DUDLEY KNOX LIBRARY
NAVAL POSTGRADUATE SCHOOL
MONTEREY CA 93943-5101

Approved for public release; distribution is unlimited.

Interaction Effects of a Lower Heated Tube on
Pool Boiling of R-124 from an Upper Horizontal Tube

by

Joseph E. Yusician, Jr.
Lieutenant, United States Navy
B.S.M.E., Drexel University, 1984

Submitted in partial fulfillment
of the requirements for the degree of

MASTER OF SCIENCE IN MECHANCIAL ENGINEERING

from the

NAVAL POSTGRADUATE SCHOOL
December 1993

Department of Mechanical Engineering

classified
urity Classification of this page

REPORT DOCUMENTATION PAGE

| | | | | |
|---|---|---|---|---|
| Report Security Classification: Unclassified | | | 1b Restrictive Markings | |
| Security Classification Authority | | | 3 Distribution/Availability of Report | |
| Declassification/Downgrading Schedule | | | Approved for public release; distribution is unlimited. | |
| Performing Organization Report Number(s) | | | 5 Monitoring Organization Report Number(s) | |
| Name of Performing Organization<br>aval Postgraduate School | 6b Office Symbol<br>34 | | 7a Name of Monitoring Organization<br>Naval Postgraduate School | |
| Address *(city, state, and ZIP code)*<br>onterey CA 93943-5000 | | | 7b Address *(city, state, and ZIP code)*<br>Monterey CA 93943-5000 | |
| Name of Funding/Sponsoring Organization<br>aval Surface Warfare Center | 6b Office Symbol<br>2272 | | 9 Procurement Instrument Identification Number | |
| dress *(city, state, and ZIP code)*<br>nnapolis, MD 21402-5067 | | | 10 Source of Funding Numbers | |
| | | | Program Element No | Project No / Task No / Work Unit Accession No |

Title *(include security classification)* INTERACTION EFFECTS OF A LOWER HEATED TUBE ON POOL BOILING OF R-124 FROM AN UPPER ORIZONTAL TUBE (UNCLASSIFIED)

Personal Author(s) Joseph E. Yusician, Jr.

| a Type of Report | 13b Time Covered From To | 14 Date of Report *(year, month, day)* | 15 Page Count |
|---|---|---|---|
| aster's Thesis | | December 1993 | 192 |

Supplementary Notation The views expressed in this thesis are those of the author and do not reflect the fficial policy or position of the Department of Defense or the U.S. Government.

| Cosati Codes | | | 18 Subject Terms *(continue on reverse if necessary and identify by block number)* |
|---|---|---|---|
| eld | Group | Subgroup | HEAT TRANSFER, INTERACTION EFFECTS OF A LOWER HEATED TUBE ON POOL BOILING FROM AN UPPER TUBE, R-124 REFRIGERANT |
| | | | |

Abstract *(continue on reverse if necessary and identify by block number)*

An investigation of the interaction effects of a lower heated tube on pool boiling of pure R-124 from an upper horizontal tube as conducted at a saturation temperature of 2.2 °C. The test tubes used were: (1) smooth tubes and (2) deformed surface URBO-B) enhanced tubes. The effects of tube spacing/configuration and lower tube heat flux on the heat transfer performance the upper tube were investigated.

For both tube arrays, the enhancing effect of bubbles from a lower tube was dramatic. This enhancement increased as lower be heat flux increased. However, when upper tube heat fluxes were greater than 20 kW/m$^2$, all enhancement disappeared.

For a smooth tube array in natural convection, the effect of a lower heated tube on the heat transfer from an upper tube was nall. In nucleate boiling, a P/D of 1.8 gave the best upper tube heat transfer performance and a vigorously nucleating lower be eliminated upper tube hysteresis. With the lower tube unheated and an upper tube heat flux of greater than 3 kW/m$^2$, the rformance using R-124 was generally better than for R-114. With a nucleating lower tube (at 10 kW/m$^2$), again the rformance of R-124 was better, but only for upper tube heat fluxes of greater than 40 kW/m$^2$.

For a TURBO-B tube array, a 30 degree offset of the upper tube reduced the upper tube heat transfer performance (compared the in-line configurations). This may indicate bubbles depart TURBO-B tubes differently than smooth tubes.

| Distribution/Availability of Abstract | 21 Abstract Security Classification | |
|---|---|---|
| X unclassified/unlimited — same as report — DTIC users | Unclassified | |
| a Name of Responsible Individual<br>Paul J. Marto | 22b Telephone *(include Area Code)*<br>408-656-2989 | 22c Office Symbol<br>ME/Mx |

FORM 1473,84 MAR 83 APR edition may be used until exhausted security classification of this pag

## ABSTRACT

An investigation of the interaction effects of a lower heated tube on pool boiling of pure R-124 from an upper horizontal tube was conducted at a saturation temperature of 2.2 °C. The test tubes used were: (1) smooth tubes and (2) deformed surface (TURBO-B) enhanced tubes. The effects of tube spacing/configuration and lower tube heat flux on the heat transfer performance of the upper tube were investigated.

For both tube arrays, the enhancing effect of bubbles from a lower tube was dramatic. This enhancement increased as lower tube heat flux increased. However, when upper tube heat fluxes were greater than 20 $kW/m^2$, all enhancement disappeared.

For a smooth tube array in natural convection, the effect of a lower heated tube on the heat transfer from an upper tube was small. In nucleate boiling, a P/D of 1.8 gave the best upper tube heat transfer performance and a vigorously nucleating lower tube eliminated upper tube hysteresis. With the lower tube unheated and an upper tube heat flux of greater than 3 $kW/m^2$, the performance using R-124 was generally better than for R-114. With a nucleating lower tube (at 10 $kW/m^2$), again the performance of R-124 was better, but only for upper tube heat fluxes of greater than 40 $kW/m^2$.

For a TURBO-B tube array, a 30 degree offset of the upper tube reduced the upper tube heat transfer performance (compared to the in-line configurations). This may indicate bubbles depart TURBO-B tubes differently than smooth tubes.

C.1

## TABLE OF CONTENTS


I. INTRODUCTION . . . . . 1

II. LITERATURE SURVEY . . . . . 5

A. POOL BOILING . . . . . 5

1. Natural Convection . . . . . 5

2. Boiling Incipience . . . . . 5

3. Nucleate Boiling . . . . . 7

B. SINGLE TUBE HEAT TRANSFER EXPERIMENTS WITH R-124 AT NAVAL POSTGRADUATE SCHOOL . . . . . 8

C. SMALL TUBE ARRAY HEAT TRANSFER PERFORMANCE . . . 9

1. Natural Convection . . . . . 10

2. Nucleate Boiling . . . . . 12

III. EXPERIMENTAL APPARATUS . . . . . 15

A. SYSTEM DESCRIPTION . . . . . 15

B. BOILING TEST SECTION . . . . . 17

1. Evaporator . . . . . 17

2. Evaporator Tubes . . . . . 18

3. Tube Configurations . . . . . 22

C. CONDENSER SECTION . . . . . 22

D. REFRIGERANT STORAGE RESERVOIR . . . . . 26

E. OIL SUBSECTION . . . . . 27

DUDLEY KNOX LIBRARY
NAVAL POSTGRADUATE SCHOOL
MONTEREY CA 93943-5101

F. COOLING SUBSYSTEM . . . . . 27
1. Ethylene-Glycol/Water Coolant Sump . . . . . 27
2. Refrigeration Plants . . . . . 27
3. Pumps and Control Valve (VC) . . . . . 28
G. APPARATUS ENCLOSURE . . . . . 28
H. INSTRUMENTATION . . . . . 30
1. Power Measurement System . . . . . 30
2. Temperature Measurement . . . . . 30
I. DATA ACQUISITION AND REDUCTION PROGRAM . . . . . 33

IV. EXPERIMENTAL PROCEDURE . . . . . 37
A. EVAPORATOR DISASSEMBLY PROCEDURE . . . . . 37
B. EVAPORATOR ASSEMBLY PROCEDURE . . . . . 38
1. Evaporator Assembly . . . . . 38
2. Leak Test . . . . . 38
3. Charging System with Refrigerant . . . . . 39
a. From Storage Reservoir . . . . . 39
b. From Refrigerant Cylinder . . . . . 40
4. Degassing Procedure . . . . . 40
5. Data Acquisition Channel Check . . . . . 41
C. STANDARD OPERATING PROCEDURE . . . . . 41
D. DATA FILES . . . . . 42

V. DISCUSSION OF RESULTS . . . . . 50
A. REPRODUCIBILITY/REPEATABILITY . . . . . 50
B. INFLUENCE OF THE LOWER TUBE . . . . . 59

1. The Effect of Tube Spacing . . . . . 62
a. Smooth Tubes with Lower Tube Unheated . . 62
b. Smooth Tubes with LTHFS of 1 kW/m$^2$ . . . . 65
c. Smooth Tubes with LTHFS of 5 kW/m$^2$ . . . . 68
d. Smooth Tubes with LTHFS of 10 kW/m$^2$ . . . 71
e. Smooth Tubes with LTHFS of 20 kW/m$^2$ . . . 73
f. Smooth Tubes with UTHFS equal LTHFS . . . 76
g. TURBO-B Tubes with Lower Tube Unheated . . 80
h. TURBO-B Tubes with LTHFS of 1 kW/m$^2$ . . . 80
i. TURBO-B Tubes with LTHFS of 5 kW/m$^2$ . . . 83
j. TURBO-B Tubes with LTHFS of 10 kW/m$^2$ . . . 83
k. TURBO-B Tubes with LTHFS of 20 kW/m$^2$ . . . 86
l. TURBO-B Tubes with UTHFS equal LTHFS . . . 86
2. The Effect of a Fixed Lower Tube Heat Flux . . 86
a. Smooth Tubes with P/D of 2.0 . . . . . 86
b. Smooth Tubes with P/D of 1.8 . . . . . 92
c. Smooth Tubes with P/D of 1.5 . . . . . 94
d. Smooth Tubes with P/D of 1.2 . . . . . 97
e. Smooth Tubes with P/D of 1.2
(Rotated 30°) . . . . . 97
f. TURBO-B Tubes with P/D of 2.0 . . . . . 102
g. TURBO-B Tubes with P/D of 1.8 . . . . . 102
h. TURBO-B Tubes with P/D of 1.5 . . . . . 106
i. TURBO-B Tubes with P/D of 1.2 . . . . . 106
j. TURBO-B Tubes with P/D of 1.2
(Rotated 30°) . . . . . 109

3. The Effect of a Variable Lower Tube Heat Flux . . . . . 109
a. Smooth Tubes with P/D of 2.0 . . . . . 109
b. Smooth Tubes with P/D of 1.8 . . . . . 112
c. Smooth Tubes with P/D of 1.5 . . . . . 115
d. Smooth Tubes with P/D of 1.2 . . . . . 115
e. Smooth Tubes with P/D of 1.2 (Rotated 30°) . . . . . 115
f. TURBO-B Tubes with P/D of 2.0 . . . . . 118
g. TURBO-B Tubes with P/D of 1.8 . . . . . 120
h. TURBO-B Tubes with P/D of 1.5 . . . . . 120
i. TURBO-B Tubes with P/D of 1.2 . . . . . 120
j. TURBO-B Tubes with P/D of 1.2 (Rotated 30°) . . . . . 124
C. R-124/R-114 PERFORMANCE COMPARISON . . . . . 124

VI. CONCLUSIONS . . . . . 129

VII. RECOMMENDATIONS . . . . . 130

APPENDIX A. PROGRAM SETUPJY . . . . . 131

APPENDIX B. PROGRAM DRPJY . . . . . 134

APPENDIX C. REPRESENTATIVE DATA SET . . . . . 147

APPENDIX D. SAMPLE CALCULATIONS . . . . . 155
A. SMOOTH TEST TUBE DIMENSIONS . . . . . 155
B. MEASURED PARAMETERS . . . . . 155
C. OUTER WALL TEMPERATURE OF THE UPPER TEST TUBE . 156
1. Surface Area of Smooth Tube . . . . . 156
2. Heater Power . . . . . 156
3. Average Inside Tube Temperature . . . . . 156
4. Outside Wall Tube Temperature . . . . . 156
5. Tube Wall Superheat . . . . . 156
D. R-124 PROPERTIES AT FILM TEMPERATURE . . . . . 157
1. Film Temperature . . . . . 157
2. Dynamic Viscosity . . . . . 157
3. Density . . . . . 157
4. Kinematic Viscosity . . . . . 157
5. Thermal Conductivity . . . . . 157
6. Specific Heat . . . . . 158
7. Thermal Diffusivity . . . . . 158
8. Volumetric Thermal Expansion Coefficient . . 158
9. Prandtl Number . . . . . 158
E. HEAT FLUX THROUGH NON-BOILING TUBE LENGTHS . . 158
F. HEAT FLUX THROUGH BOILING TUBE LENGTH . . . . . 159

APPENDIX E. UNCERTAINTY ANALYSIS . . . . . 160
A. HEAT TRANSFER RATE UNCERTAINTY . . . . . 161
B. SURFACE AREA UNCERTAINTY . . . . . 161
C. WALL SUPERHEAT UNCERTAINTY . . . . . 162

D. HEAT FLUX UNCERTAINTY . . . . . 163
E. HEAT TRANSFER COEFFICIENT UNCERTAINTY . . . . . 164

LIST OF REFERENCES . . . . . 166

INITIAL DISTRIBUTION LIST . . . . . 169

## LIST OF TABLES

TABLE 1. R-114/R-124 PHYSICAL PROPERTIES AT 2.2 °C . . 2

TABLE 2. DIMENSIONS OF TEST TUBES . . . . . 18

TABLE 3. HP-3497A CHANNEL ASSIGNMENTS . . . . . 36

TABLE 4. LIST OF DATA RUNS . . . . . 44

TABLE 5. RESULTS OF UNCERTAINTY ANALYSIS . . . . . 165

## LIST OF FIGURES


Figure 2.1 Pool Boiling Curve . . . . . 6

Figure 3.1 Schematic of Experimental Apparatus . . . . 16

Figure 3.2 Sketch of Pyrex Glass Evaporator and Cast-Iron Flange . . . . . 19

Figure 3.3 Schematic of a Test Tube . . . . . 20

Figure 3.4 Surface Profile of Enhanced (TURBO-B) Tube . 21

Figure 3.5 Sketch of an Endplate and Teflon Insert . . 23

Figure 3.6 Sketch of a Strongback . . . . . 24

Figure 3.7 Tube Configurations . . . . . 25

Figure 3.8 Schematic of R-502 Refrigeration System . . 29

Figure 3.9 Schematic of the Power Measurement System . 31

Figure 3.10 Thermocouple Positions . . . . . 32

Figure 3.11 Sketch of Thermocouple Housing . . . . . 34

Figure 5.1 Increasing Heat Flux Repeatability Runs using Smooth Tube Configuration C0 . . . . . 51

Figure 5.2 Decreasing Heat Flux Repeatability Runs using Smooth Tube Configuration C0 . . . . . 53

Figure 5.3 Decreasing Heat Flux Repeatability Runs using TURBO-B Tube Configuration C0 . . . . 55

Figure 5.4 Increasing Heat Flux Repeatability Runs using Smooth Tube Configuration C1 with the Lower Tube Unheated . . . . . 56

Figure 5.5 Decreasing Heat Flux Repeatability Runs using Smooth Tube Configuration C1 with the Lower Tube Unheated . . . . . 58
Figure 5.6 Decreasing Heat Flux Repeatability Runs using TURBO-B Tube Configuration C1 with the Lower Tube Unheated . . . . . 60
Figure 5.7 Comparison of Smooth Tube P/D Ratios for Increasing Heat Flux with the Lower Tube Unheated . . . . . 63
Figure 5.8 Comparison of Smooth Tube P/D Ratios for Decreasing Heat Flux with the Lower Tube Unheated . . . . . 64
Figure 5.9 Comparison of Smooth Tube P/D Ratios for Increasing Heat Flux with 1 $kW/m^2$ on the Lower Tube . . . . . 66
Figure 5.10 Comparison of Smooth Tube P/D Ratios for Decreasing Heat Flux with 1 $kW/m^2$ on the Lower Tube . . . . . 67
Figure 5.11 Comparison of Smooth Tube P/D Ratios for Increasing Heat Flux with 5 $kW/m^2$ on the Lower Tube . . . . . 69
Figure 5.12 Comparison of Smooth Tube P/D Ratios for Decreasing Heat Flux with 5 $kW/m^2$ on the Lower Tube . . . . . 70
Figure 5.13 Comparison of Smooth Tube P/D Ratios for Increasing Heat Flux with 10 $kW/m^2$ on the

Lower Tube . . . . . 72
Figure 5.14 Comparison of Smooth Tube P/D Ratios for Decreasing Heat Flux with 10 kW/m$^2$ on the Lower Tube . . . . . 74
Figure 5.15 Comparison of Smooth Tube P/D Ratios for Increasing Heat Flux with 20 kW/m$^2$ on the Lower Tube . . . . . 75
Figure 5.16 Comparison of Smooth Tube P/D Ratios for Decreasing Heat Flux with 20 kW/m$^2$ on the Lower Tube . . . . . 77
Figure 5.17 Comparison of Smooth Tube P/D Ratios for Increasing Heat Flux with UTHFS equal to LTHFS . . . . . 78
Figure 5.18 Comparison of Smooth Tube P/D Ratios for Decreasing Heat Flux with UTHFS equal to LTHFS . . . . . 79
Figure 5.19 Comparison of TURBO-B Tube P/D Ratios for Decreasing Heat Flux with the Lower Tube Unheated . . . . . 81
Figure 5.20 Comparison of TURBO-B Tube P/D Ratios for Decreasing Heat Flux with 1 kW/m$^2$ on the Lower Tube . . . . . 82
Figure 5.21 Comparison of TURBO-B Tube P/D Ratios for Decreasing Heat Flux with 5 kW/m$^2$ on the Lower Tube . . . . . 84
Figure 5.22 Comparison of TURBO-B Tube P/D Ratios for

Decreasing Heat Flux with 10 kW/m$^2$ on the Lower Tube . . . . . 85
Figure 5.23 Comparison of TURBO-B Tube P/D Ratios for Decreasing Heat Flux with 20 kW/m$^2$ on the Lower Tube . . . . . 87
Figure 5.24 Comparison of TURBO-B Tube P/D Ratios for Decreasing Heat Flux with the UTHFS equal to the LTHFS . . . . . 88
Figure 5.25 Comparison of Lower Tube Heat Flux Settings on Increasing Heat Flux of Smooth Tubes with P/D of 2.0 . . . . . 89
Figure 5.26 Comparison of Lower Tube Heat Flux Settings on Decreasing Heat Flux of Smooth Tubes with P/D of 2.0 . . . . . 91
Figure 5.27 Comparison of Lower Tube Heat Flux Settings on Increasing Heat Flux of Smooth Tubes with P/D of 1.8 . . . . . 93
Figure 5.28 Comparison of Lower Tube Heat Flux Settings on Decreasing Heat Flux of Smooth Tubes with P/D of 1.8 . . . . . 95
Figure 5.29 Comparison of Lower Tube Heat Flux Settings on Increasing Heat Flux of Smooth Tubes with P/D of 1.5 . . . . . 96
Figure 5.30 Comparison of Lower Tube Heat Flux Settings on Decreasing Heat Flux of Smooth Tubes with P/D of 1.5 . . . . . 98

Figure 5.31 Comparison of Lower Tube Heat Flux Settings on Increasing Heat Flux of Smooth Tubes with P/D of 1.2 . . . . . 99
Figure 5.32 Comparison of Lower Tube Heat Flux Settings on Decreasing Heat Flux of Smooth Tubes with P/D of 1.2 . . . . . 100
Figure 5.33 Comparison of Lower Tube Heat Flux Settings on Increasing Heat Flux of Smooth Tubes with P/D 1.2 (Rotated 30°) . . . . . 101
Figure 5.34 Comparison of Lower Tube Heat Flux Settings on Decreasing Heat Flux of Smooth Tubes with P/D of 1.2 (Rotated 30°) . . . . . 103
Figure 5.35 Comparison of Lower Tube Heat Flux Settings on Decreasing Heat Flux of TURBO-B Tubes with P/D of 2.0 . . . . . 104
Figure 5.36 Comparison of Lower Tube Heat Flux Settings on Decreasing Heat Flux of TURBO-B Tubes with P/D of 1.8 . . . . . 105
Figure 5.37 Comparison of Lower Tube Heat Flux Settings on Decreasing Heat Flux of TURBO-B Tubes with P/D of 1.5 . . . . . 107
Figure 5.38 Comparison of Lower Tube Heat Flux Settings on Decreasing Heat Flux of TURBO-B Tubes with P/D of 1.2 . . . . . 108
Figure 5.39 Comparison of Lower Tube Heat Flux Settings on Decreasing Heat Flux of TURBO-B Tubes

with P/D of 1.2 (Rotated 30°) . . . . . 110
Figure 5.40 Heat Transfer Performance of a Smooth Upper Tube at a Constant Heat Flux for a P/D of 2.0 . . . . . 111
Figure 5.41 Heat Transfer Performance of a Smooth Upper Tube at a Constant Heat Flux for a P/D of 1.8 . . . . . 113
Figure 5.42 Heat Transfer Performance of a Smooth Upper Tube at a Constant Heat Flux for a P/D of 1.5 . . . . . 114
Figure 5.43 Heat Transfer Performance of a Smooth Upper Tube at a Constant Heat Flux for a P/D of 1.2 . . . . . 116
Figure 5.44 Heat Transfer Performance of a Smooth Upper Tube at a Constant Heat Flux for a P/D of 1.2 (Rotated 30°) . . . . . 117
Figure 5.45 Heat Transfer Performance of a TURBO-B Upper Tube at a Constant Heat Flux for a P/D of 2.0 . . . . . 119
Figure 5.46 Heat Transfer Performance of a TURBO-B Upper Tube at a Constant Heat Flux for a P/D of 1.8 . . . . . 121
Figure 5.47 Heat Transfer Performance of a TURBO-B Upper Tube at a Constant Heat Flux for a P/D of 1.5 . . . . . 122
Figure 5.48 Heat Transfer Performance of a TURBO-B

Upper Tube at a Constant Heat Flux for a P/D of 1.2 . . . . . 123

Figure 5.49 Heat Transfer Performance of a TURBO-B Upper Tube at a Constant Heat Flux for a P/D of 1.2 (Rotated 30°) . . . . . 125

Figure 5.50 Comparison of R-124 to R-114 for Smooth Tubes with Decreasing Heat Flux and the Lower Tube Unheated . . . . . 126

Figure 5.51 Comparison of R-124 to R-114 for Smooth Tubes with Decreasing Heat Flux and a LTHFS of 10 $kW/m^2$ . . . . . 128

## NOMENCLATURE

This nomenclature reflects that which is found within programs SETUPJY (Appendix A) and DRPJY (Appendix B). Note that the upper and lower test tube dimensions are the same since like test tubes are used.

| SYMBOL | UNITS | NAME/DESCRIPTION |
|---|---|---|
| A | $m^2$ | Area |
| Ab | $m^2$ | Tube active boiling surface area |
| Ac | $m^2$ | Tube cross-sectional area |
| Cp | J/kg·K | Specific heat of upper tube |
| ACp | J/kg·K | Specific heat of lower tube |
| D | m | Diameter |
| Do | m | Tube outside diameter |
| Di | m | Tube inside diameter |
| D1 | m | Tube diameter at thermocouple positions |
| D2 | m | Tube diameter at active boiling section |
| g | $m/s^2$ | Gravitational acceleration |
| h | $W/m^2 \cdot K$ | Heat transfer coefficient of upper tube |
| Ah | $W/m^2 \cdot K$ | Heat transfer coefficient of lower tube |
| I | A | Upper tube current |
| AI | A | Lower tube current |
| Ir | A | Upper tube current from AC current sensor |
| AIr | A | Lower tube current from AC current sensor |

| | | |
|---|---|---|
| k | W/m·K | Thermal conductivity associated with the upper tube |
| Ak | W/m·K | Thermal conductivity associated with the lower tube |
| kc | W/m·K | Copper thermal conductivity |
| L | m | Tube active boiling length |
| Lu | m | Tube non-boiling length |
| Nu | | Nusselt number |
| P | m | Tube outside surface perimeter |
| Pr | | Prandtl number associated with the upper tube |
| APr | | Prandtl number associated with the lower tube |
| Pg | Pa | Gas pressure |
| Psat | Pa | Saturation pressure |
| Q | W | Upper tube boiling surface heat transfer rate |
| AQ | W | Lower tube boiling surface heat transfer rate |
| Qf | W | Upper tube heat transfer rate through one non-boiling end |
| AQf | W | Lower tube heat transfer rate through one non-boiling end |
| Qh | W | Upper tube cartridge heater heat transfer rate |
| AQh | W | Lower tube cartridge heater heat transfer rate |
| q" | $W/m^2$ | Upper tube heat flux |
| Aq" | $W/m^2$ | Lower tube heat flux |
| Ra | | Rayleigh number |
| T | °C | Temperature |

| | | |
|---|---|---|
| Tavg | °C | Upper tube average wall temperature at a thermocouple location |
| ATavg | °C | Lower tube average wall temperature at a thermocouple location |
| Tc | °C | Critical temperature |
| Tf | °C | Upper tube film temperature |
| ATf | °C | Lower tube film temperature |
| Tn | °C | Temperature at the nth thermocouple location |
| Tsat | °C | Saturation temperature |
| Two | °C | Upper tube outer wall temperature |
| ATwo | °C | Lower tube outer wall temperature |
| V | V | Upper tube cartridge heater voltage |
| AV | V | Lower tube cartridge heater voltage |
| Vr | V | Upper tube AC-DC true RMS converter output voltage |
| AVr | V | Lower tube AC-DC true RMS converter output voltage |
| $\alpha$ | $m^2/s$ | Thermal diffusivity associated with the upper tube |
| A$\alpha$ | $m^2/s$ | Thermal diffusivity associated with the lower tube |
| $\beta$ | 1/K | Upper tube volumetric thermal expansion coefficient |
| A$\beta$ | 1/K | Lower tube volumetric thermal expansion coefficient |
| $\delta$ | | Uncertainty in measurement |
| $\theta$b | K | Upper tube wall superheat (Two - Tsat) |
| A$\theta$b | K | Lower tube wall superheat (Two - Tsat) |
| $\mu$ | kg/m·s | Dynamic viscosity associated with the upper tube |

| | | |
|---|---|---|
| $A\mu$ | $kg/m \cdot s$ | Dynamic viscosity associated with the lower tube |
| $\upsilon$ | $m^2/s$ | Kinematic viscosity associated with the upper tube |
| $A\upsilon$ | $m^2/s$ | Kinematic viscosity associated with the lower tube |
| $\rho$ | $kg/m^3$ | Density associated with the upper tube |
| $A\rho$ | $kg/m^3$ | Density associated with the lower tube |

## ACKNOWLEDGMENTS

I would like to dedicate this work to my wife, Theresa, for her patience, tolerance, reassurance and everlasting support throughout my tour at the Naval Postgraduate School.

# I. INTRODUCTION

The United States Navy intends to eliminate its dependence on chlorofluorocarbons (CFC's) as soon as feasible. Currently, the Navy is using CFC-114 (Refrigerant or R-114) in most of it's chilled water air conditioning (AC) plants. These shipboard AC plants provide the chilled cooling water to cool the vital weapons systems and electronic components besides providing habitability comfort for the crew.

The Navy has identified a hydrochlorofluorocarbon, HCFC-124 or R-124, as a possible mid-term replacement for R-114 in naval shipboard AC systems. With an ozone depletion potential (ODP) of only 2% compared to 70% for R-114, R-124 is a much more tolerable fluid to use until an acceptable alternative refrigerant can be found that has zero ODP.

Although both refrigerants operate near the same evaporating temperature (2.2 °C), the characteristics of R-124 under similar conditions as R-114 are quite different. For example, the refrigeration components (i.e., heat exchangers, piping, etc.) must be able to withstand: (1) the higher operating pressures of R-124 (11 psig at 2.2 °C compared to 0 psig for R-114) and (2) the higher vapor pressure after the system is secured (in a main engineering space at 100 °F, R-124 would reach 66 psig compared to 31 psig for R-114). Given the system components can operate safely at these higher

pressures of R-124, then the hardware modifications to the system should be limited to:

1. Modifying the compressor to maintain rated capacity and use a miscible alkylbenzene oil for lubrication.
2. Reset/replace the system safety devices to account for the higher pressures of R-124.
3. Replace the system seals with neoprene seals, which resist deterioration when in contact with R-124, to maintain leak tight integrity.

Besides hardware modifications, another main concern is how does the heat transfer characteristics of R-124 compare to R-114. Table 1, from Bertsch [Ref. 1], provides

**TABLE 1. R-114/R-124 PHYSICAL PROPERTIES AT 2.2 °C**

| **Property** | **R-114** | **R-124** |
|---|---|---|
| Psat (kPa) | 96 | 177 |
| $\rho$(liq) (kg/m$^2$) | 1526 | 1429 |
| $\rho$(vapor) (kg/m$^2$) | 7.5 | 11.3 |
| Cp(liq) (J/kg·K) | 932 | 1060 |
| $h_{fg}$ (kJ/kg) | 134.7 | 158.9 |
| k(liq) (W/m·K) | 0.0701 | 0.0744 |
| $\mu$(liq) (g/m·s) | 0.4449 | 0.3375 |
| $\sigma$ (N/m) | 0.0136 | 0.0129 |

the physical properties of R-114 and R-124 at a saturation temperature of 2.2 °C. As seen from Table 1, R-124 has higher latent heat of vaporization, vapor density and

thermal conductivity than R-114 at 2.2 °C and a considerably lower liquid viscosity. Therefore, it is reasonable for one to assume that R-124 would have better heat transfer performance at 2.2 °C than R-114. Bertsch [Ref. 1] evaluated and compared the heat transfer performance of R-114 and R-124 for a single horizontal smooth tube and various enhanced tubes using pure refrigerant and refrigerant/oil mixtures. One of his conclusions was:

> For smooth and finned tubes, significant improvements in heat transfer (>50%) were obtained in pure R-124 compared with pure R-114 at the same saturation temperature. This was attributed to the higher saturation pressure of R-124 activating more nucleation sites and the higher latent heat of vaporization, vapor density and thermal conductivity of R-124 over R-114.

Perry [Ref. 2] investigated the effect of oil, pressurization and subcooling on the onset of nucleate boiling of R-124 from a single horizontal tube. When Perry [Ref. 2] compared his results to Bertsch [Ref. 1] for pure R-124, he found a larger incipient wall superheat was being obtained, but almost identical data trends were observed at high heat fluxes and decreasing heat fluxes. He attributed the larger incipience to his degassing procedure of the refrigerent system after reassembly.

Now, what if multiple tubes are arranged in a bundle configuration? How do the lower tubes influence the heat transfer performance of the upper tubes? Lake [Ref. 3] in search of an answer to these questions, used a configuration

of two horizontal tubes (smooth and enhanced tubes) in vertical alignment, submerged in a pool of R-114, separated by a pitch-to-diameter (P/D) ratio. After using various combinations of P/D ratios and lower tube heat fluxes, Lake [Ref. 3] found that a nucleating lower tube significantly enhanced the heat transfer performance of an upper tube, particularly at low heat fluxes. Also, a P/D ratio of 1.8 gave the best heat transfer performance for smooth tubes at high heat fluxes (no P/D effect was found using the enhanced tubes).

To fully understand the nucleate pool boiling characteristics of R-124 and to directly compare the heat transfer performance of R-124 to R-114, multiple tube pool boiling data for R-124 is needed. Therefore, the following thesis objectives were established:

1. Collect natural convection and pool boiling heat transfer data of pure R-124 using a single smooth and enhanced tube and check the repeatability with the existing R-124 data of Bertsch [Ref. 1] and Perry [Ref. 2].
2. Collect natural convection and pool boiling heat transfer data of R-124 over a range of increasing and decreasing heat fluxes using two tubes while varying the spacing between the tubes and the heat flux on the lower tube.
3. Compare the R-124 data to the R-114 data obtained by Lake [Ref. 3].

# II. LITERATURE SURVEY

## A. POOL BOILING

Pool boiling occurs when a heated surface is submerged below the free surface of a liquid pool, at a temperature sufficiently above the local saturation temperature to cause bubbles to form from the surface. Figure 2.1, from Bar-Cohen [Ref. 4], is a pool boiling curve for a highly wetting liquid with several regimes displayed. Only the natural convection (or single phase convection), boiling incipience and nucleate boiling regimes are discussed.

### 1. Natural Convection

The regime (a-b) in Figure 2.1, is where heat transfer occurs because of the liquid flow caused by buoyancy forces due to density differences in the liquid pool. In this regime, the heat flux from the heated surface is proportional to some power of wall superheat (i.e., $q'' \propto \Delta T_w^{1.25}$ or $\Delta T_w^{1.33}$). This proportionality remains valid until the wall superheat reaches a value where vapor bubbles first form on the heated surface.

### 2. Boiling Incipience

The onset of nucleate boiling (ONB) or incipient boiling is a random phenomenon (You et al. [Ref. 5]) which

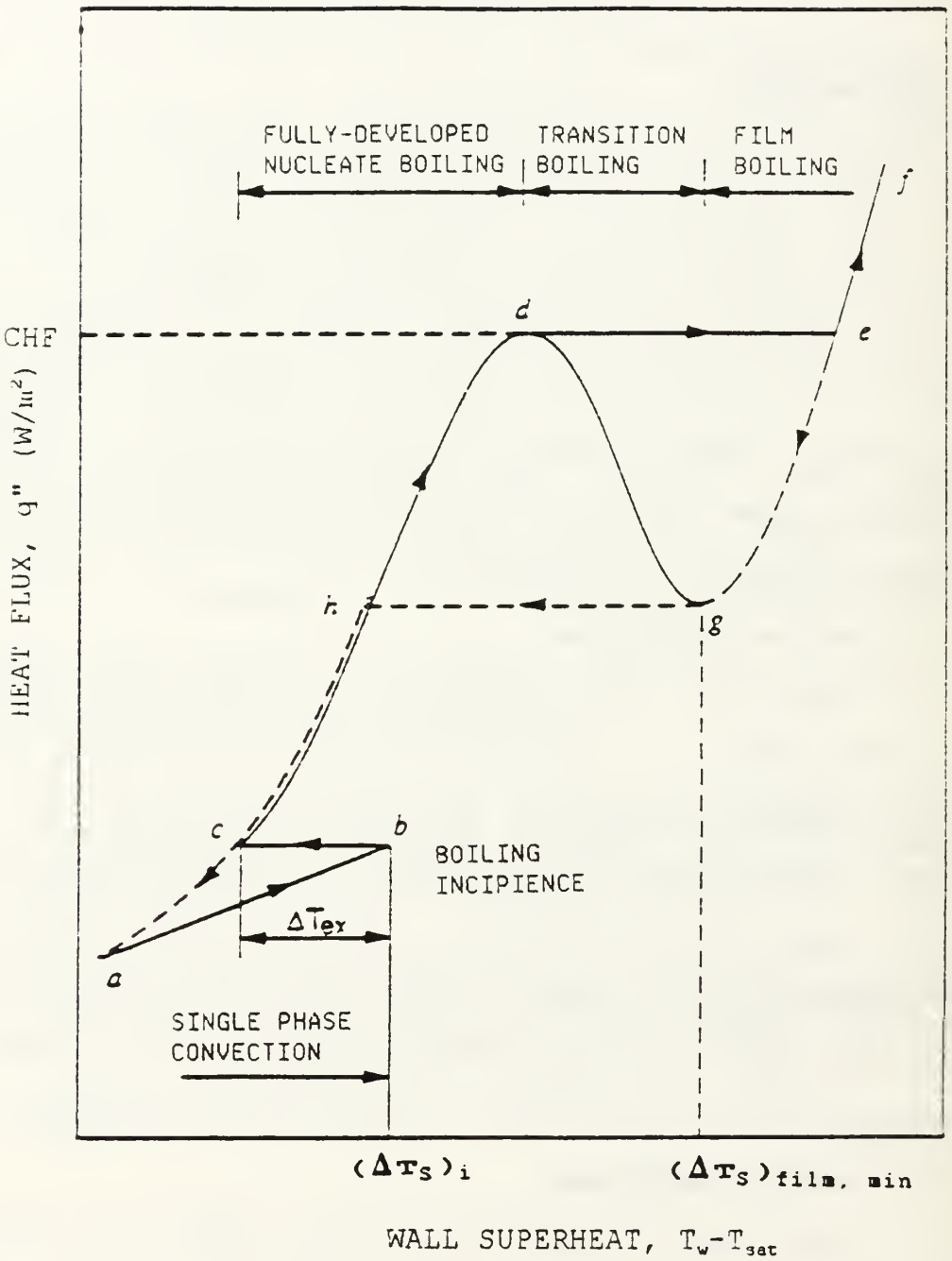


**Figure 2.1 Pool Boiling Curve**

is influenced by factors such as surface condition of the heated surface, liquid properties and dissolved gases in the liquid pool. Bar-Cohen and Simon [Ref. 6] and Tong et al. [Ref. 7] investigated boiling incipience of highly-wetting liquids using refrigerants and dielectrics. They found that these liquids effectively flood the micro-cavities on a tube surface, causing fewer active embryos (micro-cavities containing trapped vapor). Ultimately, these highly-wetting liquids require larger wall superheats to initialize bubble growth in the flooded micro-cavities. As a result of the larger wall superheats (up to 100 °C, Bar-Cohen and Simon [Ref. 6]), nucleation at (b), in Figure 2.1, occurs in an explosive manner. This explosive boiling from the active micro-cavities causes the larger inactive cavities to activate, rapidly decreasing the required wall superheat to sustain boiling, noted as $\Delta T_{ex}$ in Figure 2.1. This drift from (b) to (c) only occurs during increasing heat flux and is referred to as thermal overshoot or superheat excursion.

### 3. Nucleate Boiling

The regime (c-d) in Figure 2.1 is the fully developed nucleate boiling region. At (c), small isolated bubbles are leaving the heated surface at low heat fluxes. As the heat flux is increased, these small bubbles become more numerous as more active sites are created. At high heat fluxes, these bubbles begin to coalesce, forming slugs of vapor, which grow

and depart from the surface. According to Thome [Ref. 8], in this regime, heat removal is accomplished by sensible heat in the form of superheated liquid or as latent heat in vapor bubbles. Also, the principal mechanisms of heat transfer are: (1) liquid-phase convection, enhanced by the stripping of the thermal boundary layer by the departing vapor bubbles, and (2) evaporation of the thin liquid micro-layer trapped between a growing vapor bubble and the heated surface.

## B. SINGLE TUBE HEAT TRANSFER EXPERIMENTS WITH R-124 AT NAVAL POSTGRADUATE SCHOOL

Bertsch [Ref. 1] and Perry [Ref. 2] independently studied the heat transfer performance of single smooth and enhanced tubes submerged in a liquid pool of R-124 at 2.2 °C. Perry [Ref. 2] determined that in natural convection the experimentally based correlation, equation (1), developed by Churchill and Chu [Ref. 9] fairly well predicted the heat transfer performance of a smooth tube.

$$Nu = \left[0.6 + 0.387\left(\frac{Ra}{(1+(0.559/Pr)^{9/16})^{16/9}}\right)^{1/6}\right]^2 \qquad (1)$$

where Nu = Nusselt number = hDo/k

Ra = Rayleigh number = $(g \cdot \beta \cdot \{Twall - Tsat\} \cdot Do^3)/(\upsilon \cdot \alpha)$

During nucleate boiling, most correlations available to predict the heat transfer performance of a smooth tube are expressed as heat flux as a function of tube wall superheat. Bertsch [Ref. 1] used a best fit correlation through his experimental nucleate boiling data to express the heat flux from a smooth single tube in pure R-124 as:

$$q'' = (17.0)\Delta T_w^3 \quad (W/m^2) \qquad (2)$$

In the above equation, the wall superheat $\Delta T_w$ is expressed in degrees Celsius.

For a single enhanced tube, Bertsch [Ref. 1] concluded that nucleate pool boiling enhancement (i.e., improvements in heat transfer compared to a single smooth tube) were as much as 6.2 times for re-entrant cavity surfaces (TURBO-B and HIGH FLUX). Thome [Ref. 10] attributes these enhancements to the numerous re-entrant cavities that trap vapor, which create a large boiling site density, reducing the wall superheat required to sustain nucleation.

## C. SMALL TUBE ARRAY HEAT TRANSFER PERFORMANCE

The effect of a lower tube on the heat transfer performance of an upper tube is very important when designing flooded evaporators. It is essential to understand the mechanisms that affect the heat transfer performance in small

tube arrays in natural convection and nucleate boiling for both smooth and enhanced surfaces.

**1. Natural Convection**

In natural convection, the interaction effects of a lower heated tube on the heat transfer performance of an upper tube are the result of two offsetting mechanisms. With a lower tube heated, a rising heated buoyant plume impinges on and flows around an upper tube, which subjects the upper tube to local forced convection effects. This forced convection increases the local fluid velocity around the upper tube and raises the upper tube heat transfer coefficient. Additionally, the heated plume from the lower tube increases the local ambient temperature of the fluid impinging on the upper tube. This reduces the natural convection buoyancy driving force for this tube, decreasing the upper tube heat transfer coefficient. Therefore, the presence of a lower heated tube has opposing influences on the heat transfer performance of an upper tube. Which of these influences is dominant depends on the tube spacing, local heat flux and the thermophysical properties of the fluid.

Sparrow and Niethammer [Ref. 11] studied the effect of vertical separation between two horizontal cylinders on the heat transfer performance of an upper cylinder in natural convection using air. It was discovered that heat transfer

enhancement[1] increased as the distance between the tubes increased with a maximum enhancement of approximately 1.3 for $7 < P/D < 9$. Also, for a $P/D < 3$, the enhancement decreases below 1.0. Al-Alusi and Bushnell [Ref. 12] and Tokura et al. [Ref. 13] also working with a small array of horizontal smooth cylinders in air, found generally the same results. As the distance between the cylinders increased, the heat transfer enhancement increased, reaching a maximum, then returning to a lower value of enhancement.

Sparrow and Boessneck [Ref. 14] investigated the effect of transverse misalignment of a lower cylinder on the heat transfer performance of an upper cylinder, for $2 \leq P/D \leq 9$, using air. For the perfectly aligned upper and lower cylinders, the heat transfer enhancement of the upper cylinder increased as the P/D ratio increased. Again, the largest enhancement was found with a P/D of 9 and the P/D of 2 produced the lowest enhancment. As misalignment was increased, the enhancement began to merge to a common value of about 1.03 at sufficiently large offsets (about 2.5 cylinder diameters). Sparrow and Boessneck concluded that this behavior is caused by the rising plume from the lower cylinder presenting a pre-heated quasi-forced-convection flow to the

[1]Enhancement is defined for a small tube array as the upper cylinder heat transfer coefficient when both cylinders are heated divided by the upper cylinder heat transfer coefficient when the lower tube is unheated.

upper cylinder. At smaller P/D ratios, the increased local ambient temperatures of the fluid impinging on the upper cylinder dominates and decreases the upper cylinder heat transfer performance. At larger P/D ratios, the forced convection effects are more dominant and increase the heat transfer from the upper cylinder.

Inagaki and Komori [Ref. 15] studied natural convection heat transfer from two vertically aligned horizontal cylinders in water. As discovered with air, a decrease in enhancement which falls below 1.0, is found for $P/D < 1.0$. A maximum enhancement of 1.25 occurs between $2.5 \leq P/D \leq 3.0$ and at larger P/D ratios, the enhancement decreases to 1.0. Inagaki and Komori attribute this behavior to the same two opposing influences discussed previously.

**2. Nucleate Boiling**

For small tube arrays in nucleate boiling, the most significant mechanism of enhancement within the array, is the well documented bundle effect[2]. Cornwell and associates [Refs. 16-19] studied fluid flow in tube bundles and found significiant enhancements in heat transfer in the upper portions of the bundles, concluding that forced convection and bubbly flow from the lower tubes, creating sliding bubbles

[2]Bundle effect is the enhancement of an upper tube due to the activation (i.e., the nucleation of bubbles) of lower tubes within the bundle.

around the upper tube, cause significant enhancement at low heat flux conditions.

Fujita et al. [Ref. 20] conducted tests with an array of three horizontal smooth tubes in R-113 at 0.1 MPa. For heat fluxes < 20 $kW/m^2$, the bundle effect enhanced the upper tube heat transfer performance. Fujita et al. [Ref. 20] also used an array of two smooth tubes, where the lower tube heat flux was held constant and the upper tube heat flux was decreased uniformly. The upper tube enhancement increased as the lower tube heat flux was raised. Lake [Ref. 3] investigated the effect of P/D ratio and lower tube heat flux on the heat transfer performance of an upper tube, using an array of two smooth tubes in R-114 at 1 atmosphere. For these tests, the bottom tube heat flux was held constant and the upper tube heat flux was raised and lowered steadily. Lake found that for an upper tube heat flux of < 20 $kW/m^2$, the enhancement of the upper tube was due to a bundle effect and the amount of enhancement increased with increased lower tube heat flux, which is consistent with Fujita et al. [Ref. 20]. Also, Lake found that for upper tube heat fluxes of > 20 $kW/m^2$, all bundle effects faded and that the P/D ratio of 1.8 provided the best upper tube heat transfer performance.

For a small array of enhanced tubes, several authors report findings similar to those found for the smooth tube arrays. Stephan and Mitrovic [Ref. 21], using a small array of three horizontal T-shaped finned tubes in R-114 at 0.2 MPa

and R-12 at 0.15 MPa, found bundle effects present at heat fluxes < 20 $kW/m^2$, with these effects disappearing as the heat flux was raised. Hahne and associates [Refs. 22-24], using two different fin arrays in R-11 at 0.1 MPa, also found significant bundle effects for heat fluxes of < 20 $kW/m^2$, which subside at higher heat fluxes. Hahne et al. [Ref. 24] also investigated the influence of P/D ratio on upper tube heat transfer. For heat fluxes < 20 $kW/m^2$, the maximum P/D ratio tested (P/D of 3.0) produced the best heat transfer performance for both finned arrays. Above 20 $kW/m^2$, neither P/D ratio nor tube fin pitch affected the upper tube heat transfer. Lake [Ref. 3], in conjunction with his testing of smooth tube performance above, found no effect of P/D ratio on HIGH FLUX tube (porous coated tube) performance at any heat flux and that there was no effect from a lower heated tube on the heat transfer performance of a nucleating upper HIGH FLUX tube. Fujita et al. [Ref. 20], like Lake, also tested porous coated tubes using the same testing conditions as for the smooth tubes and he concluded that the lower tube heat flux setting had no influence on the heat transfer coefficient of the upper tube, which agrees with the conclusions of Lake [Ref. 3].

# III. EXPERIMENTAL APPARATUS

## A. SYSTEM DESCRIPTION

A schematic diagram of the experimental apparatus is shown in Figure 3.1. Details of the apparatus design, construction and calibration are discussed by Karasabun [Ref. 25], Reilley [Ref. 26] and Sugiyama [Ref. 27]. The apparatus is very similar to the one used by Lake [Ref. 3] to conduct pool boiling of pure R-114 with a two tube configuration. The only major change being the replacement of the Pyrex-glass Tees used as the condenser and evaporator. Bertsch [Ref. 1] replaced the Pyrex-glass Tees with fiberglass reinforced Pyrex-glass Tees enabling the system to withstand the increased operating pressure of R-124.

As shown in Figure 3.1, the present system contains the following components: (1) a reinforced Pyrex-glass Tee, used as the evaporator to boil the refrigerant; (2) a reinforced Pyrex-glass Tee, used as the condenser to condense the refrigerant vapor; (3) a liquid refrigerant storage reservoir; (4) an oil storage and mixing subsystem (not used); (5) a vacuum pump; (6) an ethylene-glycol/water mixture cooling subsystem; (7) a condenser pump; (8) aluminum framework with plexiglass siding which houses

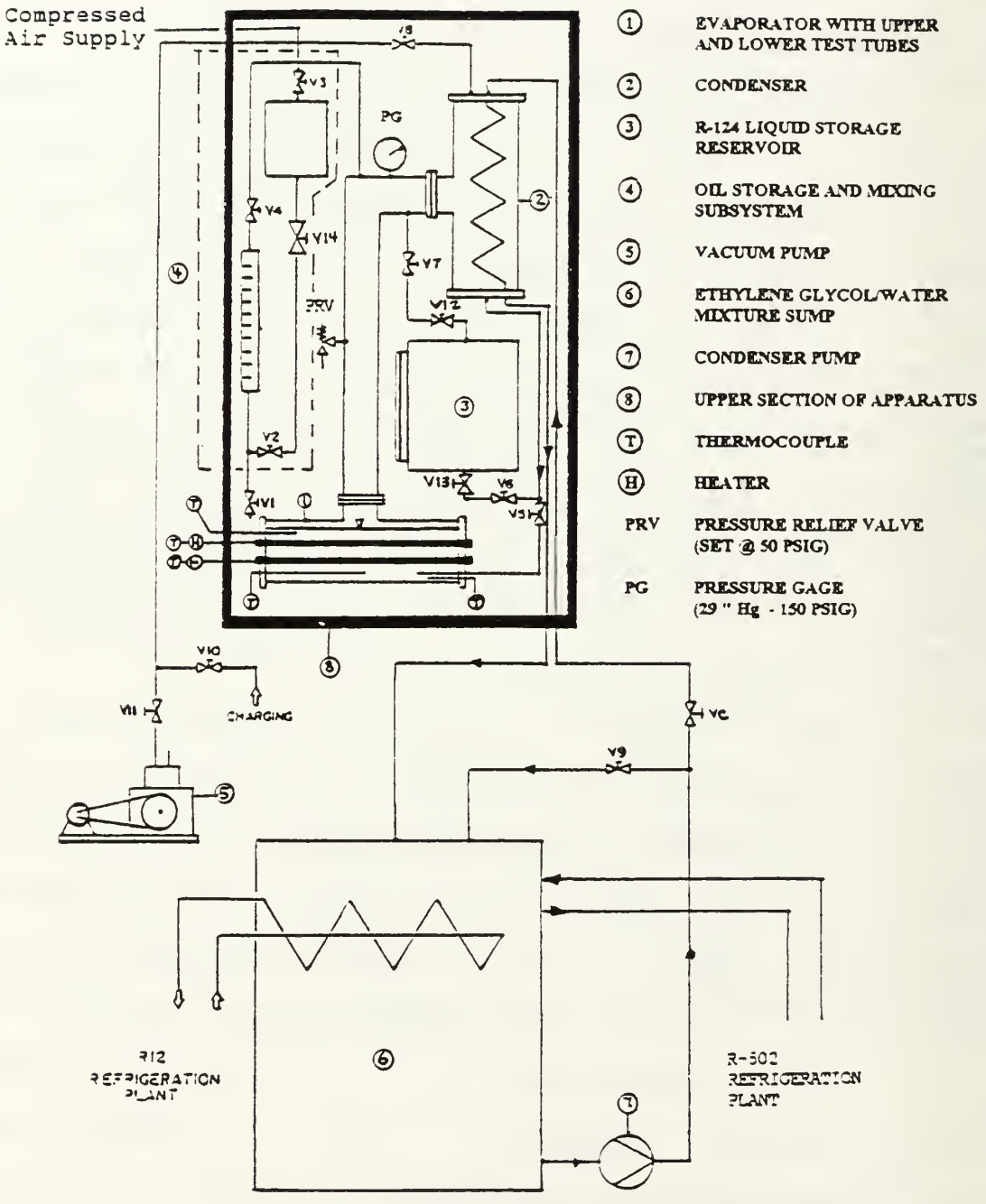


Figure 3.1 Schematic of Experimental Apparatus

components (1) through (4); and (9) a data acquisition and instrumentation system (not shown in Figure 3.1).

The system operates in a closed loop with vapor being generated by the heated tubes submerged in the R-124 liquid pool in the evaporator. The vapor travels to the condenser, via a two inch diameter aluminum L-shaped pipe, where it's condensed on a copper coil cooled by the chilled ethylene-glycol/water mixture. The condensed liquid refrigerant is gravity fed back to the evaporator via the return line.

## B. BOILING TEST SECTION

### 1. Evaporator

The evaporator is a Corning Pyrex-glass Tee section (three inch nominal inner diameter) coated with a continuous winding of fiberglass impregnated filaments bonded with a modified epoxy resin. It was installed horizontally with the side-arm of the Tee vertical and hydrostatically safety tested to 75 psig by Bertsch [Ref. 1]. Aluminum endplates, 210 mm diameter and 12.7 mm thick, house the thermocouple wells, an oil entry fitting (not used) and the Teflon inserts, which hold the test tubes in position. The endplates are mated to the evaporator using cast-iron flanges. At the very bottom of the evaporator sits the refrigerant liquid return line from the condenser. A copper deflector plate was installed just above the return line to prevent any vapor bubbles that might

rise off the return line from impinging on the test tubes. The liquid refrigerant level in the evaporator is approximately 10 mm below the top of the evaporator and approximately 10 mm above the top of the upper tube. Figure 3.2 is a sketch of the evaporator and a cast-iron flange.

**2. Evaporator Tubes**

Figure 3.3 is a schematic of a boiling tube. Two different tube types were used in this study: a smooth tube and a TURBO-B enhanced surface tube. Table 2 provides the dimensions of each tube type while Figure 3.4 shows an

**TABLE 2. DIMENSIONS OF TEST TUBES**

| Tube | D1 mm | D2 mm | Di mm | Do mm | L mm | Lu mm | kc W/m·K |
|---|---|---|---|---|---|---|---|
| smooth | 12.4 | 15.9 | 12.7 | 15.9 | 203.2 | 76.2 | 344 |
| TURBO-B | 11.6 | 13.8 | 11.8 | 15.9 | 203.2 | 76.2 | 398 |

expanded view of the enhanced surface of the TURBO-B tube. Each tube is heated by a 1 kW, 240 volt stainless-steel cartridge heater. The heater measures 6.35 mm outside diameter, 203.2 mm overall length with a heated length of 190 mm and is centered inside the test tube. The tubes are instrumented with eight thermocouples at various locations to

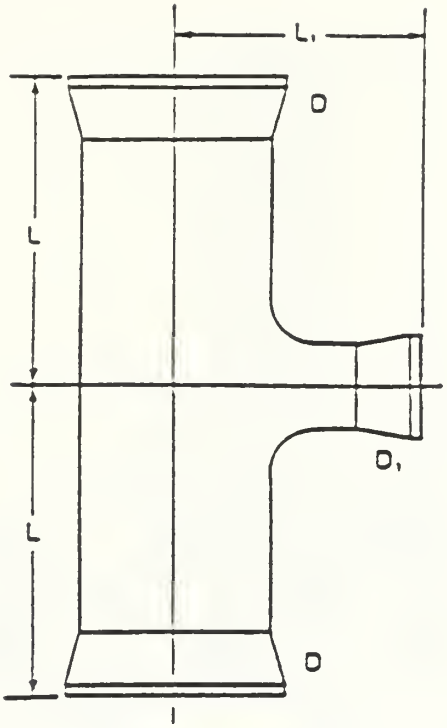


Corning Pyrex Glass Evaporator ($D \times D_1$ = 402x51 mm, $L$ = 178 mm, $L_1$ = 127 mm)

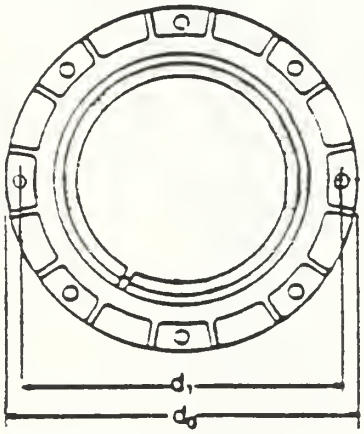


Cast Iron Flange ($d_i$ = 190 mm, $d_o$ = 210 mm)

Figure 3.2 Sketch of Pyrex Glass Evaporator and Cast-Iron Flange

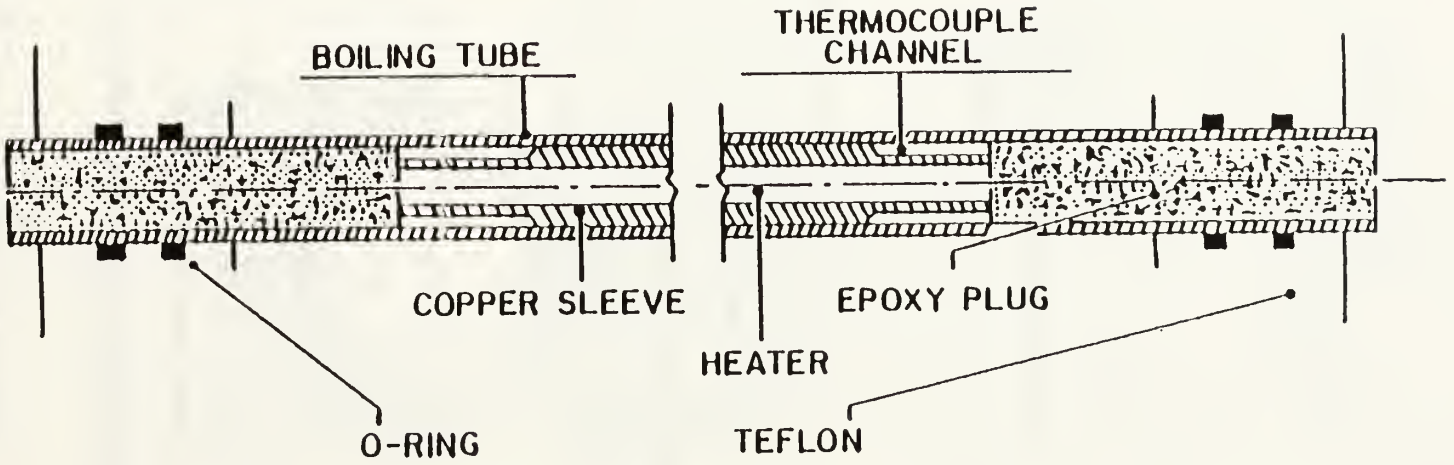


Figure 3.3 Schematic of a Test Tube

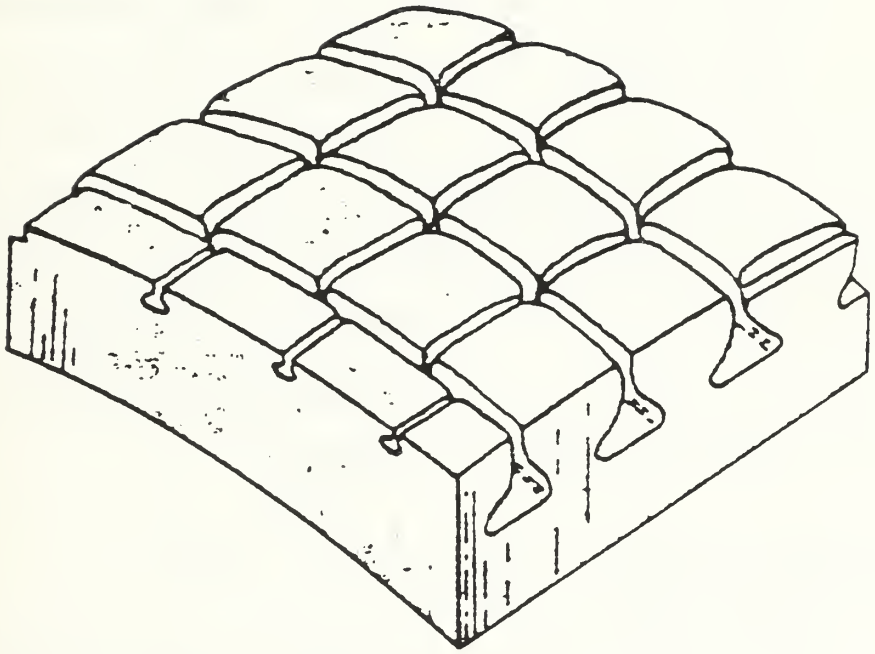

Figure 3.4 Surface Profile of Enhanced (TURBO-B) Tube

monitor the tube wall temperatures. Bertsch [Ref. 1] provides a detailed assembly procedure for the manufacturing and instrumentation of a test tube.

The test tubes are secured in the evaporator by Teflon inserts and sealed with o-rings (Figure 3.5). Strong-backs, shown in Figure 3.6, are used to anchor the Teflon inserts in the endplates.

### 3. Tube Configurations

Figure 3.7 shows the six tube configurations that were used. Configuration C0 is the single tube configuration used by Bertsch [Ref. 1] and Perry [Ref. 2]. In configurations C1 through C4, the top tube is fixed relative to the evaporator while the lower tube position is varied. Configuration C5 consists of rotating the Teflon insert used for C4 through an angle of 30°. Note that when rotation is completed, the upper tube position has moved off the evaporator centerline and the lower tube position remains unchanged.

## C. CONDENSER SECTION

The condenser is also a fiberglass-epoxy coated Corning Pyrex-glass Tee section identical in size, shape and substance to the evaporator shown in Figure 3.2. It is mounted vertically (see Figure 3.1) with aluminum endplates bolted to cast-iron flanges, similar to the evaporator arrangement. The

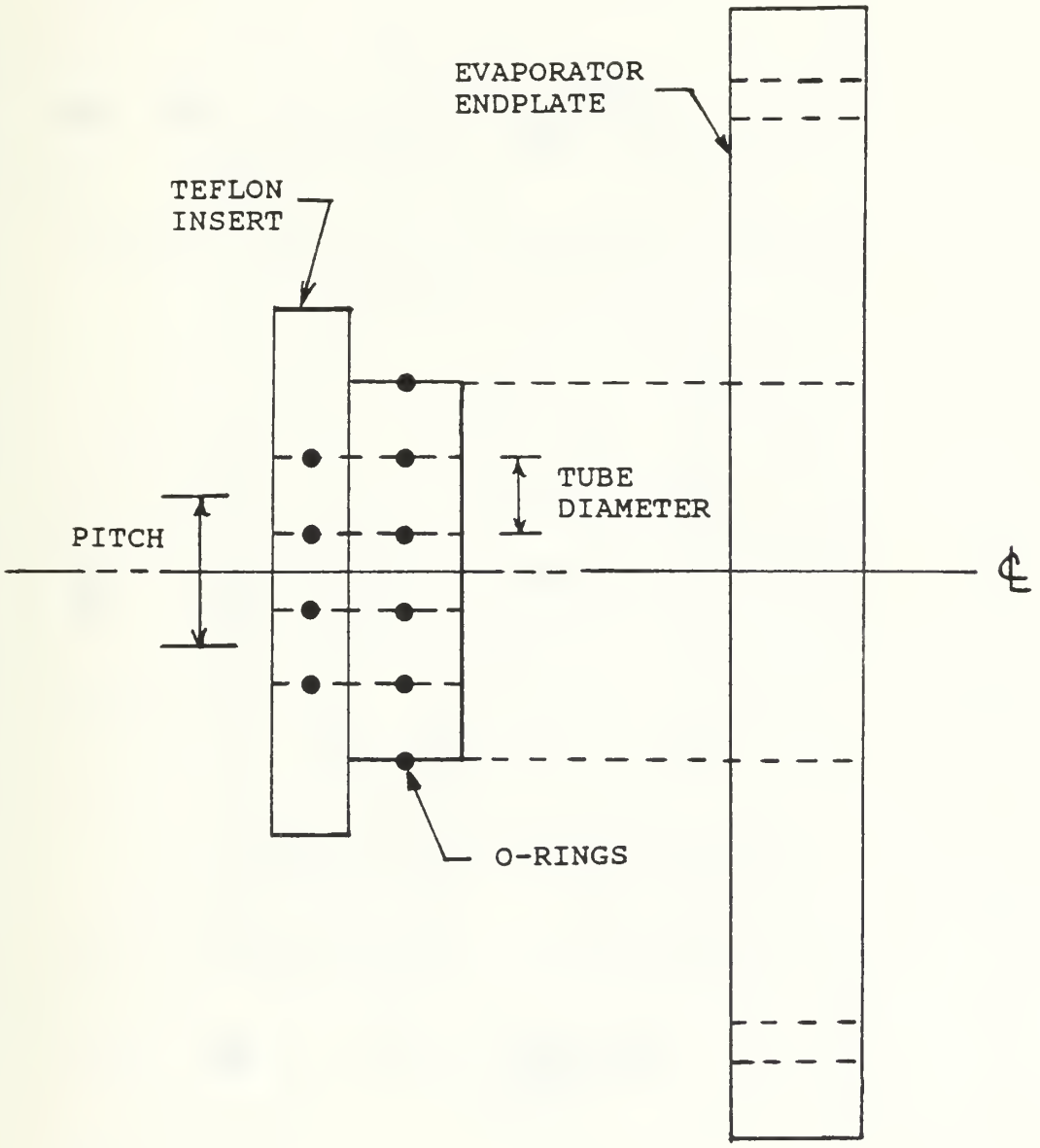


Figure 3.5 Sketch of an Endplate and Teflon Insert

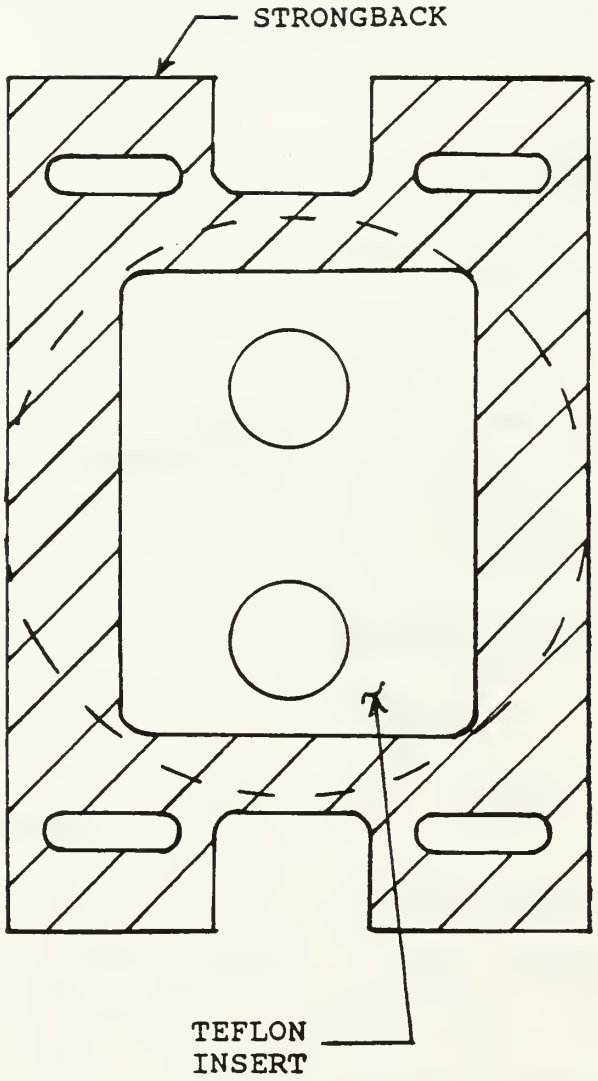


Figure 3.6 Sketch of a Strongback

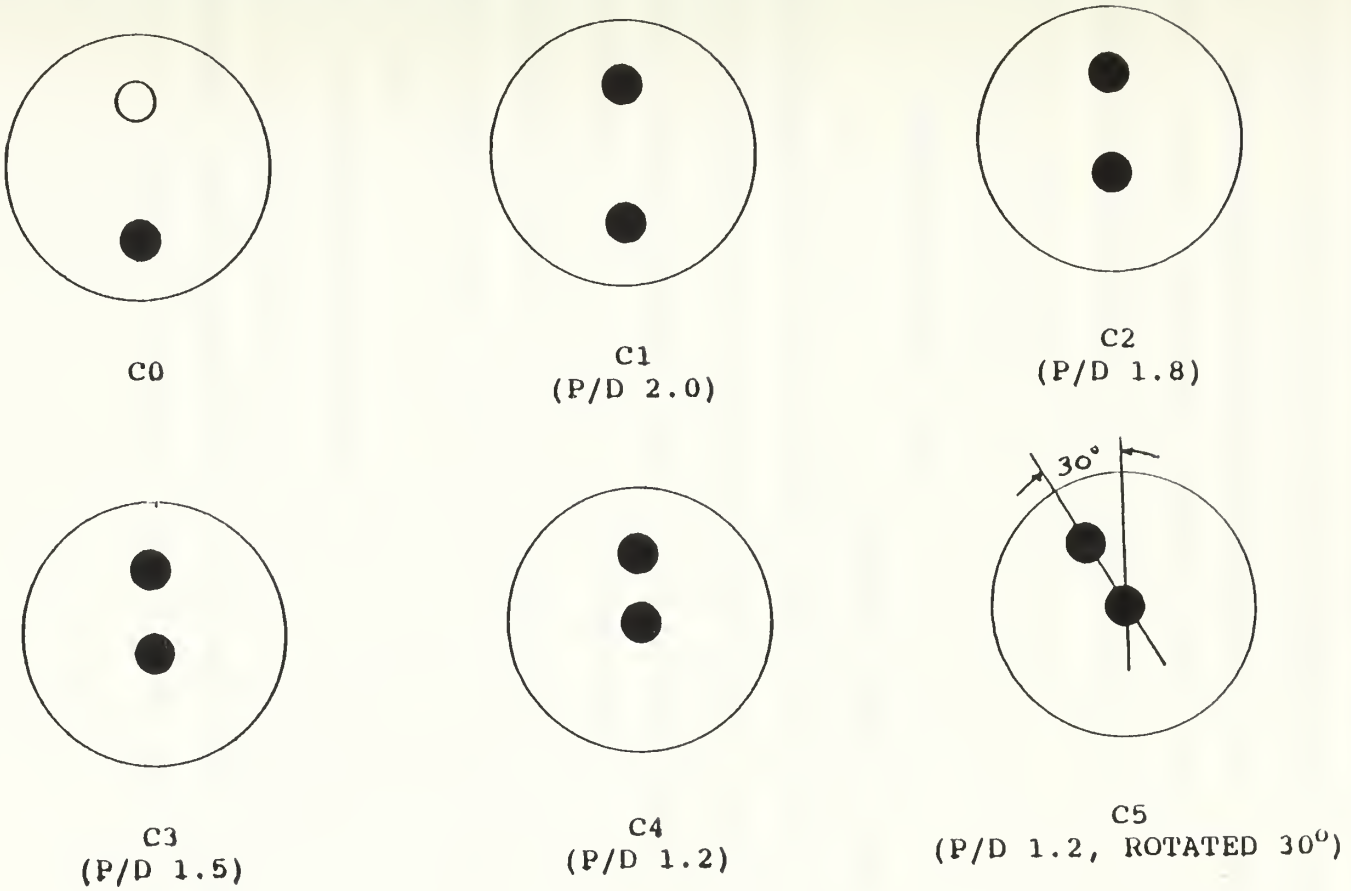


Figure 3.7 Tube Configurations

top endplate is fitted with connections for refrigerant charging/vacuum operations and the ethylene-glycol/water coolant inlet tube. The bottom endplate is fitted with connections for the gravity feed return line to the evaporator and the ethylene-glycol/water coolant outlet tube. The refrigerant vapor rises from the evaporator, passing through the L-shaped aluminum pipe and enters the condenser where it is condensed on a 3/8 inch outside diameter copper tube which is helically coiled inside the condenser.

## D. REFRIGERANT STORAGE RESERVOIR

The refrigerant storage reservoir is an aluminum cylinder, 230 mm in diameter and 254 mm in height. It is located within the apparatus enclosure above the evaporator and below the condenser (see Figure 3.1). The reservoir enables the operator to store the liquid R-124 instead of releasing it into the atmosphere, prior to changing out the test tubes. The installed sight glass allows monitoring of the liquid level during replenishing from an outside source (i.e., 145 lb. storage cylinder) or refilling the evaporator after a test tube changeout. The reservoir is isolated from or aligned to the system by means of valves V6, V7, V12 and V13.

## E. OIL SUBSECTION

This study was devoted to pure R-124. In order to ensure that no oil contaminated the system, the oil line from the oil cylinder to the evaporator was removed (see Figure 3.1) and the access on the evaporator endplate was capped. Perry [Ref. 2] describes the oil subsection components and the oil addition procedure for a refrigerant/oil mixture study.

## F. COOLING SUBSYSTEM

### 1. Ethylene-Glycol/Water Coolant Sump

At the base of the apparatus sits a 0.15 cubic meter plexiglass tank containing approximately 30 gallons of ethylene-glycol/water mixture producing a freezing point of -25 °C. The sump rests on a wood platform and is wrapped with 22 mm thick foam rubber sheet for insulation. Supply and discharge connections for the condenser and sump pump as well as a thermocouple to monitor the sump temperature are installed.

### 2. Refrigeration Plants

A 1/2 ton R-502 and 1/4 ton R-12 refrigeration plants are used simultaneously to maintain the ethylene-glycol/water coolant temperature at about -15° C. Both plants are located close to the sump and contain the following components: (1) hermetically sealed compressor assembly; (2) air-cooled condenser; (3) receiver; (4) filter-dryer; (5) pressure

regulator; (6) temperature control switch; and (7) thermostatic expansion valve. The R-502 plant (Figure 3.8) uses a counter flow heat exchanger as the system evaporator while the R-12 plant uses a 9.5 mm diameter coiled copper tubing submerged in the sump tank as the system evaporator (Figure 3.1).

**3. Pumps and Control Valve (VC)**

A positive displacement sump pump, rated at 8 gpm, is connected to the discharge connection of the coolant sump with a one inch diameter PVC pipe. It circulates coolant from the sump through the R-502 evaporator and back to the sump. A similar pump, called the condenser pump, circulates coolant from the sump to the condenser, via the control valve VC, and back to the sump (see Figure 3.1). Valve VC is used by the operator to control the refrigerant pool saturation temperature. A manually operated bypass valve (V9, Figure 3.1) is installed upstream of valve VC to prevent overloading the condenser pump when valve VC is closed.

## G. APPARATUS ENCLOSURE

A welded aluminum frame measuring 214 cm high, 61 cm wide and 51 cm deep is used to contain most of the system components. The upper half of the frame contains the evaporator, condenser, oil subsystem, and refrigerant storage reservoir (see Figure 3.1). The lower half of the frame

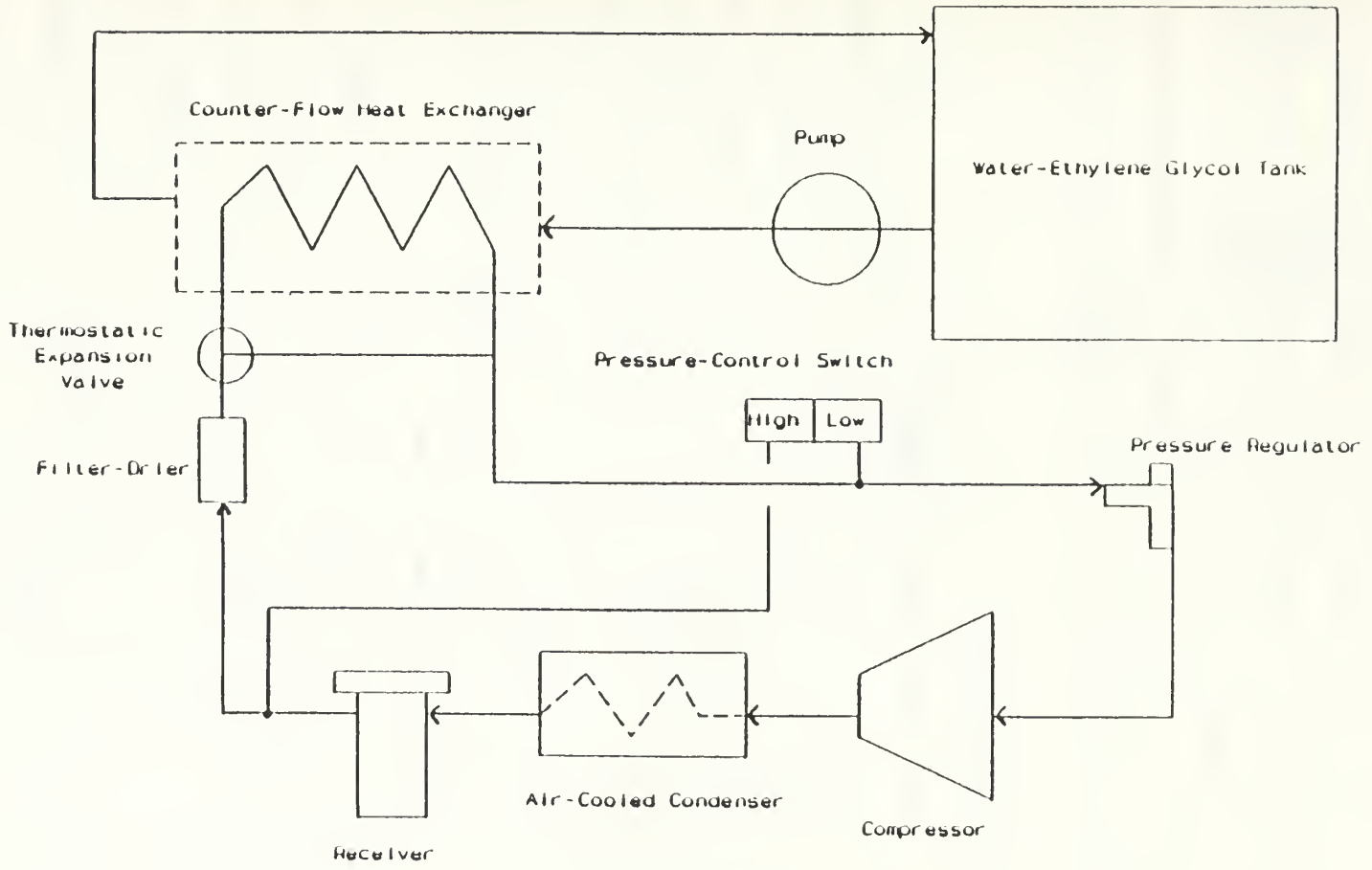


Figure 3.8 Schematic of R-502 Refrigeration System

contains the coolant sump tank. For operator safety and to reduce heat leakage into the evaporator and condenser, all sides of the upper half of the frame are covered with 13 mm thick plexiglass, hinged on both sides to allow access to the system components. Holes in the front plexiglass cover allow operation of valves V1 through V8 while maintaining the integrity of the enclosed upper frame.

## H. INSTRUMENTATION

### 1. Power Measurement System

Figure 3.9 is a schematic of the power measurement system. Each boiling tube heater is powered by a 240 volt AC source controlled by a variac. The variac output ranges from 0-220 volt and 0-5 amp, adjustable by the operator to obtain the desired heat flux at the tube surface. The current and voltage sensors convert the AC input signal into DC voltages which are used as input by the Data Acquisition Unit.

### 2. Temperature Measurement

Temperatures are measured using 30 gauge (0.25 mm diameter) copper-constantan (type T) thermocouples. For each test tube, eight thermocouples are spaced over the heater sleeve, as shown in Figure 3.10, to measure the wall temperatures. Three thermocouples are inserted into housings that penetrate the evaporator endplate and are submerged in

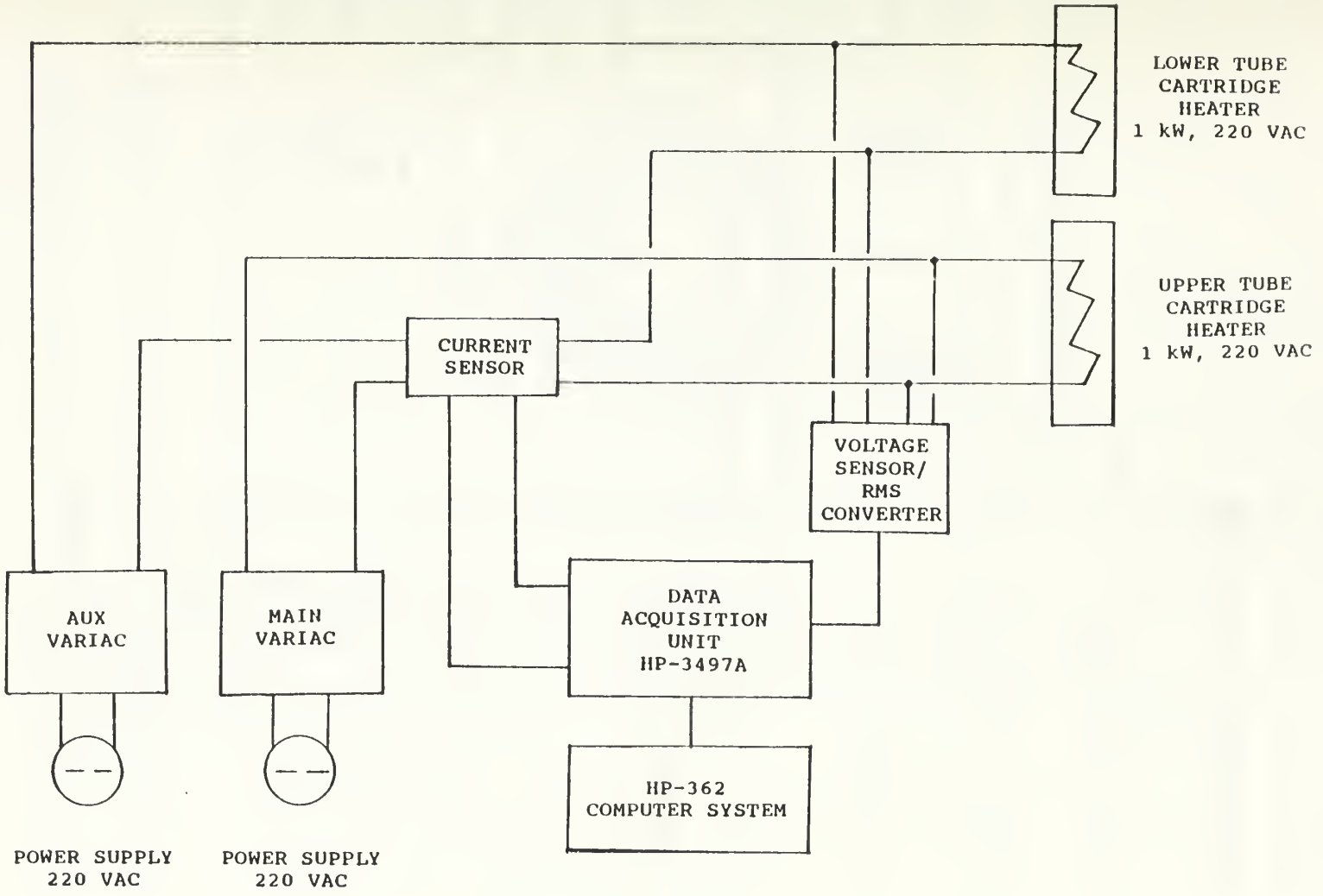


Figure 3.9 Schematic of the Power Measurement System

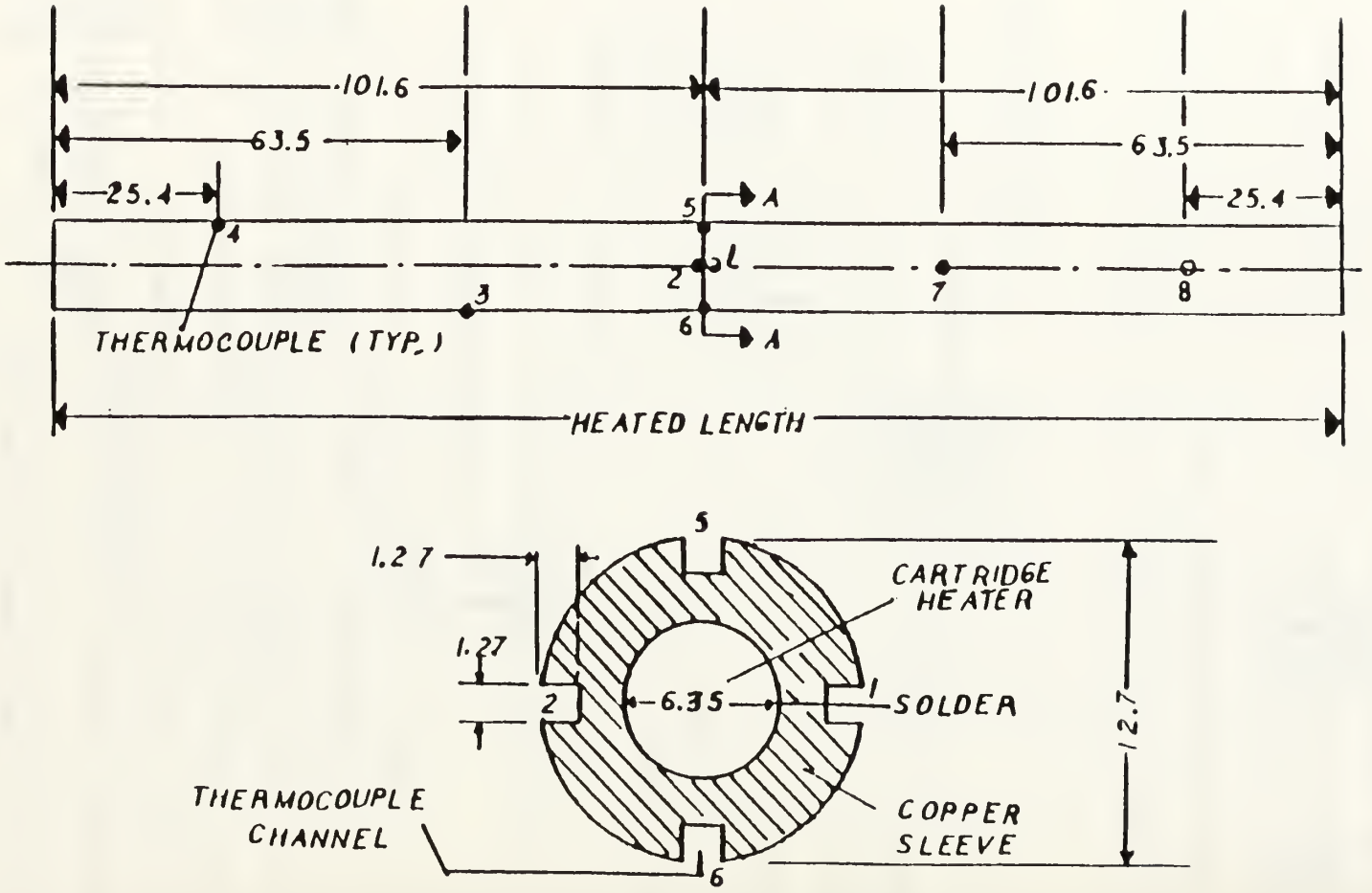


Figure 3.10 Thermocouple Positions

the refrigerant liquid pool at different locations (see Figure 3.1). Each housing is constructed of a low conductivity stainless steel body and a high conductivity copper tip (Figure 3.11). This minimizes the errors in pool temperature measurements caused by heat conduction through the housing. A single thermocouple is located in the coolant sump tank to measure the sump temperature.

Thermocouples were read by the a Hewlett-Packard (HP) 3497A Data Acquisition Unit which is controlled by an HP 326 Computer System.

## I. DATA ACQUISITION AND REDUCTION PROGRAM

Data acquisition and reduction program DRP72, used by Lake [Ref. 3], was modified to incorporate the thermophysical properties of saturated R-124. Bertsch [Ref. 1] discusses the generation of the equations used in the program calculations. The modified DRP72 program was renamed DRPJY. Appendix B contains the program DRPJY. The program DRPJY directs the HP 362 Computer System and the HP 3497A Data Acquisition Unit to read and process all thermocouple, current and R.M.S. voltage readings. Using this information, DRPJY performs the following calculations (from Bertsch [Ref. 1]):

1. Converts voltage readings into tube temperatures and power.
2. Computes heat transfer rate from cartridge heaters.

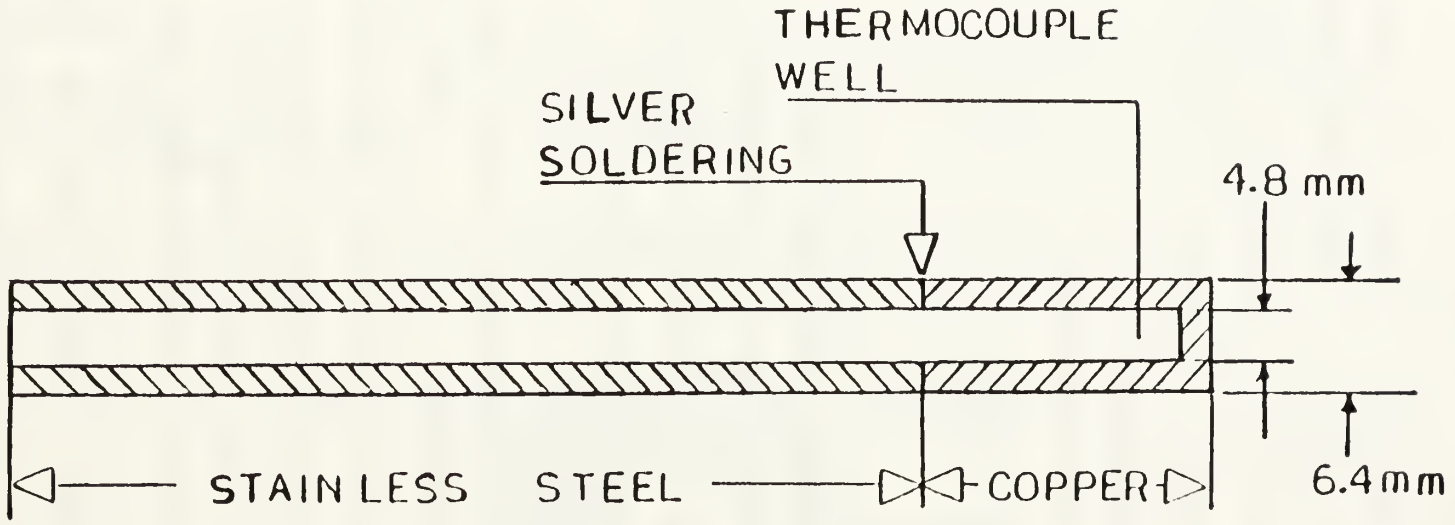


Figure 3.11 Sketch of Thermocouple Housing

3. Computes average test tube wall temperatures and wall superheat (Twall - Tsat).

4. Computes physical properties of R-124 using property correlations from RefProp [Ref. 28] at the film temperature (Twall + Tsat)/2.

5. Computes heat transfer coefficient of R-124 from the unheated ends and heated length of the test tubes.

6. Computes heat losses from the unheated ends of the test tubes.

7. Computes heat flux from heated length of test tubes.

The processed output data was printed by an HP Inkjet printer and stored on the computer hard drive. As a precaution, each output data file was copied to a 3.5 inch floppy disk in the event the computer hard drive becomes unreadable. Table 3 lists the channel assignments that are sensor inputs to the Data Acquisition Unit.

TABLE 3. HP-3497A CHANNEL ASSIGNMENTS

| Channel | Channel Assignments |
|---|---|
| 00-07 | Upper test tube wall temperature (T1-T8) |
| 08-15 | Lower test tube wall temperature (T9-T16) |
| 16 | Liquid pool thermocouple (Tld1) |
| 17 | Liquid pool thermocouple (Tld2) |
| 18 | Liquid pool thermocouple (Tv) |
| 19 | Sump coolant temperature |
| 20 | R.M.S. voltage of tube heaters |
| 21 | Upper tube current sensor |
| 22 | Lower tube current sensor |

# IV. EXPERIMENTAL PROCEDURE

## A. EVAPORATOR DISASSEMBLY PROCEDURE

The following procedure is used to transfer the liquid refrigerant from the evaporator to the reservoir to facilitate test tube changeouts:

1. Operate both R-502 and R-12 refrigeration systems to cool the sump tank temperature to approximately -15 °C.
2. Start the condenser pump and using control valve VC, adjust the coolant supply pressure to 1 psig.
3. Close valve V5 to isolate the evaporator from the condensing refrigerant vapor (see Figure 3.1).
4. Align the refrigerant storage reservoir to the system by opening valves V6, V7, V12 and V13.
5. Position and energize the high volume air dryer (set for high heat) so the heated air stream is blowing on the center of the evaporator. Adjust valve VC to ensure the refrigerant vapor is condensing.
6. After 1-2 hours, the evaporator should be dry with the liquid refrigerant in the reservoir and a small amount in the return line.
7. Close valves V6, V7, V12 and V13, isolating the reservoir from the system.
8. Secure and remove the air dryer.
9. Stop the condenser pump.
10. Open valves V8 and V10 to reduce to system pressure to atmospheric. Close valve V8 and V10 when the system pressure reads 0 psig on the system pressure gage.
11. Disconnect the test tube heater and thermocouple leads.

12. Remove strongbacks.

13. Remove Teflon inserts and test tubes.

## B. EVAPORATOR ASSEMBLY PROCEDURE

### 1. Evaporator Assembly

Before installing smooth test tubes, rinse with acetone then wipe clean with lint-free wipes or if installing TURBO-B test tubes, brush the enhanced surfaces with a soft bristle brush (i.e., toothbrush) using ethyl alcohol then repeat the brushing using acetone and let the tubes air dry. Check the Teflon insert o-rings for damage and replace as necessary. Before installing the test tubes, wipe the evaporator interior clean with lint-free wipes. Install the test tubes in the evaporator using the Teflon inserts to secure the tubes in place. Snug the strongbacks up to the Teflon inserts and connect the thermocouple leads. Prior to connecting the heater leads, check the resistance between the heater leads and the outer tube wall using a multimeter. One megohm resistance or greater is satisfactory.

### 2. Leak Test

After assembling the evaporator and before charging the system with refrigerant, perform a vacuum test to verify the integrity of the system. Evacuate the system by starting the vacuum pump and opening valves V11 and V8 (see Figure 3.1). After evacuating the system to approximately 29

in. Hg, close valves V11 and V8, then stop the vacuum pump. If no drop in vacuum is detected (i.e., no leak) within 30 minutes, charge the system with R-124.

If a leak is detected, open valves V8 and V11 and pressurize the system with air to 20 psig. Apply a soap/water solution to the system sealing surfaces to identify the leak location (bubbles will be seen from the leak source). After identifying and repairing the leak, retest the system for leaks.

**3. Charging System with Refrigerant**

Once the system integrity is assured, fill the evaporator with R-124, using one of the following procedures, to a level ***just below the top of the evaporator*** (NOTE: some refrigerant will be lost during the degas procedure, therefore, it is important to fill the evaporator above the level needed to conduct data runs):

***a. From Storage Reservoir***

Open valves V12 and V7 to equalize the pressure between the storage reservoir and the system. Open valves V13, V6 and V5 to gravity fill the evaporator with liquid refrigerant. When the evaporator is filled to the proper level, close valves V6, V13, V7 and V12 to isolate the storage reservoir from the system.

*b. From Refrigerant Cylinder*

Connect the cylinder to valve V10 using the charging hose (Figure 3.1). Open valves V5, V8 and V10 and then open the cylinder liquid valve to release the refrigerant from the cylinder into the system. Close valves V8, V10 and the cylinder liquid valve when the evaporator is filled to the proper level. Disconnect the charging hose from valve V10 and stow the cylinder.

**4. Degassing Procedure**

This degas procedure is similar to Perry's [Ref. 3] degassing procedure B. Degas the system by boiling the refrigerant, using a upper test tube heat flux of 85 $KW/m^2$ and a lower test tube heat flux of 20 $KW/m^2$, for 30 minutes. Ensure the condenser pump is running and control valve VC is open to prevent overpressurizing the system. During the boiling process, air and non-condensible gases rise in the system and collect in the condenser. After the 30 minute boiling time has elapsed, secure the heat flux to the test tubes and stop the condenser pump. Let the system set for 30 minutes allowing the condensed refrigerant to drain to the evaporator. After the 30 minute set time has elapsed, start the vacuum pump and open valve V11, then open valve V8 for 20 seconds to remove the accumulated air and non-condensible gases. After closing valve V8, stop the vacuum pump and close valve V11.

### 5. Data Acquisition Channel Check

After all evaporator thermocouples (test tubes and pool) are connected, load and run program SETUPJY to verify the output of each thermocouple is correct. Any output that is inconsistent or suspect is either fixed or noted and later excluded from the calculations in program DRPJY.

## C. STANDARD OPERATING PROCEDURE

The following procedure is used to conduct each data collection run:

1. Operate the R-502 and R-12 refrigeration systems to cool the sump to approximately -15 °C.
2. Energize the HP-362 Computer System, Data Acquisition Unit and the variac control panel.
3. Load and run program SETUPJY. Verify the thermocouple outputs are consistent.
4. Verify control valve VC is closed, then start the condenser pump.
5. Slowly open valve VC until the coolant pressure gage reads 1/8 psig. This pressure setting will ensure that the refrigerant pool will be slowly cooled.
6. Monitor the thermocouple outputs with SETUPJY until confident the thermocouples are operating properly. Note which thermocouples are inconsistent and must be excluded from program DRPJY.
7. When the refrigerant pool temperature is approaching 5 °C, load and run program DRPJY. Select 'TAKE DATA' option.
8. At the prompt, enter the filename that the data is to be stored under (page 38 explains the file naming scheme used).

9. At the prompt, enter the number of defective upper tube thermocouples that were identified by SETUPJY.

10. At the prompt, enter the defective upper tube thermocouple locations that were identified by SETUPJY.

11. At the prompt, enter the number of defective lower tube thermocouples that were identified by SETUPJY.

12. At the prompt, enter the defective lower tube thermocouple locations that were identified by SETUPJY.

13. Select the type of test tubes installed.

14. From the main menu, select 'SET Tsat'. Monitor the pool thermocouples and, if required, adjusted valve VC to maintain the desired pool saturation temperature of 2.22 ± 0.1 °C.

15. From the main menu, select 'SET UPPER TUBE HEAT FLUX', then adjust the main variac to the desired heat flux. Initial heat flux setting is 500-600 $KW/m^2$.

16. Press the keyboard button f1 to return to the main menu and select 'SET LOWER TUBE HEAT FLUX'. Adjust the aux variac to the desired heat flux.

17. From the main menu, select 'SET Tsat'. Adjust valve VC to maintain the desired pool saturation temperature while monitoring the pool thermocouples.

18. Once the pool saturation temperature is stable, return to the main menu and select 'TAKE DATA'.

19. For each heat flux setting steps 15-18 are repeated.

## D. DATA FILES

Data were filed using the following convention:

Example (D0904ASC1):

1. First letter D indicates the file is a data file.

2. The following four characters indicate the date; in this example September 04, 1993.

3. The next letter indicates the order in which the data run was completed on that day; no letter - 1st run, A - 2nd run, B - 3rd run, etc.

4. The next one or two letters indicate the tubes used; S - smooth, TB - TURBO-B.

5. The last letter and number combination represent the tube configuration used.

Table 4 is a summarized list of the data runs completed.

**TABLE 4. LIST OF DATA RUNS**

| Data File | Tube Type | Purpose |
|---|---|---|
| D0728ASC0 | Smooth | Repeatability; single tube |
| D0804ASC0 | Smooth | Repeatability; single tube |
| D0816SC0 | Smooth | Repeatability; single tube |
| D0520SC1 | Smooth | Repeatability; P/D = 2.0; no power on lower tube |
| D0714SC1 | Smooth | Repeatability; P/D = 2.0; no power on lower tube |
| D0831SC1 | Smooth | Data; repeatability; P/D = 2.0; no power on lower tube |
| D0901SC1 | Smooth | Data; P/D = 2.0; 1 $kW/m^2$ on lower tube |
| D0902SC1 | Smooth | Data; P/D = 2.0; 5 $kW/m^2$ on lower tube |
| D0902BSC1 | Smooth | Data; P/D = 2.0; 20 $kW/m^2$ on lower tube |
| D0903SC1 | Smooth | Data; P/D = 2.0; q" on both tubes inc/dec together |
| D0904SC1 | Smooth | Data; P/D = 2.0; 5 $kW/m^2$ on upper tube |
| D0904ASC1 | Smooth | Data; P/D = 2.0; 10 $kW/m^2$ on upper tube |
| D0905SC1 | Smooth | Data; P/D = 2.0; 20 $kW/m^2$ on upper tube |
| D0906SC2 | Smooth | Data; P/D = 1.8; no power on lower tube |
| D0906ASC2 | Smooth | Data; P/D = 1.8; 1 $kW/m^2$ on lower tube |
| D0907SC2 | Smooth | Data; P/D = 1.8; 5 $kW/m^2$ on lower tube |
| D0907ASC2 | Smooth | Data; P/D = 1.8; 10 $kW/m^2$ on lower tube |

TABLE 4. LIST OF DATA RUNS (continued)

| Data File | Tube Type | Purpose |
|---|---|---|
| D0908SC2 | Smooth | Data; P/D = 1.8; 20 kW/m$^2$ on lower tube |
| D0908ASC2 | Smooth | Data; P/D = 1.8; q" on both tubes inc/dec together |
| D0908ASC2 | Smooth | Data; P/D = 1.8; 5 kW/m$^2$ on upper tube |
| D0909SC2 | Smooth | Data; P/D = 1.8; 10 kW/m$^2$ on upper tube |
| D0909ASC2 | Smooth | Data; P/D = 1.8; 20 kW/m$^2$ on lower tube |
| D0910SC3 | Smooth | Data; P/D = 1.5; no power on lower tube |
| D0910ASC3 | Smooth | Data; P/D = 1.5; 1 kW/m$^2$ on lower tube |
| D0917SC3 | Smooth | Data; P/D = 1.5; 5 kW/m$^2$ on lower tube |
| D0919SC3 | Smooth | Data; P/D = 1.5; 10 kW/m$^2$ on lower tube |
| D0919ASC3 | Smooth | Data; P/D = 1.8; 20 kW/m$^2$ on lower tube |
| D0920SC3 | Smooth | Data; P/D = 1.8; q" on both tubes inc/dec together |
| D0920ASC3 | Smooth | Data; P/D = 1.5; 5 kW/m$^2$ on upper tube |
| D0920BSC3 | Smooth | Data; P/D = 1.5; 10 kW/m$^2$ on upper tube |
| D0920CSC3 | Smooth | Data; P/D = 1.5; 20 kW/m$^2$ on upper tube |
| D0921SC4 | Smooth | Data; P/D = 1.2; no power on lower tube |
| D0921ASC4 | Smooth | Data; P/D = 1.2; 1 kW/m$^2$ on lower tube |
| D0921BSC4 | Smooth | Data; P/D = 1.2; 5 kW/m$^2$ on lower tube |

**TABLE 4. LIST OF DATA RUNS (continued)**

| Data File | Tube Type | Purpose |
|---|---|---|
| D0921CSC4 | Smooth | Data; P/D = 1.2; 10 kW/m$^2$ on lower tube |
| D0922SC4 | Smooth | Data; P/D = 1.2; 20 kW/m$^2$ on lower tube |
| D0922ASC4 | Smooth | Data; P/D = 1.2; q" on both tubes inc/dec together |
| D0922BSC4 | Smooth | Data; P/D = 1.2; 5 kW/m$^2$ on upper tube |
| D0922CSC4 | Smooth | Data; P/D = 1.2; 10 kW/m$^2$ on upper tube |
| D0922DSC4 | Smooth | Data; P/D = 1.2; 20 kW/m$^2$ on upper tube |
| D0930SC5 | Smooth | Data; P/D = 1.2 rotated 30°; no power on lower tube |
| D0930ASC5 | Smooth | Data; P/D = 1.2 rotated 30°; 1 kW/m$^2$ on lower tube |
| D0930BSC5 | Smooth | Data; P/D = 1.2 rotated 30°; 5 kW/m$^2$ on lower tube |
| D0930CSC5 | Smooth | Data; P/D = 1.2 rotated 30°; 10 kW/m$^2$ on lower tube |
| D0929CSC5 | Smooth | Data; P/D = 1.2 rotated 30°; 20 kW/m$^2$ on lower tube |
| D0929DSC5 | Smooth | Data; P/D = 1.2 rotated 30°; q" on both tubes inc/dec together |
| D0929BSC5 | Smooth | Data; P/D = 1.2 rotated 30°; 5 kW/m$^2$ on upper tube |
| D0929ASC5 | Smooth | Data; P/D = 1.2 rotated 30°; 10 kW/m$^2$ on upper tube |
| D0929SC5 | Smooth | Data; P/D = 1.2 rotated 30°; 20 kW/m$^2$ on upper tube |
| D1012TBC0 | TURBO-B | Repeatability; single tube |
| D1012ATBC0 | TURBO-B | Repeatability; single tube |
| D1012BTBC0 | TURBO-B | Repeatability; single tube |

TABLE 4. LIST OF DATA RUNS (continued)

| Data File | Tube Type | Purpose |
|---|---|---|
| D1019TBC1 | TURBO-B | Repeatability; P/D = 2.0; no power on lower tube |
| D1018ATBC1 | TURBO-B | Repeatability; P/D = 2.0; no power on lower tube |
| D1018BTBC1 | TURBO-B | Data; repeatability; P/D = 2.0; no power on lower tube |
| D1018CTBC1 | TURBO-B | Data; P/D = 2.0; 1 $kW/m^2$ on lower tube |
| D1018DTBC1 | TURBO-B | Data; P/D = 2.0; 5 $kW/m^2$ on lower tube |
| D1019TBC1 | TURBO-B | Data; P/D = 2.0; 10 $kW/m^2$ on lower tube |
| D1019ATBC1 | TURBO-B | Data; P/D = 2.0; 20 $kW/m^2$ on lower tube |
| D1019ETBC1 | TURBO-B | Data; P/D = 2.0; q" on both tubes decreased together |
| D1019CTBC1 | TURBO-B | Data; P/D = 2.0; 5 $kW/m^2$ on upper tube |
| D1019DTBC1 | TURBO-B | Data; P/D = 2.0; 10 $kW/m^2$ on upper tube |
| D1019ETBC1 | TURBO-B | Data; P/D = 2.0; 20 $kW/m^2$ on upper tube |
| D1020TBC2 | TURBO-B | Data; P/D = 1.8; no power on lower tube |
| D1020ATBC2 | TURBO-B | Data; P/D = 1.8; 1 $kW/m^2$ on lower tube |
| D1020BTBC2 | TURBO-B | Data; P/D = 1.8; 5 $kW/m^2$ on lower tube |
| D1020CTBC2 | TURBO-B | Data; P/D = 1.8; 10 $kW/m^2$ on lower tube |
| D1020DTBC2 | TURBO-B | Data; P/D = 1.8; 20 $kW/m^2$ on lower tube |

**TABLE 4. LIST OF DATA RUNS (continued)**

| Data File | Tube Type | Purpose |
|---|---|---|
| D1020ETBC2 | TURBO-B | Data; P/D = 1.8; q" on both tubes decreased together |
| D1021TBC2 | TURBO-B | Data; P/D = 1.8; 5 kW/m$^2$ on upper tube |
| D1021ATBC2 | TURBO-B | Data; P/D = 1.8; 10 kW/m$^2$ on upper tube |
| D1021ATBC2 | TURBO-B | Data; P/D = 1.8; 20 kW/m$^2$ on upper tube |
| D1021CTBC3 | TURBO-B | Data; P/D = 1.5; no power on lower tube |
| D1021BTBC3 | TURBO-B | Data; P/D = 1.5; 1 kW/m$^2$ on lower tube |
| D1021ETBC3 | TURBO-B | Data; P/D = 1.5; 5 kW/m$^2$ on lower tube |
| D1021FTBC3 | TURBO-B | Data; P/D = 1.5; 10 kW/m$^2$ on lower tube |
| D1022TBC3 | TURBO-B | Data; P/D = 1.5; 20 kW/m$^2$ on lower tube |
| D1022ATBC3 | TURBO-B | Data; P/D = 1.5; q" on both tubes decreased together |
| D1022BTBC3 | TURBO-B | Data; P/D = 1.5; 5 kW/m$^2$ on upper tube |
| D1022CTBC3 | TURBO-B | Data; P/D = 1.5; 10 kW/m$^2$ on upper tube |
| D1022DTBC3 | TURBO-B | Data; P/D = 1.5; 20 kW/m$^2$ on upper tube |
| D1022ETBC4 | TURBO-B | Data; P/D = 1.2; no power on lower tube |
| D1022FTBC4 | TURBO-B | Data; P/D = 1.2; 1 kW/m$^2$ on lower tube |
| D1025TBC4 | TURBO-B | Data; P/D = 1.2; 5 kW/m$^2$ on lower tube |
| D1025ATBC4 | TURBO-B | Data; P/D = 1.2; 10 kW/m$^2$ on lower tube |

TABLE 4. LIST OF DATA RUNS (continued)

| Data File | Tube Type | Purpose |
|---|---|---|
| D1025BTBC4 | TURBO-B | Data; P/D = 1.2; 20 kW/m$^2$ on lower tube |
| D1025CTBC4 | TURBO-B | Data; P/D = 1.2; q" on both tubes decreased together |
| D1025DTBC4 | TURBO-B | Data; P/D = 1.2; 5 kW/m$^2$ on upper tube |
| D1025ETBC4 | TURBO-B | Data; P/D = 1.2; 10 kW/m$^2$ on upper tube |
| D1025FTBC4 | TURBO-B | Data; P/D = 1.2; 20 kW/m$^2$ on upper tube |
| D1026TBC5 | TURBO-B | Data; P/D = 1.2 rotated 30°; no power on lower tube |
| D1026ATBC5 | TURBO-B | Data; P/D = 1.2 rotated 30°; 1 kW/m$^2$ on lower tube |
| D1026BTBC5 | TURBO-B | Data; P/D = 1.2 rotated 30°; 5 kW/m$^2$ on lower tube |
| D1026CTBC5 | TURBO-B | Data; P/D = 1.2 rotated 30°; 10 kW/m$^2$ on lower tube |
| D1026DTBC5 | TURBO-B | Data; P/D = 1.2 rotated 30°; 20 kW/m$^2$ on lower tube |
| D1026ETBC5 | TURBO-B | Data; P/D = 1.2 rotated 30°; q" on both tubes decreased together |
| D1027TBC5 | TURBO-B | Data; P/D = 1.2 rotated 30°; 5 kW/m$^2$ on upper tube |
| D1027ATBC5 | TURBO-B | Data; P/D = 1.2 rotated 30°; 10 kW/m$^2$ on upper tube |
| D1027BTBC5 | TURBO-B | Data; P/D = 1.2 rotated 30°; 20 kW/m$^2$ on upper tube |

# V. DISCUSSION OF RESULTS

## A. REPRODUCIBILITY/REPEATABILITY

To verify that the equipment and operating procedure being used were consistent with those used by Bertsch [Ref. 1] and Perry [Ref. 2], six reproducibility/repeatability runs were performed. Program DRPGP (from Perry's single tube work [Ref. 2]) was used for the runs conducted with a single test tube and DRPJY was used for all runs conducted with two test tubes. Figures 5.1 and 5.2 are plots of increasing and decreasing heat flux using a smooth tube in configuration C0 (which is identical to the configuration used by Perry [Ref. 2]). In Figure 5.1, the three runs completed are in very good agreement with each other. At lower heat fluxes ( $< 4$ kW/m$^2$) some scatter is present which disappears at mid-range heat fluxes (4-8 kW/m$^2$). Perry [Ref. 2] found the same phenomenon and attributed the scatter to convection regime thermal gradients where mixing is inefficient within the liquid pool, after discovering large local variations in the tube wall and pool thermocouples of up to 5%. In this study, local variations in the tube wall and pool thermocouples were found to be up to 7% at lower heat fluxes and decreasing as heat flux increased, which supports Perry's theory. In

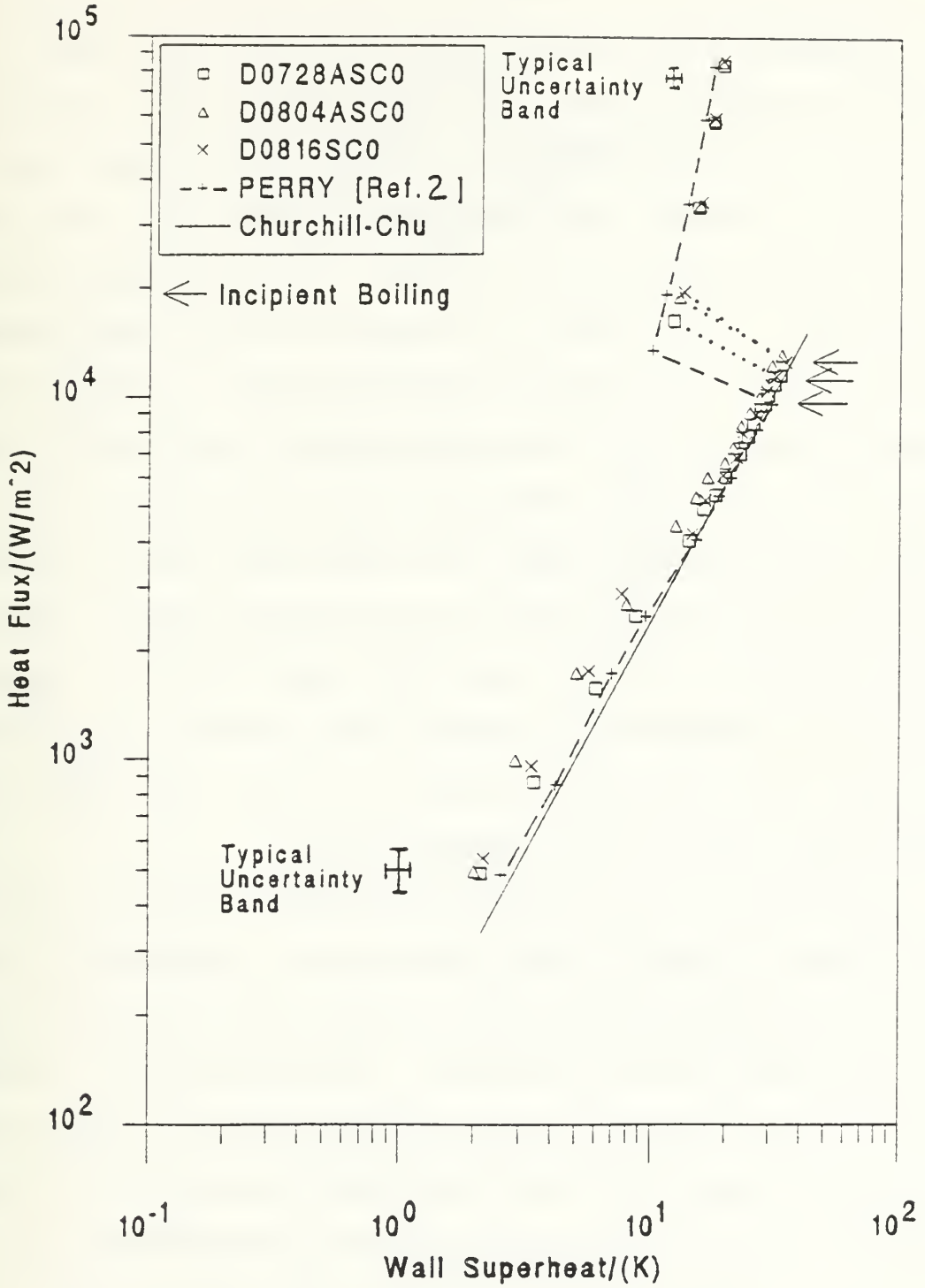


Figure 5.1 Increasing Heat Flux Repeatability Runs using Smooth Tube Configuration C0

natural convection, the three data runs started to the left of the Churchill and Chu correlation [Ref. 9] (shown as a solid line) at low heat fluxes and converged toward the Churchill-Chu line as the heat flux was increased. This slight shift to the left, although consistent during the three runs, was within the uncertainty in the region. Good repeatability was also found at the onset of nucleate boiling (indicated by arrows) and in the nucleate boiling region. Comparing the repeatability runs to the representative data set of Perry [Ref. 2], at low heat fluxes the data vary slightly but are within the uncertainty band. The data merge up to the point of incipience, but why Perry's run nucleated earlier than the present data is unclear since the runs were, in essence, identical. In the boiling region, Perry's data is slightly to the left of the present data but again lie within the uncertainty band for that region.

In Figure 5.2, good repeatability is again shown for all heat fluxes. Comparing the three present repeatability runs to the representative data set of Perry [Ref. 2], again shows good reproducibility throughout. For heat fluxes $< 1$ kW/m$^2$, the slopes of the data curves change, which indicates the transition from nucleate boiling back to natural convection. Based on Figures 5.1 and 5.2, data reproducibility is considered satisfactory with the single smooth tube work carried out by Perry [Ref. 2] on the same apparatus.

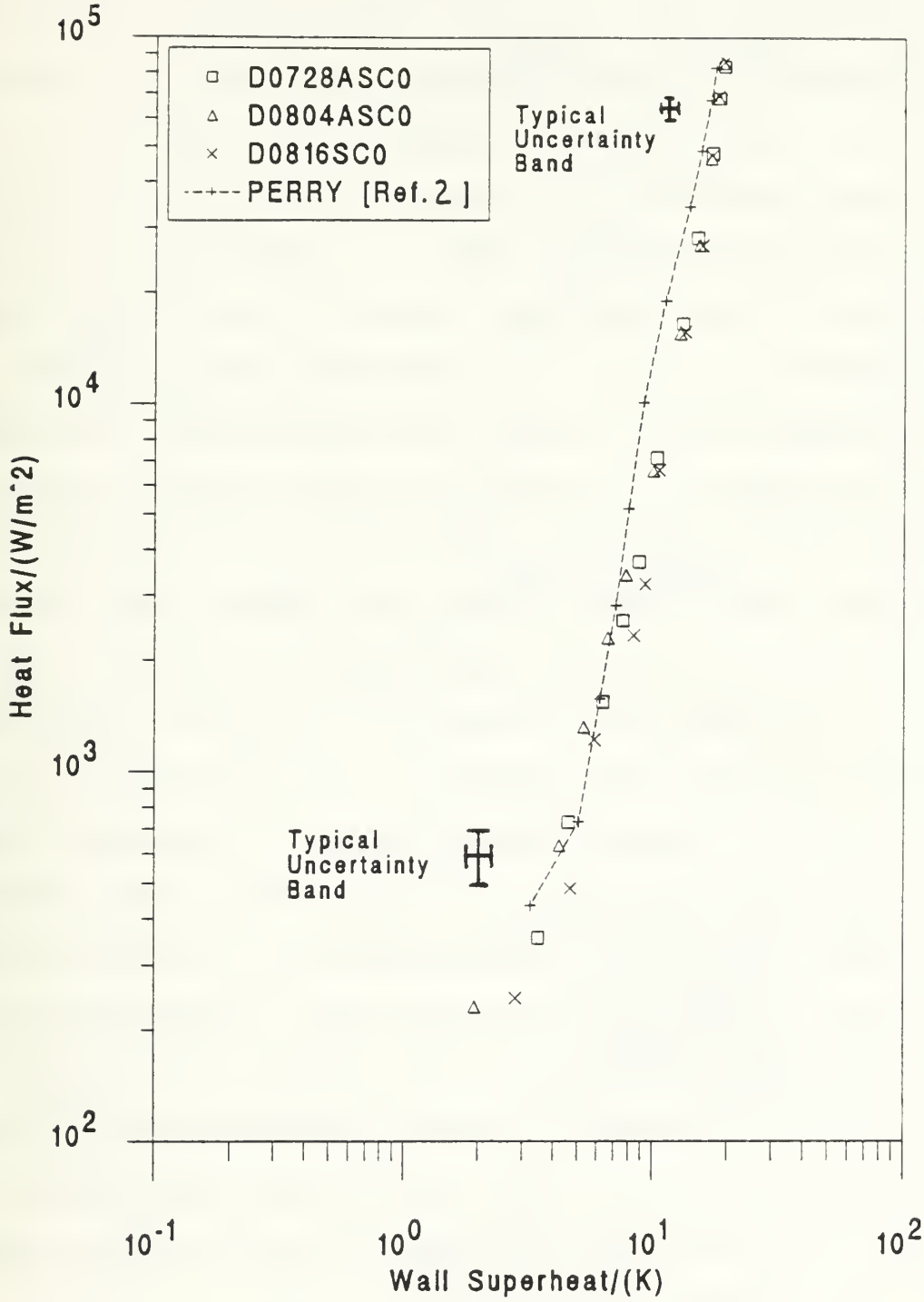


Figure 5.2 Decreasing Heat Flux Repeatability Runs using Smooth Tube Configuration C0

Figure 5.3 is a comparison of decreasing heat flux repeatability runs using an enhanced tube (TURBO-B) in configuration C0 with the single tube data of Bertsch [Ref. 1]. For the present data, good repeatability is again obtained throughout. In comparing the current data with the data collected by Bertsch [Ref. 1], different boiling curves are easily seen. This was a result of two different TURBO-B test tubes being used. After examining both test tubes under a microscope (using 50x and 100x magnification), the TURBO-B test tube used in this study had wider notches between the 'mushroom-like pedestals' (see Figure 3.4), indicating that a different fabrication process was used to make the tube. Above 20 $kW/m^2$ on the plot, the current data curves are to the left of Bertsch's data (about 2 °C less wall superheat), indicating better heat transfer. It is believed this is due to the wider notches in the tube surface allowing more bubbles to depart the tube surface at higher heat fluxes, removing more heat than the tube used by Bertsch. At about 10 $kW/m^2$, the trend is reversed, the current data crosses and continues to fall below Bertsch's data (about 0.3 °C more wall superheat). At low heat fluxes, the wider notches allow the refrigerant to flood back into the boiling channels (see Figure 3.4) and reduce the number of active sites, reducing the heat transfer from the tube.

Figure 5.4 is a comparison of increasing heat flux repeatability runs using smooth tube configuration C1 with the

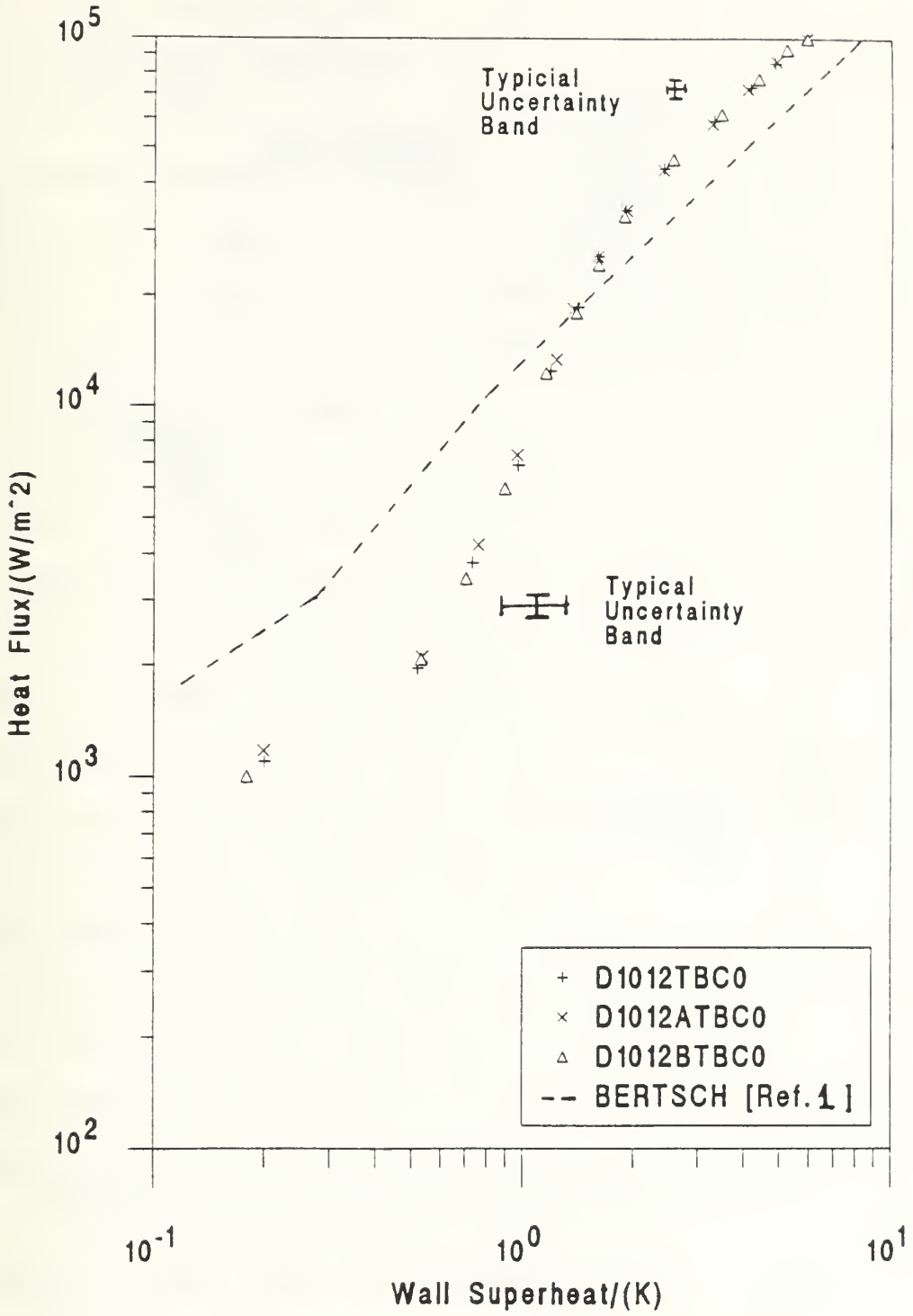


Figure 5.3 Decreasing Heat Flux Repeatability Runs using TURBO-B Tube Configuration C0

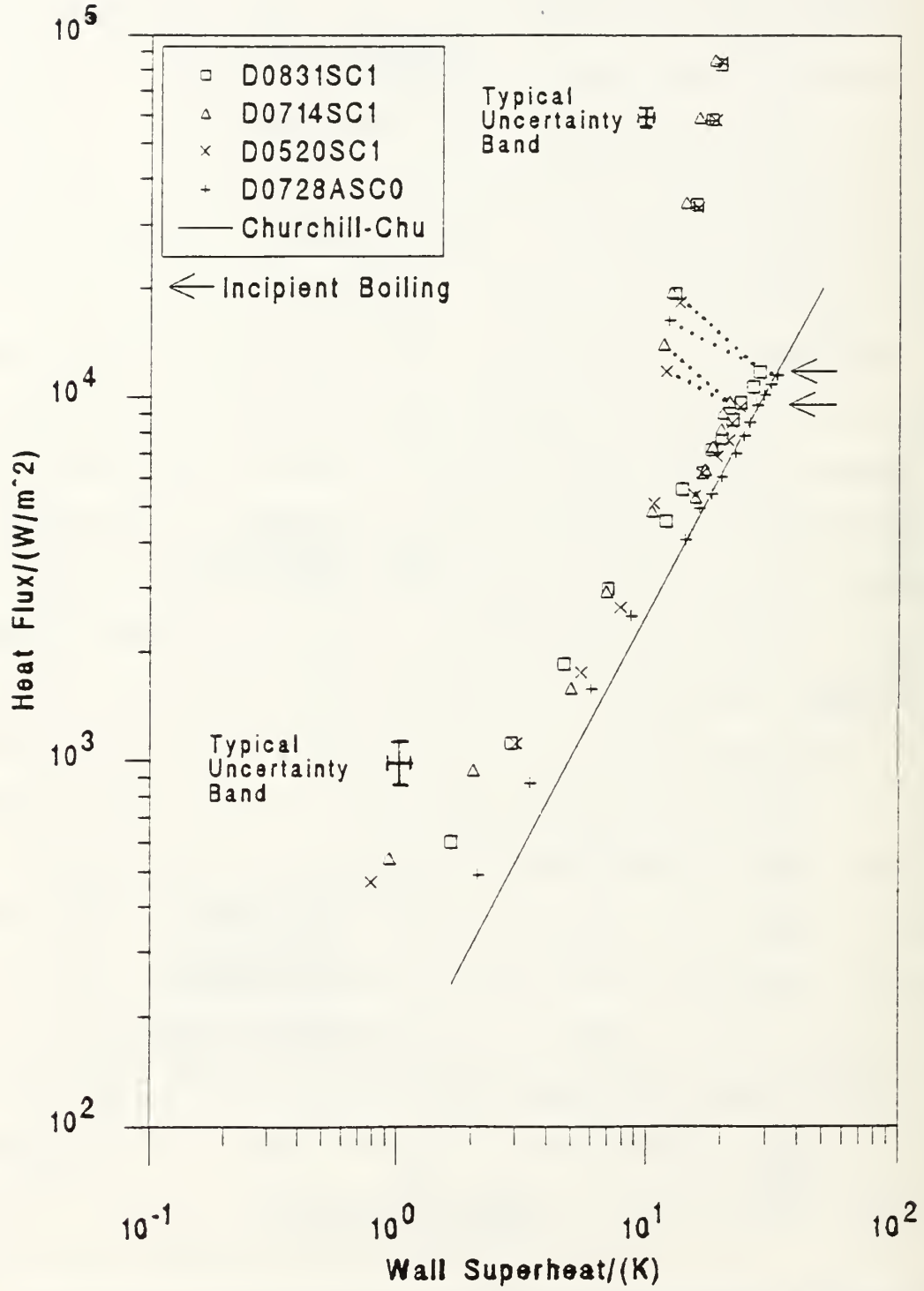


Figure 5.4 Increasing Heat Flux Repeatability Runs using Smooth Tube Configuration C1 with the Lower Tube Unheated

lower tube unheated and a single smooth tube data set (D0728ASC0) from Figure 5.1. The plot shows some scatter of data at low heat fluxes that is attributed to the liquid pool temperature gradients, as discussed previously. Again, good repeatability is found in the mid-range heat flux and boiling regions. In comparison to the single tube data (configuration C0) and the Churchill and Chu correlation [Ref. 9], the upper tube heat transfer performance of the C1 configuration is clearly enhanced in natural convection. This enhancement is probably due to the liquid pool surface being much closer to the upper test tube (approximately 10 mm) when it is position C1, increasing the circulation (i.e., local fluid velocity) around the upper tube and ultimately increasing heat transfer performance of the tube. Lake [Ref. 3], in his comparison of single tube R-114 data to his C1 configuration data, found the same enhancement. He concluded that the lower tube must be modifying the flow over the upper tube. In actuality, it is probably a combination of both the decreased distance to the pool surface and the lower tube modifying the flow over the upper tube that causes the enhancement. From this plot, it was concluded that the program DRPJY was performing properly.

Figure 5.5 is the corresponding decreasing heat flux data runs for Figure 5.4. Good repeatability is again found for the C1 configuration runs. Comparing the single tube data (D0728ASC0 from Figure 5.2) to the C1 configuration data,

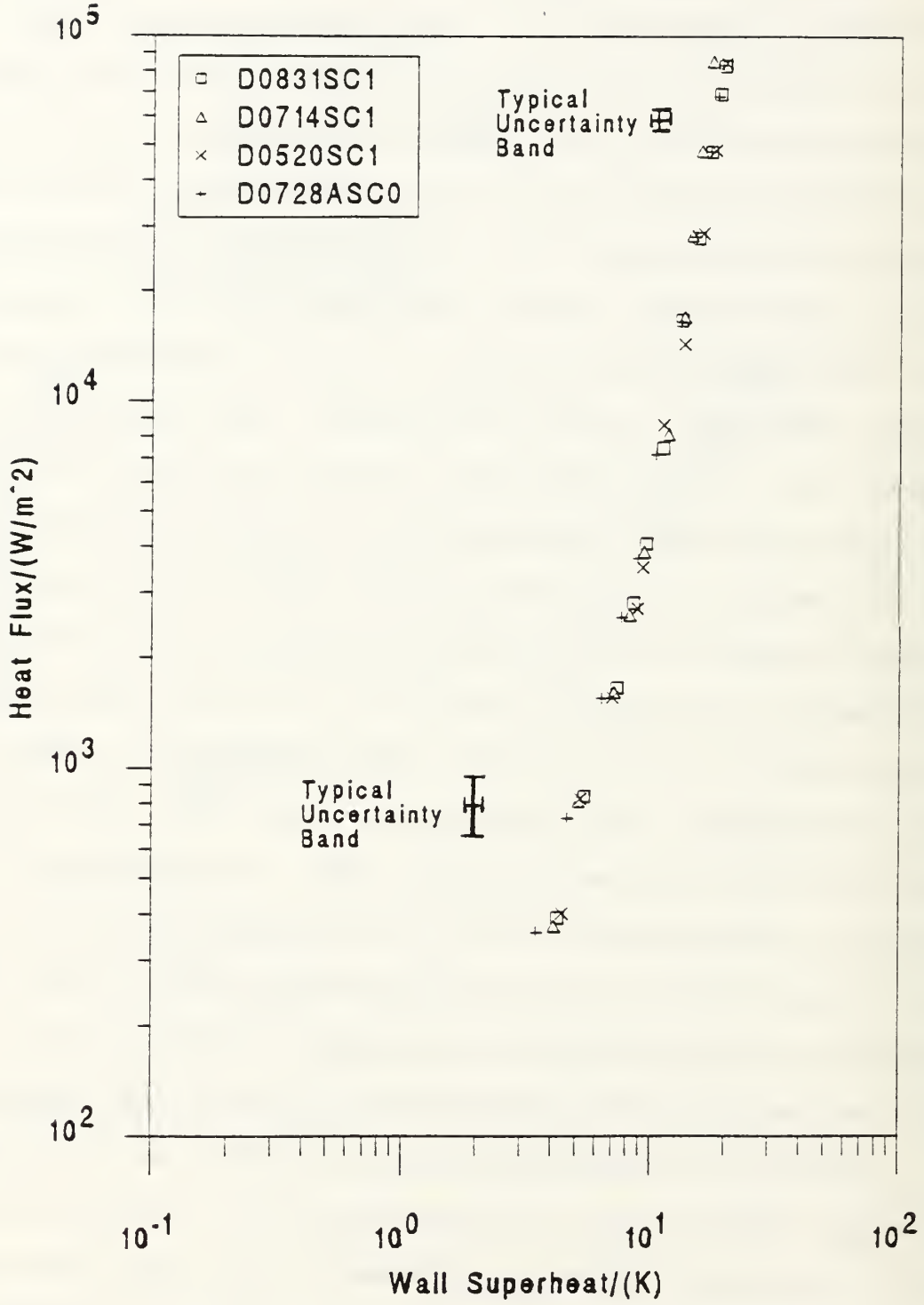


Figure 5.5 Decreasing Heat Flux Repeatability Runs using Smooth Tube Configuration C1 with the Lower Tube Unheated

indicates that in nucleate boiling with decreasing heat fluxes, both tube configurations perform equally well.

Figure 5.6 is the decreasing heat flux repeatability runs using TURBO-B tubes in configuration C1 with the lower tube unheated. Good repeatability is evident. Comparing the single TURBO-B data set (D1012TBC0) from Figure 5.3 to the C1 data, at high heat fluxes both tube configurations perform equally well, as was for the smooth tube case (Figure 5.5). At low heat fluxes (< 8 $kW/m^2$), the C1 configuration data is to the left of the C0 configuration data, indicating an enhancement due to the addition of the lower tube and moving the test tube closer to the surface of the liquid pool; this was not seen for the smooth tube case (Figure 5.5). As will be discussed later, the addition of a lower tube heat flux, shifts the C1 data curve even more towards the left.

Based on Figures 5.1 through 5.6, the repeatability of the current data and reproducibility of previous single tube work performed by Perry [Ref. 2], is considered satisfactory.

## B. INFLUENCE OF THE LOWER TUBE

To investigate the effects of a lower heated tube on an upper tube, five different tube configurations and fixed lower tube heat flux settings were used. The five tube configurations selected were P/D ratios of 2.0, 1.8, 1.5, 1.2

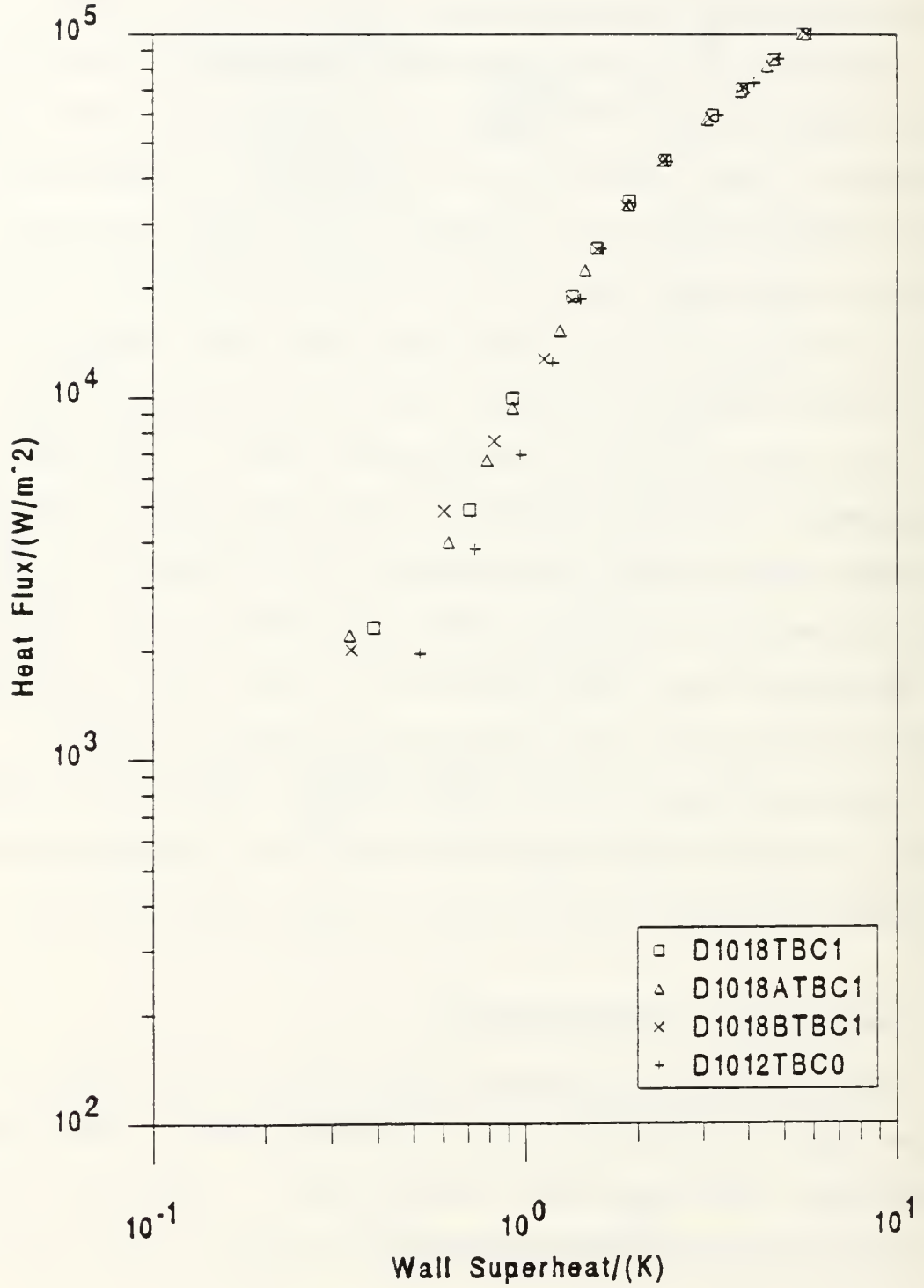


Figure 5.6 Decreasing Heat Flux Repeatability Runs using TURBO-B Tube Configuration C1 with the Lower Tube Unheated

and 1.2 (rotated 30°). P/D of 2.0 was selected because it matches not only the vertical pitch used in naval shipboard flooded evaporators, but also the pitch used in the flooded evaporator bundle apparatus at the Naval Postgraduate School Heat Transfer Laboratory. The fixed lower tube heat flux settings (LTHFS) used were 0, 1, 5, 10 and 20 $kW/m^2$. In addition to these runs, data runs for each tube configuration were also done using a lower tube heat flux setting that was equal to the upper tube heat flux setting (UTHFS). Finally, at a fixed UTHFS of 5, 10 and 20 $kW/m^2$, the LTHFS was varied to investigate the influence of the strength of the convection effects from below. For each data run, the same tube surface was used for the upper and lower tube; mixing of the tube types was not allowed. For the smooth tube runs, the upper tube was started in the natural convection region at low heat fluxes, was run up and down through various heat flux settings, and was returned to the natural convection region. For the TURBO-B tubes, only decreasing upper tube heat flux runs were recorded to prevent overlapping/repeating data (the TURBO-B tubes did not enter the natural convection region at low heat fluxes).

To evaluate the effect of a lower heated tube on an upper tube, the data is presented by the effect of changing the P/D ratio for a common LTHFS, the effect of varying the LTHFS for a common P/D ratio and the effect of varying the lower tube heat flux for a fixed upper tube heat flux setting.

### 1. The Effect of Tube Spacing

#### *a. Smooth Tubes with Lower Tube Unheated*

Figure 5.7 shows the increasing heat flux data taken for the five tube configurations (C1-C5) with the lower tube unheated and the corresponding Churchill and Chu correlation [Ref. 9]. As seen in the repeatability runs, at low heat fluxes the data is shifted to the left of the Churchill-Chu line and as the heat flux is increased, the data tends to approach the Churchill-Chu line up to the incipient boiling point (indicated by arrows). This implies that the circulation occurring within the evaporator enhances the natural convection that occurs from a single tube immersed in an *infinite* expanse of fluid. Following nucleation of the upper tube, the boiling curve for P/D of 1.8 is to the left of the others and appears to be yielding the best heat transfer performance. It is unclear why this is so, because it is so repeatable and the same smooth test tubes were used. Lake [Ref. 3] also found that P/D of 1.8 gave the best heat transfer performance.

Figure 5.8 shows the corresponding decreasing heat flux data for Figure 5.7. With decreasing heat flux, a P/D of 1.8 again provides the best heat transfer performance until the lowest heat flux region, as did Lake's data [Ref. 3].

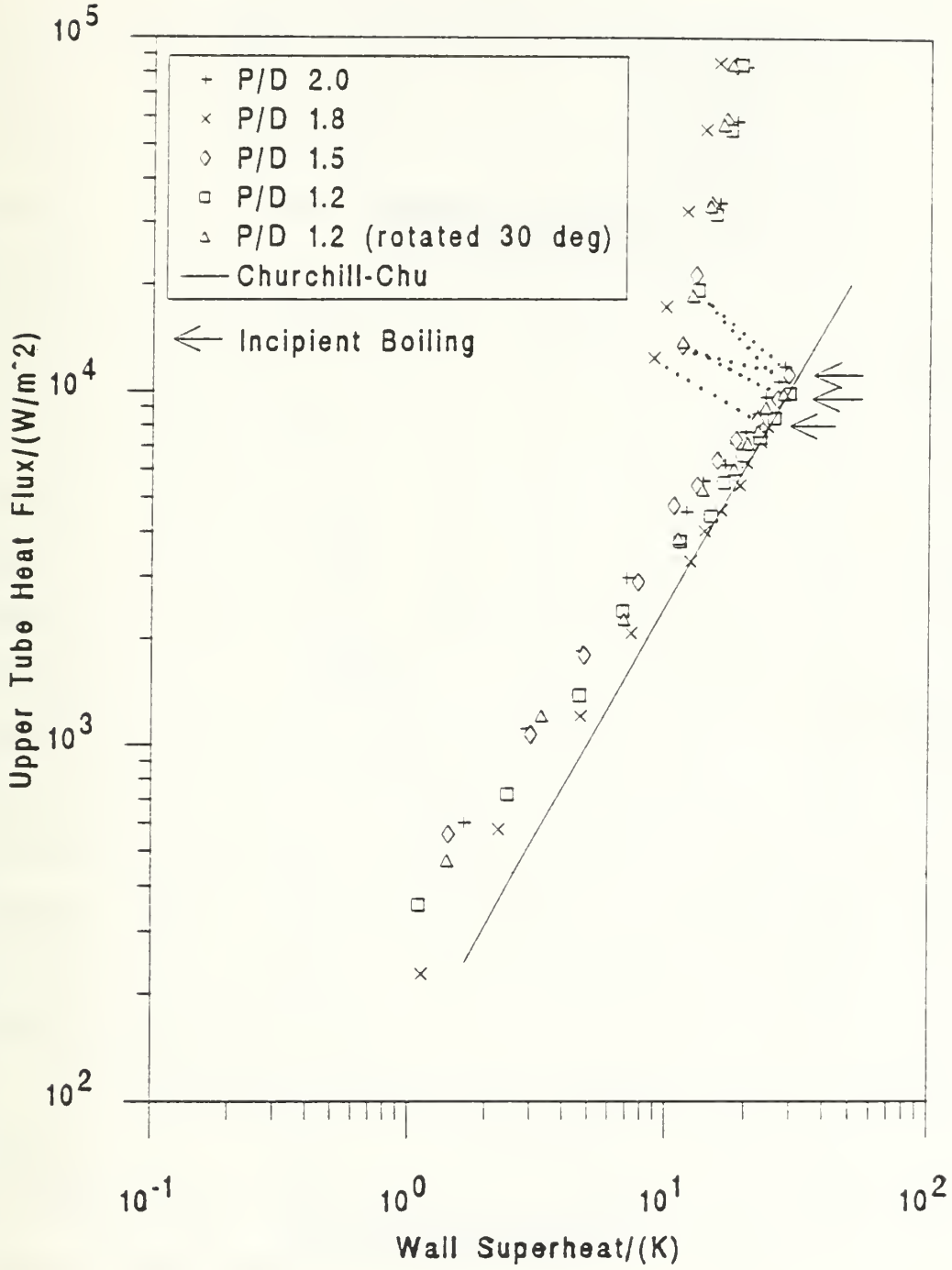


Figure 5.7 Comparison of Smooth Tube P/D Ratios for Increasing Heat Flux with the Lower Tube Unheated

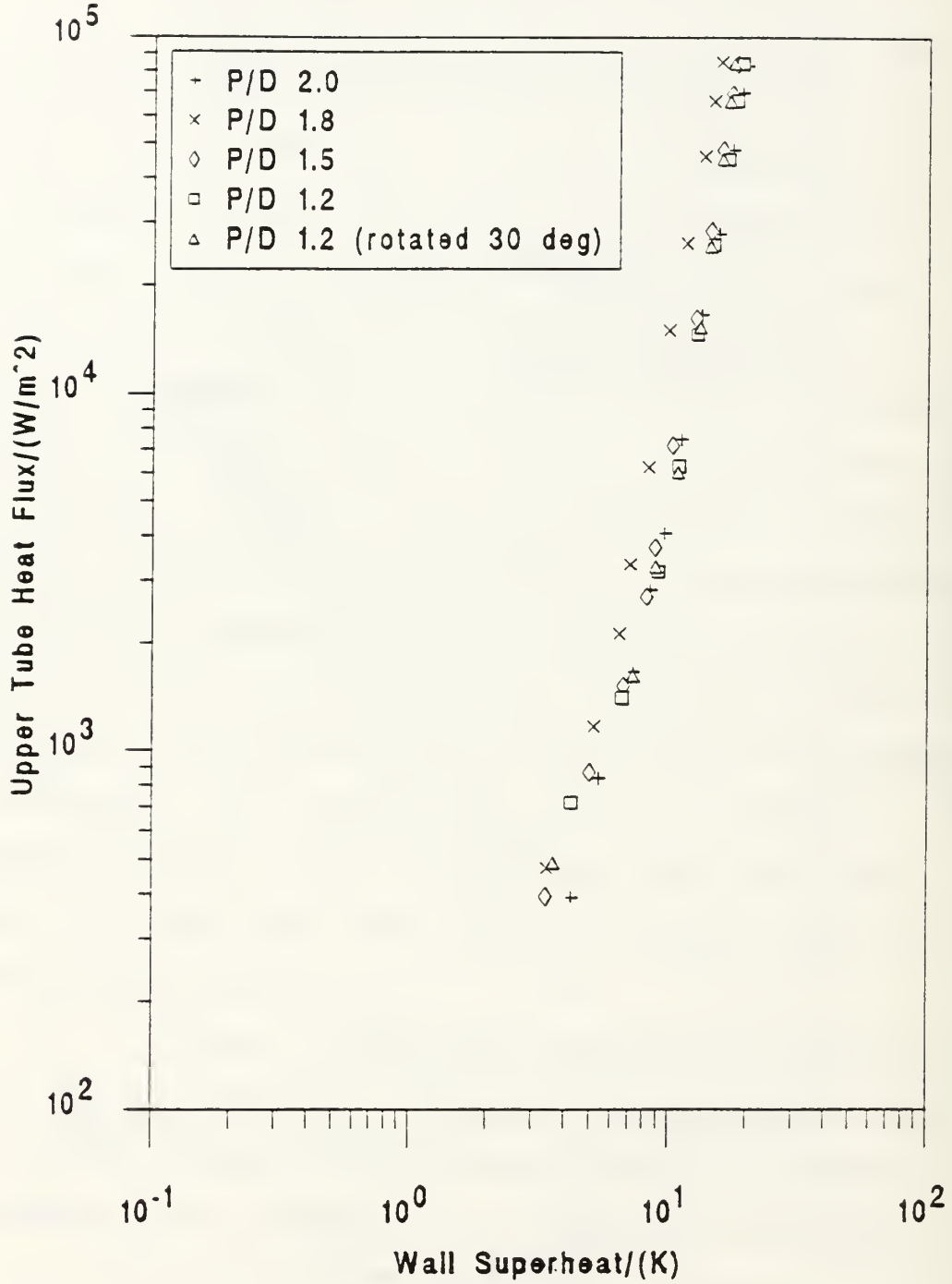


Figure 5.8 Comparison of Smooth Tube P/D Ratios for Decreasing Heat Flux with the Lower Tube Unheated

*b. Smooth Tubes with LTHFS of 1 kW/m²*

Figure 5.9 shows the increasing heat flux data taken for the five tube configurations (C1-C5) with a heat flux of 1 kW/m² on the lower tube. Both the upper and lower tubes for all configurations started in the natural convection region. At low heat fluxes, some scatter is present which becomes smaller as the data approaches the incipient boiling points and tends towards the Churchill and Chu correlation [Ref. 9], as seen previously. Note that the data for a P/D of 1.2 crosses the Churchill-Chu line and appears to nucleate earlier than the others. For this small spacing, the heated plume from the lower tube can actually reduce natural convection from the top tube since the local ambient pool temperature is increased. This creates a larger wall temperature and a larger wall superheat (Twall - Tsat). After nucleation, a P/D of 1.8 again provides better heat transfer in the boiling region than the other P/D ratios. This trend suggests that in the boiling region the enhancement provided by a P/D of 1.8 is due to the tube spacing itself and not from heating the lower tube.

Figure 5.10 is the decreasing heat flux data for to Figure 5.9. A P/D of 1.8 provides the best heat transfer performance until approximately 4 kW/m², which is where the boiling curves seem to merge. With a LTHFS of 1 kW/m², it appears to force the decreasing boiling curves to merge at a

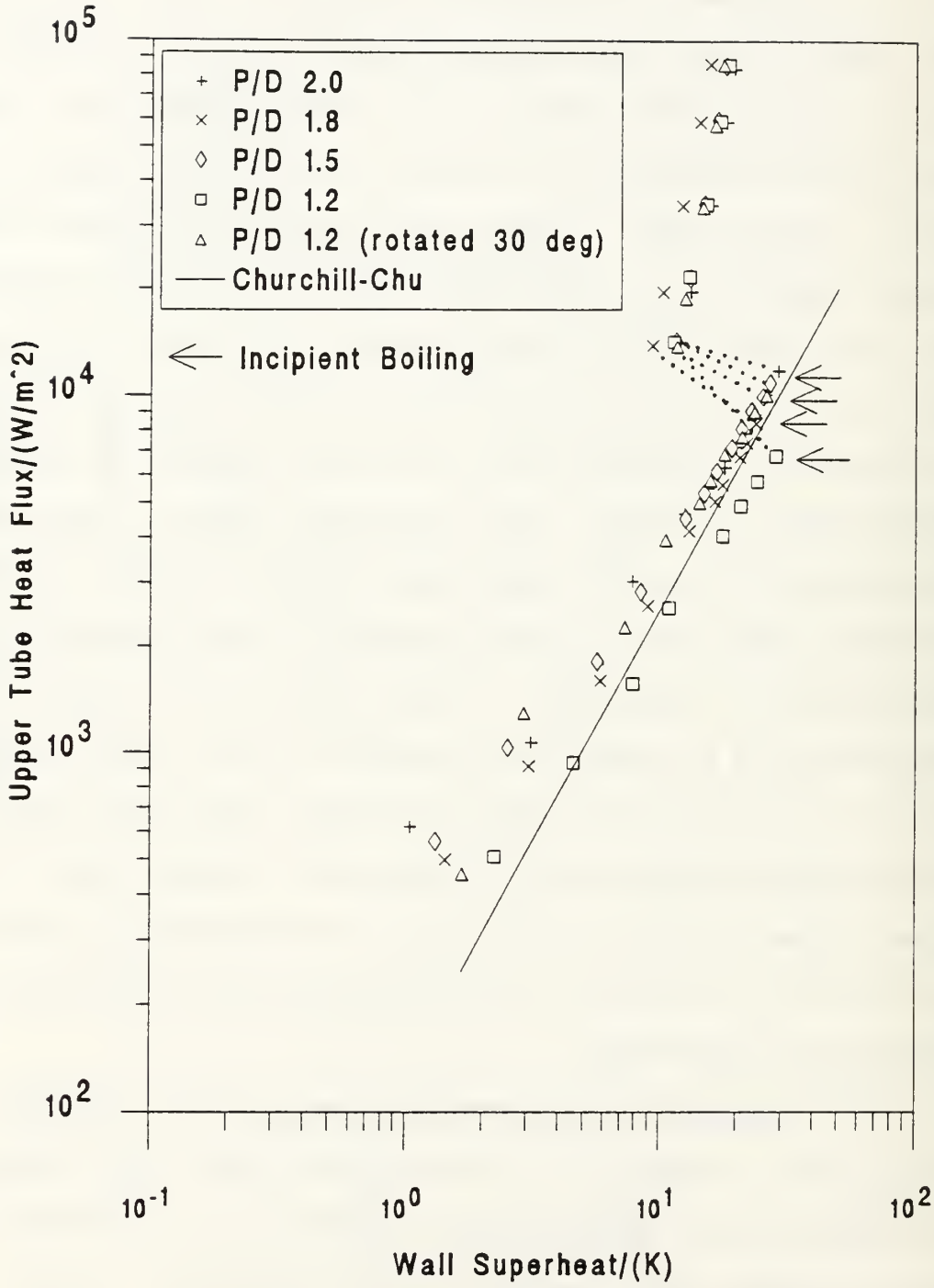


Figure 5.9 Comparison of Smooth Tube P/D Ratios for Increasing Heat Flux with 1 kW/m$^2$ on the Lower Tube

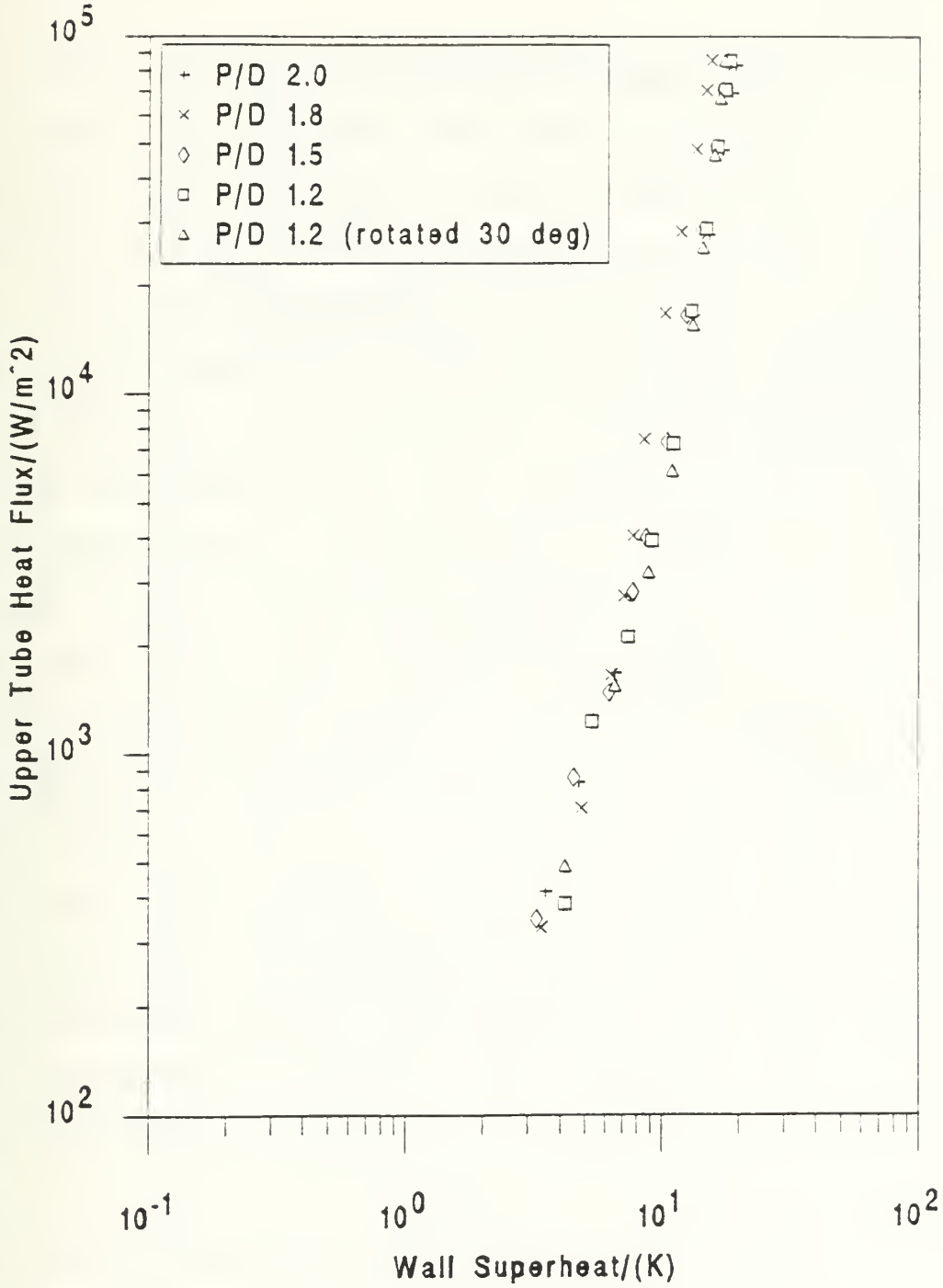


Figure 5.10 Comparison of Smooth Tube P/D Ratios for Decreasing Heat Flux with 1 $kW/m^2$ on the Lower Tube

higher heat flux (4 $kW/m^2$) than with the lower tube unheated (< 1 $kW/m^2$).

### *c. Smooth Tubes with LTHFS of 5 $kW/m^2$*

Figure 5.11 shows the increasing heat flux data taken for the five tube configurations (C1-C5) with 5 $kW/m^2$ on the lower tube. Both upper and lower tubes for all the configurations started in the natural convection region. At low heat fluxes, the data is to the left of the Churchill and Chu correlation [Ref. 9], as seen in Figures 5.7 and 5.9. As the heat flux is increased, some interesting things happen. The data for a P/D of 1.2 (rotated 30°) quickly crosses the Churchill-Chu line and begins to parallel it, then nucleates at a low heat flux of about 3 $kW/m^2$. This is believed to be an anomaly and not an effect. Of the remaining P/D ratios, 1.8 is the only one to tend toward the Churchill-Chu line with increasing heat flux. The P/D ratios of 2.0, 1.5 and 1.2 seem to parallel the Churchill-Chu line, probably due to the LTHFS intensifying the forced convection around the upper tube. In all cases, the lower tube remained in natural convection until the upper tube nucleated. Once the upper tube nucleated, the lower tube also nucleated. In the boiling region, a P/D of 1.8 again gave the best enhancement.

Figure 5.12 is the decreasing heat flux data for Figure 5.11. Above 10 $kW/m^2$, P/D of 1.8 is clearly providing

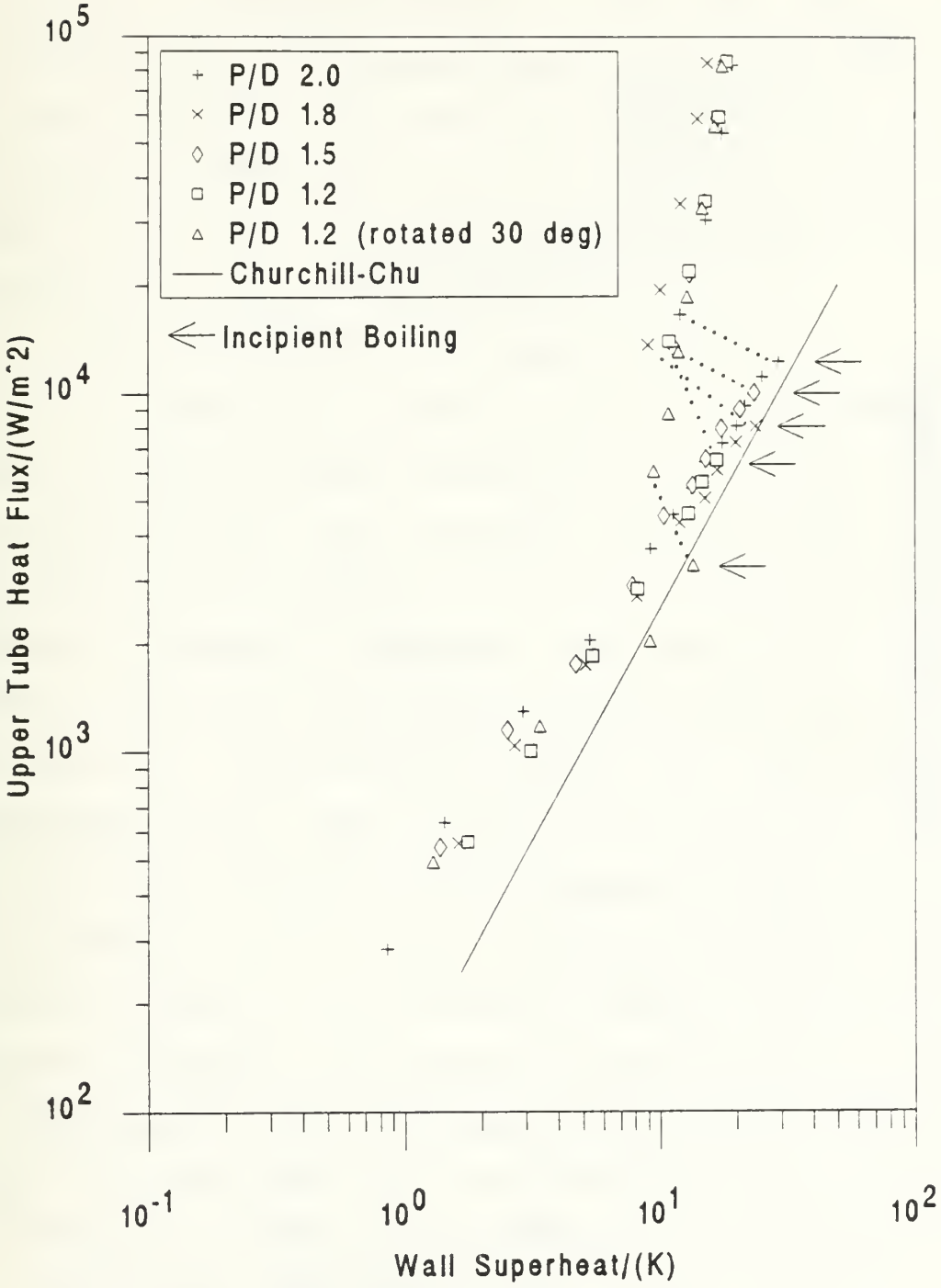


Figure 5.11 Comparison of Smooth Tube P/D Ratios for Increasing Heat Flux with 5 kW/m$^2$ on the Lower Tube

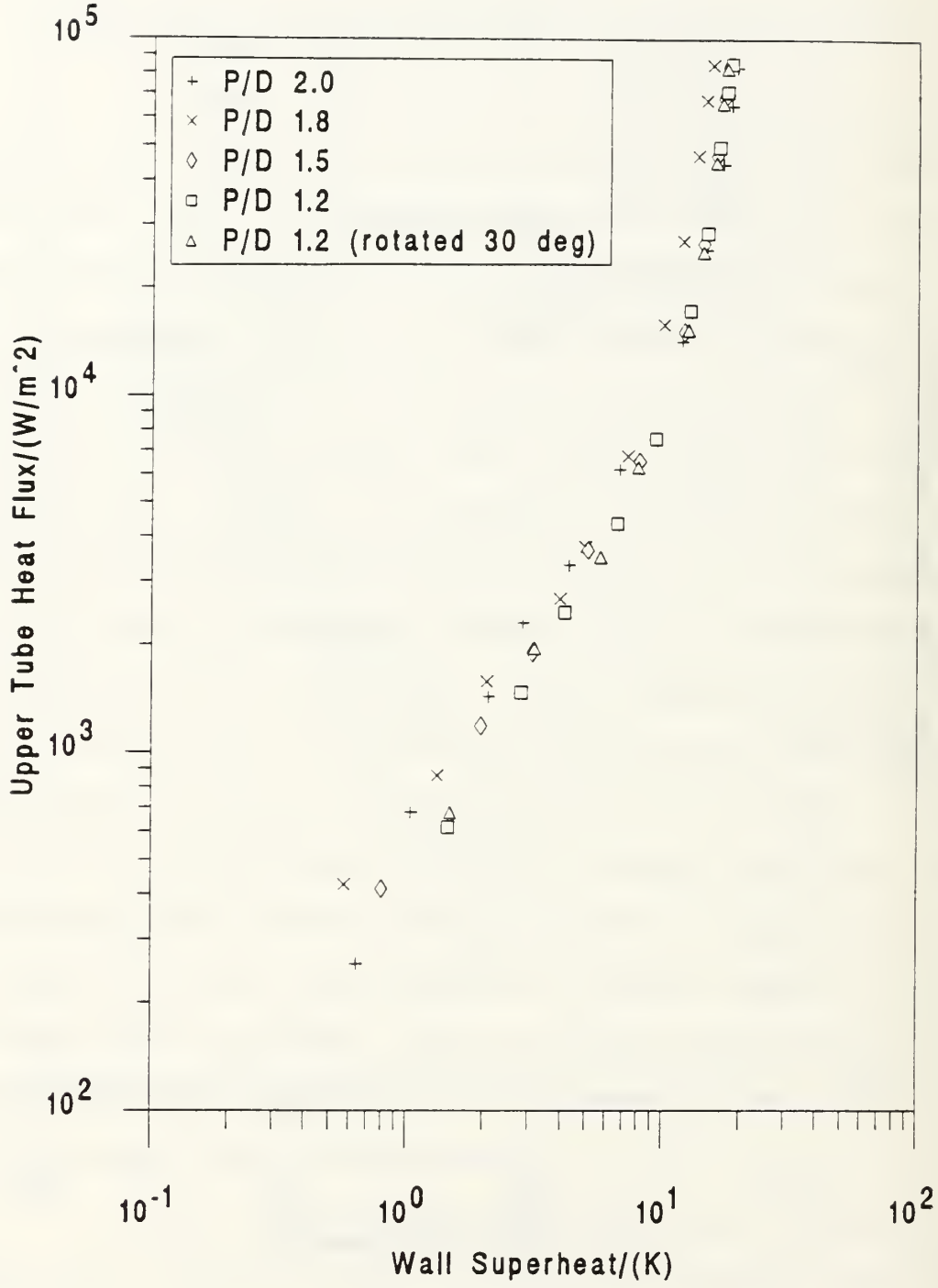


Figure 5.12 Comparison of Smooth Tube P/D Ratios for Decreasing Heat Flux with 5 kW/m$^2$ on the Lower Tube

the best heat transfer. Below 10 $kW/m^2$, the upper tube is returning to natural convection, but the lower tube is still nucleating. The bubbles departing the lower tube impinge upon the upper tube causing a significant increase in heat transfer performance, from bubble sweeping, compared to the data for a LTHFS of 0 and 1 $kW/m^2$. Also, a LTHFS of 5 $kW/m^2$ eliminates any upper tube hysteresis effect.

***d. Smooth Tubes with LTHFS of 10 $kW/m^2$***

Figure 5.13 shows the increasing heat flux data taken for the five tube configurations (C1-C5) with 10 $kW/m^2$ on the lower tube. For this LTHFS, the lower tube nucleated at the start of the run for a P/D of 1.5, but the upper tube remained in natural convection. The effect of the bubbles from the lower tube impacting and sweeping over the upper tube is seen to significantly enhance the heat transfer performance of the upper tube in the low heat flux regions. For the other P/D ratios, the incipient boiling points were very random; at the largest spacing, nucleation occurred quickly, whereas at the smallest spacing, nucleation was delayed. Possibly, the largest spacing (P/D of 2.0) allowed the heated plume from the lower tube to thin the boundary layer around the upper tube, but the closest spacing (P/D of 1.2) enabled the heated plume to 'skirt' around the upper tube and not disturb the upper tube boundary layer as much, delaying the point of incipience. Again, once the upper tube

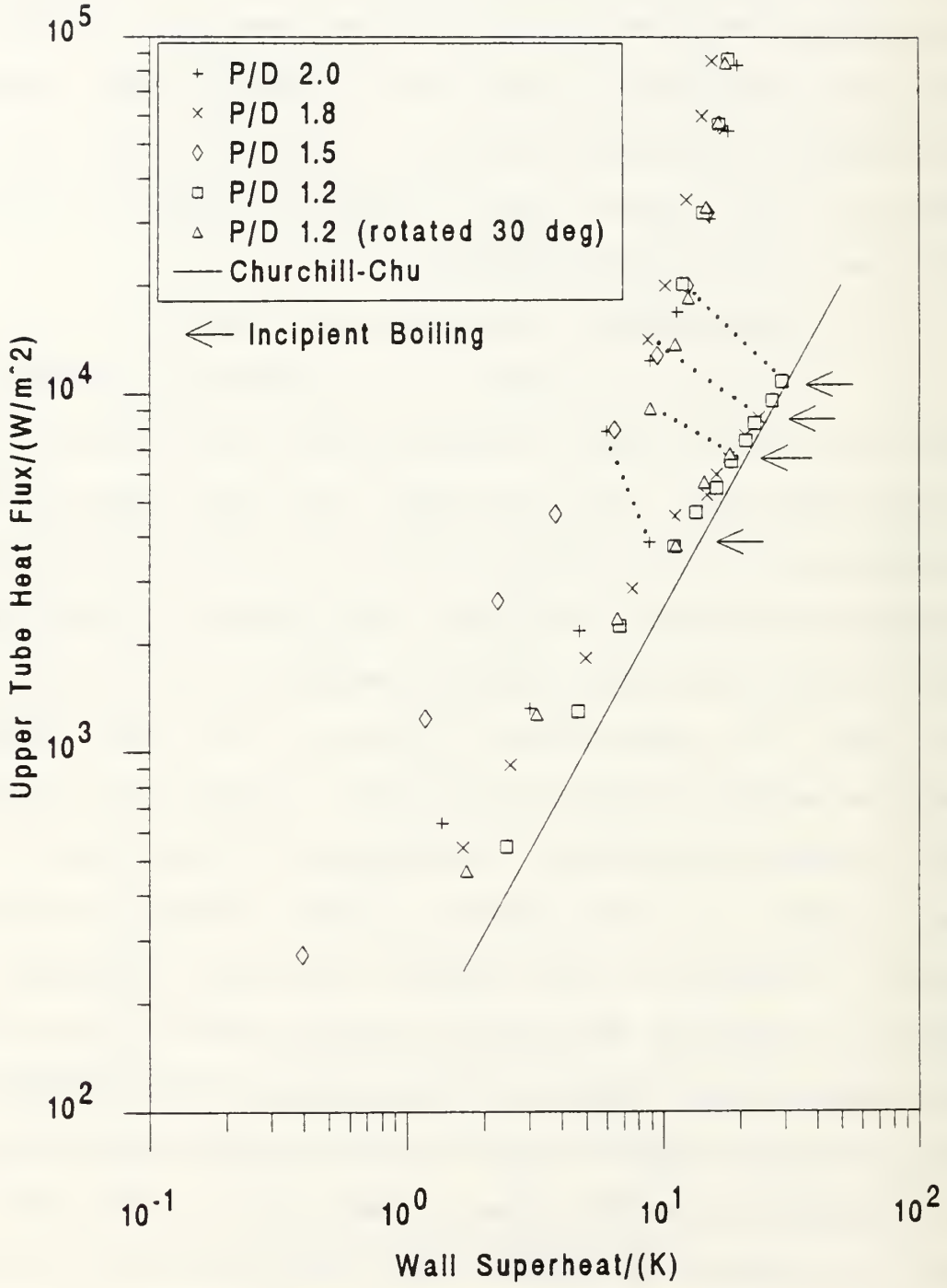


Figure 5.13 Comparison of Smooth Tube P/D Ratios for Increasing Heat Flux with 10 kW/m$^2$ on the Lower Tube

nucleated, the lower tube also nucleated shortly thereafter. In the fully developed nucleate boiling region, a P/D of 1.8 still gives the best performance.

Figure 5.14 is the decreasing heat flux data for Figure 5.13. A P/D of 1.8 provided the best heat transfer until the heat flux was lowered to about 15 $kW/m^2$, where no gain over the other P/D ratios is noticed. This concurs with the findings of Lake [Ref. 3]. Below 10 $kW/m^2$, the nucleating lower tube is definitely enhancing the upper tube performance for all P/D ratios, although, the P/D of 1.2 (rotated 30°) is slightly to the right of the other curves. This is probably caused by the angular offset of the upper tube, not allowing the bubbles from the lower tube to directly impinge upon the upper tube. Therefore, a 30° rotation slightly decreases the performance of the upper tube compared to an in-line tube configuration.

***e. Smooth Tubes with LTHFS of 20 $kW/m^2$***

Figure 5.15 shows the increasing heat flux data taken for the five tube configurations (C1-C5) with 20 $kW/m^2$ on the lower tube. In each run, the lower tube was nucleating at the beginning of the run and remained nucleating throughout. The only effect from P/D spacing is noticed above 20 $kW/m^2$ where a P/D of 1.8 again provides the best performance.

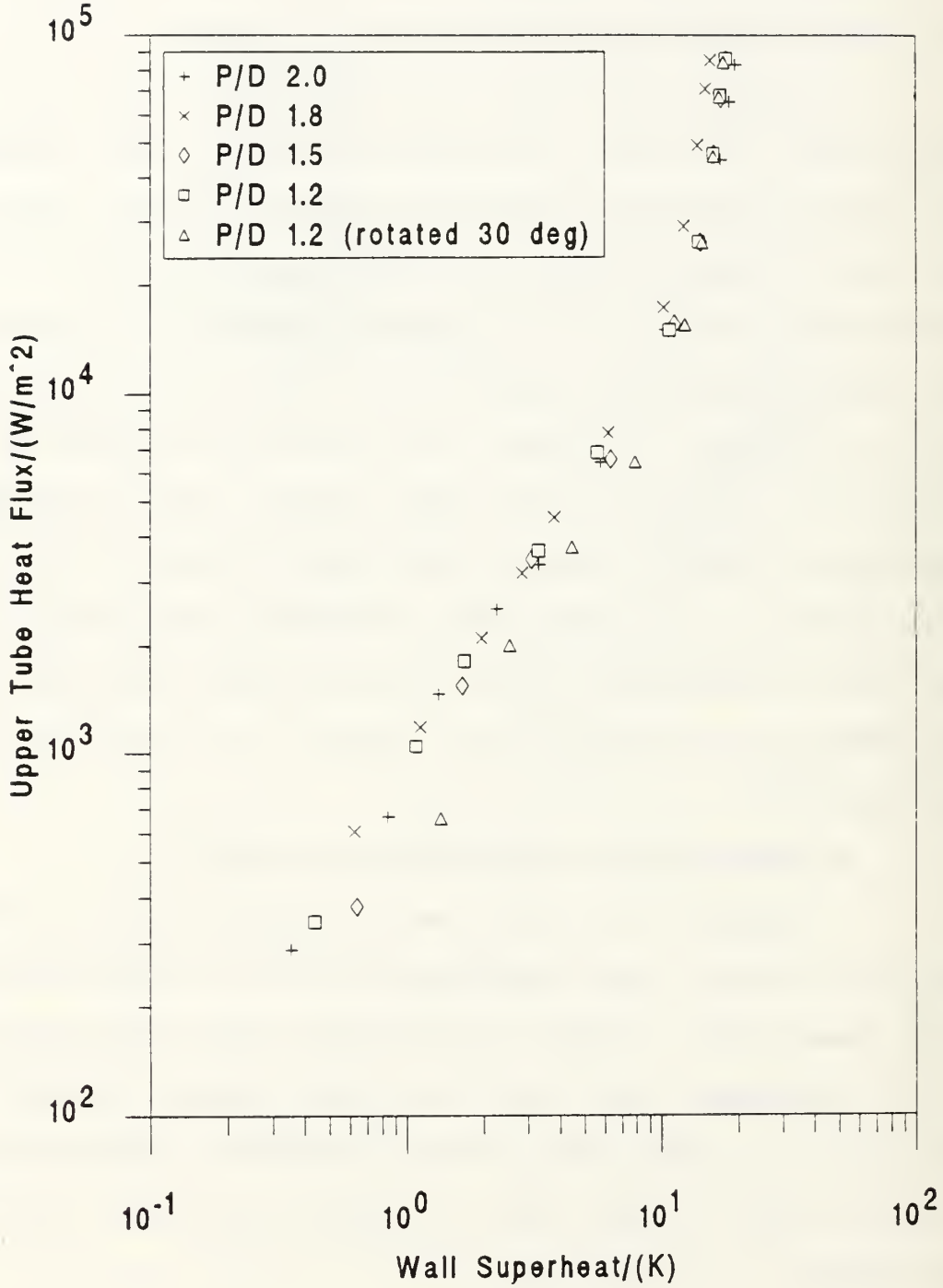


Figure 5.14 Comparison of Smooth Tube P/D Ratios for Decreasing Heat Flux with 10 kW/m$^2$ on the Lower Tube

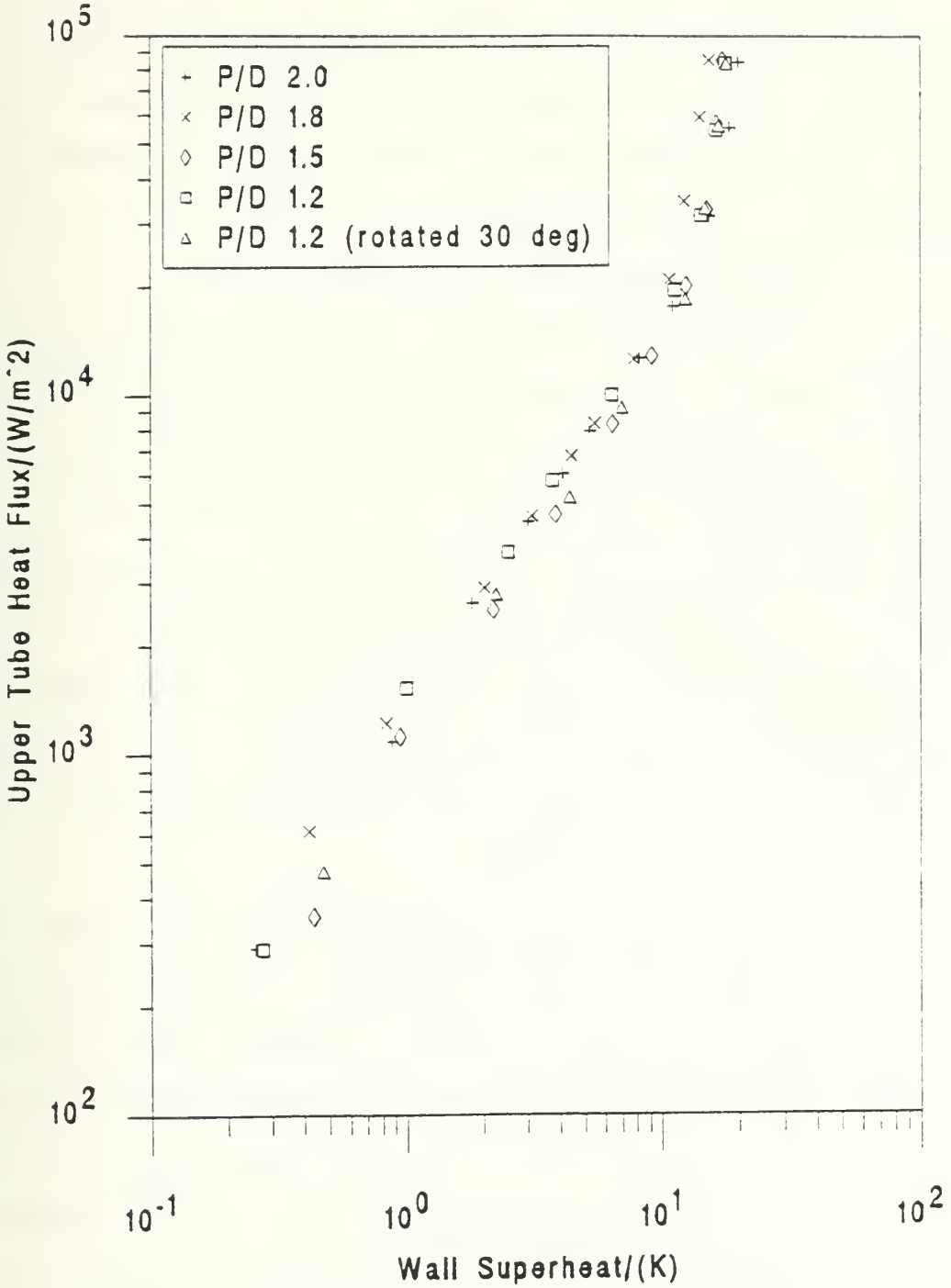


Figure 5.15 Comparison of Smooth Tube P/D Ratios for Increasing Heat Flux with 20 kW/m$^2$ on the Lower Tube

Figure 5.16 is the decreasing heat flux data for Figure 5.15. Again, below 20 $kW/m^2$, only a P/D of 1.2 (rotated 30°) drops slightly below the other curves at mid-range heat fluxes. It appears that this LTHFS enables more bubbles from the lower tube to impinge upon the upper tube, compared to a LTHFS of 10 $kW/m^2$.

***f. Smooth Tubes with UTHFS equal LTHFS***

Figure 5.17 shows the increasing heat flux data taken for the five tube configurations (C1-C5) with the UTHFS equal to the LTHFS throughout the entire length of the run. At the beginning of all the runs, both tubes were in the natural convection region. In the natural convection region, a P/D of 1.2 (rotated 30°) is the only configuration that is very close to the Churchill and Chu correlation [Ref. 9]. This was not expected nor can be explained. Again, a random incipient point was obtained and in the boiling region, a P/D of 1.8 was the best performer.

Figure 5.18 is the decreasing heat flux data for Figure 5.17. Above 20 $kW/m^2$, a P/D of 1.8 still provides the best performance and below 20 $kW/m^2$ it appears that as the P/D decreases, so does the enhancement of the upper tube. Between 9 and 5 $kW/m^2$, it's believed that the tubes shift from the boiling region back to natural convection. This may cause the decrease of enhancement because, as speculated earlier, as the

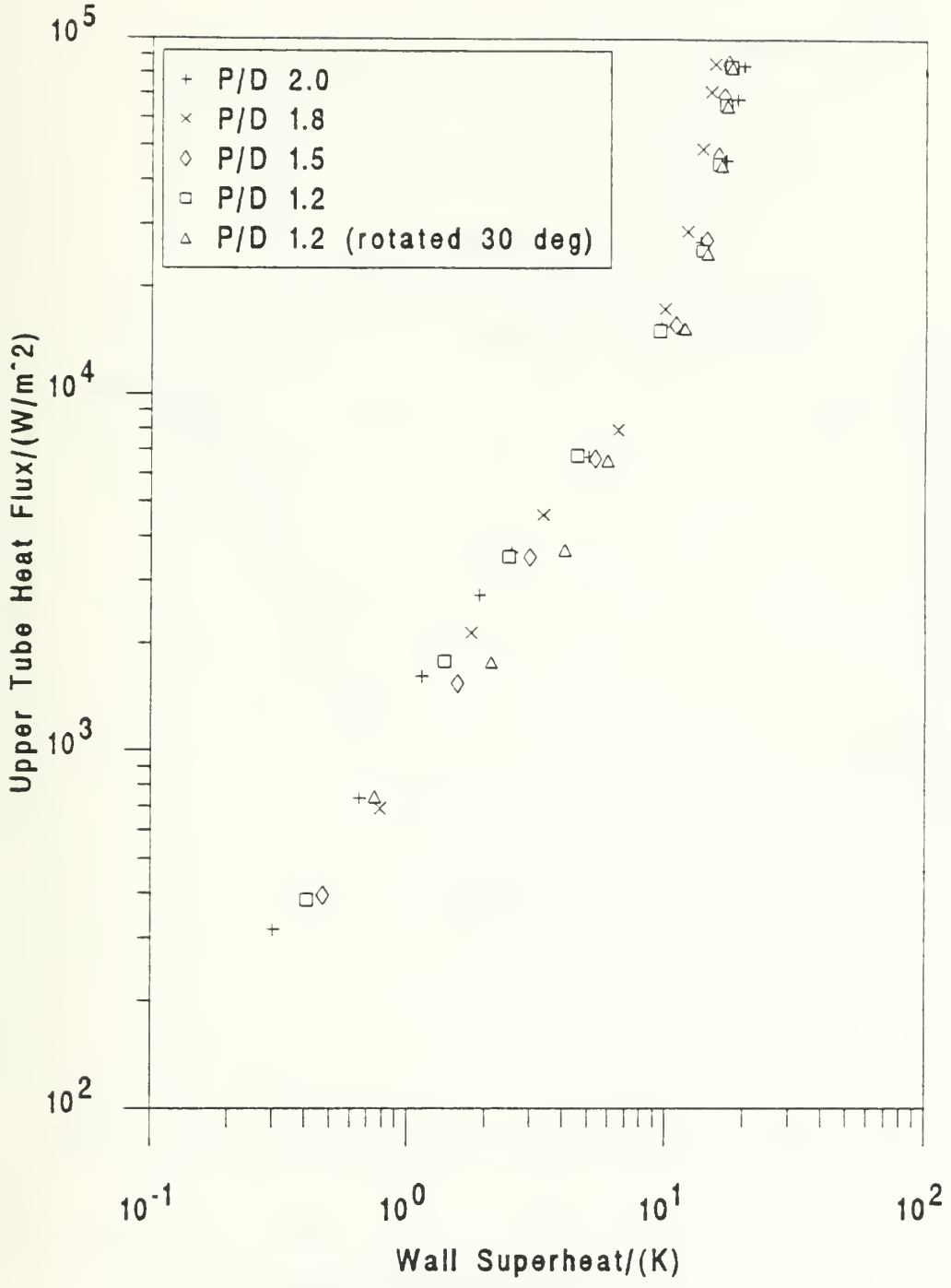


Figure 5.16 Comparison of Smooth Tube P/D Ratios for Decreasing Heat Flux with 20 kW/m$^2$ on the Lower Tube

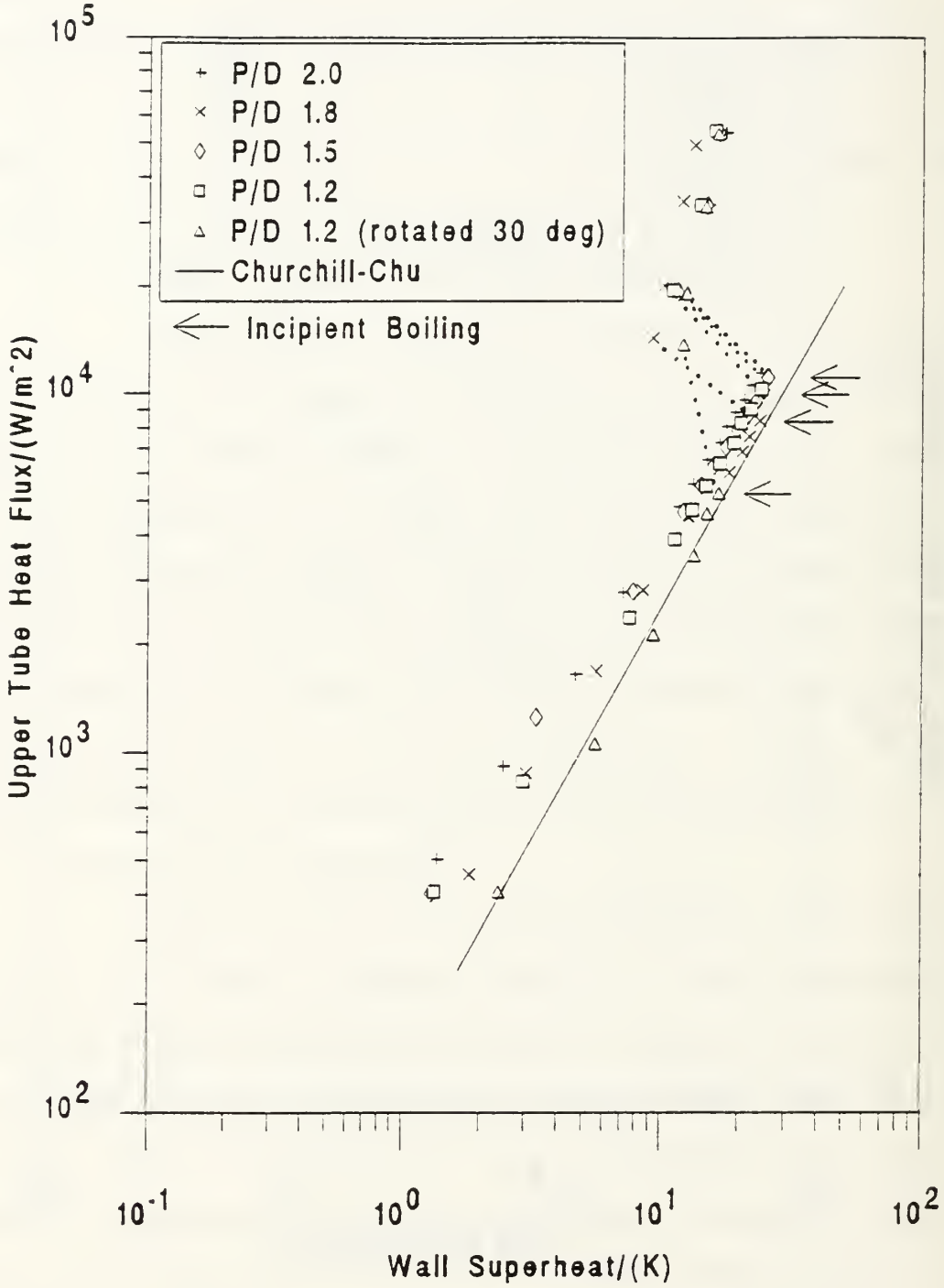


Figure 5.17 Comparison of Smooth Tube P/D Ratios for Increasing Heat Flux with UTHFS equal to LTHFS

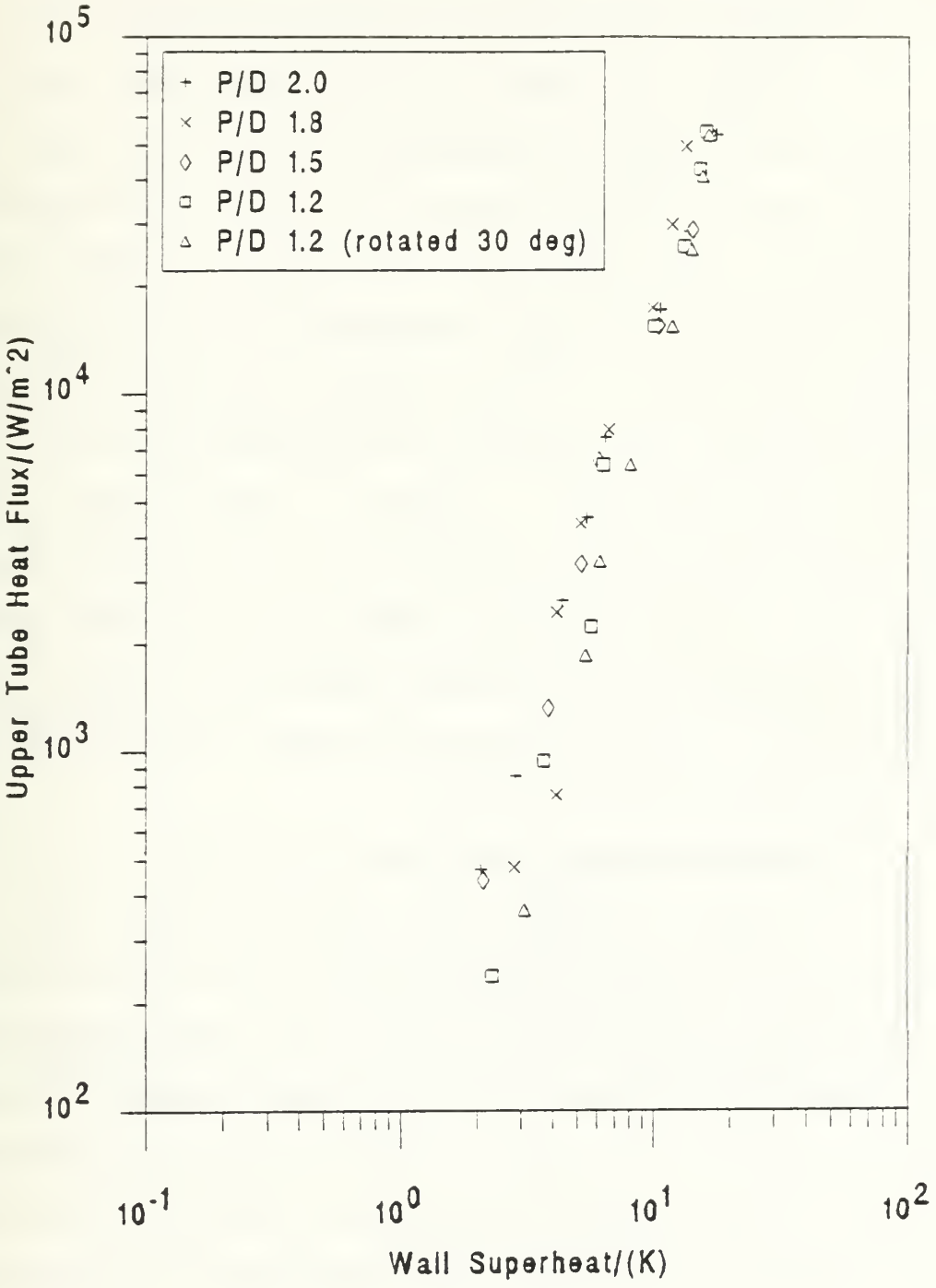


Figure 5.18 Comparison of Smooth Tube P/D Ratios for Decreasing Heat Flux with UTHFS equal to LTHFS

P/D is decreased so too are the convection effects from the lower tube.

### *g. TURBO-B Tubes with Lower Tube Unheated*

Figure 5.19 shows the decreasing heat flux data taken for the five tube configurations (C1-C5) with lower tube unheated. At the start of each run, an undetermined amount of nucleation was occurring from the lower tube due to the vigorous boiling action off the upper tube at the run start heat flux (100 $kW/m^2$). A very consistent boiling curve above 10 $kW/m^2$ indicates that there is no enhancement from the lower tube at any P/D ratio. Below 5 $kW/m^2$, the rotated configuration data agrees well with the single tube data in Figure 5.3. This indicates that the lower tube is not modifying the flow around the upper tube and the upper tube is performing as a single tube which provides less heat transfer than the in-line configurations.

### *h. TURBO-B Tubes with LTHFS of 1 $kW/m^2$*

Figure 5.20 shows the decreasing heat flux data taken for the five tube configurations (C1-C5) with 1 $kW/m^2$ on the lower tube. At the start of each run, both the upper and lower tubes were nucleating. Very little change is noticed between Figures 5.19 and 5.20. Above 20 $kW/m^2$, the plots are identical. Below 10 $kW/m^2$, the LTHFS of 1 $kW/m^2$ moved the data curves slightly to the left. This indicates that the greater

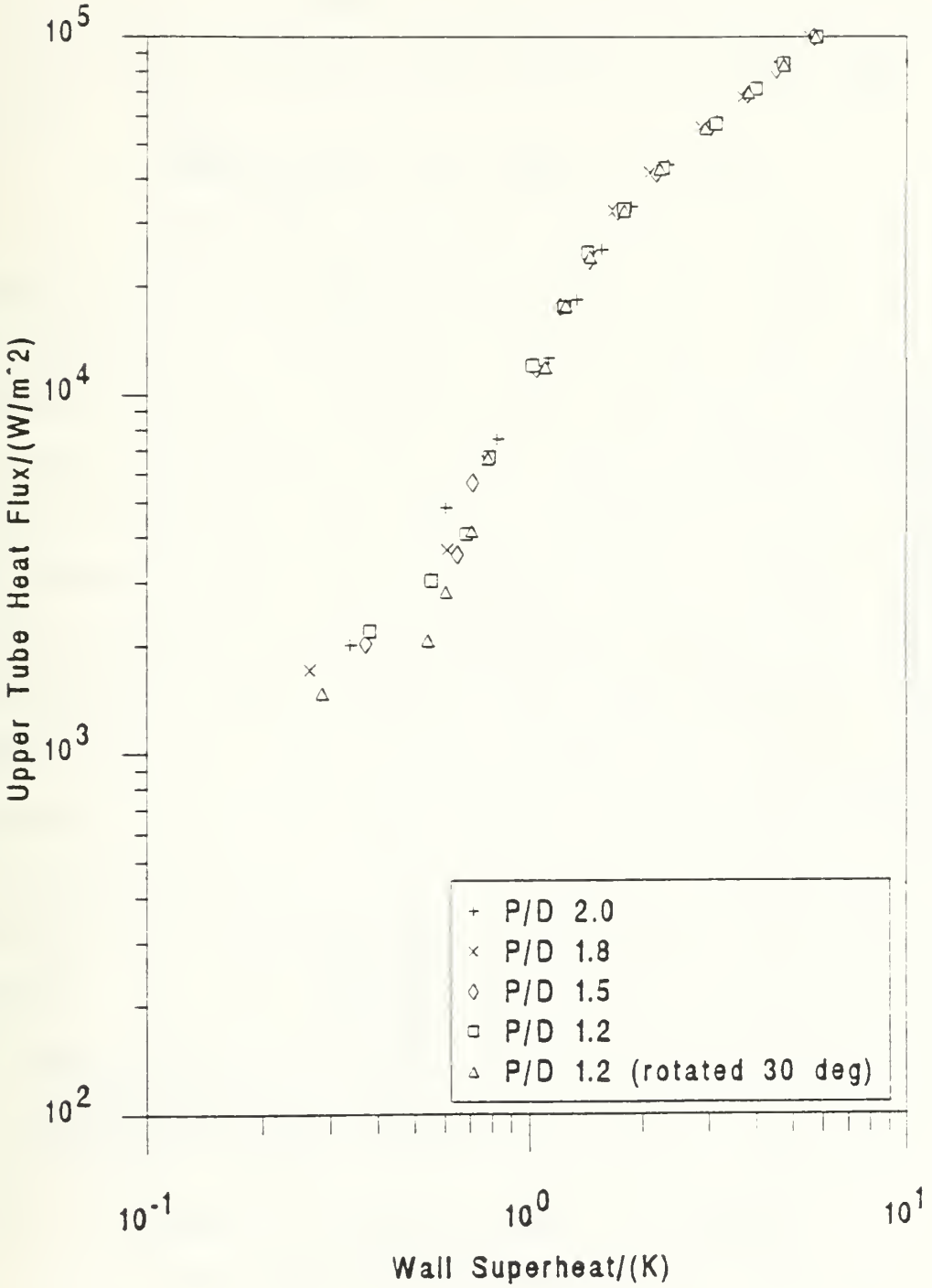


Figure 5.19 Comparison of TURBO-B Tube P/D Ratios for Decreasing Heat Flux with the Lower Tube Unheated

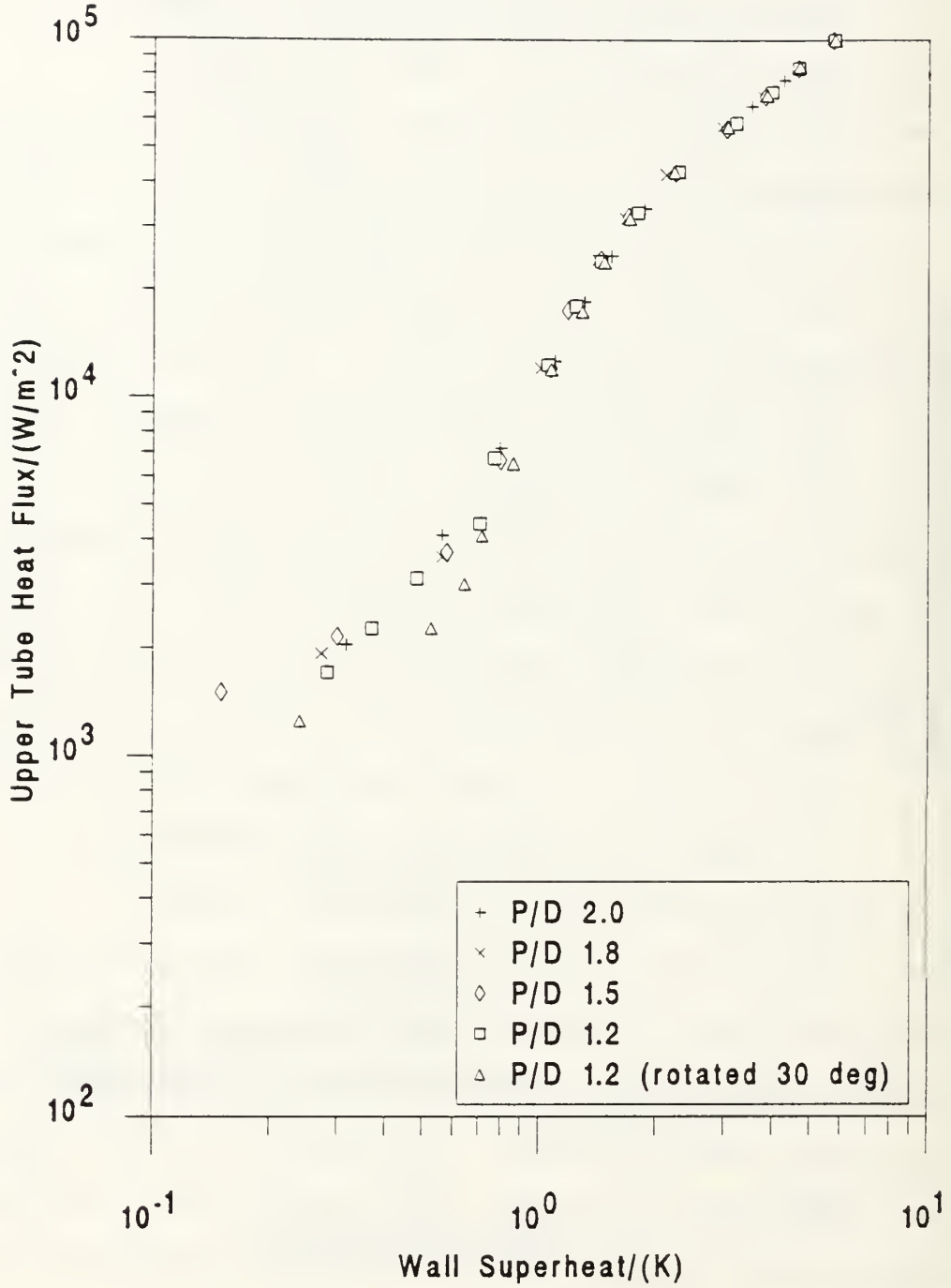


Figure 5.20 Comparison of TURBO-B Tube P/D Ratios for Decreasing Heat Flux with 1 kW/m$^2$ on the Lower Tube

the LTHFS, the more enhanced the mid-range and lower heat flux region becomes. As seen in the previous figure, a P/D of 1.2 (rotated 30°) is again less enhanced than the other P/D ratios.

*i. TURBO-B Tubes with LTHFS of 5 kW/m²*

Figure 5.21 shows the decreasing heat flux data taken for the five tube configurations (C1-C5) with 5 kW/m² on the lower tube. At the start of each run, both tubes were vigorously boiling. Above 20 kW/m², the data is consistent with the two previous plots, but below 10 kW/m², a definite separation between a P/D of 1.2 (rotated 30°) and the other P/D ratios is seen. Also for heat fluxes < 10 kW/m², the in-line configurations provide better heat transfer than the same configurations seen in Figure 5.20. This indicates that as LTHFS increases, more bubbles depart the lower tube and increase the upper tube heat transfer performance for the in-line configurations. For the rotated configuration, the bubbles must be departing the lower TURBO-B tube differently (compare to a lower smooth tube) and are not impinging upon the upper TURBO-B tube. This explains the approximately 40 - 45% decrease in heat transfer performance for the rotated configuration compared to the in-line configurations.

*j. TURBO-B Tubes with LTHFS of 10 kW/m²*

Figure 5.22 shows the decreasing heat flux data taken for the five tube configurations (C1-C5) with 10 kW/m²

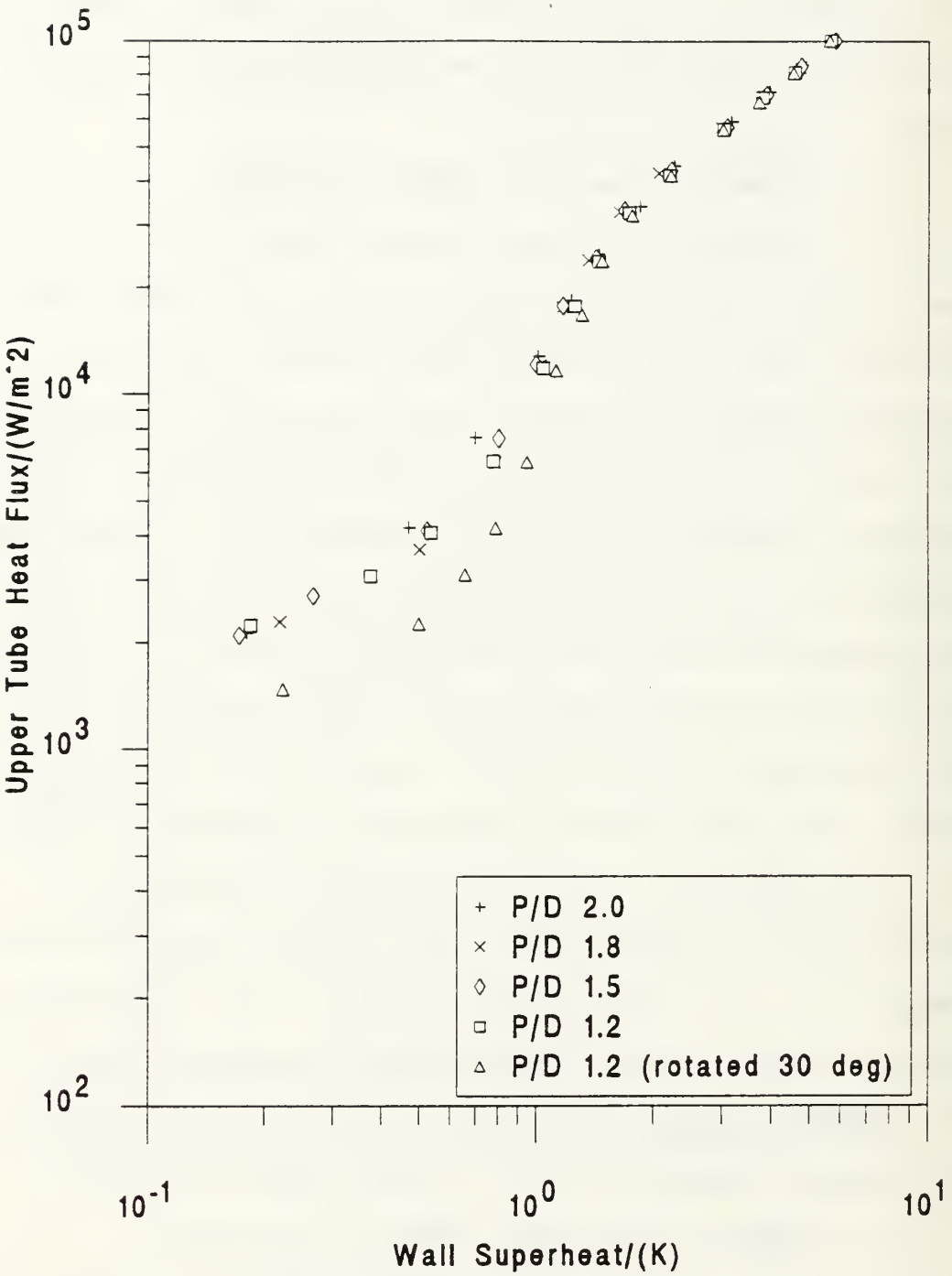


Figure 5.21 Comparison of TURBO-B Tube P/D Ratios for Decreasing Heat Flux with 5 kW/m$^2$ on the Lower Tube

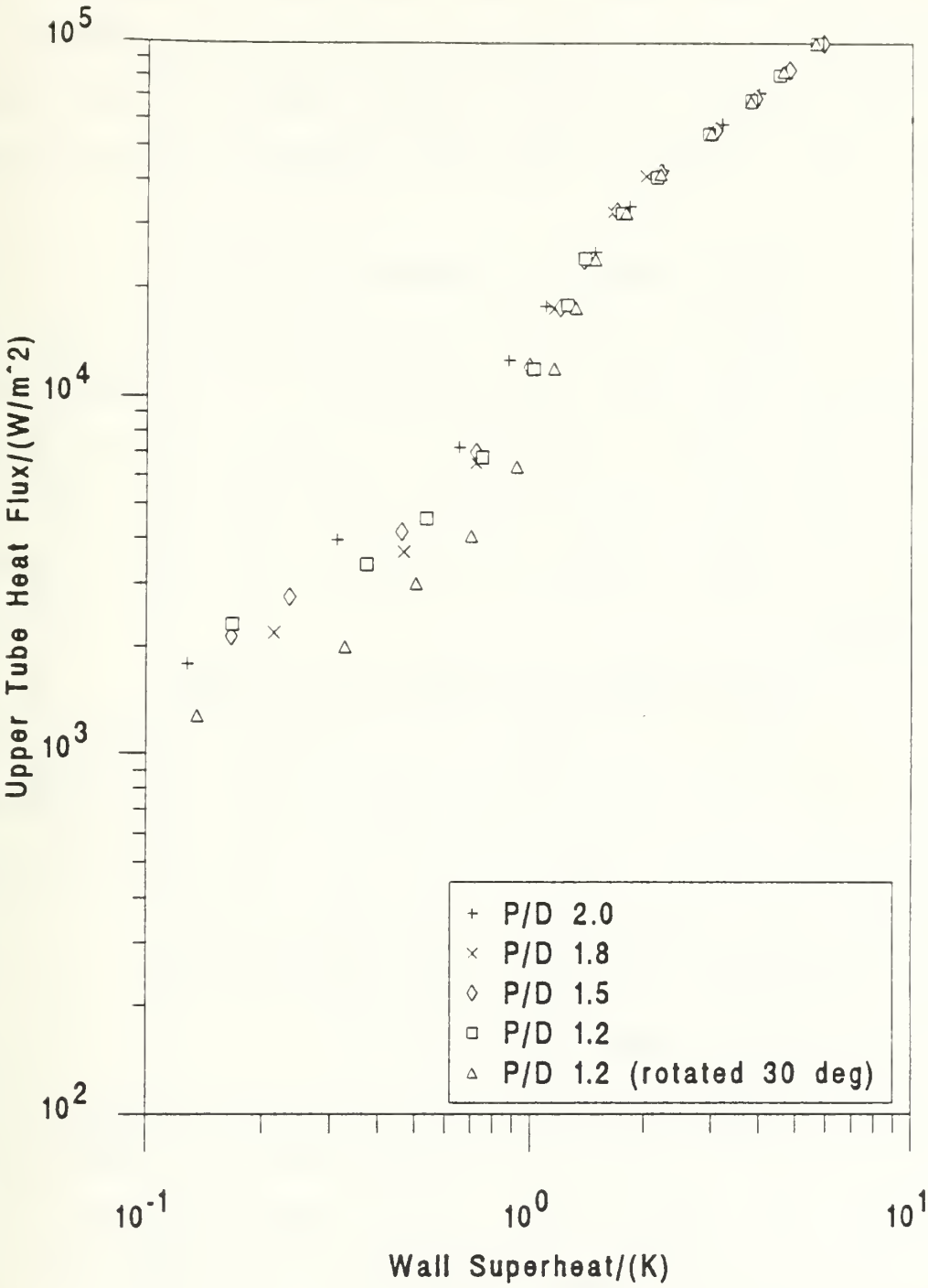


Figure 5.22 Comparison of TURBO-B Tube P/D Ratios for Decreasing Heat Flux with 10 kW/m$^2$ on the Lower Tube

on the lower tube. Again, both tubes were nucleating at the beginning of each run. There are no obvious changes above 20 $kW/m^2$ from the previous plots. Below 10 $kW/m^2$, all the curves seem to have shifted to the left compared to the previous case.

*k. TURBO-B Tubes with LTHFS of 20 $kW/m^2$*

Figure 5.23 shows the decreasing heat flux data taken for the five tube configurations (C1-C5) with 20 $kW/m^2$ on the lower tube. Figures 5.22 and 5.23 show similar results, therefore, increasing the LTHFS from 10 to 20 $kW/m^2$ provides a small change in upper tube heat transfer performance.

*l. TURBO-B Tubes with UTHFS equal LTHFS*

Figure 5.24 shows the decreasing heat flux data taken for the five tube configurations (C1-C5) with the UTHFS equal to the LTHFS. There is not much change in this plot relative to the trend set by the previous plots.

**2. The Effect of a Fixed Lower Tube Heat Flux**

*a. Smooth Tubes with P/D of 2.0*

Figure 5.25 shows the increasing heat flux data taken for a P/D of 2.0 at five different heat flux settings on the lower tube. The Churchill and Chu correlation [Ref. 9] is also shown for comparison. For a LTHFS of 20 $kW/m^2$, the lower tube had nucleated immediately at the beginning of the run and remained nucleating for the length of the run. All other

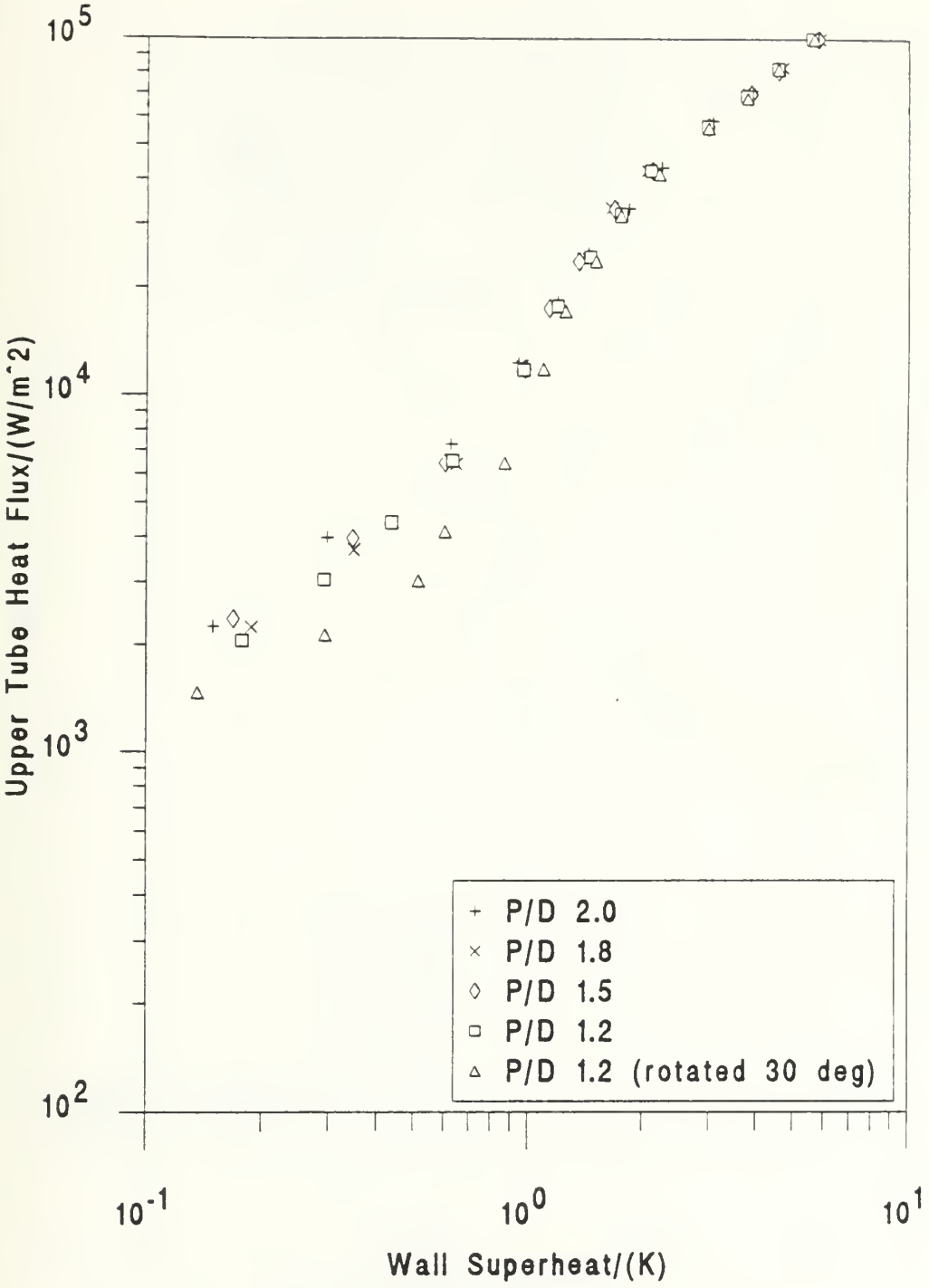


Figure 5.23 Comparison of TURBO-B Tube P/D Ratios for Decreasing Heat Flux with 20 kW/m$^2$ on the Lower Tube

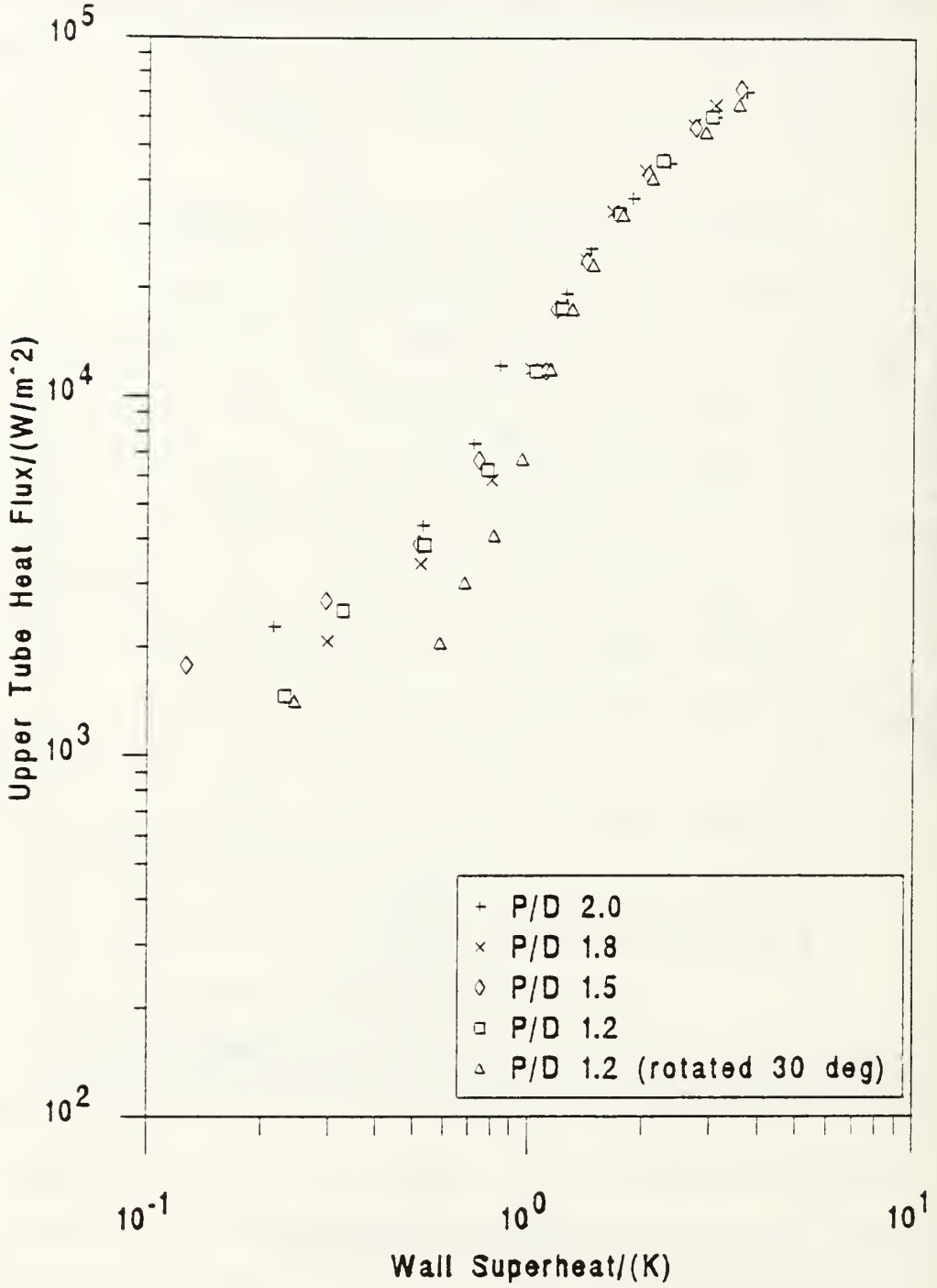


Figure 5.24 Comparison of TURBO-B Tube P/D Ratios for Decreasing Heat Flux with the UTHFS equal to the LTHFS

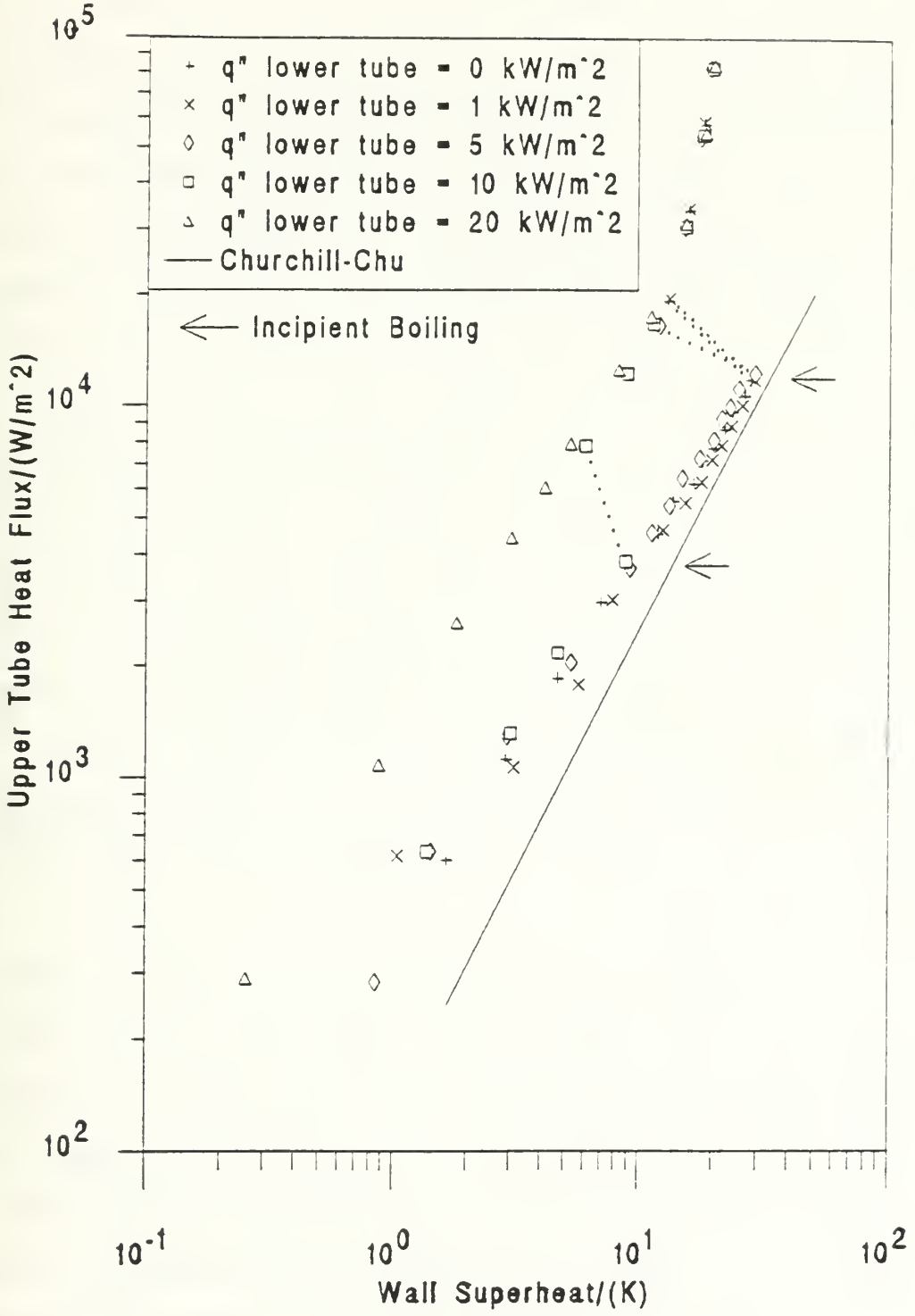


Figure 5.25 Comparison of Lower Tube Heat Flux Settings on Increasing Heat Flux of Smooth Tubes with P/D of 2.0

LTHFS data runs, started in natural convection. In the natural convection region, the data are shifted to the left of the Churchill and Chu correlation [Ref. 9], but approach it as heat flux is increased. This is probably caused by strong circulation patterns within the small evaporator enhancing the heat transfer mentioned previously. In natural convection, the effect of a LTHFS had little influence on the upper tube heat transfer behavior; in fact, this is repeated for all the P/D ratios. The point of incipience was very repeatable, with the exception of a LTHFS of 10 $kW/m^2$. A heat flux of 10 $kW/m^2$ is approximately the heat flux that 'trips' the nucleation sites causing boiling to occur from a smooth tube, so shortly after the run started, the lower tube nucleated and caused the upper tube to nucleate quickly. At high heat fluxes, all the data falls on one nucleate boiling curve indicating that the LTHFS has little effect on the heat transfer from the upper tube in this region.

Figure 5.26 shows the decreasing heat flux data for the data run for Figure 5.25. Important to note that the upper tube starts and finishes each run in natural convection, but the lower tube might not. For a LTHFS of 0 and 1 $kW/m^2$, the lower tube starts and finishes in natural convection; for a LTHFS of 20 $kW/m^2$, it starts and finishes in nucleate boiling; and for a LTHFS of 5 and 10 $kW/m^2$, it starts in natural convection and finishes in nucleate boiling. At high heat fluxes, all the data lay on one nucleate boiling curve as

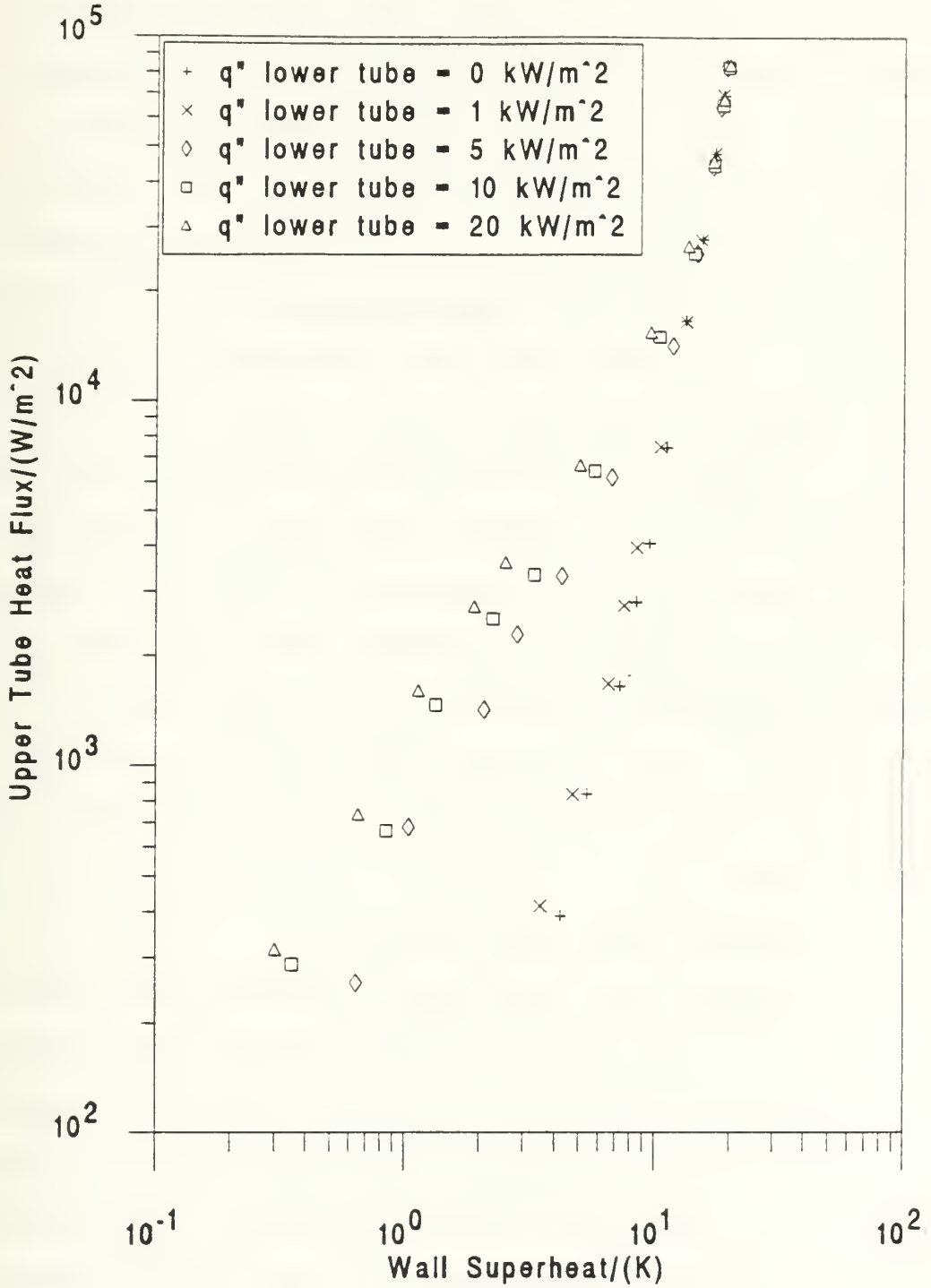


Figure 5.26 Comparison of Lower Tube Heat Flux Settings on Decreasing Heat Flux of Smooth Tubes with P/D of 2.0

expected. Below 20 $kW/m^2$, five separate curves are seen. The curves with a LTHFS of 0 and 1 $kW/m^2$ return to the natural convection region, indicating a deactivation of the nucleation sites as the upper tube heat flux is decreased, showing the hysteresis effect of the upper tube. At a heat flux below 5 $kW/m^2$, the curves with a LTHFS of 5, 10 and 20 $kW/m^2$ begin to parallel the natural convection curve found on the increasing heat flux plot and have significant enhancement over the 0 and 1 $kW/m^2$ curves at low heat fluxes. Also, the hysteresis effect is eliminated by the vigorously nucleating lower tube. This same phenomena was found by Lake [Ref. 3]. He attributed this enhancement to strong convection effects on the upper tube from the bubbles nucleating off the lower tube. Therefore, significant enhancement of heat transfer of an upper tube is possible when the lower tube is nucleating and very little enhancement is noticed when both tubes are in natural convection.

***b. Smooth Tubes with P/D of 1.8***

Figure 5.27 shows the increasing heat flux data taken for a P/D of 1.8 at five lower tube heat flux settings. For a LTHFS of 20 $kW/m^2$, the lower tube had nucleated immediately at the beginning of the run and remained nucleating for the entire length of the run. All other LTHFS started in natural convection. In the natural convection region, the data are shifted to the left of the Churchill and

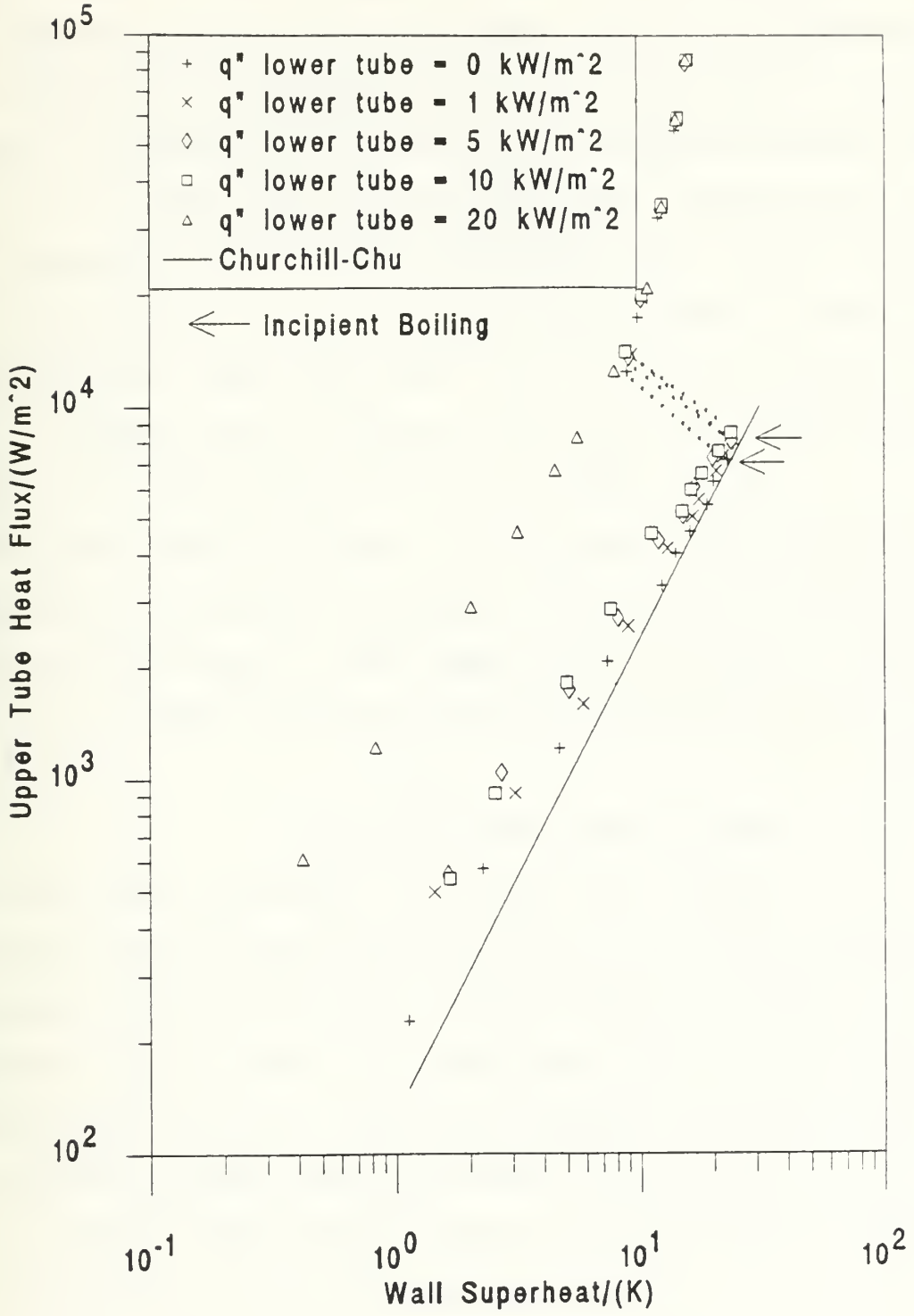


Figure 5.27 Comparison of Lower Tube Heat Flux Settings on Increasing Heat Flux of Smooth Tubes with P/D of 1.8

Chu correlation [Ref. 9], but approach it as heat flux is increased, as was the case with a P/D of 2.0. Again, the effect of the LTHFS had little influence of the upper tube heat transfer behavior. The point of incipience was again, very repeatable. This time, unlike for a P/D of 2.0, the lower tube remained in natural convection until the upper tube nucleated. Again, at high heat fluxes, all the data falls on one nucleate boiling curve indicating that the LTHFS has little effect upon the heat transfer in this region.

Figure 5.28 shows the decreasing heat flux data for the data runs for Figure 5.27. The data trend is similar to that found in Figure 5.26. Therefore, significant enhancement of heat transfer from an upper tube is again seen when the lower tube is nucleating with larger than 5 $kW/m^2$ on the lower tube.

### *c. Smooth Tubes with P/D of 1.5*

Figure 5.29 shows the increasing heat flux data taken for a P/D of 1.5 at five lower tube heat flux settings. For a LTHFS of 10 and 20 $kW/m^2$, the lower tube had nucleated immediately at the beginning of the run and remained nucleating for the length of the run. All other LTHFS started in natural convection. This plot shows similar results seen on Figure 5.27 and most of the comments still apply.

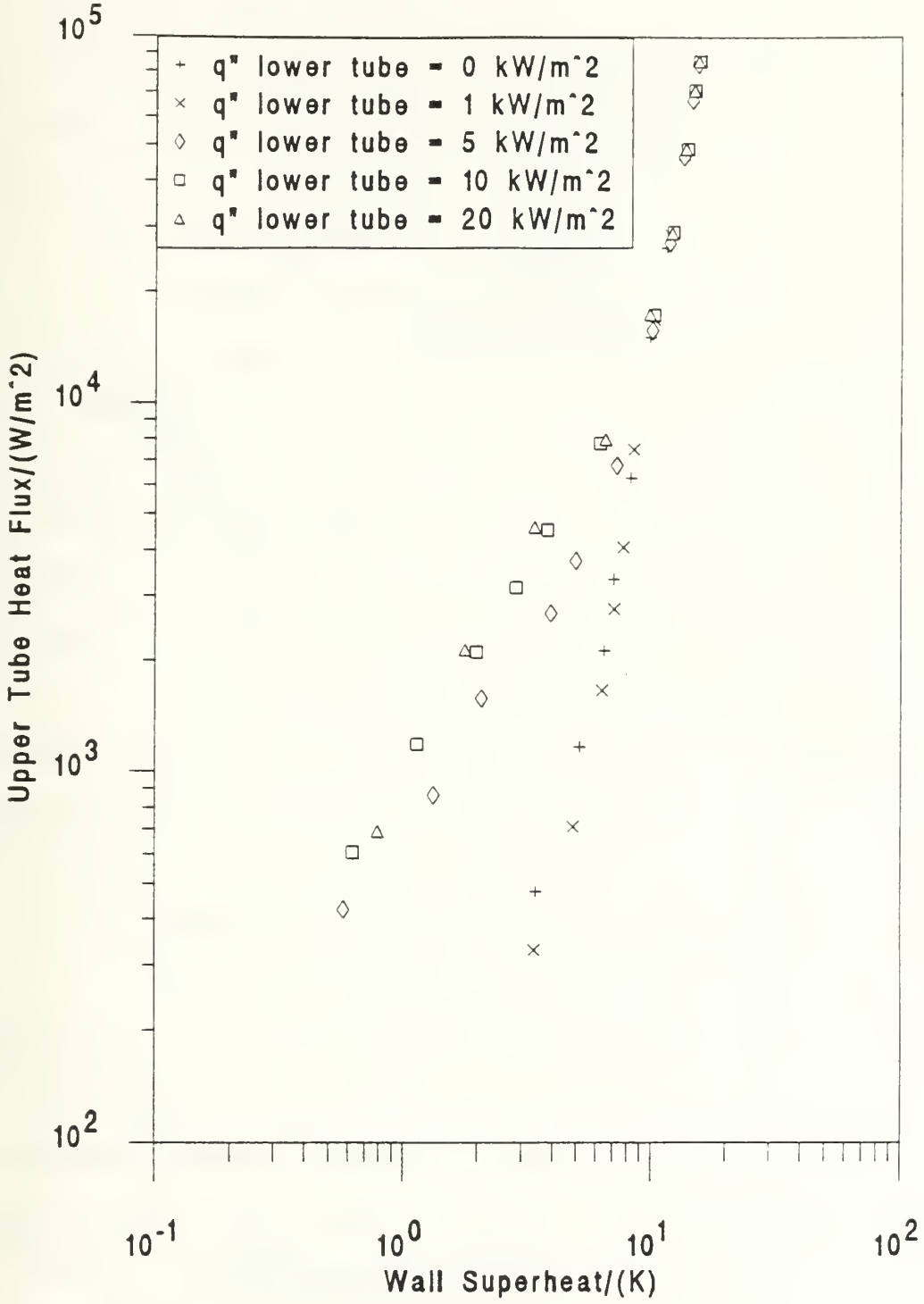


Figure 5.28 Comparison of Lower Tube Heat Flux Settings on Decreasing Heat Flux of Smooth Tubes with P/D of 1.8

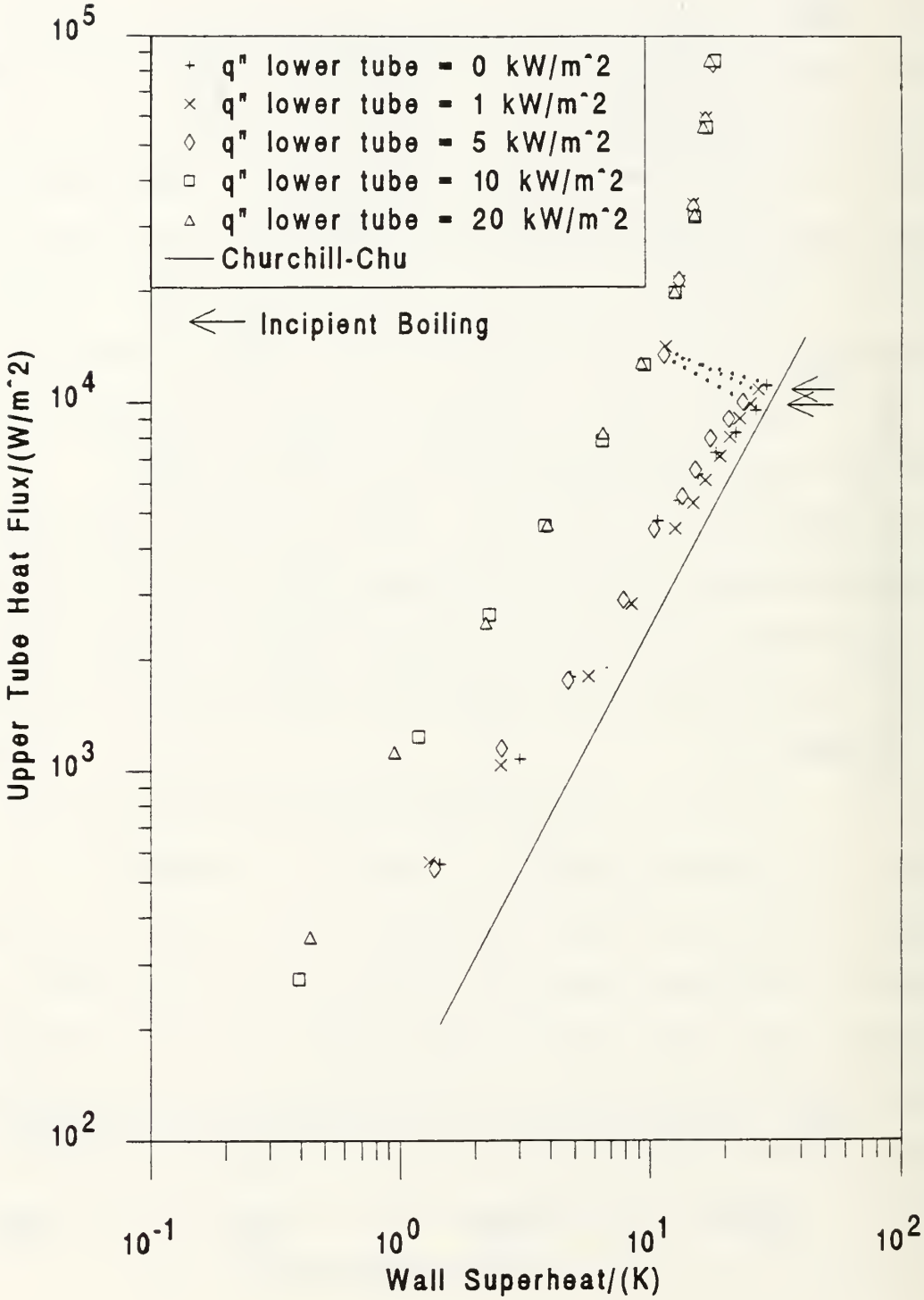


Figure 5.29 Comparison of Lower Tube Heat Flux Settings on Increasing Heat Flux of Smooth Tubes with P/D of 1.5

Figure 5.30 shows the decreasing heat flux data for the data runs shown in Figure 5.29. Again, similar results are obtained as before. Significant enhancement in the heat transfer from an upper tube is obtained when the lower tube is nucleating with a heat flux larger than 5 $kW/m^2$.

***d. Smooth Tubes with P/D of 1.2***

Figure 5.31 shows the increasing heat flux data taken for a P/D of 1.2 at five lower tube heat flux settings. For a LTHFS of 20 $kW/m^2$, the lower tube had nucleated immediately at the beginning of the run and remained nucleating for the length of the run. All other LTHFS started in natural convection. This plot shows similar results seen on Figure 5.29 and most of the comments still apply.

Figure 5.32 shows the decreasing heat flux data for the data runs shown in Figure 5.31. This plot shows similar results seen on Figure 5.30 and again, most of the comments still apply.

***e. Smooth Tubes with P/D of 1.2 (Rotated 30°)***

Figure 5.33 shows the increasing heat flux data taken for a P/D of 1.2 (rotated 30°), at five lower tube heat flux settings. For a LTHFS of 20 $kW/m^2$, the lower tube had nucleated immediately at the beginning of the run and remained nucleating for the length of the run. All other LTHFS started in natural convection. The increasing data for this configuration is more concentrated than the others seen

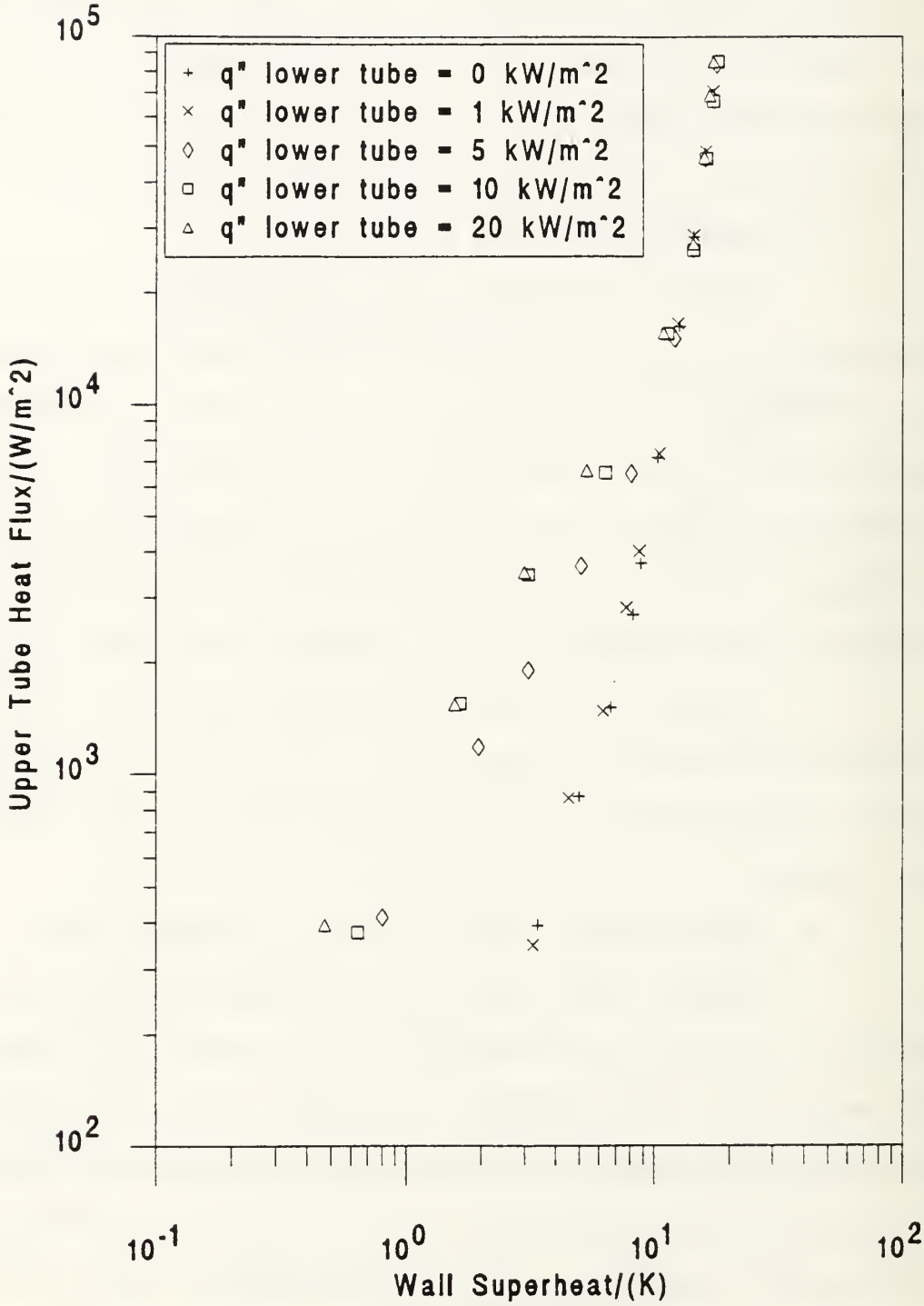


Figure 5.30 Comparison of Lower Tube Heat Flux Settings on Decreasing Heat Flux of Smooth Tubes with P/D of 1.5

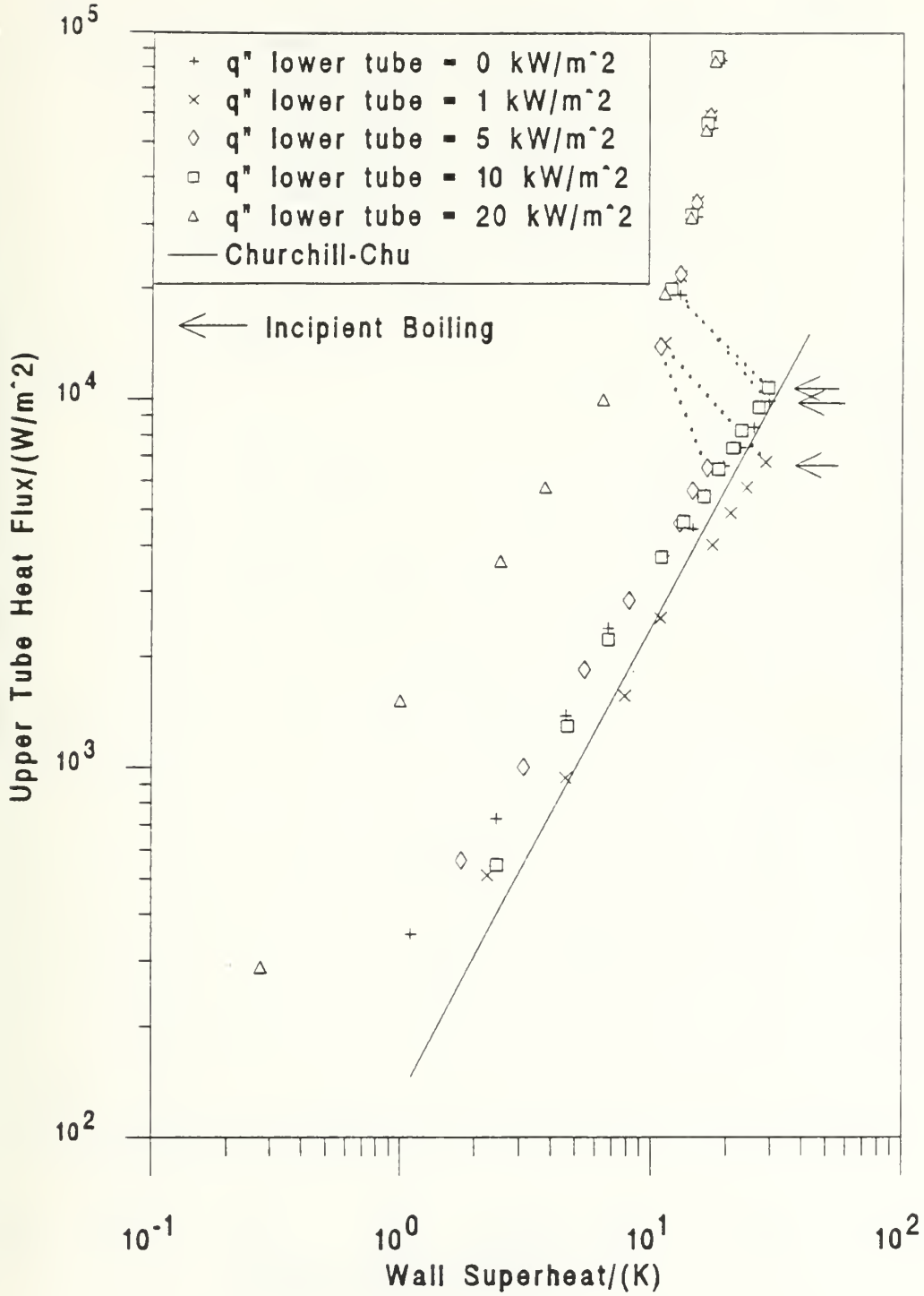


Figure 5.31 Comparison of Lower Tube Heat Flux Settings on Increasing Heat Flux of Smooth Tubes with P/D of 1.2

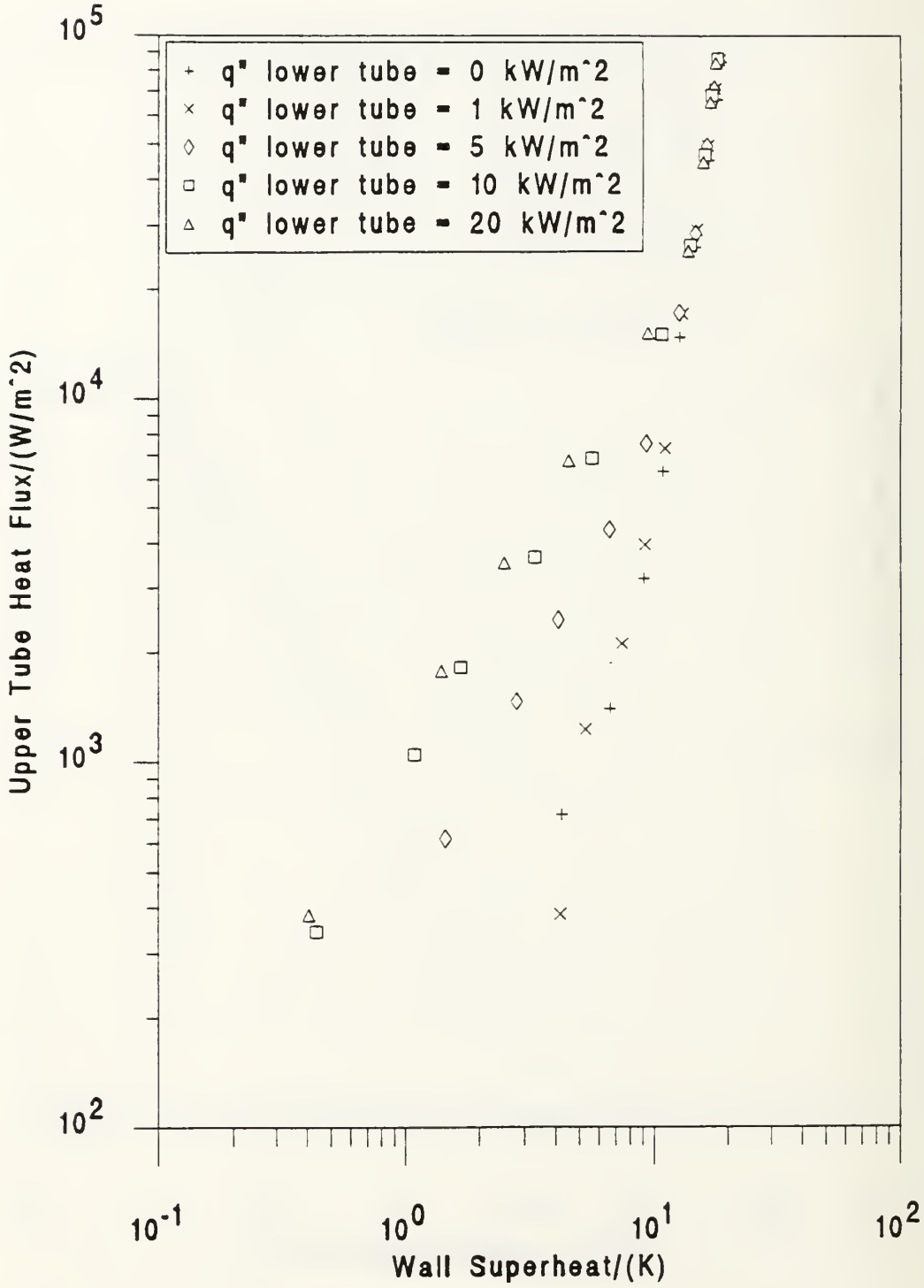


Figure 5.32 Comparison of Lower Tube Heat Flux Settings on Decreasing Heat Flux of Smooth Tubes with P/D of 1.2

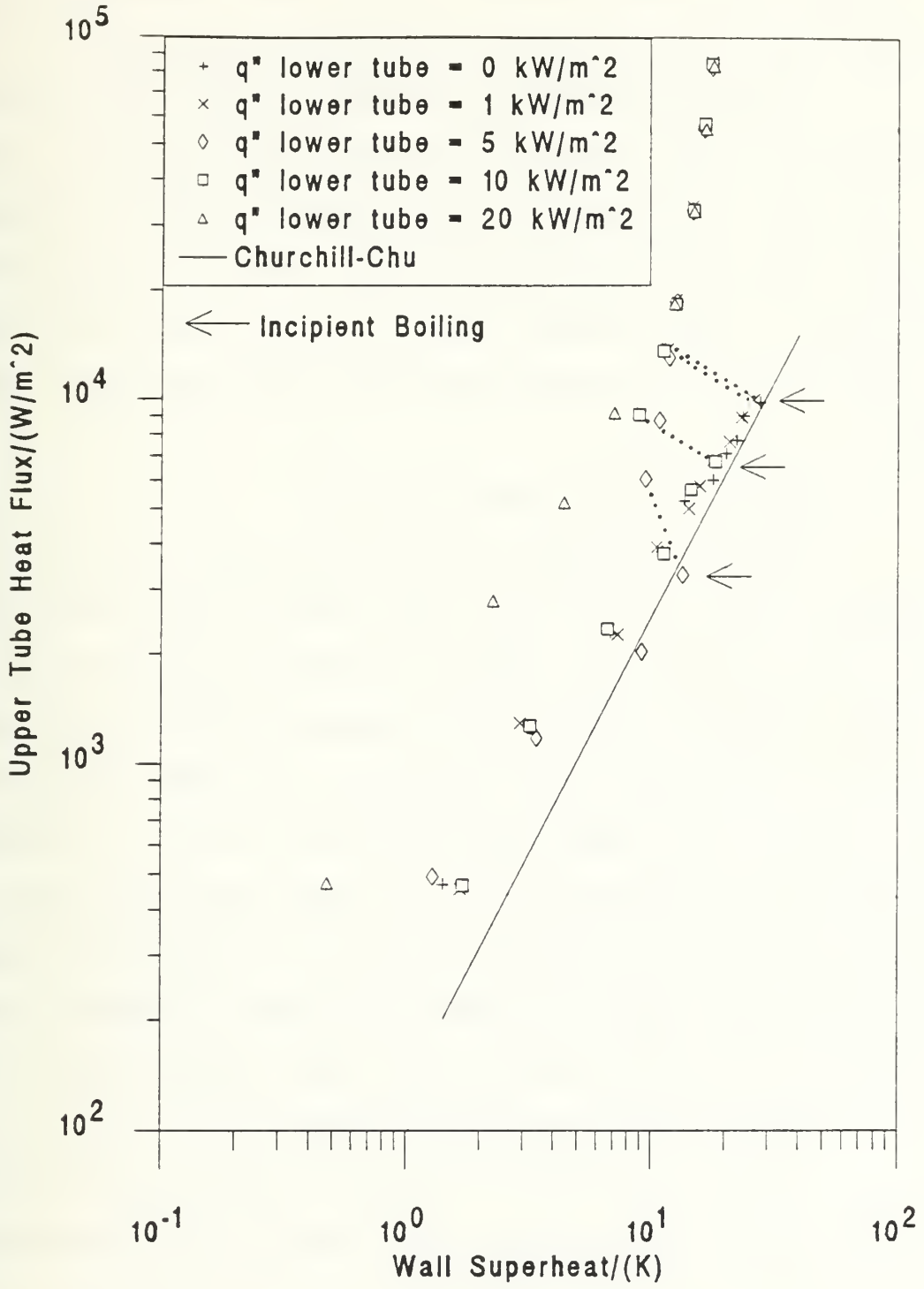


Figure 5.33 Comparison of Lower Tube Heat Flux Settings on Increasing Heat Flux of Smooth Tubes with P/D of 1.2 (Rotated 30°)

previously. This might be due to the offset orientation of the upper tube causing the data to be less scattered.

Figure 5.34 shows the decreasing heat flux data for the data runs shown in Figure 5.33. At high heat fluxes, all the data lay on one nucleate boiling curve. Below 10 $kW/m^2$, separate curves are formed and as seen before. Significant enhancement of heat transfer from an upper tube is obtained when the lower tube is nucleating with a heat flux larger than 5 $kW/m^2$.

***f. TURBO-B Tubes with P/D of 2.0***

Figure 5.35 shows the decreasing heat flux data for the TURBO-B tubes taken at five lower tube heat flux settings. At the start of each run, a very consistent boiling curve is seen above 20 $kW/m^2$, indicating that above a UTHFS of 20 $kW/m^2$, there is no enhancement from increasing the LTHFS. Below 10 $kW/m^2$, raising the LTHFS does increase the heat transfer performance of the upper tube. At an upper tube heat flux of 2 $kW/m^2$, an increase in performance of 2.4 is found going from an unheated lower tube to a LTHFS of 20 $kW/m^2$, compared to an increase of 3.6 for the smooth tube array (Figure 5.26).

***g. TURBO-B Tubes with P/D of 1.8***

Figure 5.36 shows the decreasing heat flux data for the TURBO-B tubes taken at five lower tube heat flux settings. Similar results are found compared to the P/D of 2.0 case. At

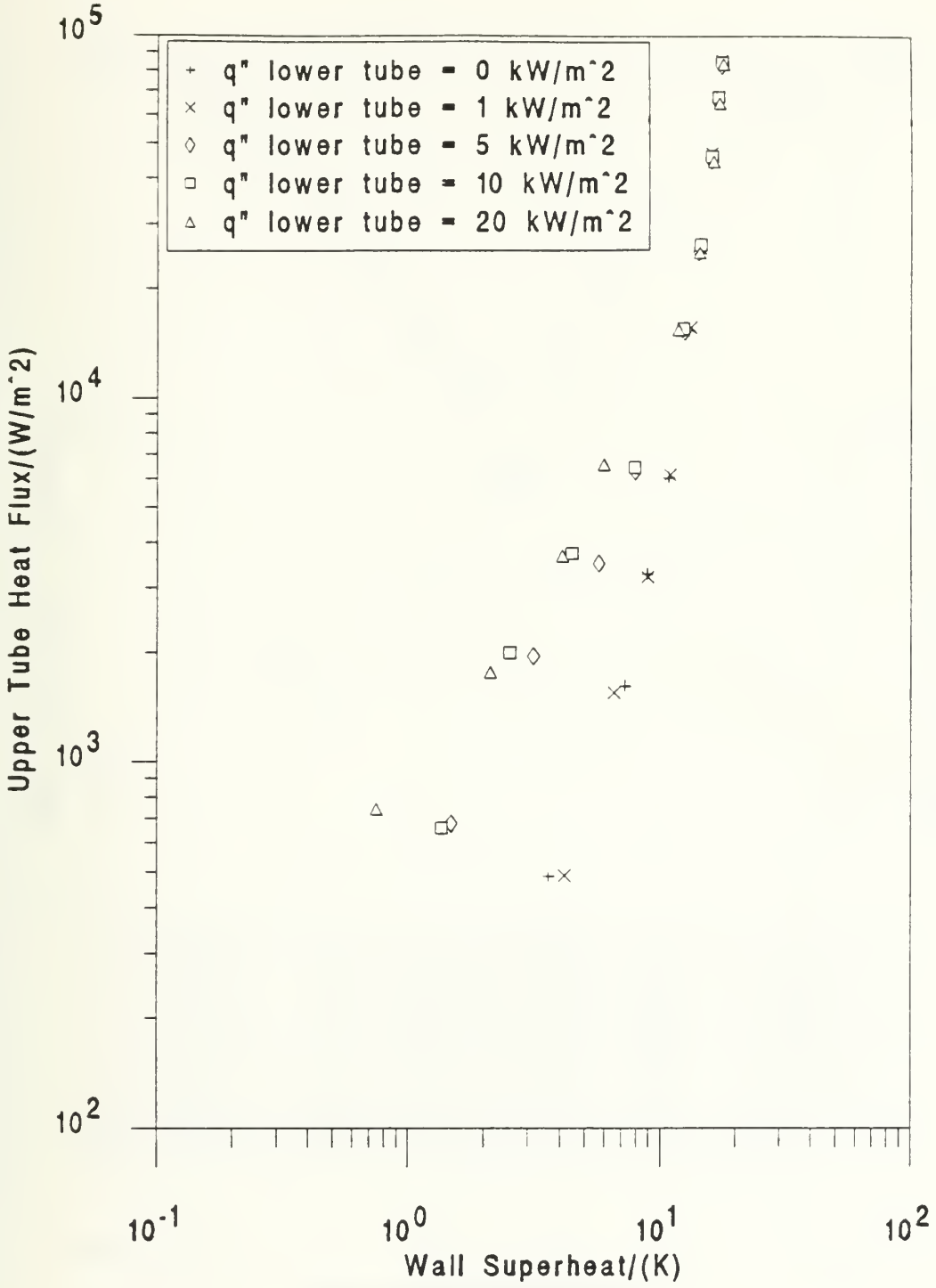


Figure 5.34 Comparison of Lower Tube Heat Flux Settings on Decreasing Heat Flux of Smooth Tubes with P/D of 1.2 (Rotated 30°)

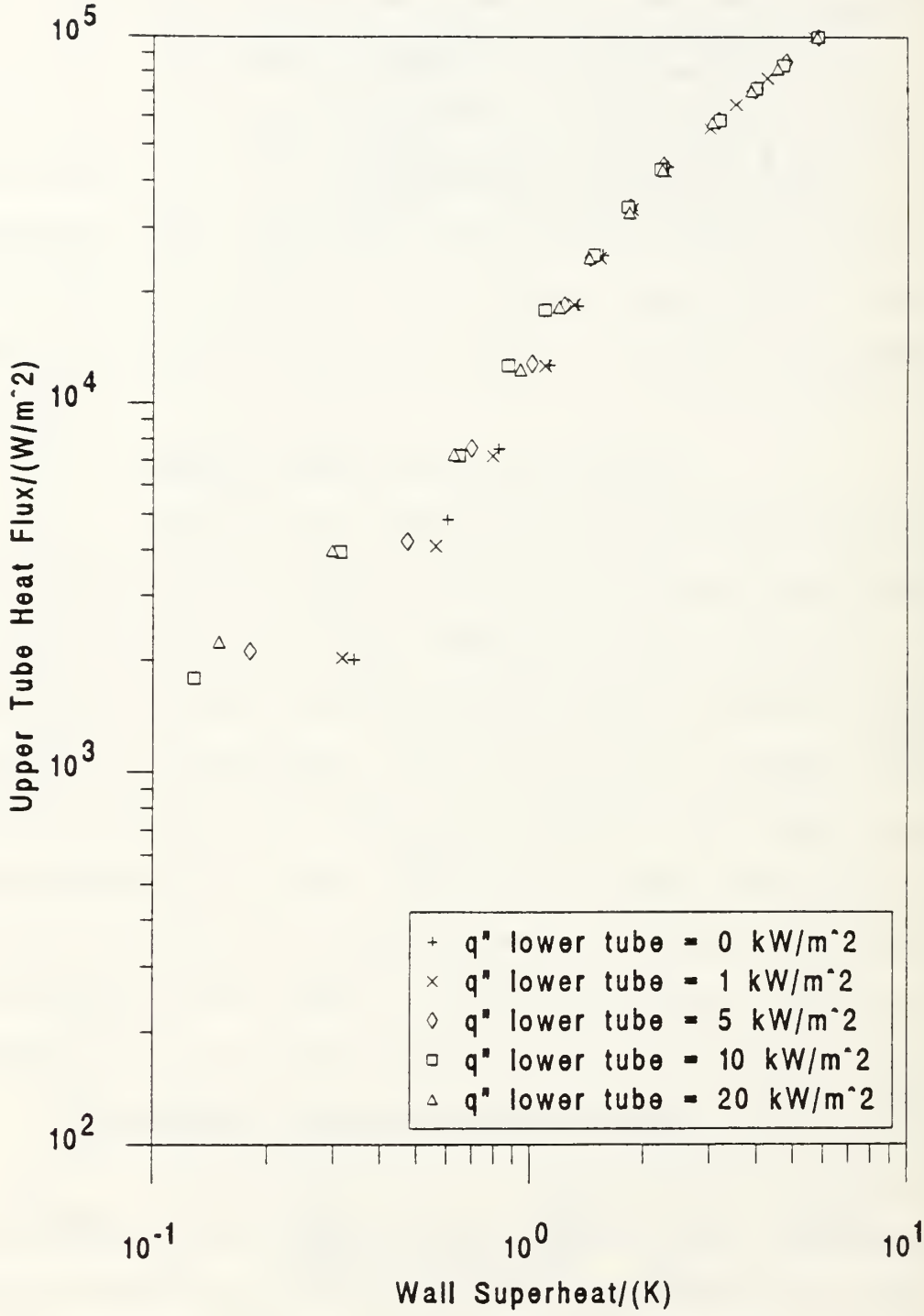


Figure 5.35 Comparison of Lower Tube Heat Flux Settings on Decreasing Heat Flux of TURBO-B Tubes with P/D of 2.0

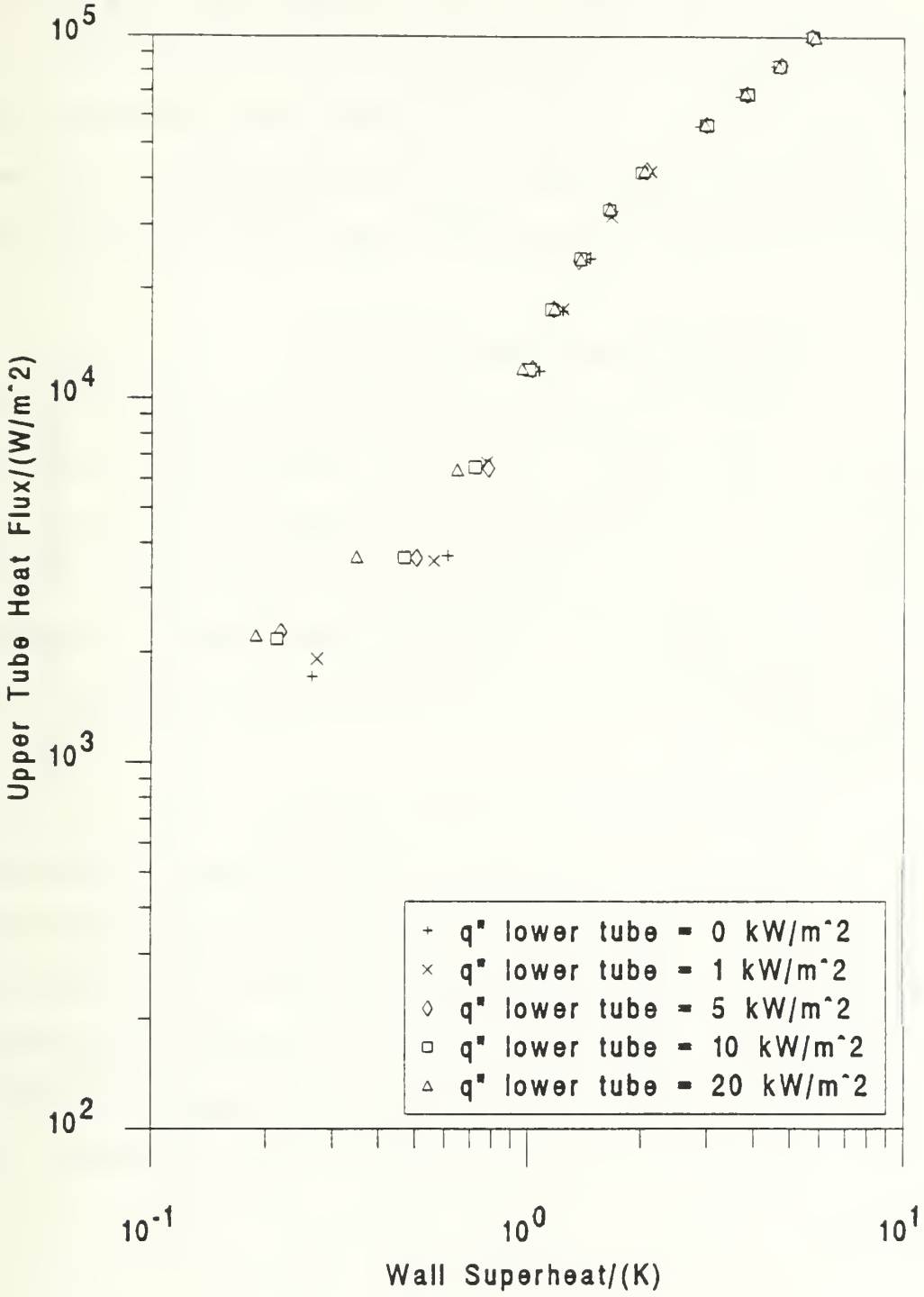


Figure 5.36 Comparison of Lower Tube Heat Flux Settings on Decreasing Heat Flux of TURBO-B Tubes with P/D of 1.8

an upper tube heat flux of 2 $kW/m^2$, an increase in performance of 1.6 is found going from a unheated lower tube to a LTHFS of 20 $kW/m^2$, compared to an increase of 3.7 for the smooth tube array (Figure 5.28). Unlike the smooth tube case where a P/D of 1.8 produced the best heat transfer performance in nucleate boiling, no optimal P/D ratio was found for the TURBO-B tube array.

***h. TURBO-B Tubes with P/D of 1.5***

Figure 5.37 shows the decreasing heat flux data for the TURBO-B tubes taken at five lower tube heat flux settings. Similar results are found compared to the P/D of 1.8 case. At an upper tube heat flux of 2 $kW/m^2$, an increase in performance of 2.2 is found going from a unheated lower tube to a LTHFS of 20 $kW/m^2$, compared to an increase of 3.5 for the smooth tube array (Figure 5.30).

***i. TURBO-B Tubes with P/D of 1.2***

Figure 5.38 shows the decreasing heat flux data for the TURBO-B tubes taken at five lower tube heat flux settings. Similar results are found compared to the P/D of 1.5 case. At an upper tube heat flux of 2 $kW/m^2$, an increase in performance of 2.2 is found going from a unheated lower tube to a LTHFS of 20 $kW/m^2$, compared to an increase of 5.4 for the smooth tube array (Figure 5.32).

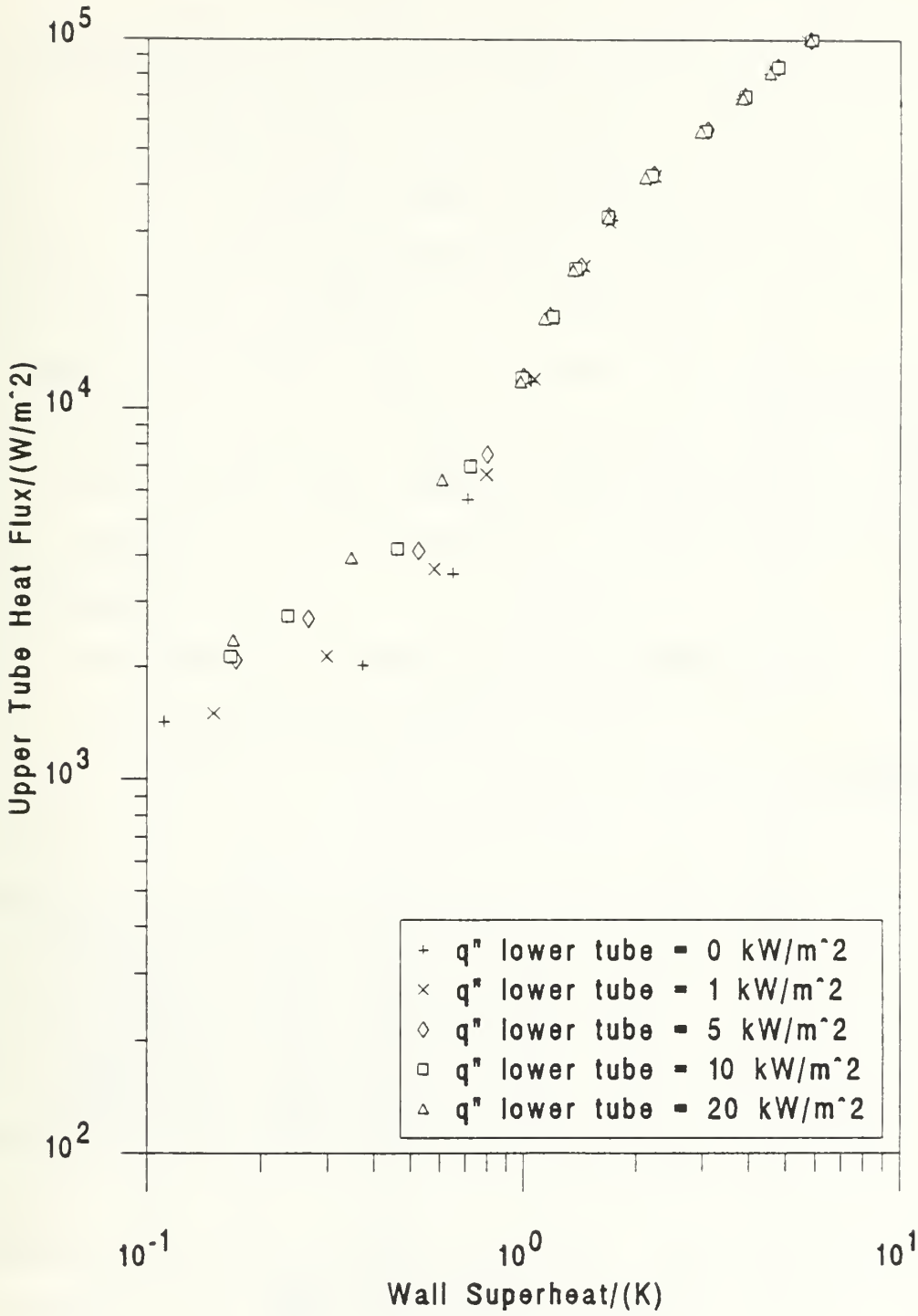


Figure 5.37 Comparison of Lower Tube Heat Flux Settings on Decreasing Heat Flux of TURBO-B Tubes with P/D of 1.5

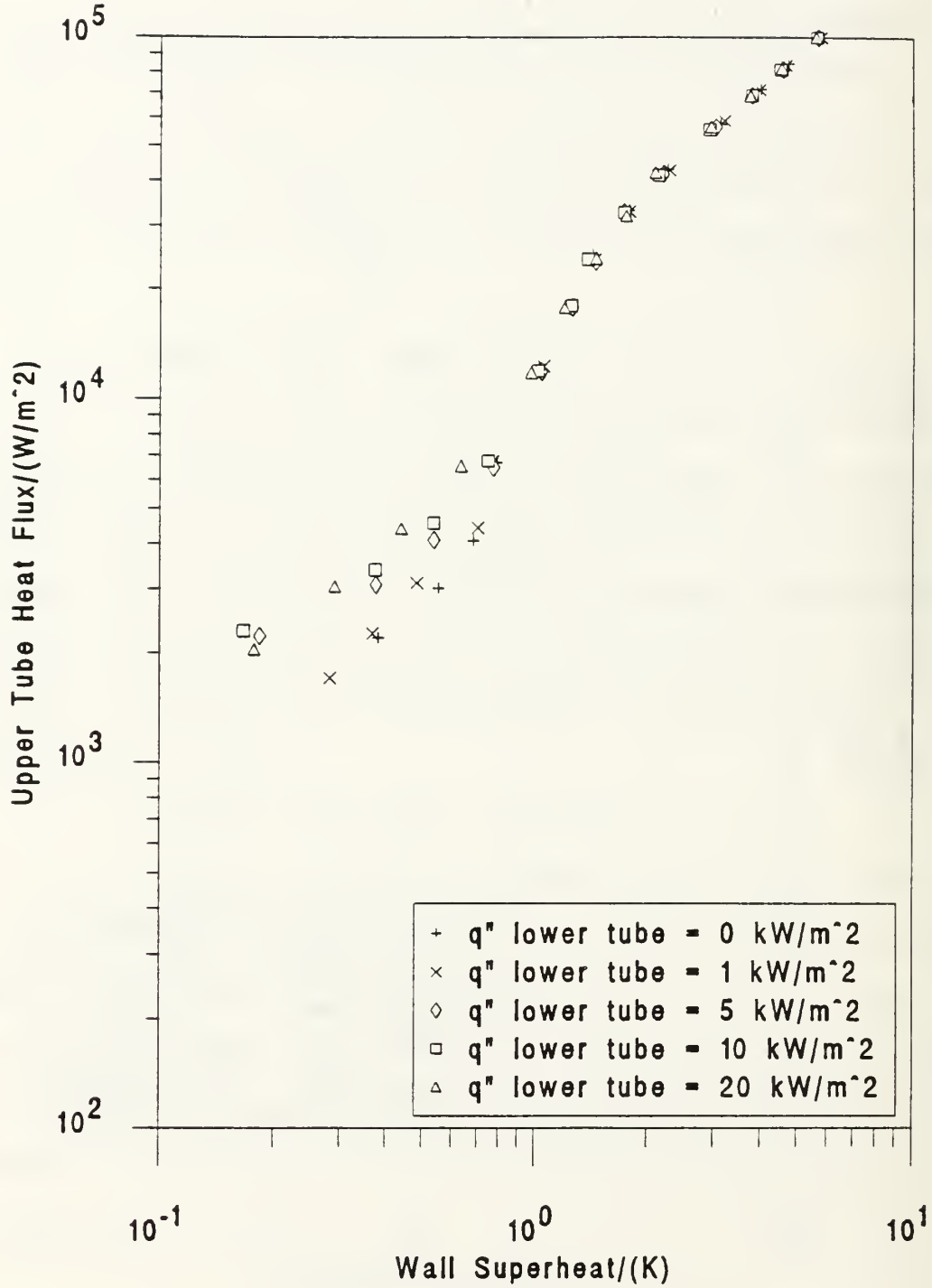


Figure 5.38 Comparison of Lower Tube Heat Flux Settings on Decreasing Heat Flux of TURBO-B Tubes with P/D of 1.2

*j. TURBO-B Tubes with P/D of 1.2 (Rotated 30°)*

Figure 5.39 shows the decreasing heat flux data for the TURBO-B tubes taken at five lower tube heat flux settings. A very consistent boiling curve is again seen above 10 $kW/m^2$. Below 10 $kW/m^2$, the data seems less scattered and slightly to the left of any other configuration, indicating that rotating the upper tube reduces the enhancement produced from increasing the LTHFS in the low heat flux regions. At an upper tube heat flux of 2 $kW/m^2$, an increase in performance of 1.7 is found going from a unheated lower tube to a LTHFS of 20 $kW/m^2$, compared to an increase of 3.5 for the smooth tube array (Figure 5.34).

**3. The Effect of a Variable Lower Tube Heat Flux**

*a. Smooth Tubes with P/D of 2.0*

Figure 5.40 shows the heat transfer performance of an upper tube, held at a constant heat flux, as the lower tube heat flux is varied. The three fixed UTHFS used were 5, 10 and 20 $kW/m^2$. The labeling in the plot legend describes which data were taken using increasing or decreasing lower tube heat flux. The sharp transitions in the increasing curves are the points where the lower tube nucleated and caused the upper tube to shift from natural convection to nucleate boiling (visually verified during the data run), significantly increasing the upper tube heat transfer coefficient, as expected. The maximum upper tube heat transfer coefficient

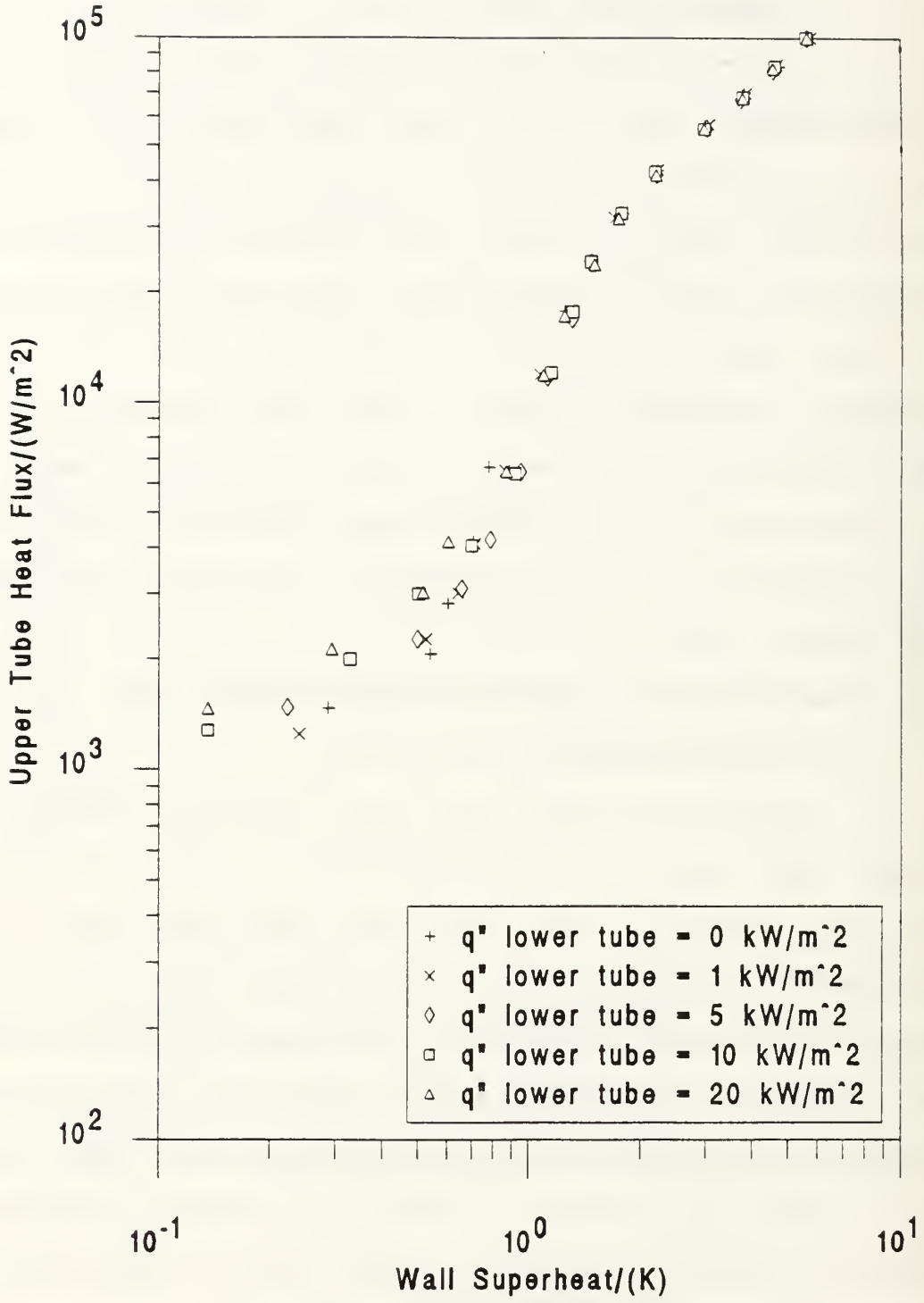


Figure 5.39 Comparison of Lower Tube Heat Flux Setting on Decreasing Heat Flux of TURBO-B Tubes with P/D of 1.2 (Rotated 30°)

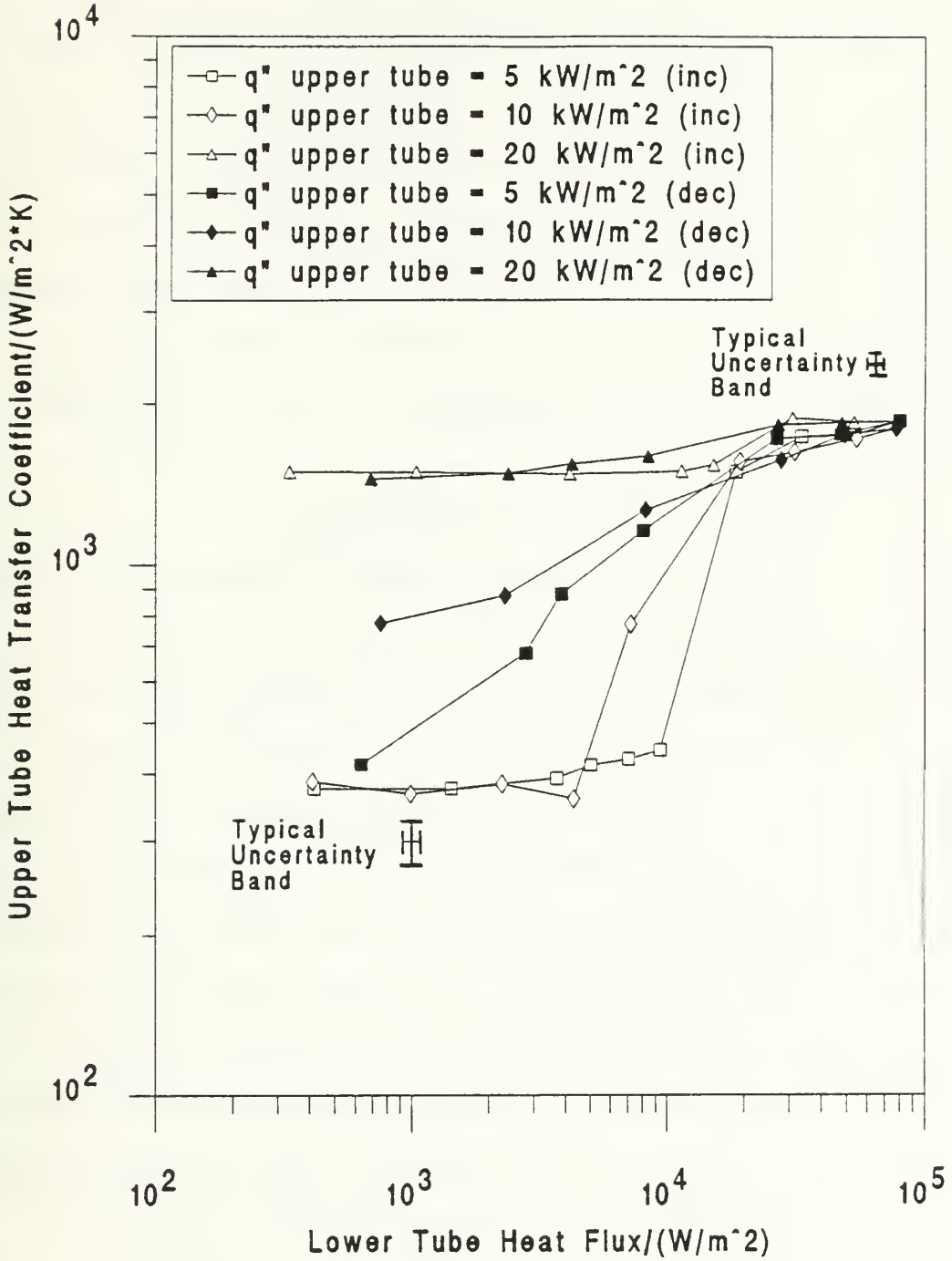


Figure 5.40 Heat Transfer Performance of a Smooth Upper Tube at a Constant Heat Flux for a P/D of 2.0

for all three UTHFS was 1850 $W/m^2 \cdot K$, which indicates that at a lower tube heat flux of 80 $kW/m^2$, the heat transfer performance of the upper tube is independent of the lower tube heat flux. The decreasing curves show that for an UTHFS of 20 $kW/m^2$, the lower tube heat flux has little influence on the upper tube heat transfer. For the UTHFS of 10 $kW/m^2$, as the lower tube heat flux is decreased, the upper tube remains in nucleate boiling, but for the UTHFS of 5 $kW/m^2$, the upper tube returns to the natural convection region as the lower tube heat flux is decreased.

***b. Smooth Tubes with P/D of 1.8***

Figure 5.41 shows the heat transfer performance of an upper tube, held at a constant heat flux, as the lower tube heat flux is varied. Similar results were obtained as in the P/D of 2.0 case, except that the curves did not merge at the highest heat flux setting. The maximum heat transfer coefficient for the UTHFS of 5 and 10 $kW/m^2$ converged at approximately 1700 $W/m^2 \cdot K$ and for the UTHFS of 20 $kW/m^2$ the value was about 1900 $W/m^2 \cdot K$. It is not known why the curves did not merge at high lower tube heat fluxed. Comparing these results to the P/D of 2.0 results, at the smallest lower tube heat fluxes, the P/D of 1.8 provides better heat transfer.

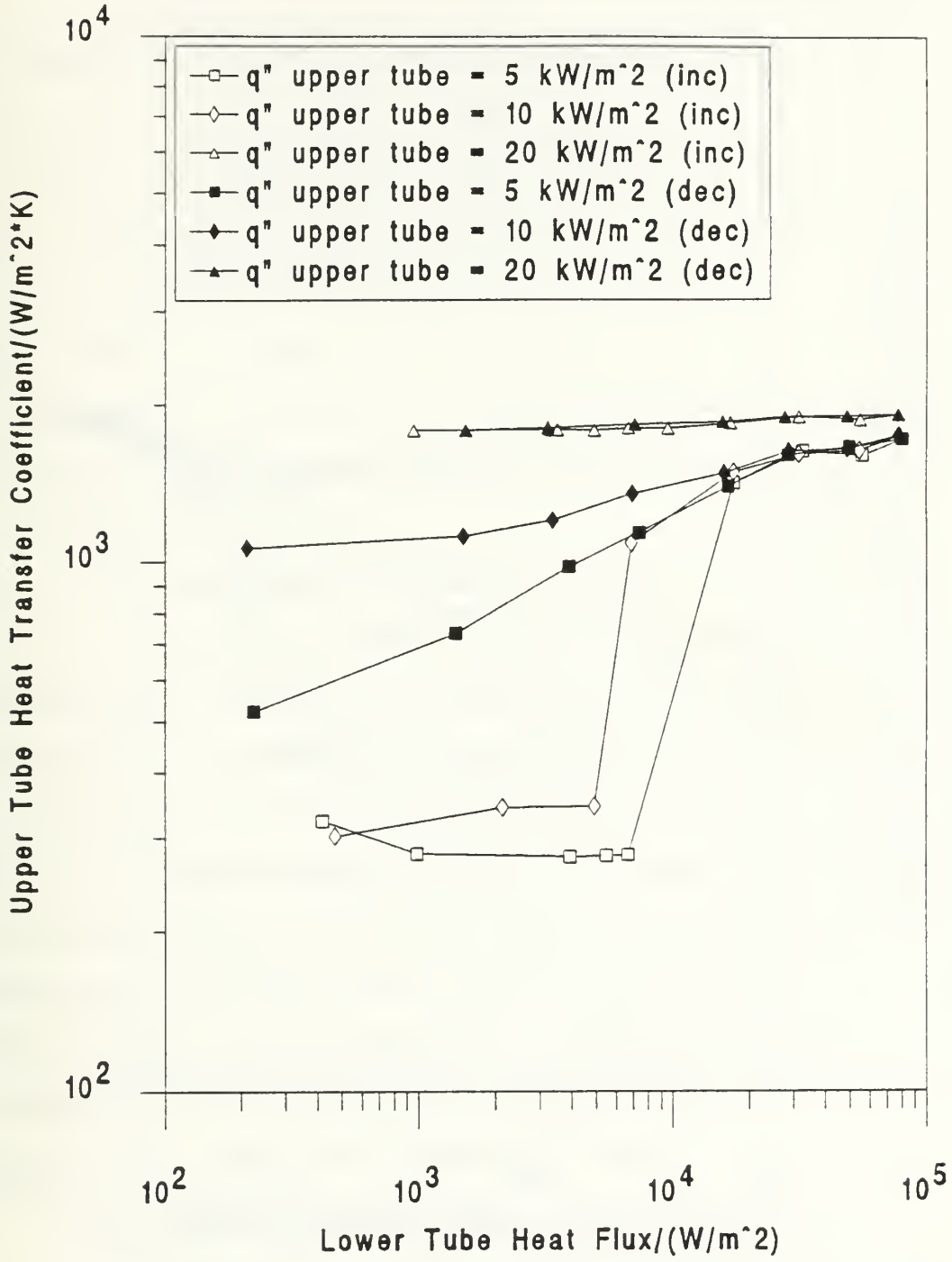


Figure 5.41 Heat Transfer Performance of a Smooth Upper Tube at a Constant Heat Flux for a P/D of 1.8

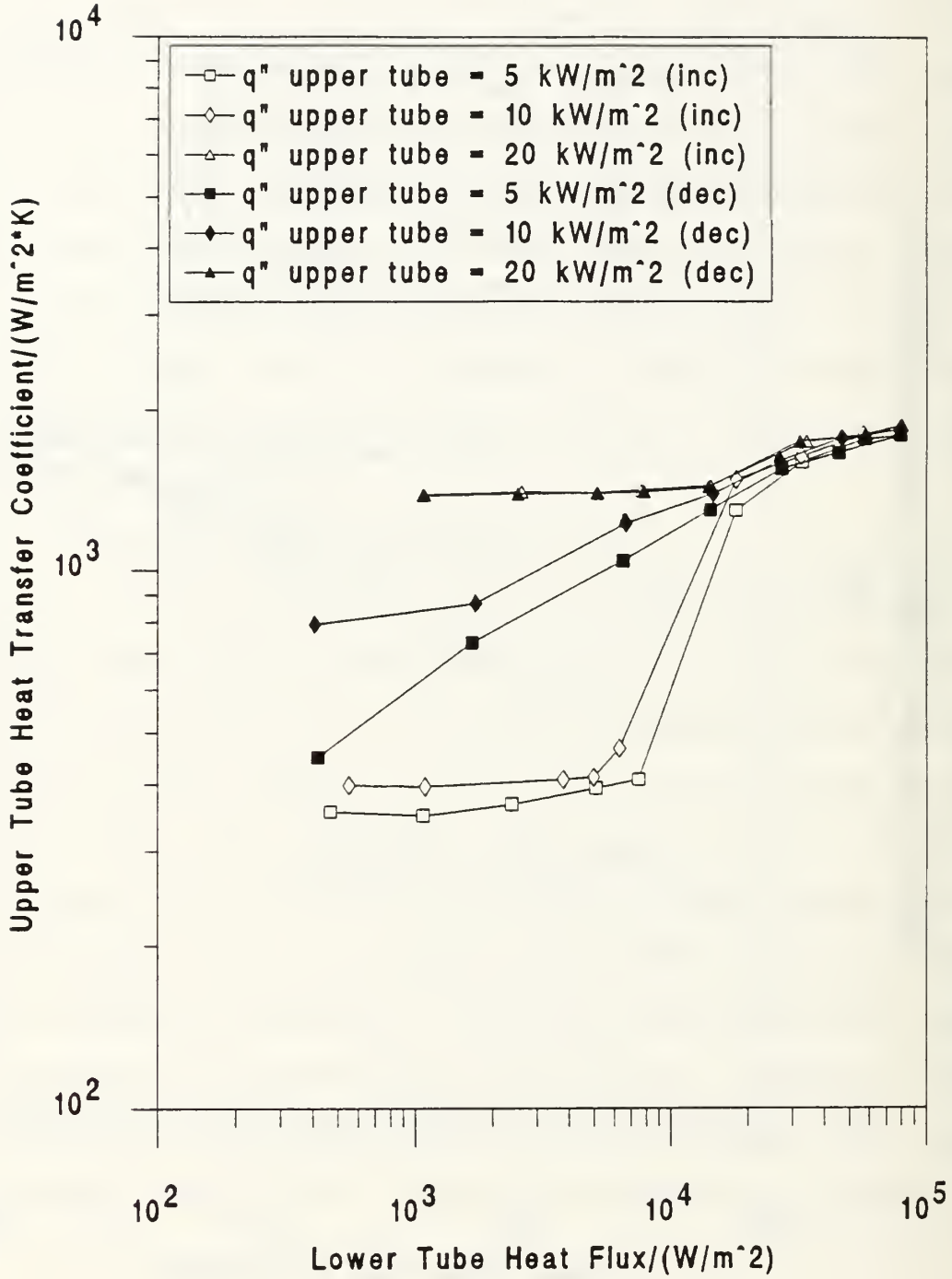


Figure 5.42 Heat Transfer Performance of a Smooth Upper Tube at a Constant Heat Flux for a P/D of 1.5

*c. Smooth Tubes with P/D of 1.5*

Figure 5.42 shows the heat transfer performance of an upper tube, held at a constant heat flux, as the lower tube heat flux is varied. The maximum heat transfer coefficient for all three of the UTHFS converged at approximately 1800 $W/m^2 \cdot K$, similar to the P/D of 2.0 case. The decreasing curves show very similar behavior found at a P/D of 2.0. Comparing these results to data of a P/D of 2.0 and 1.8, a P/D of 2.0 and 1.5 are similar in the amount of enhancement achieved, whereas a P/D of 1.8 outperforms them both, in the mid to low heat flux regions.

*d. Smooth Tubes with P/D of 1.2*

Figure 5.43 shows the heat transfer performance of an upper tube, held at a constant heat flux, as the lower tube heat flux is increased. The maximum heat transfer coefficient for all three of the UTHFS converged, as did the P/D of 2.0 and 1.5, at approximately 1990 $W/m^2 \cdot K$, highest value of all the configurations tested. Therefore, the best heat transfer performance was given by a P/D ratio of 1.8 when the lower tube heat flux was held constant, but a P/D ratio of 1.2 when the upper tube heat flux was held constant. No decreasing curves were recorded for these data runs.

*e. Smooth Tubes with P/D of 1.2 (Rotated 30°)*

Figure 5.44 shows the heat transfer performance of an upper tube, held at a constant heat flux, as the lower tube

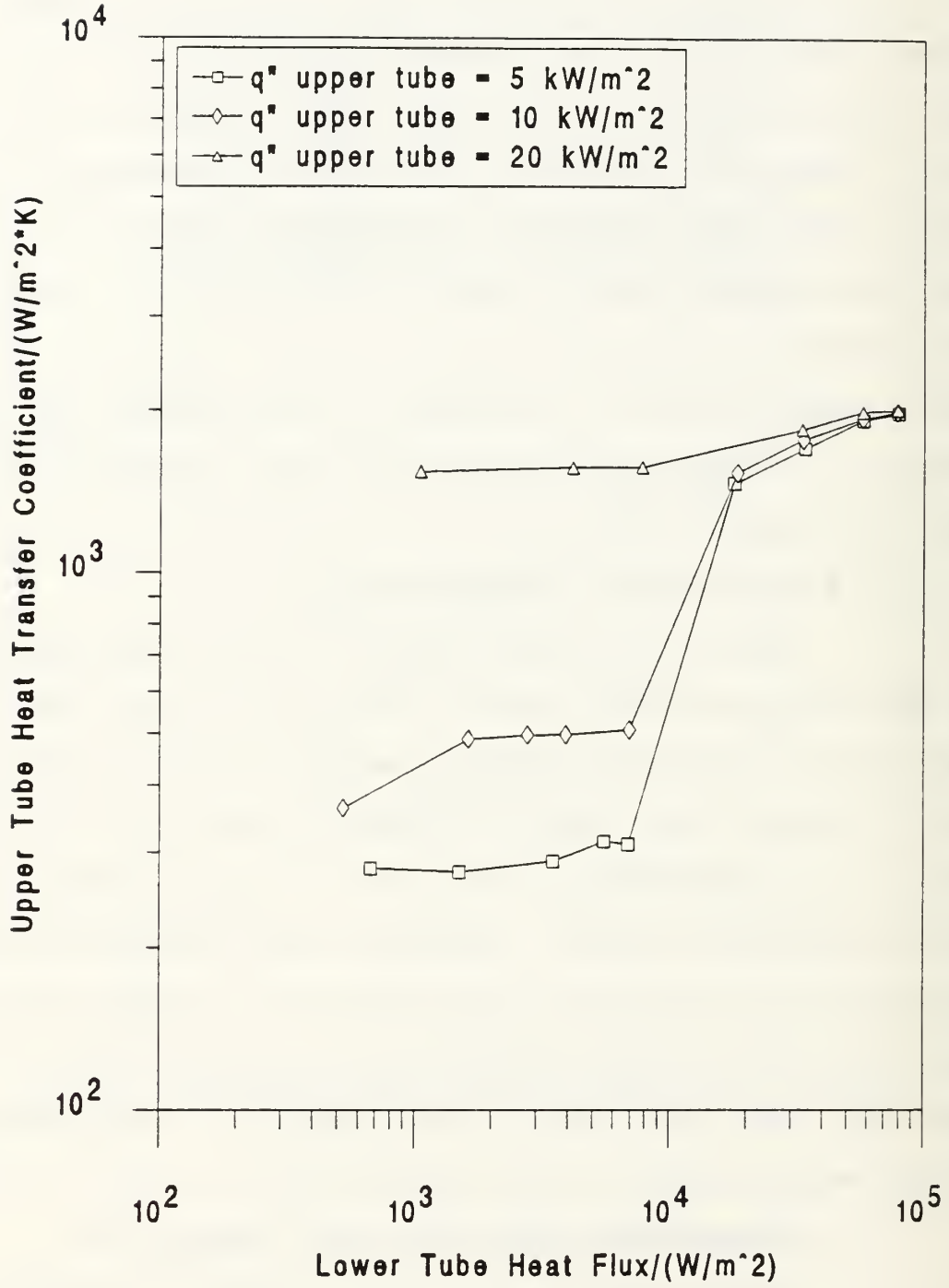


Figure 5.43 Heat Transfer Performance of a Smooth Upper Tube at a Constant Heat Flux for a P/D of 1.2

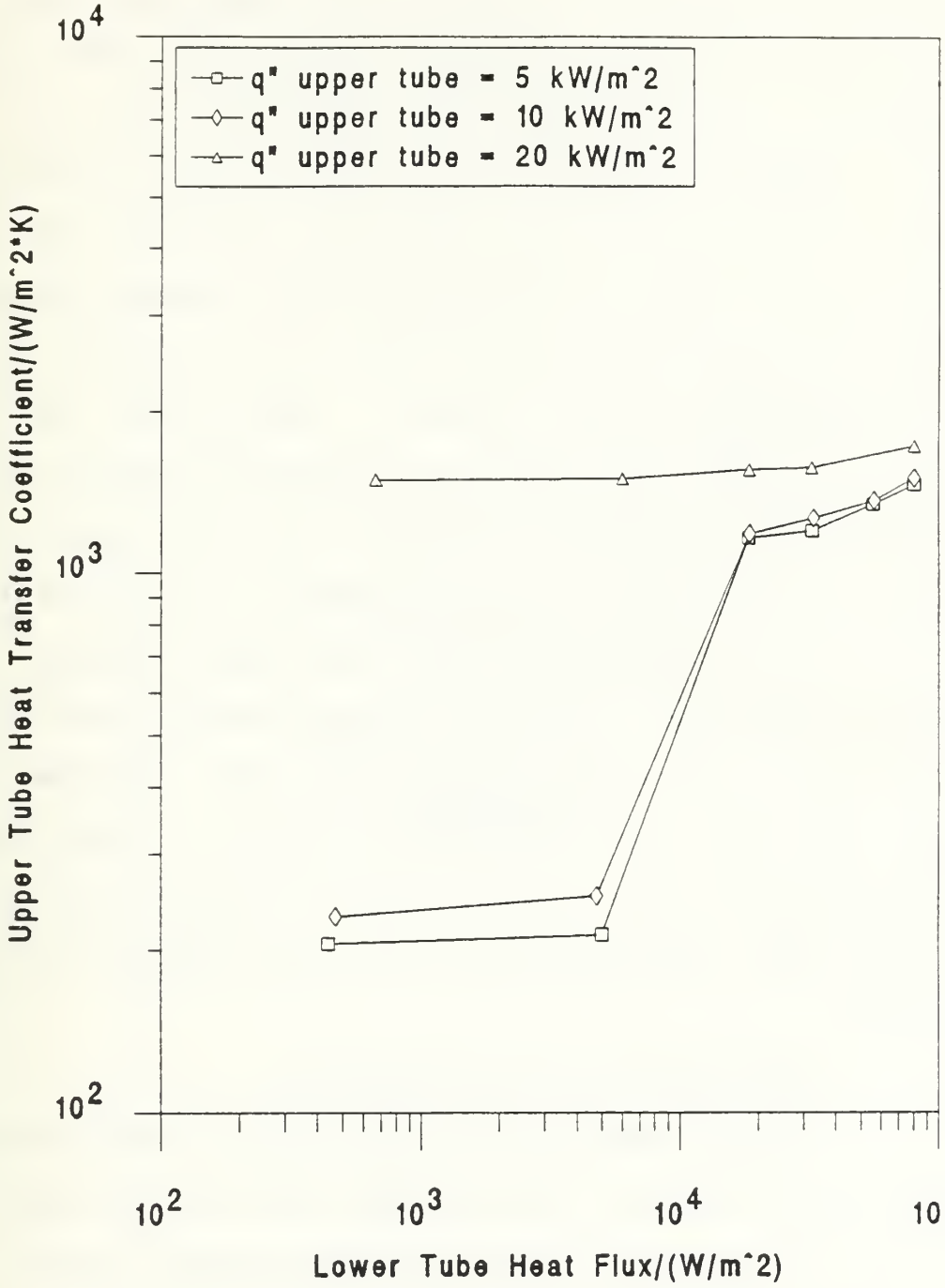


**Figure 5.44 Heat Transfer Performance of a Smooth Upper Tube at a Constant Heat Flux for a P/D of 1.2 (Rotated 30°)**

heat flux is increased. As seen for the P/D of 1.8 case, the curves do not merge at the highest lower tube heat flux. The maximum heat transfer coefficient for the two lower curves converged at about 1500 $W/m^2 \cdot K$ and the upper curve was 1725 $W/m^2 \cdot K$. Comparing Figures 5.43 and 5.44, for an UTHFS of 20 $kW/m^2$, the data curves are identical for lower tube heat fluxes up to 8 $kW/m^2$, indicating that the forced convection effects from the lower tube have very little influence on the upper tube heat transfer behavior. Above lower tube heat fluxes of 10 $kW/m^2$, the in-line configuration provides better heat transfer performance because the lower tube is in nucleate boiling and all of the bubbles are impacting the upper tube providing enhancement by *bubble pumping;* as opposed to the offset configuration, where most of the bubbles coming off the lower tube miss the upper tube. The same idea holds true for the other data curves. The in-line configurations are more enhanced due to *bubble pumping* from the lower tube. No decreasing curves were recorded for these data runs.

***f. TURBO-B Tubes with P/D of 2.0***

Figure 5.45 shows the heat transfer performance of an upper tube, held at a constant heat flux, as the lower tube heat flux is decreased. At high lower tube heat fluxes, all three of the UTHFS appear to perform almost equally. For an UTHFS of 20 $kW/m^2$, the lower tube heat flux has little

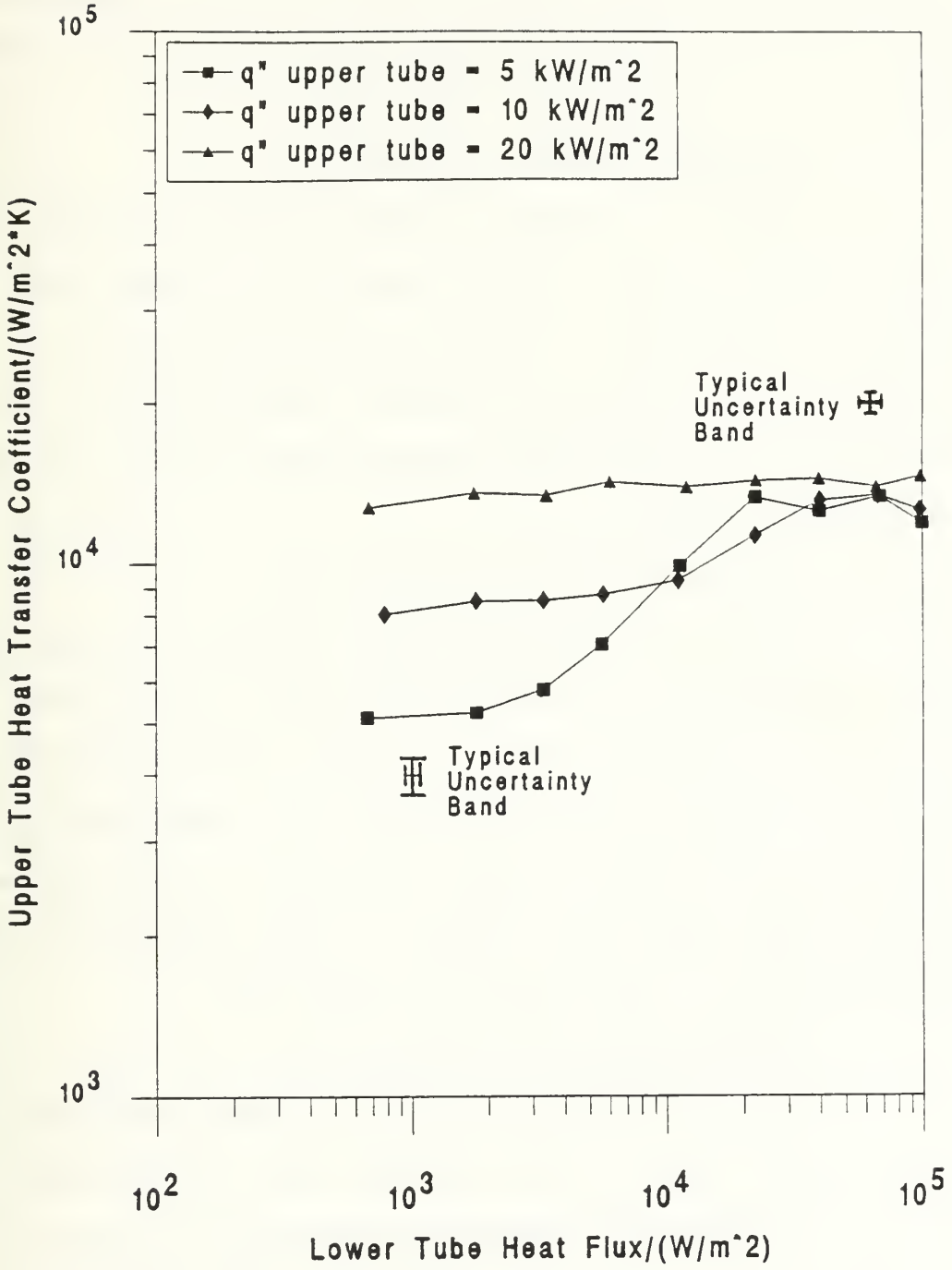


Figure 5.45 Heat Transfer Performance of a TURBO-B Upper Tube at a Constant Heat Flux for a P/D of 2.0

influence on the upper tube heat transfer and for an UTHFS of 5 and 10 $kW/m^2$, as the lower tube heat flux is decreased so follows the performance of the upper tube (more for 5 than 10 $kW/m^2$).

***g. TURBO-B Tubes with P/D of 1.8***

Figure 5.46 shows the heat transfer performance of an upper tube, held at a constant heat flux, as the lower tube heat flux is decreased. Comparing these curves to the ones for a P/D of 2.0, a small enhancement in performance is gained in the mid and low heat flux regions using a P/D of 1.8, which is an expected result.

***h. TURBO-B Tubes with P/D of 1.5***

Figure 5.47 shows the heat transfer performance of an upper tube, held at a constant heat flux, as the lower tube heat flux is decreased. There is very little difference in performance between a P/D of 1.5 and 1.8. Comparing the P/D of 1.5 to the 2.0 data, a small decrease in performance is noted for lower tube heat fluxes > 20 $kW/m^2$ using the P/D of 1.5 configuration, which cannot be explained.

***i. TURBO-B Tubes with P/D of 1.2***

Figure 5.48 shows the heat transfer performance of an upper tube, held at a constant heat flux, as the lower tube heat flux is decreased. Similar performance is noted for a P/D ratio of 1.2 and 1.5, therefore, the comments made previously still apply.

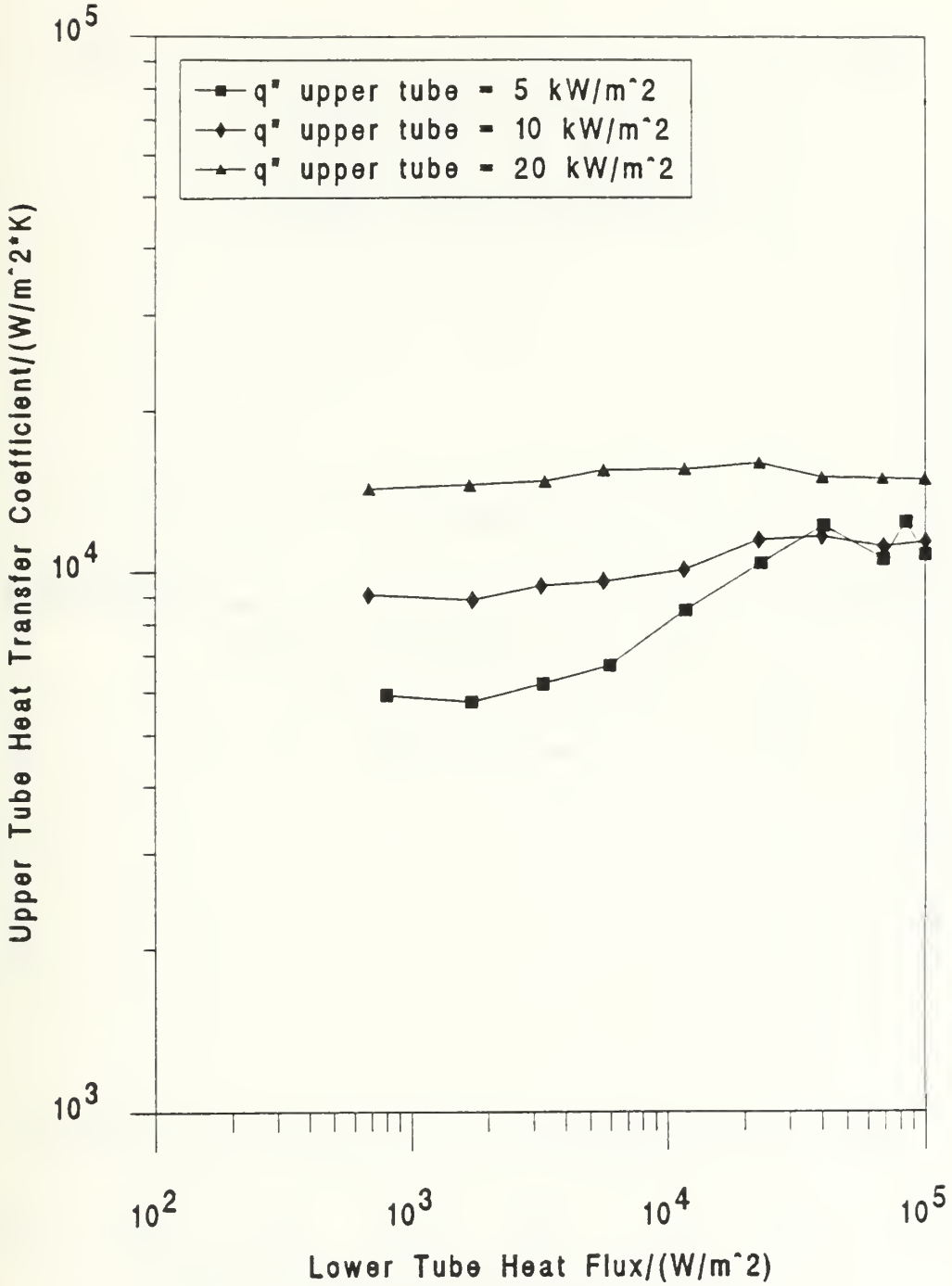


Figure 5.46 Heat Transfer Performance of a TURBO-B Upper Tube at a Constant Heat Flux for a P/D of 1.8

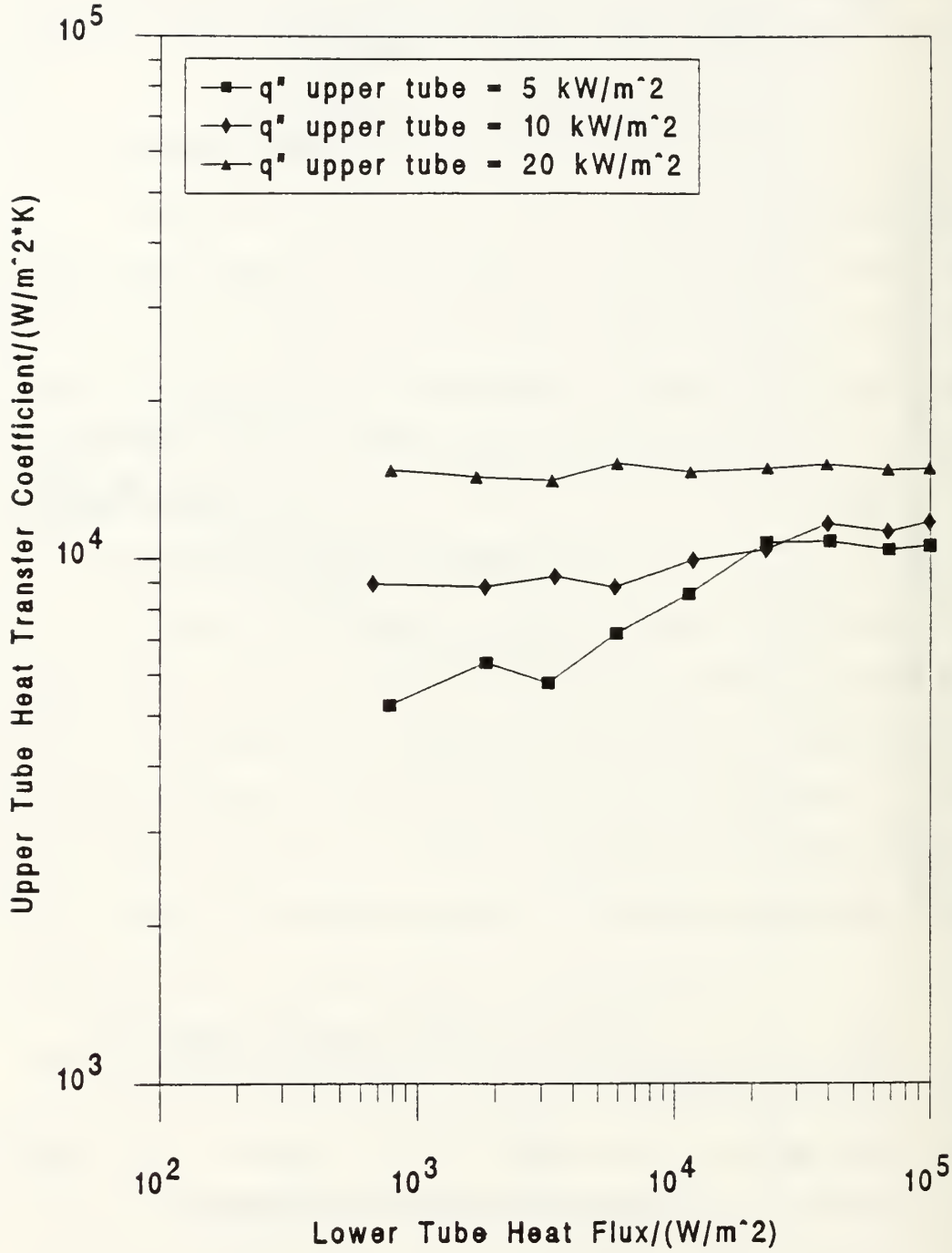


Figure 5.47 Heat Transfer Performance of a TURBO-B Upper Tube at a Constant Heat Flux for a P/D of 1.5

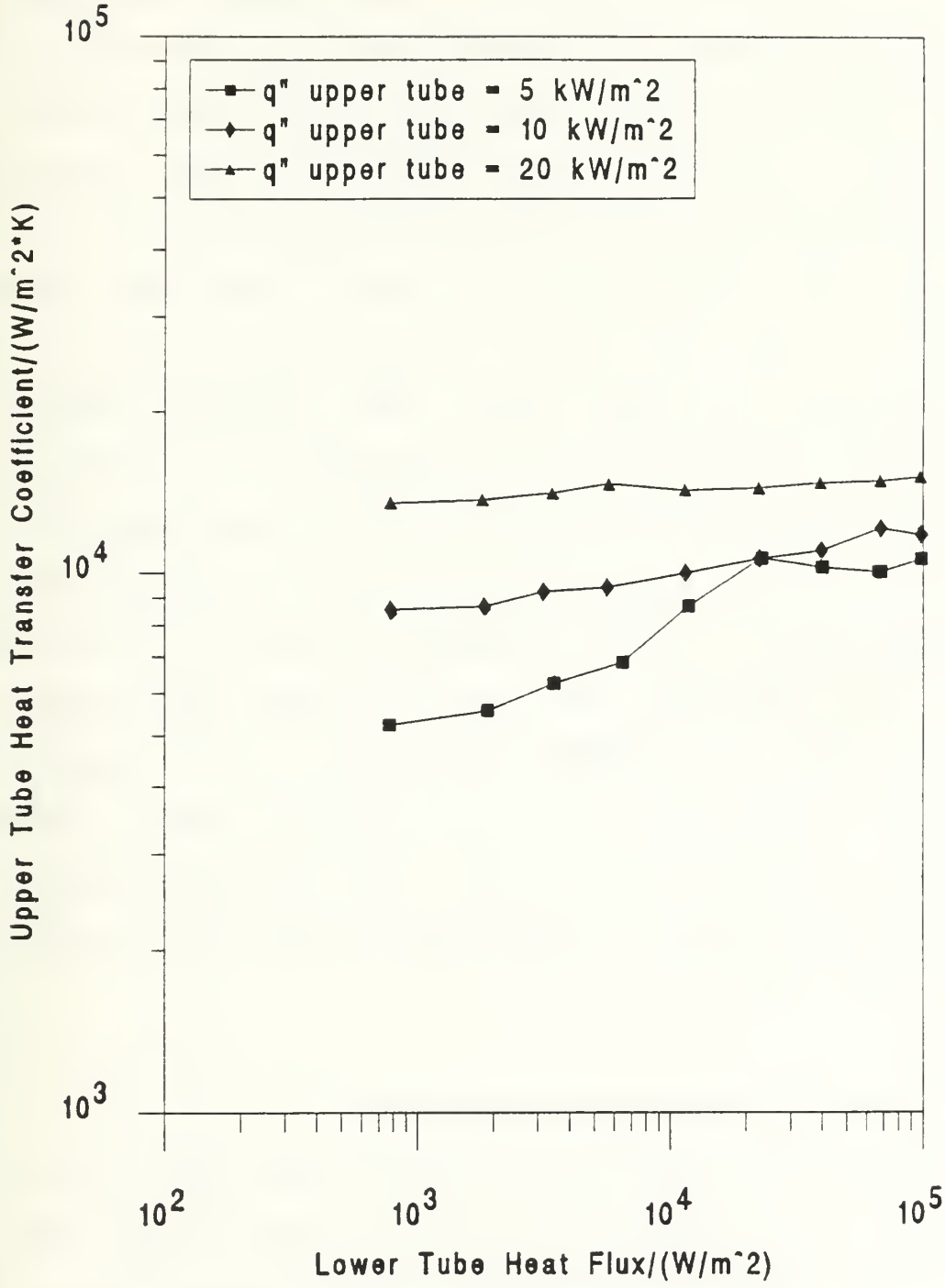


Figure 5.48 Heat Transfer Performance of a TURBO-B Upper Tube at a Constant Heat Flux for a P/D of 1.2

*j. TURBO-B Tubes with P/D of 1.2 (Rotated 30°)*

Figure 5.49 shows the heat transfer performance of an upper tube, held at a constant heat flux, as the lower tube heat flux is decreased. Comparing Figures 5.48 and 5.49, for an UTHFS of 20 $kW/m^2$, the data curves are almost identical, indicating that the lower tube orientation and heat flux have very little influence on the upper tube heat transfer behavior. For the other two data curves, the in-line configuration provides better heat transfer performance because of *bubble pumping,* discussed earlier. For the offset configuration, all of the data curves do not merge and are almost horizontal lines, indicating there is no enhancement by *bubble pumping.* It is believed that most of the bubbles coming off the lower tube miss the upper tube because the bubbles depart the TURBO-B tube surface at the upper most section of the tube, which is different than how bubbles depart the smooth tube surface. This phenomena needs to be further investigated. No decreasing curves were recorded for these data runs.

## C. R-124/R-114 PERFORMANCE COMPARISON

Figure 5.50 compares the decreasing heat flux data for R-124 found in this study with the R-114 data of Lake [Ref. 3] for smooth tube configurations listed in the plot legend, with the lower tube unheated. In the mid to high heat flux

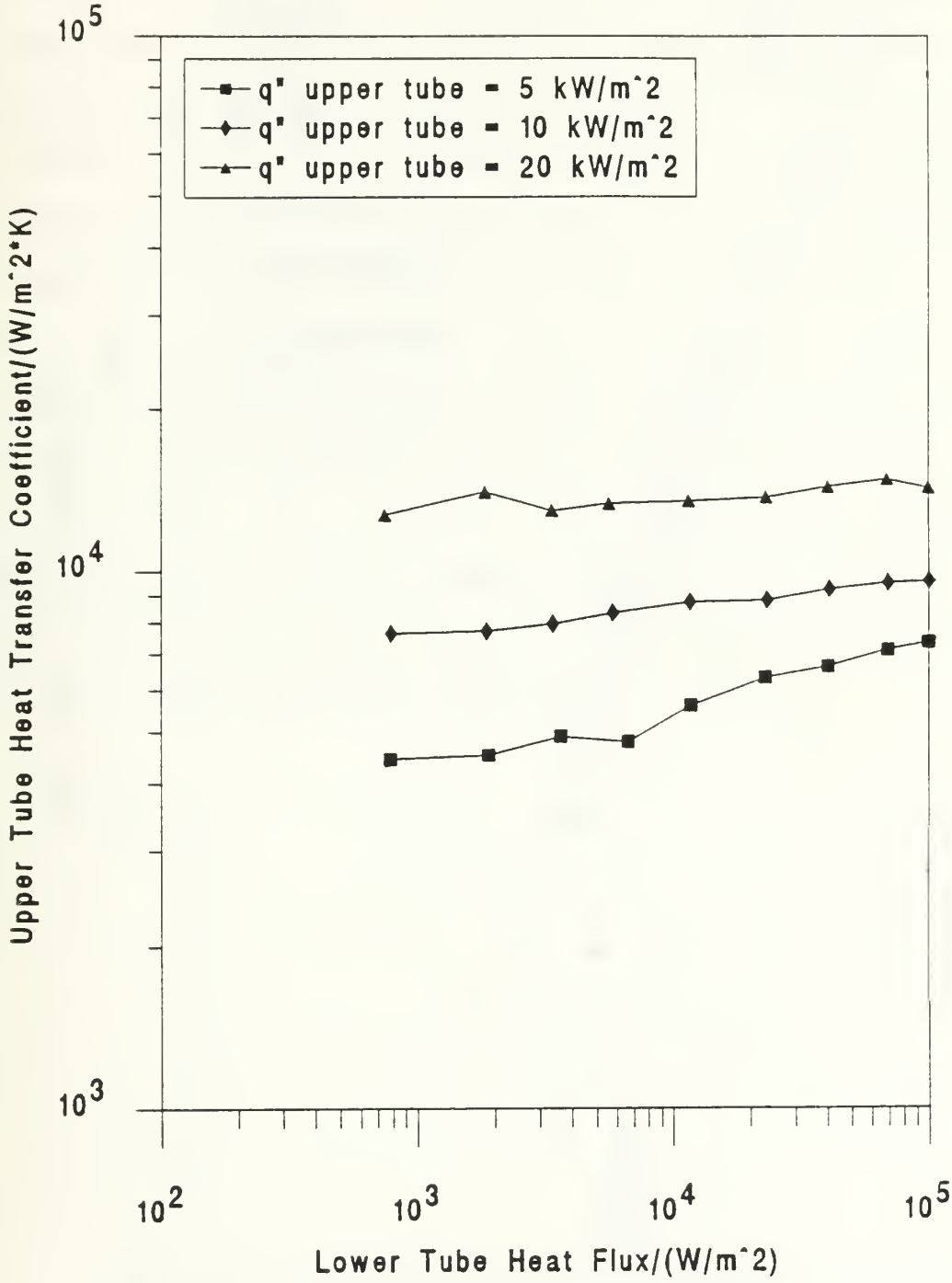


Figure 5.49 Heat Transfer Performance of a TURBO-B Upper Tube at a Constant Heat Flux for a P/D of 1.2 (Rotated 30°)

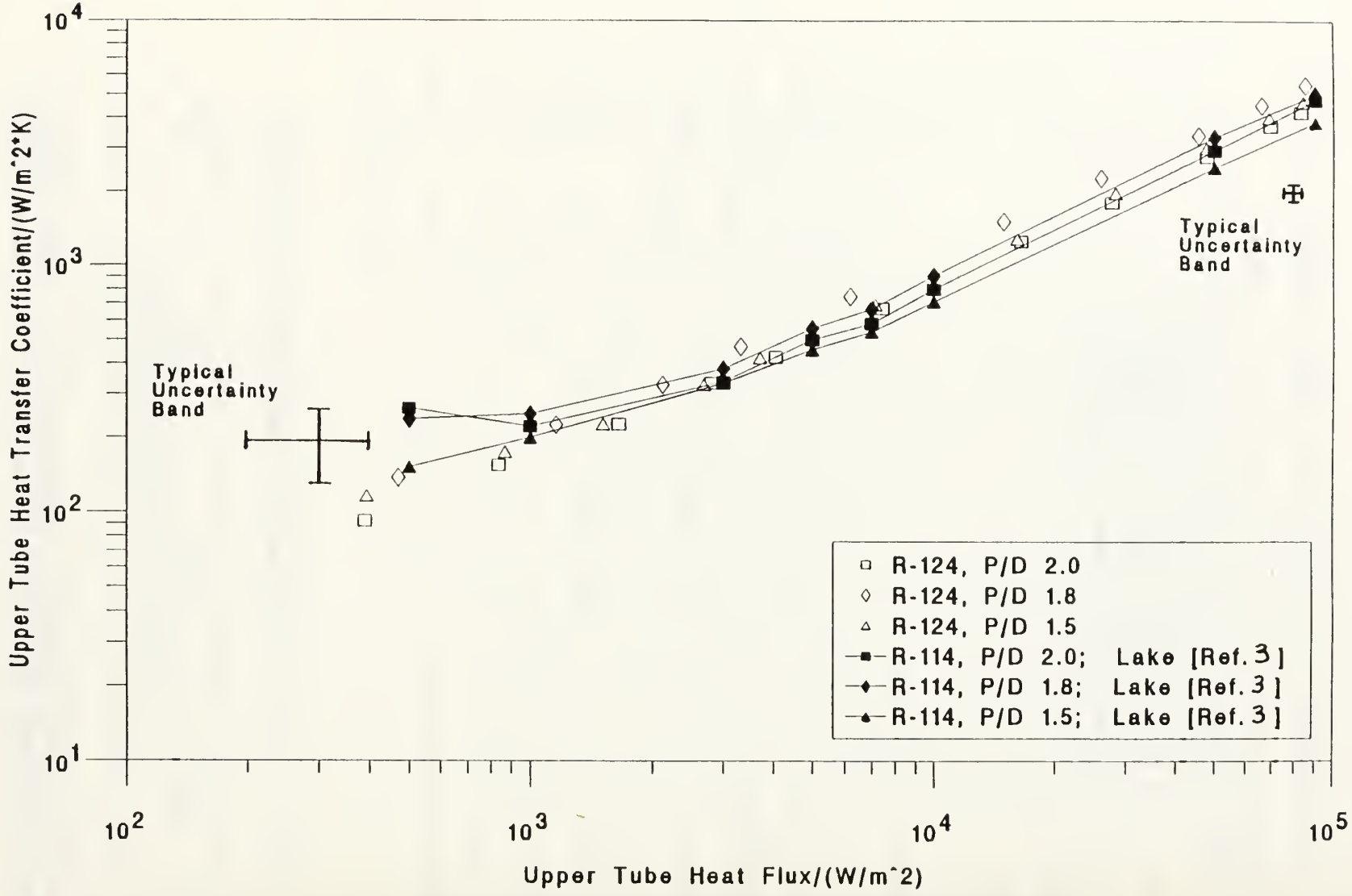


Figure 5.50 Comparison of R-124 to R-114 for Smooth Tubes with Decreasing Heat Flux and the Lower Tube Unheated

regions, the P/D ratios of 1.8 and 1.5 demonstrated improved performance with the R-124, but with a P/D of 2.0, little or no improvement was found. In the low heat flux region, the uncertainty is too large to make any definitive conclusions.

Figure 5.51 compares the decreasing heat flux data for R-124 with the R-114 data of Lake [Ref. 3] for the smooth tube configurations listed in the plot legend, with 10 $kW/m^2$ on the lower tube. In the high heat flux region, a P/D of 1.8 and 1.5 again provided better performance using R-124, but for R-114, a P/D of 2.0 displayed slightly better performance. In the mid-range heat fluxes, R-114 exhibited improved performance in each of the three configurations. Again, in the low heat flux region, there was too much uncertainty in the data to draw any viable conclusions.

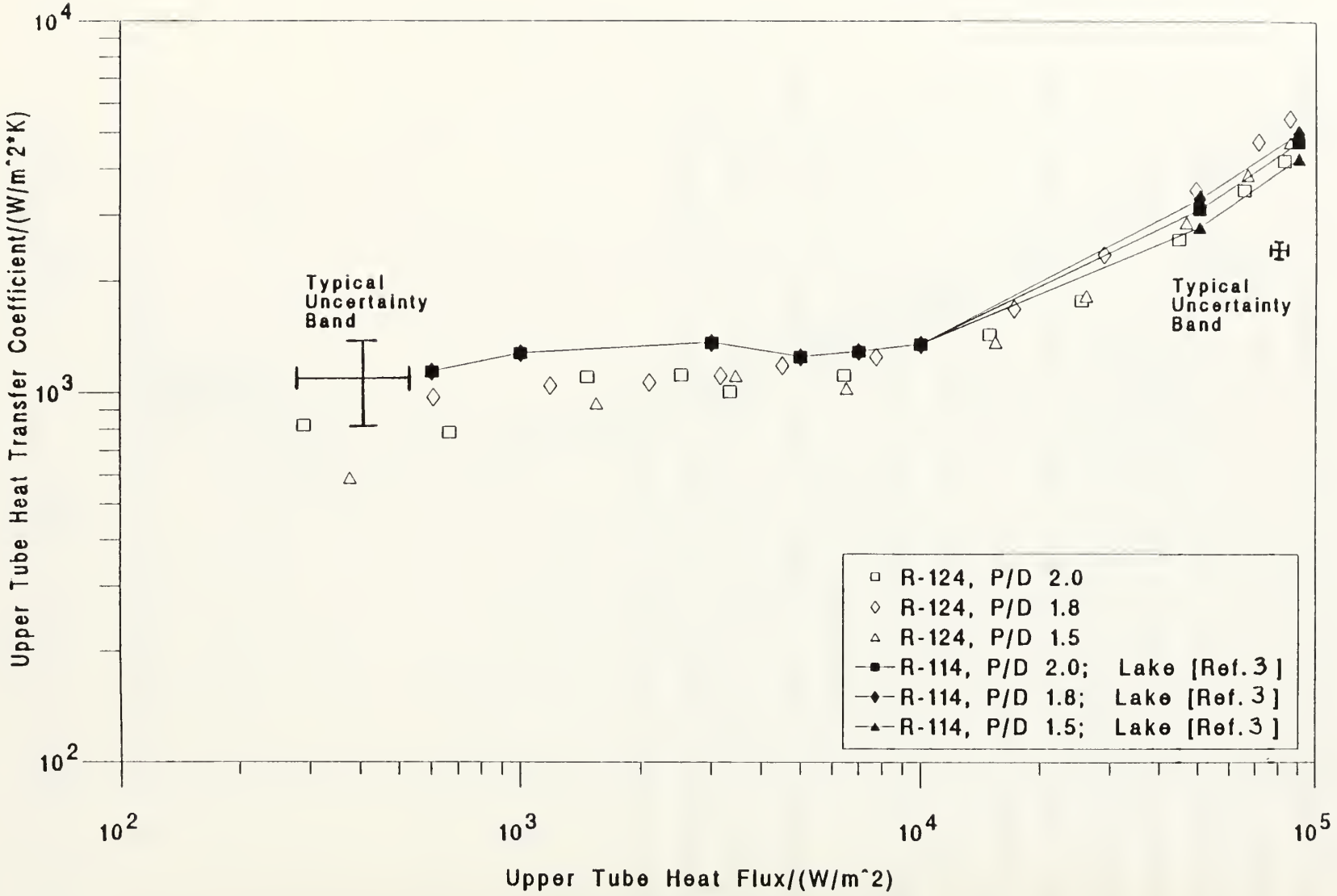


Figure 5.51 Comparison of R-124 to R-114 for Smooth Tubes with Decreasing Heat Flux and a LTHFS of 10 kW/m$^2$

# VI. CONCLUSIONS

The interaction effects of a lower heated tube on pool boiling of R-124 from an upper horizontal tube has been studied for tube two types: smooth and TURBO-B. Based on the data obtained, the following conclusions are made:

1. In natural convection, the effect of a lower heated tube on the heat transfer from an upper tube was small.

2. For a smooth tube array, a vigorously nucleating lower tube eliminated upper tube hysteresis.

3. For a smooth tube array in nucleate boiling, P/D of 1.8 gave the best upper tube heat transfer performance. No optimal P/D was found for the TURBO-B tube array.

4. For both arrays with upper tube heat fluxes < 5 $kW/m^2$, the enhancing effect of bubbles from a lower tube was dramatic. This enhancement increased as lower tube heat flux increased. When upper tube heat fluxes were > 20 $kW/m^2$, all enhancement disappeared.

5. For a TURBO-B tube array, a 30 degree offset of the upper tube reduced the upper tube heat transfer performance (compared to the in-line configurations). This may indicate bubbles depart TURBO-B tubes differently than smooth tubes.

6. For a smooth tube array with the lower tube unheated and an upper tube heat flux of > 3 $kW/m^2$, the performance of R-124 compared to R-114, improved as the P/D ratio was reduced. With a nucleating lower tube (at 10 $kW/m^2$), again the performance of R-124 improved as the P/D ratio decreased, but only for upper tube heat fluxes of > 40 $kW/m^2$.

# VII. RECOMMENDATIONS

1. Conduct further studies using TURBO-B tubes to verify that bubbles do depart the TURBO-B tubes differently than smooth tubes.

2. Conduct similar tests using different enhanced tubes to better understand the influence of a lower heated enhanced tube on the heat transfer behavior of an upper tube.

3. Modify the existing evaporator to accept a larger number of tubes (three and four smooth or enhanced tubes) and conduct tests to study the effect of multiple heated lower tubes on the heat transfer performance of an upper tube.

4. Conduct similar tests using multiple tube configurations with R-124/oil mixtures to determine the effect of oil on the heat transfer performance of an upper tube.

## APPENDIX A. PROGRAM SETUPJY

Program SETUPJY was used to evaluate the system performance prior to commencing a data collection run. This program is written in Hewlett-Packard Basic 5.0 language and enables the operator to:

1. Monitor the coolant sump temperature.
2. Monitor the evaporator liquid pool average temperature.
3. Monitor all the thermocouple channel output temperatures.
4. Monitor the voltage, current and power supplied to the upper tube heater (main heater) as well as the heater element electrical resistance.
5. Monitor the voltage, current and power supplied to the lower tube heater (auxiliary heater) as well as the heater element electrical resistance.

```
10!   PROGRAM: SETUPJY
20!   DATE:    MAY 15, 1993
30!   PROGRAMMER: LT DEAN SUGIYAMA
40!   MODIFIED BY LANNIE LAKE JAN 22, 1992
50!   MODIFIED BY GEORGE D. PERRY 10 APR 1993
60!   MODIFIED BY JOE YUSICIAN MAY 15, 1993
70    COM /Cc/ C(7)
80    DATA 0.10086091,25727.94369,-767345.8295,78025595.81,-9247486589,6.97688E+
11,-2.66192E+13
90    DATA 3.94078E+14
100   READ C(*)
110   ON KEY 1,15 GOTO 150
120   PRINTER IS 1
150   PRINT USING "2X,""SELECT OPTION"""
160   PRINT USING "6X,""0=MONITOR SUMP"""
170   PRINT USING "6X,""1=MONITOR LIQUID"""
180   PRINT USING "6X,""2=CHECK THERMOCOUPLES"""
190   PRINT USING "6X,""3=CHECK MAIN HEATER"""
200   PRINT USING "6X,""4=CHECK AUX HEATERS"""
210   PRINT USING "6X,""5=EXIT PROGRAM"""
230   BEEP
240   INPUT Ido
250   IF Ido>5 THEN Ido=5
260   IF Ido=0 THEN 340
270   IF Ido=1 THEN 520
280   IF Ido=2 THEN 690
290   IF Ido=3 THEN 870
300   IF Ido=4 THEN 870
310   IF Ido=5 THEN 1170
340   PRINT
350   PRINT "SUMP TEMPERATURE DEG C "
360   PRINT
370   OUTPUT 709;"AR AF19 AL19 VR5"
380   OUTPUT 709;"AS SA"
390   Sum=0
400   FOR J=1 TO 5
410   ENTER 709;E
420   Sum=Sum+E
430   NEXT J
440   Eave=Sum/5
450   Temp=FNTvsv(Eave)
460   PRINT USING "4X,MDD.DD";Temp
470   BEEP
480   PRINT
490   WAIT 5
500   GOTO 340
510!
520   PRINT
530   PRINT "LIQUID TEMPERATURE DEG C"
540   PRINT
550   OUTPUT 709;"AR AF16 AL18 VR5"
560   Sum=0
570   FOR I=1 TO 2
580   OUTPUT 709;"AS SA"
590   ENTER 709;E
600   Sum=Sum+E
610   NEXT I
620   Eave=Sum/2
630   Temp=FNTvsv(Eave)
640   PRINT USING "4X,MDD.DD";Temp
650   BEEP
660   WAIT 5
670   GOTO 610
```

```
680!
690   PRINT
700   PRINT "TEMPERATURE          DEG C"
710   OUTPUT 709;"AR AF00 AL19 VR5"
720   FOR I=1 TO 20
730   OUTPUT 709;"AS SA"
740   Sum=0
750   FOR J=1 TO 5
760   ENTER 709;E
770   Sum=Sum+E
780   NEXT J
790   Eave=Sum/5
800   Temp=FNTvsv(Eave)
810   PRINT TAB(3);I;TAB(15);Temp
820   NEXT I
830   BEEP
840   WAIT 5
850   GOTO 690
860!
870   PRINT
880   OUTPUT 709;"AR AF20 AL22 VR5"
890   FOR I=1 TO 3
900   OUTPUT 709;"AS SA"
910   Sum=0
920   FOR J=1 TO 5
930   ENTER 709;E
940   Sum=Sum+E
950   NEXT J
960   IF I=1 THEN Volt=Sum/5
970   IF I=2 AND Ido=3 THEN
980   PRINT "MAKE SURE VOLTAGE BOX IS SET TO MAIN HEATERS"
990   Amp=Sum/5
1000  END IF
1010  IF I=3 AND Ido=4 THEN
1020  PRINT "MAKE SURE VOLTAGE BOX IS SET TO AUX HEATERS"
1030  Amp=Sum/5
1040  END IF
1050  NEXT I
1060  Amp=ABS(Amp*1.9182)
1070  Volt=ABS(Volt*25)
1080  Power=Volt*Amp
1090  Resistance=Volt/Amp
1100  PRINT
1110  BEEP
1120  PRINT "VOLTAGE(V) CURRENT(A) RESISTENCE(ohms) POWER(W)"
1130  PRINT
1140  PRINT USING "1X,5(MDDDD.DD,4X)";Volt,Amp,Resistence,Power
1150  WAIT 5
1160  GOTO 870
1170  BEEP
1180  PRINT
1190  PRINT "SETUP COMPLETE"
1200  END
1210  DEF FNTvsv(V)
1220  COM /Cc/ C(7)
1230  T=C(0)
1240  FOR I=1 TO 7
1250  T=T+C(I)*V^I
1260  NEXT I
1270  T=T+8.626897E-2+T*(3.761199E-3-T*5.0689259E-5)
1280  RETURN T
1290  FNEND
```

## APPENDIX B. PROGRAM DRPJY

This data acquisition/reduction program is written in Hewlett-Packard Basic 5.0 language and is listed on the following pages.

```
10   ! FILE NAME: DRPJY
20   ! DATE:      MAY 15, 1993
30   ! REVISED VERSION OF DRP72 FOR R-124 (2 INSTRUMENTED TUBES)
40   ! REVISED BY LT. GEORGE PERRY & LT. JOE YUSICIAN
50     COM /Idp/ Idp
60     PRINTER IS 1
70     CALL Select
80     BEEP
90     PRINT
100    PRINT "DATA COLLECTION COMPLETE"
110    END
120!
130    SUB Main
140    COM /Iprop/ Ift
150    COM /Idp/ Idp
160    COM /Cc/ C(7),Ical
170    COM /Wil/ D2,Di,Do,L,Lu,Kcu
180    DIM Emf(20),T(20),D1a(13),D2a(13),Dia(13),Doa(13),La(13),Lua(13),Kcua(13),
Et(19),Tn$(4)[15]
190    DATA 0.10086091,25727.94369,-767345.8295,78025595.81
200    DATA -9247486589,6.97688E+11,-2.66192E+13,3.94078E+14
210    READ C(*)
220    DATA Smooth,High Flux,Turbo-B,High Flux Mod,Turbo-B Mod
230    READ Tn$(*)
240    PRINTER IS 701
250    PRINT
260    PRINT "          Date :",DATE$(TIMEDATE)
270    PRINT
280    PRINT USING "10X,""NOTE: Program name : DRPJY"""
290    BEEP
300!   INPUT "ENTER INPUT MODE (0=3054A,1=FILE)",Im
310    Im=0
320!   INPUT "SELECT FLUID (0=R-114,1=R-124)",Ift
330    Ift=1
340!   INPUT "1 OR 2 TUBE OPERATION (ENTER 1 OR 2)",Hwmntu
350    Hwmntu=2
360!   INPUT "SELECT HEATING MODE (0=ELEC; 1=WATER)",Ihm
370    Ihm=0
380!   INPUT "ENTER THERMOCOUPLE TYPE (0=NEW,1=OLD)",Ical
390    Ical=0
400    INPUT "GIVE A NAME FOR THE RAW DATA FILE",D2_file$
410    PRINT USING "16X,""New file name: "",15A";D2_file$
420    Size1=20
430    CREATE BDAT D2_file$,Size1
440    ASSIGN @File2 TO D2_file$
450 !
460 ! DUMMY FILE UNTIL Nrun KNOWN
470    D1_file$="DUMMY"
480    CREATE BDAT D1_file$,Size1
490    ASSIGN @File1 TO D1_file$
500    OUTPUT @File1;Date$
510    BEEP
520    INPUT "ENTER NR OF DEFECTIVE UPPER TUBE TCS (0=DEFAULT, 2 MAX.)",Idtc
530    IF Idtc=0 THEN
540    Ldtc1=0
550    Ldtc2=0
560    PRINT USING "16X,""No defective UPPER TUBE TCs exist"""
570    END IF
580    IF Idtc=1 THEN
590    BEEP
600    INPUT "ENTER DEFECTIVE UPPER TUBE TC LOCATION (TEMP 1-8)",Ldtc1
610    PRINT USING "16X,""UPPER TUBE TC is defective at LOCATION:"",DD";Ldtc1
620    Ldtc2=0
630    END IF
640    IF Idtc=2 THEN
650    BEEP
660    INPUT "ENTER DEFECTIVE UPPER TUBE TC LOCATIONS (TEMP 1-8)",Ldtc1,Ldtc2
670    PRINT USING "16X,""UPPER TUBE TC are defective at LOCATIONS:"",DD,4X,DD";L
dtc1,Ldtc2
```

```
680   END IF
690   IF Idtc>2 THEN
700   BEEP
710   PRINTER IS 1
720   BEEP
730   PRINT "INVALID ENTRY"
740   PRINTER IS 701
750   GOTO 510
760   END IF
770   OUTPUT @File1;Ldtc1,Ldtc2
780   IF Hwmntu=1 THEN GOTO 1190
790   INPUT "ENTER NUMBER OF DEFECTIVE LOWER TUBE TCS (0=DEFAULT, 2 MAX)",Aidtc
800   IF Aidtc=0 THEN
810   Aldtc1=0
820   Aldtc2=0
830   PRINT USING "16X,""No defective LOWER TUBE TCs exist"""
840   END IF
850   IF Aidtc=1 THEN
860   BEEP
870   INPUT "ENTER DEFECTIVE TC LOWER TUBE LOCATIONS (TEMP 9-16)",Aldtc1
880   PRINT USING "16X,""LOWER TUBE TC is defective at LOCATION:"",DD";Aldtc1
890   Aldtc2=0
900   END IF
910   IF Aidtc=2 THEN
920   BEEP
930   INPUT "ENTER DEFECTIVE LOWER TUBE TC LOCATIONS (TEMP 9-16)",Aldtc1,Aldtc2
940   PRINT USING "16X,""LOWER TUBE TC are defective at LOCATIONS:"",DD,4X,DD";A
ldtc1,Aldtc2
950   END IF
960   IF Aidtc>2 THEN
970   BEEP
980   PRINTER IS 1
990   BEEP
1000  PRINT "INVALID ENTRY"
1010  PRINTER IS 701
1020  GOTO 790
1030  END IF
1040  OUTPUT @File1;Aldtc1,Aldtc2
1050  PRINTER IS 1
1060  BEEP
1070  PRINT USING "2X,""Select tube number"""
1080  PRINT USING "6X,""4  Wieland Hard 8 inch"""
1090  PRINT USING "6X,""5  HIGH FLUX 8 inch"""
1100! PRINT USING "6X,""6  GEWA-K 40 Fins/in"""
1110! PRINT USING "6X,""7  GEWA-K 26 Fins/in"""
1120! PRINT USING "6X,""8  GEWA-T 19 Fins/in"""
1130! PRINT USING "6X,""9  GEWA-T OR GEWA-TY 26 Fins/in"""
1140! PRINT USING "6X,""10 THERMOEXCEL-E"""
1150! PRINT USING "6X,""11 THERMOEXCEL-HE"""
1160  PRINT USING "6X,""12 TURBO-B"""
1170! PRINT USING "6X,""13 GEWA-K 19 Fins/in"""
1180  INPUT Itt
1190  OUTPUT @File1;Itt
1200  PRINTER IS 701
1210  IF Itt=4 THEN PRINT USING "16X,""Tubes:  Wieland Hard 8 inch"""
1220  IF Itt=12 THEN PRINT USING "16X,""Tubes:  Turbo-B"""
1230  IF Itt=5 THEN PRINT USING "16X,""Tubes:  High Flux 8 inch"""
1240! IF Itt<10 THEN PRINT USING "16X,""Tube Number:   "",D";Itt
1250! IF Itt>9 THEN PRINT USING "16X,""Tube Number:   "",DD";Itt
1260! INPUT "ENTER OUTPUT VERSION (0=LONG,1=SHORT,2=NONE)",Iov
1270  Iov=0
1280! INPUT "SELECT (0=LIQ,1=VAP,2=(LIQ+VAP)/2)",Ilqv
1290  Ilqv=2
1300!
1310! DIMENSIONS FOR TESTED TUBES
1320!
1330! D1=Diameter at thermocouple positions
1340  DATA .0111125,.0111125,.0111125,.0129540,.012446,.0129540,.0100965
1350  DATA .0100965,.01157,.01157,.01157,.01157,.01157,.0100965
1360  READ D1a(*)
1370  D1=D1a(Itt)
```

```
1380!
1390! D2=Diameter of test section to the base of fins
1400  DATA .015875,.015875,.015875,.015824,.015875,.015824,.01270
1410  DATA .0127,.0138,.0138,.0138,.0138,.0138,.0127
1420  READ D2a(*)
1430  D2=D2a(Itt)
1440!
1450! Di=Inside diameter of unenhanced ends
1460  DATA .0127,.0127,.0127,.0132,.0127,.0132,.0111125,.0111125
1470  DATA .0118,.0118,.0118,.0118,.0118,.0111125
1480  READ Dia(*)
1490  Di=Dia(Itt)
1500!
1510! Do=Outside diameter of unenhanced ends
1520  DATA .015875,.015875,.015875,.015824,.015875,.015824,.01270,.01270
1530  DATA .01331,.01331,.01331,.01331,.0158,.0127
1540  READ Doa(*)
1550  Do=Doa(Itt)
1560!
1570! L=Length of enhanced surface
1580  DATA .1016,.1016,.1016,.1016,.2032,.2032,.2032,.2032,.2032,.2032,.2032,.20
32,.2032,.2032
1590  READ La(*)
1600  L=La(Itt)
1610!
1620! Lu=Length of unenhanced surface at the ends
1630  DATA .0254,.0254,.0254,.0254,.0762,.0762,.0762,.0762,.0762,.0762,.0762,.07
62,.0762,.0762
1640  READ Lua(*)
1650  Lu=Lua(Itt)
1660!
1670! Kcu=Thermal Conductivity of tube
1680  DATA 398,344,344,45,344,45,344,344,398,398,398,398,398,344
1690  READ Kcua(*)
1700  Kcu=Kcua(Itt)
1710!
1720  Xn=.8
1730  Fr=.3
1740  Cf=3.7037E+10
1750  A=PI*(Do^2-Di^2)/4
1760  P=PI*Do
1770  Nsub=0
1780  Ntc=20
1790  J=1
1800 Repeat: !
1810  Dtld=2.22
1820  Ido=2
1830  ON KEY 1,15 RECOVER 1800
1840  PRINTER IS 1
1850  PRINT USING "2X,""SELECT OPTION"""
1860  PRINT USING "6X,""0=TAKE DATA"""
1870  PRINT USING "6X,""1=SET UPPER TUBE HEAT FLUX (MAIN)"""
1880  PRINT USING "6X,""2=SET Tsat"""
1890  PRINT USING "6X,""3=SET LOWER TUBE HEAT FLUX (AUX)"""
1900  BEEP
1910  INPUT Ido
1920  IF Ido>3 THEN Ido=3
1930  IF Ido=0 THEN 3680
1940!
1950! LOOP TO SET UPPER TUBE HEAT FLUX
1960  IF Ido=1 THEN
1970  OUTPUT 709;"AR AF20 AL21 VR5"
1980  PRINT "SET VOLT BOX TO MAIN"
1990  BEEP
2000  INPUT "ENTER DESIRED Qdp",Dqdp
2010  PRINT USING "4X,""DESIRED Qdp  ACTUAL Qdp"""
```

```
2020  Err=1000
2030  FOR I=1 TO 2
2040  OUTPUT 709;"AS SA"
2050  Sum=0
2060  FOR Ji=1 TO 5
2070  ENTER 709;E
2080  Sum=Sum+E
2090  NEXT Ji
2100  IF I=1 THEN Volt=Sum/5
2110  IF I=2 THEN Amp=Sum/5
2120  NEXT I
2130  Amp=ABS(Amp*1.9182)
2140  Volt=ABS(Volt*25)
2150  Aqdp=Volt*Amp/(PI*D2*L)
2160  IF ABS(Aqdp-Dqdp)>Err THEN
2170  IF Aqdp>Dqdp THEN
2180  BEEP 4000,.2
2190  BEEP 4000,.2
2200  BEEP 4000,.2
2210  ELSE
2220  BEEP 250,.2
2230  BEEP 250,.2
2240  BEEP 250,.2
2250  END IF
2260  PRINT USING "4X,MZ.3DE,2X,MZ.3DE";Dqdp,Aqdp
2270  WAIT 2
2280  GOTO 2030
2290  ELSE
2300  BEEP
2310  PRINT USING "4X,MZ.3DE,2X,MZ.3DE";Dqdp,Aqdp
2320  Err=500
2330  WAIT 2
2340  GOTO 2030
2350  END IF
2360  END IF
2370!
2380! LOOP TO SET Tsat
2390  IF Ido=2 THEN
2400  IF Ikdt=1 THEN 2440
2410  Dtld=2.22
2420! PRINT USING "4X,"" DTsat  ATsat   Rate    Tv     Rate"""
2430  Ikdt=1
2440  Old1=0
2450  Old2=0
2460  Nn=1
2470  Nrs=Nn MOD 15
2480  Nn=Nn+1
2490  IF Nrs=1 THEN
2500  PRINT USING "4X,""  Tsat    Tld1    Tld2     Tv    Tsump"""
2510  END IF
2520  OUTPUT 709;"AR AF16 AL19 VR5"
2530  FOR I=1 TO 6
2540  IF I>4 THEN 2700
2550  Sum=0
2560  OUTPUT 709;"AS SA"
2570  FOR Ji=1 TO 20
2580  ENTER 709;Eliq
2590  Sum=Sum+Eliq
2600  NEXT Ji
2610  Eliq=Sum/20
2620  Tld=FNTvsv(Eliq)
2630  IF I=1 THEN Tld1=Tld
2640  IF I=2 THEN Tld2=Tld
2650  IF I=3 THEN Tv=Tld
2660  IF I=4 THEN Tsump=Tld
2670  IF I=5 THEN Tinlet=Tld
2680  IF I=6 THEN Tout=Tld
```

```
2690  NEXT I
2700  Atld=(Tld1+Tld2)*.5
2710  IF ABS(Atld-Dtld)>.2 THEN
2720  IF Atld>Dtld THEN
2730  BEEP 4000,.2
2740  BEEP 4000,.2
2750  BEEP 4000,.2
2760  ELSE
2770  BEEP 250,.2
2780  BEEP 250,.2
2790  BEEP 250,.2
2800  END IF
2810  Err1=Atld-Old1
2820  Old1=Atld
2830  Err2=Tv-Old2
2840  Old2=Tv
2850  IF Tld1>100. THEN 2880
2860  PRINT USING "4X,5(MDD.DD,2X)";Dtld,Tld1,Tld2,Tv,Tsump
2870  WAIT 2
2880  GOTO 2470
2890  ELSE
2900  IF ABS(Atld-Dtld)>.1 THEN
2910  IF Atld>Dtld THEN
2920  BEEP 3000,.2
2930  BEEP 3000,.2
2940  ELSE
2950  BEEP 800,.2
2960  BEEP 800,.2
2970  END IF
2980  Err1=Atld-Old1
2990  Old1=Atld
3000  Err2=Tv-Old2
3010  Old2=Tv
3020  PRINT USING "4X,5(MDDD.DD,2X)";Dtld,Tld1,Tld2,Tv,Tsump
3030  WAIT 2
3040  GOTO 2470
3050  ELSE
3060  BEEP
3070  Err1=Atld-Old1
3080  Old1=Atld
3090  Err2=Tv-Old2
3100  Old2=Tv
3110  PRINT USING "4X,5(MDDD.DD,2X)";Dtld,Tld1,Tld2,Tv,Tsump
3120  WAIT 2
3130  GOTO 2470
3140  END IF
3150  END IF
3160  END IF
3170  !
3180! LOOP TO SET LOWER TUBE HEAT FLUX
3190  IF Ido=3 THEN
3200  PRINT " SET VOLT BOX TO AUX"
3210  OUTPUT 709;"AR AF20 AL22 VR5"
3220  BEEP
3230  INPUT "ENTER DESIRED AuQdp",Duxqdp
3240  PRINT USING "2X,""DESIRED AuxQdp  ACTUAL AuxQdp"""
3250  Err=1000
3260  FOR I=1 TO 3
3270  OUTPUT 709;"AS SA"
3280  Sum=0
3290  FOR Ji=1 TO 5
3300  ENTER 709;E
3310  Sum=Sum+E
3320  NEXT Ji
3330  IF I=1 THEN Volt=Sum/5
3340  IF I=3 THEN Amp=Sum/5
3350  NEXT I
```

```
3360  Amp=ABS(Amp*1.9182)
3370  Volt=ABS(Volt*25)
3380  Auxqdp=Volt*Amp/(PI*D2*L)
3390  IF ABS(Auxqdp-Duxqdp)>Err THEN
3400  IF Auxqdp>Duxqdp THEN
3410  BEEP 4000,.2
3420  BEEP 4000,.2
3430  BEEP 4000,.2
3440  ELSE
3450  BEEP 250,.2
3460  BEEP 250,.2
3470  BEEP 250,.2
3480  END IF
3490  PRINT USING "4X,MZ.3DE,2X,MZ.3DE";Duxqdp,Auxqdp
3500  WAIT 2
3510  GOTO 3260
3520  ELSE
3530  BEEP
3540  PRINT USING "4X,MZ.3DE,2X,MZ.3DE";Duxqdp,Auxqdp
3550  Err=500
3560  WAIT 2
3570  GOTO 3260
3580  END IF
3590  GOTO 1850
3600  END IF
3610! ERROR TRAP FOR Ido OUT OF BOUNDS
3620  IF Ido>3 THEN
3630  BEEP
3640  GOTO 1850
3650  END IF
3660!
3670! TAKE DATA LOOP
3680  IF Ikol=1 THEN 3730
3690  BEEP
3700  Ikol=1
3710  INPUT "ENTER BULK OIL %",Bop
3720  Ikol=1
3730  OUTPUT 709;"AR AF00 AL19 VR5"
3740  Ntc=20
3750  FOR I=1 TO Ntc
3760  OUTPUT 709;"AS SA"
3770  Sum=0
3780  FOR Ji=1 TO 20
3790  ENTER 709;E
3800  Sum=Sum+E
3810  IF I=(17-Nsub) OR I=(18-Nsub) THEN Et(Ji-1)=E
3820  NEXT Ji
3830  Kdl=0
3840  IF I=(17-Nsub) OR I=(18-Nsub) THEN
3850  Eave=Sum/20
3860  Sum=0.
3870  FOR Jk=0 TO 19
3880  IF ABS(Et(Jk)-Eave)<5.0E-6 THEN
3890  Sum=Sum+Et(Jk)
3900  ELSE
3910  Kdl=Kdl+1
3920  END IF
3930  NEXT Jk
3940  IF I=(17-Nsub) OR I=(18-Nsub) THEN PRINT USING "4X,""Kdl = "",DD";Kdl
3950  IF Kdl>20 THEN
3960  BEEP
3970  BEEP
3980  PRINT USING "4X,""Too much scattering in data - repeat data set"""
3990  GOTO 1840
4000  END IF
4010  END IF
4020  Emf(I)=Sum/(20-Kdl)
```

```
4030  NEXT I
4040  Coun=0.
4050  OUTPUT 709;"AR AF20 AL22 VR5"
4060  FOR I=1 TO 3
4070  OUTPUT 709;"AS SA"
4080  Sum=0
4090  FOR Ji=1 TO 5
4100  ENTER 709;E
4110  Sum=Sum+E
4120  NEXT Ji
4130  IF Coun=0. THEN
4140  IF I=1 THEN Vr=Sum/5
4150  IF I=2 THEN Ir=Sum/5
4160  ELSE
4170  IF I=1 THEN Avr=Sum/5
4180  IF I=3 THEN Air=Sum/5
4190  END IF
4200  NEXT I
4210  IF Coun=0 THEN
4220  PRINT "SHIFT VOLT BOX TO AUX"
4230  END IF
4240  IF Coun=1 THEN GOTO 4290
4250  INPUT "TAKE AUX READINGS(1=YES)?",Ccon
4260  IF Ccon>1 THEN GOTO 4250
4270  Coun=Coun+Ccon
4280  GOTO 4060
4290!
4300! CONVERT emf'S TO TEMP,VOLT,CURRENT
4310  Twa=0
4320  Atwa=0
4330  FOR I=1 TO Ntc
4340  IF Idtc>0 THEN
4350  IF I=Ldtc1 OR I=Ldtc2 THEN
4360  T(I)=-99.99
4370  GOTO 4470
4380  END IF
4390  END IF
4400  IF Aidtc>0 THEN
4410  IF I=Aldtc1 OR I=Aldtc2 THEN
4420  T(I)=-99.99
4430  GOTO 4470
4440  END IF
4450  END IF
4460  T(I)=FNTvsv(Emf(I))
4470  NEXT I
4480  Twa=Twa/(4-Idtc)
4490  FOR I=1 TO 8
4500  IF I=Ldtc1 OR I=Ldtc2 THEN
4510  Twa=Twa
4520  ELSE
4530  Twa=Twa+T(I)
4540  END IF
4550  NEXT I
4560  Tw=Twa/(8-Idtc)
4570  FOR I=9 TO 16
4580  IF I=Aldtc1 OR I=Aldtc2 THEN
4590  Atwa=Atwa
4600  ELSE
4610  Atwa=Atwa+T(I)
4620  END IF
4630  NEXT I
4640  Atw=Atwa/(8-Aidtc)
4650  Tld=T(17-Nsub)
4660  Tld2=T(18-Nsub)
4670  Tlda=(Tld+Tld2)*.5
4680  Tv=T(19-Nsub)
4690  Tsump=T(20-Nsub)
```

```
4700  Amp=ABS(Ir*1.9182)
4710  Volt=ABS(Vr)*25
4720  Q=Volt*Amp
4730  Auamp=ABS(Air*1.9182)
4740  Auvolt=ABS(Avr)*25
4750  Auq=Auvolt*Auamp
4760  Kcu=Kcua(Itt)
4770!
4780! FOURIER CONDUCTION EQUATION WITH CONTACT RESISTANCE NEGLECTED
4790  Tw=Tw-Q*LOG(D2/D1)/(2*PI*Kcu*L)
4800  Atw=Atw-Auq*LOG(D2/D1)/(2*PI*Kcu*L)
4810  Tsat=(Tlda+Tv)*.5
4820!
4830! COMPUTE THETHAB
4840  Thetab=Tw-Tsat
4850  Athetab=Atw-Tsat
4860  IF Thetab<0 THEN
4870  BEEP
4880  INPUT "UPPER TWALL<TSAT (0=CONTINUE, 1=END)",Iev
4890  IF Iev=0 THEN GOTO 3150
4900  IF Iev=1 THEN 1850
4910  END IF
4920  IF Athetab<0 THEN
4930  BEEP
4940  INPUT "LOWER TWALL<TSAT (0=CONTINUE, 1=END)",Aiev
4950  IF Aiev=0 THEN GOTO 3150
4960  IF Aiev=1 THEN 1850
4970  END IF
4980!
4990! COMPUTE VARIOUS PROPERTIES
5000  Tfilm=(Tw+Tsat)*.5
5010  Rho=FNRho(Tfilm)
5020  Mu=FNMu(Tfilm)
5030  K=FNK(Tfilm)
5040  Cp=FNCp(Tfilm)
5050  Beta=FNBeta(Tfilm)
5060  Hfg=FNHfg(Tsat)
5070  Ni=Mu/Rho
5080  Alpha=K/(Rho*Cp)
5090  Pr=Ni/Alpha
5100  Psat=FNPsat(Tsat)
5110!
5120! COMPUTE VARIOUS PROPERTIES FOR AUX TUBE
5130  Atfilm=(Atw+Tsat)*.5
5140  Arho=FNRho(Atfilm)
5150  Amu=FNMu(Atfilm)
5160  Ak=FNK(Atfilm)
5170  Acp=FNCp(Atfilm)
5180  Abeta=FNBeta(Atfilm)
5190  Ani=Amu/Arho
5200  Aalpha=Ak/(Arho*Acp)
5210  Apr=Ani/Aalpha
5220!
5230! COMPUTE NATURAL-CONVECTIVE HEAT-TRANSFER COEFFICIENT
5240! FOR UNENHANCED END(S)
5250  Hbar=190
5260  Fe=(Hbar*P/(Kcu*A))^.5*Lu
5270  Tanh=FNTanh(Fe)
5280  Theta=Thetab*Tanh/Fe
5290  Xx=(9.81*Beta*Thetab*Do^3*Tanh/(Fe*Ni*Alpha))^.166667
5300  Yy=(1+(.559/Pr)^(9/16))^(8/27)
5310  Hbarc=K/Do*(.6+.387*Xx/Yy)^2
5320  IF ABS((Hbar-Hbarc)/Hbarc)>.001 THEN
5330  Hbar=(Hbar+Hbarc)*.5
5340  GOTO 5260
5350  END IF
5360!
5370! COMPUTE NATURAL-CONVECTIVE HEAT-TRANSFER COEFFICIENT
5380! FOR UNENHANCED END(S) FOR AUX TUBE
5390  Ahbar=190
5400  Fe=(Ahbar*P/(Kcu*A))^.5*Lu
5410  Atanh=FNTanh(Fe)
```

```
5420  Atheta=Athetab*Atanh/Fe
5430  Axx=(9.81*Abeta*Athetab*Do^3*Atanh/(Fe*Ani*Aalpha))^.166667
5440  Ayy=(1+(.559/Apr)^(9/16))^(8/27)
5450  Ahbarc=Ak/Do*(.6+.387*Axx/Ayy)^2
5460  IF ABS((Ahbar-Ahbarc)/Ahbarc)>.001 THEN
5470  Ahbar=(Ahbar+Ahbarc)*.5
5480  GOTO 5400
5490  END IF
5500!
5510! COMPUTE HEAT LOSS RATE THROUGH UNENHANCED END(S)
5520  Q1=(Hbar*P*Kcu*A)^.5*Thetab*Tanh
5530  Qc=Q-2*Q1
5540  As=PI*D2*L
5550 !
5560 !COMPUTE HEAT LOSS RATE THROUGH UNENHANCED END(S) OF AUX TUBE
5570  Aq1=(Ahbar*P*Kcu*A)^.5*Athetab*Atanh
5580  Aqc=Auq-2*Aq1
5590!
5600! COMPUTE ACTUAL HEAT FLUX AND BOILING COEFFICIENT
5610  Qdp=Qc/As
5620  Htube=Qdp/Thetab
5630  Csf=(Cp*Thetab/Hfg)/(Qdp/(Mu*Hfg)*(.014/(9.81*Rho)^.5)^(1/3.)*Pr^1.7)
5640!
5650! COMPUTE ACTUAL HEAT FLUX AND BOILING COEFFICIENT FOR AUX TUBE
5660  Auqdp=Aqc/As
5670  Ahtube=Auqdp/Athetab
5680  Acsf=(Acp*Athetab/Hfg)/(Auqdp/(Amu*Hfg)*(.014/(9.81*Arho)^.5)^(1/3.)*Apr^1
.7)
5690!
5700! COMPUTE CHURCHILL-CHU CORRELATION FOR UPPER TUBE
5710  Cc=Hbar*Thetab
5720!
5730! RECORD TIME OF DATA TAKING
5740  OUTPUT 709;"TD"
5750  ENTER 709;Told$
5760!
5770! OUTPUT DATA TO PRINTER
5780  PRINTER IS 701
5790  PRINT
5800  PRINT USING "10X,""Data Set Number = "",DDD,2X,""Bulk Oil % = "",DD.D";J,B
op
5810  PRINT "          TIME:",TIME$(TIMEDATE)
5820  PRINT
5830  PRINT USING "10X,""TC No:    1      2      3      4      5      6      7
    8"""
5840  PRINT USING "10X,""Temp :"",8(1X,MDD.DD)";T(1),T(2),T(3),T(4),T(5),T(6),T(
7),T(8)
5850  PRINT USING "10X,""TC No:    9      10     11     12     13     14     15
    16"""
5860  PRINT USING "10X,""Temp :"",8(1X,MDD.DD)";T(9),T(10),T(11),T(12),T(13),T(1
4),T(15),T(16)
5870  PRINT
5880  PRINT USING "10X,""  Twa   ATwa   Tliqd   Tliqd2  Tvapr  Psat   Tsat   Tsu
mp"""
5890  PRINT USING "10X,3(MDD.DD,1X),1X,MDD.DD,1X,3(1X,MDD.DD),2X,MDD.D";Tw,Atw,T
ld,Tld2,Tv,Psat,Tsat,Tsump
5900  PRINT USING "10X,""     Vr        Ir       Cc""
5910  PRINT USING "10X,2(MDDD.DD,3X),1X,MZ.3DE";Vr,Ir,Cc
5920  PRINT USING "10X,"" Thetab    Htube      Qdp      Athetab  Ahtube     AuQd
p"""
5930  PRINT USING "10X,MDD.3D,1X,MZ.3DE,1X,MZ.3DE,1X,MDD.3D,1X,MZ.3DE,1X,MZ.3DE"
;Thetab,Htube,Qdp,Athetab,Ahtube,Auqdp
5940  PRINT
5950  BEEP
5960  INPUT "OK TO STORE THIS DATA SET (1=Y,0=N)?",Ok
5970  IF Ok=1 THEN J=J+1
5980  IF Ok=1 AND Im=0 THEN
5990  OUTPUT @File1;Bop,Told$,Emf(*),Vr,Ir,Avr,Air
6000  END IF
6010  IF Iuf=1 THEN OUTPUT @Ufile;Vw,Uo
6020  IF Ire=1 THEN OUTPUT @Refile;Fms,Rew
6030  BEEP
```

```
6040  INPUT "WILL THERE BE ANOTHER RUN (1=Y,0=N)?",Go_on
6050  Nrun=J
6060  IF Go_on=0 THEN 6080
6070  IF Go_on<>0 THEN Repeat
6080  BEEP
6090  PRINT
6100  PRINT USING "10X,""NOTE: "",ZZ,"" data runs were stored in file "",15A";J-
1,D2_file$
6110  ASSIGN @File1 TO *
6120  OUTPUT @File2;Nrun-1
6130  ASSIGN @File1 TO D1_file$
6140  ENTER @File1;Date$,Ldtc1,Ldtc2,Itt
6150  ENTER @File1;Aldtc1,Aldtc2
6160  OUTPUT @File2;Date$,Ldtc1,Ldtc2,Itt
6170  OUTPUT @File2;Aldtc1,Aldtc2
6180  FOR I=1 TO Nrun-1
6190  ENTER @File1;Bop,Told$,Emf(*),Vr,Ir
6200  ENTER @File1;Avr,Air
6210  OUTPUT @File2;Bop,Told$,Emf(*),Vr,Ir
6220  OUTPUT @File2;Avr,Air
6230  NEXT I
6240  ASSIGN @File1 TO *
6250  PRINTER IS 1
6260  PURGE "DUMMY"
6270  PRINT
6280  PRINT "DUMMY FILE PURGED"
6290  SUBEND
6300!
6310! CURVE FITS OF PROPERTY FUNCTIONS
6320!
6330  DEF FNKcu(T)
6340! OFHC COPPER 250 TO 300 K
6350  Tk=T+273.15      !C TO K
6360  K=434-.112*Tk
6370  RETURN K
6380  FNEND
6390!
6400  DEF FNMu(T)
6410  COM /Iprop/ Ift
6420  IF Ift=1 THEN
6430  !223 TO 373 K
6440! 170 TO 360 K CURVE FIT OF VISCOUSITY
6450  Tk=T+273.15      !C TO K
6460  Mu=EXP(-4.4636+(1011.47/Tk))*1.0E-3
6470  END IF
6480  IF Ift=1 THEN
6490! 223 TO 373 K
6500  Mu=3.4593-4.26E-2*T+3.9485E-4*T^2-4.193E-6*T^3+2.0709E-8*T^4
6510  Mu=Mu*1.0E-4
6520  END IF
6530  RETURN Mu
6540  FNEND
6550!
6560  DEF FNCp(T)
6570  COM /Iprop/ Ift
6580  IF Ift=0 THEN
6590! 180 TO 400 K CURVE FIT OF Cp
6600  Tk=T+273.15      !C TO K
6610  Cp=.40188+1.65007E-3*Tk+1.51494E-6*Tk^2-6.67853E-10*Tk^3
6620  Cp=Cp*1000
6630  END IF
6640  IF Ift=1 THEN
6650! 223 TO 373 K CURVE FIT Cp(R124)
6660  Cp=1.0542+2.1405E-3*T+1.0709E-5*T^2-6.4721E-8*T^3-1.4324E-9*T^4+4.136E-11*
T^5
6670  Cp=Cp*1000
6680  END IF
6690  RETURN Cp
6700  FNEND
```

```
6710!
6720  DEF FNRho(T)
6730  COM /Iprop/ Ift
6740  IF Ift=0 THEN
6750  Tk=T+273.15      !C TO K
6760  X=1-(1.8*Tk/753.95)  !K TO R
6770  Ro=36.32+61.146414*X^(1/3)+16.418015*X+17.476838*X^.5+1.119828*X^2
6780  Ro=Ro/.062428
6790  END IF
6800  IF Ift=1 THEN
6810! 223 TO 373 K (R124)
6820  Ro=1434.8-2.8619*T-6.7267E-3*T^2-7.2852E-5*T^3
6830  END IF
6840  RETURN Ro
6850  FNEND
6860!
6870  DEF FNK(T)
6880  COM /Iprop/ Ift
6890  IF Ift=0 THEN
6900! T<360 K WITH T IN C
6910  K=.071-.000261*T
6920  END IF
6930! RETURN K
6940  IF Ift=1 THEN
6950! 223 TO 373 K (R-124)
6960  K=7.5191E-2-3.5436E-4*T-1.9545E-7*T^2+3.1835E-9*T^3
6970  END IF
6980  RETURN K
6990  FNEND
7000!
7010  DEF FNTanh(X)
7020  P=EXP(X)
7030  Q=1/P
7040  Tanh=(P-Q)/(P+Q)
7050  RETURN Tanh
7060  FNEND
7070!
7080  DEF FNTvsv(V)
7090  COM /Cc/ C(7),Ical
7100  T=C(0)
7110  FOR I=1 TO 7
7120  T=T+C(I)*V^I
7130  NEXT I
7140  IF Ical=1 THEN
7150  T=T-6.7422934E-2+T*(9.0277043E-3-T*(-9.3259917E-5))
7160  ELSE
7170  T=T+8.626897E-2+T*(3.76199E-3-T*5.0689259E-5)
7180  END IF
7190  RETURN T
7200  FNEND
7210!
7220  DEF FNBeta(T)
7230  Rop=FNRho(T+.1)
7240  Rom=FNRho(T-.1)
7250  Beta=-2/(Rop+Rom)*(Rop-Rom)/.2
7260  RETURN Beta
7270  FNEND
7280!
7290  DEF FNHfg(T)
7300  COM /Iprop/ Ift
7310  IF Ift=0 THEN
7320  Hfg=1.3741344E+5-T*(3.3094361E+2+T*1.2165143)
7330  END IF
7340  IF Ift=1 THEN
7350! 223 TO 373 K CURVE FIT (R124)
7360  Hfg=159.93-.4609*T-1.458E-3*T^2-1.3715E-5*T^3
7370  Hfg=Hfg*1000
```

```
7380  END IF
7390  RETURN Hfg
7400  FNEND
7410!
7420  DEF FNPsat(Tc)
7430  COM /Iprop/ Ift
7440  IF Ift=0 THEN
7450! 0 TO 80 deg F CURVE FIT OF Psat
7460  Tf=1.8*Tc+32
7470  Pa=5.945525+Tf*(.15352082+Tf*(1.4840963E-3+Tf*9.6150671E-6))
7480  Pg=Pa-14.7
7490  END IF
7500  IF Ift=1 THEN
7510! 223 TO 373 K CURVE FIT (R-124)
7520  Pa=(162.68+5.946*Tc+9.2081E-2*Tc^2+6.9359E-4*Tc^3)*.14504
7530  Pg=Pa-14.7
7540  END IF
7550  IF Pg>0 THEN       ! +=PSIG,-=in Hg
7560  Psat=Pg
7570  ELSE
7580  Psat=Pg*29.92/14.7
7590  END IF
7600  RETURN Psat
7610  FNEND
7620 !
7630 !
7640  SUB Purg
7650  BEEP
7660  INPUT "ENTER FILE NAME TO BE DELETED",File$
7670  PURGE File$
7680  GOTO 7650
7690  SUBEND
7700 !
7710 !
7720  SUB Select
7730  COM /Idp/ Idp
7740  BEEP
7750  PRINTER IS 1
7760  PRINT USING "2X,""Select option:"""
7770  PRINT USING "6X,"" 0 TAKE DATA"""
7780  PRINT USING "6X,"" 1 PURGE FILES"""
7790  INPUT Idp
7800  IF Idp=0 THEN CALL Main
7810  IF Idp=1 THEN CALL Purg
7820  SUBEND
```

# APPENDIX C. REPRESENTATIVE DATA SET

```
Date :      7 Sep 1993

NOTE: Program name : DRPJY
      New file name: 00907SC2
      UPPER TUBE TC are defective at LOCATIONS: 7      8
      LOWER TUBE TC is defective at LOCATION: 9
      Tubes:  Wieland Hard 8 incn

Data Set Number =   1  Bulk Oil % =  0.0
TIME:      13:13:35

TC No:     1       2       3       4       5       6       7       8
Temp :   3.85    3.73    3.75    3.66    3.87    3.89  -99.99  -99.99
TC No:     9      10      11      12      13      14      15      16
Temp : -99.99   20.20   18.36   20.46   19.64   20.49   18.63   17.30

  Twa    ATwa    Tliqd    Tliqd2   Tvapr   Psat    Tsat    Tsump
  3.79   19.36    2.20     2.22     2.11   10.82    2.16   -10.3
     Vr           Ir         Cc
    .84          .17      2.388E+02
 Thetab      Htube       Qdp        Athetab   Ahtube      AuQdp
  1.525   3.408E+02   5.542E+02   17.194   1.832E+02   3.150E-03


Data Set Number =   2  Bulk Oil % =  0.0
TIME:      13:14:38

TC No:     1       2       3       4       5       6       7       9
Temp :   4.37    4.31    4.32    4.32    4.96    5.10  -99.99  -99.99
TC No:     9      10      11      12      13      14      15      16
Temp : -99.99   20.49   19.22   20.57   20.07   20.32   18.38   17.68

  Twa    ATwa    Tliqd    Tliqd2   Tvapr   Psat    Tsat    Tsump
  4.94   19.55    2.29     2.36     2.18   10.90    2.25   -10.8
     Vr           Ir         Cc
   1.13         .23      4.530E+02
 Thetab      Htube       Qdp        Athetab   Ahtube      AuQdp
  2.688   3.368E+02   1.040E+03   17.397   1.793E+02   3.120E+03


Data Set Number =   3  Bulk Oil % =  0.0
TIME:      13:16:14

TC No:     1       2       3       4       5       6       7       8
Temp :   7.38    7.12    7.12    6.82    7.19    7.43  -99.99  -99.99
TC No:     9      10      11      12      13      14      15      16
Temp : -99.99   20.08   18.76   20.32   19.41   20.16   18.35   16.96

  Twa    ATwa    Tliqd    Tliqd2   Tvapr   Psat    Tsat    Tsump
  7.17   19.12    2.07     2.13     2.02   10.73    2.06   -10.3
     Vr           Ir         Cc
   1.49         .31      1.025E+03
 Thetab      Htube       Qdp        Athetab   Ahtube      AuQdp
  5.104   3.410E+02   1.740E+03   17.057   1.860E+02   3.172E+03
```

```
Data Set Number =   4  Bulk Oil % =  0.0
TIME:      13:17:49

TC No:     1       2       3       4       5       6       7       8
Temp :  10.40   10.10   10.12    3.64   10.01   10.30  -99.99  -99.99
TC No:     9      10      11      12      13      14      15      16
Temp : -99.99   20.02   18.77   20.12   19.61   20.29   18.32   17.29

  Twa    ATwa    Tliqd    Tliqd2   Tvapr   Psat    Tsat    Tsump
 10.11   19.18    1.95     2.15     1.92   10.66    1.99   -10.7
     Vr          Ir         Cc
   1.87         .39      1.855E+03
 Thetab     Htube       Qdp       Athetab  Ahtube      AuQdp
  8.121   3.319E+02  2.695E+03   17.189   1.834E+02   3.152E+03


Data Set Number =   5  Bulk Oil % =  0.0
TIME:      13:18:54

TC No:     1       2       3       4       5       6       7       8
Temp :  14.37   14.17   14.12   13.47   13.75   14.60  -99.99  -99.99
TC No:     9      10      11      12      13      14      15      16
Temp : -99.99   20.49   19.23   20.42   20.02   20.52   18.47   17.87

  Twa    ATwa    Tliqd    Tliqd2   Tvapr   Psat    Tsat    Tsump
 14.05   19.52    2.01     2.25     2.04   10.76    2.09   -10.8
     Vr          Ir         Cc
   2.36         .50      3.046E+03
 Thetab     Htube       Qdp       Athetab  Ahtube      AuQdp
 11.960   3.630E+02  4.342E+03   17.429   1.780E+02   3.102E+03


Data Set Number =   6  Bulk Oil % =  0.0
TIME:      13:20:03

TC No:     1       2       3       4       5       6       7       8
Temp :  17.69   17.40   17.30   16.51   16.64   17.63  -99.99  -99.99
TC No:     9      10      11      12      13      14      15      16
Temp : -99.99   20.21   18.86   20.32   19.69   20.48   18.47   17.08

  Twa    ATwa    Tliqd    Tliqd2   Tvapr   Psat    Tsat    Tsump
 17.16   19.27    2.04     2.32     2.09   10.80    2.13   -10.7
     Vr          Ir         Cc
   2.58         .55      4.084E+03
 Thetab     Htube       Qdp       Athetab  Ahtube      AuQdp
 15.024   3.379E+02  5.077E+03   17.139   1.834E+02   3.143E+03
```

```
Data Set Number =   7  Bulk Oil % =  0.0
TIME:      13:21:13

TC No:     1       2       3       4       5       6       7       8
Temp :  19.40   19.10   18.35   18.05   18.12   18.37 -99.99 -99.99
TC No:     9      10      11      12      13      14      15      16
Temp : -99.99   19.39   18.74   19.34   19.50   20.11   18.08   17.07

  Twa    ATwa    Tliqd    Tliqd2   Tvapr  Psat    Tsat    Tsump
 18.79   19.03    1.89     2.21     1.36  10.68    2.00   -10.7
     Vr          Ir         Cc
   2.80         .60      4.707E+03
 Thetab      Htube       Qdp       Athetab  Ahtube      AuQdp
 16.783   3.612E+02  6.061E+03   17.027   1.848E+02   3.146E+03


Data Set Number =   8  Bulk Oil % =  0.0
TIME:      13:22:11

TC No:     1       2       3       4       5       6       7       8
Temp :  22.76   22.21   21.96   20.86   21.04   22.51 -99.99 -99.99
TC No:     9      10      11      12      13      14      15      16
Temp : -99.99   19.75   18.48   19.79   19.35   20.05   18.04   16.85

  Twa    ATwa    Tliqd    Tliqd2   Tvapr  Psat    Tsat    Tsump
 21.84   18.87    1.81     2.19     1.90  10.63    1.35   -10.7
     Vr          Ir         Cc
   3.07         .65      5.358E+03
 Thetab      Htube       Qdp       Athetab  Ahtube      AuQdp
 19.389   3.552E+02  7.263E+03   16.325   1.364E+02   3.155E+03


Data Set Number =   9  Bulk Oil % =  0.0
TIME:      13:23:55

TC No:     1       2       3       4       5       6       7       8
Temp :  26.91   26.51   26.32   25.12   24.95   26.71 -99.99 -99.99
TC No:     9      10      11      12      13      14      15      16
Temp : -99.99   20.53   19.25   20.45   20.10   20.75   18.59   17.71

  Twa    ATwa    Tliqd    Tliqd2   Tvapr  Psat    Tsat    Tsump
 26.03   19.60    2.14     2.47     2.23  10.32    2.27   -10.7
     Vr          Ir         Cc
   3.29         .70      7.369E+03
 Thetab      Htube       Qdp       Athetab  Ahtube      AuQdp
 23.757   3.391E+02  8.056E+03   17.329   1.785E+02   3.094E+03
```

```
Data Set Number =  10  Bulk Oil % =  0.0
TIME:      13:27:26

TC No:     1       2       3       4       5       6       7       8
Temp :  10.92   11.50   11.27   11.74   11.29   10.85  -99.99  -99.99
TC No:     9      10      11      12      13      14      15      16
Temp : -99.99   17.36   15.38   17.50   17.07   18.05   16.48   14.36

  Twa    ATwa    Tliqd    Tliqd2  Tvapr  Psat    Tsat    Tsump
 11.16   16.54    2.25     2.25    2.09  10.33    2.17   -10.5
     Vr          Ir        Cc
   3.79        .81      2.114E+03
 Thetab     Htube       Qdp       Athetab  Ahtube      AuQdp
  8.991  1.510E+03  1.357E+04   14.471  2.455E+02  3.553E-03


Data Set Number =  11  Bulk Oil % =  0.0
TIME:      13:29:22

TC No:     1       2       3       4       5       6       7       8
Temp :  11.77   12.52   12.23   12.73   12.40   11.81  -99.99  -99.99
TC No:     9      10      11      12      13      14      15      16
Temp : -99.99   16.30   15.33   16.98   16.60   17.31   16.36   13.76

  Twa    ATwa    Tliqd    Tliqd2  Tvapr  Psat    Tsat    Tsump
 12.14   16.21    2.23     2.22    2.01  10.78    2.12   -10.6
     Vr          Ir        Cc
   4.48        .96      2.430E-03
 Thetab     Htube       Qdp       Athetab  Ahtube      AuQdp
 10.027  1.924E+03  1.929E+04   14.092  4.218E+02  5.944E+03


Data Set Number =  12  Bulk Oil % =  0.0
TIME:      13:30:20

TC No:     1       2       3       4       5       6       7       8
Temp :  13.80   14.46   14.14   14.73   14.52   13.94  -99.99  -99.99
TC No:     9      10      11      12      13      14      15      16
Temp : -99.99   16.21   14.70   16.26   15.95   17.07   15.51   13.21

  Twa    ATwa    Tliqd    Tliqd2  Tvapr  Psat    Tsat    Tsump
 14.07   15.53    2.11     2.14    1.93  10.70    2.03   -10.6
     Vr          Ir        Cc
   5.88       1.25      3.072E+03
 Thetab     Htube       Qdp       Athetab  Ahtube      AuQdp
 12.039  2.792E+03  3.361E+04   13.502  2.755E+02  3.720E+03
```

Data Set Number = 13 Bulk Oil % = 0.0
TIME: 13:31:43

| TC No: | 1 | 2 | 3 | 4 | 5 | 6 | 7 | 8 |
|---|---|---|---|---|---|---|---|---|
| Temp : | 16.12 | 16.75 | 16.45 | 17.02 | 16.87 | 16.17 | -99.99 | -99.99 |
| TC No: | 9 | 10 | 11 | 12 | 13 | 14 | 15 | 16 |
| Temp : | -99.99 | 15.79 | 14.44 | 15.87 | 15.71 | 16.83 | 15.49 | 13.23 |

| Twa | ATwa | Tliqd | Tliqd2 | Tvapr | Psat | Tsat | Tsumo |
|---|---|---|---|---|---|---|---|
| 16.24 | 15.34 | 2.21 | 2.32 | 2.16 | 10.87 | 2.21 | -10.6 |

| Vr | Ir | Cc |
|---|---|---|
| 7.71 | 1.64 | 3.739E+03 |

| Thetab | Htube | Qdo | Athetab | Ahtube | AuQdo |
|---|---|---|---|---|---|
| 14.030 | 4.162E+03 | 5.839E+04 | 13.125 | 2.869E+02 | 3.756E+03 |

Data Set Number = 14 Bulk Oil % = 0.0
TIME: 13:32:48

| TC No: | 1 | 2 | 3 | 4 | 5 | 6 | 7 | 8 |
|---|---|---|---|---|---|---|---|---|
| Temp : | 17.77 | 18.27 | 17.93 | 18.48 | 18.53 | 17.70 | -99.99 | -99.99 |
| TC No: | 9 | 10 | 11 | 12 | 13 | 14 | 15 | 16 |
| Temp : | -99.99 | 15.53 | 14.22 | 15.56 | 15.39 | 15.51 | 14.39 | 12.90 |

| Twa | ATwa | Tliqd | Tliqd2 | Tvapr | Psat | Tsat | Tsumo |
|---|---|---|---|---|---|---|---|
| 17.64 | 15.03 | 2.29 | 2.36 | 2.21 | 10.92 | 2.27 | -10.6 |

| Vr | Ir | Cc |
|---|---|---|
| 8.23 | 1.86 | 4.207E+03 |

| Thetab | Htube | Qdo | Athetab | Ahtube | AuQdo |
|---|---|---|---|---|---|
| 15.375 | 5.453E+03 | 8.384E+04 | 12.760 | 2.372E+02 | 3.792E+03 |

Data Set Number = 15 Bulk Oil % = 0.0
TIME: 13:34:20

| TC No: | 1 | 2 | 3 | 4 | 5 | 6 | 7 | 8 |
|---|---|---|---|---|---|---|---|---|
| Temp : | 16.36 | 17.52 | 17.20 | 17.74 | 17.69 | 16.30 | -99.99 | -99.99 |
| TC No: | 9 | 10 | 11 | 12 | 13 | 14 | 15 | 16 |
| Temp : | -99.99 | 15.59 | 14.13 | 15.58 | 15.39 | 16.64 | 15.18 | 12.94 |

| Twa | ATwa | Tliqd | Tliqd2 | Tvapr | Psat | Tsat | Tsumo |
|---|---|---|---|---|---|---|---|
| 16.35 | 15.05 | 2.40 | 2.54 | 2.31 | 11.03 | 2.39 | -10.4 |

| Vr | Ir | Cc |
|---|---|---|
| 8.23 | 1.75 | 3.325E+03 |

| Thetab | Htube | Qdo | Athetab | Ahtube | AuQdo |
|---|---|---|---|---|---|
| 14.563 | 4.572E+03 | 6.658E+04 | 12.662 | 2.387E+02 | 3.782E+03 |

```
Data Set Number =  16  Bulk Oil % =  0.0
TIME:      13:35:45

TC No:     1       2       3       4       5       6       7       8
Temp :   15.31   16.29   15.38   16.59   16.32   15.60 -99.99 -99.99
TC No:     9      10      11      12      13      14      15      16
Temp : -99.99   15.49   14.01   15.51   15.31   16.33   14.86   12.72

  Twa    ATwa    Tliqd    Tliqd2  Tvapr  Psat    Tsat    Tsumo
 15.30   14.86    2.33     2.35    2.25  10.34    2.29   -10.4
     Vr          Ir         Cc
   5.38        1.47      3.560E+03
 Thetab     Htube       Qdp       Athetab  Ahtube      AuQdp
 13.503  3.431E+03  4.634E+04   12.568  3.038E+02  3.918E+03


Data Set Number =  17  Bulk Oil % =  0.0
TIME:      13:36:51

TC No:     1       2       3       4       5       6       7       8
Temp :   13.76   14.46   14.18   14.81   14.21   13.65 -99.99 -99.99
TC No:     9      10      11      12      13      14      15      16
Temp : -99.99   15.21   13.75   15.17   15.10   16.15   14.60   12.42

  Twa    ATwa    Tliqd    Tliqd2  Tvapr  Psat    Tsat    Tsumo
 14.02   14.60    2.25     2.29    2.08  10.33    2.17   -10.2
     Vr          Ir         Cc
   5.28        1.13      3.010E+03
 Thetab     Htube       Qdp       Athetab  Ahtube      AuQdp
 11.348  2.271E+03  2.690E+04   12.427  3.095E+02  3.347E+03


Data Set Number =  18  Bulk Oil % =  0.0
TIME:      13:38:09

TC No:     1       2       3       4       5       6       7       8
Temp :   11.86   12.64   12.42   12.98   12.20   11.69 -99.99 -99.99
TC No:     9      10      11      12      13      14      15      16
Temp : -99.99   15.29   13.82   15.29   15.25   16.45   15.07   12.61

  Twa    ATwa    Tliqd    Tliqd2  Tvapr  Psat    Tsat    Tsumo
 12.21   14.80    2.28     2.24    2.06  10.32    2.16   -10.1
     Vr          Ir         Cc
   4.06         .87      2.437E+03
 Thetab     Htube       Qdp       Athetab  Ahtube      AuQdp
 10.048  1.556E+03  1.563E+04   12.638  3.005E+02  3.797E+03
```

```
Data Set Number =  19  Bulk Oil % =  0.0
TIME:      13:39:28

TC No:     1       2       3       4       5       6       7       8
Temp :   9.20    9.58    9.45    9.80    9.85    9.39  -99.99  -99.99
TC No:     9      10      11      12      13      14      15      16
Temp : -99.99   15.63   14.21   15.46   15.66   16.68   15.32   13.16

  Twa    ATwa    Tliqd    Tliqd2   Tvapr   Psat    Tsat    Tsump
 9.50   15.13    2.28     2.35     2.17   10.30    2.24   -10.1
    Vr          Ir         Cc
  2.72        .58      1.609E+03
 Thetab     Htube       Qdp       Athetab   Ahtube      AuQdp
 7.251   9.245E+02  6.712E+03   12.890   2.368E-02   3.696E+03


Data Set Number =  20  Bulk Oil % =  0.0
TIME:      13:40:18

TC No:     1       2       3       4       5       6       7       8
Temp :   7.12    7.13    7.03    7.10    7.79    7.23  -99.99  -99.99
TC No:     9      10      11      12      13      14      15      16
Temp : -99.99   15.65   14.29   15.45   15.68   16.67   15.31   13.21

  Twa    ATwa    Tliqd    Tliqd2   Tvapr   Psat    Tsat    Tsump
 7.21   15.15    2.25     2.32     2.22   10.91    2.25   -10.1
    Vr          Ir         Cc
  2.04        .43      9.373E+02
 Thetab     Htube       Qdp       Athetab   Ahtube      AuQdp
 4.956   7.498E+02  3.717E+03   12.900   2.322E+02   3.769E-03


Data Set Number =  21  Bulk Oil % =  0.0
TIME:      13:41:00

TC No:     1       2       3       4       5       6       7       8
Temp :   6.17    6.12    6.04    6.02    6.77    6.33  -99.99  -99.99
TC No:     9      10      11      12      13      14      15      16
Temp : -99.99   15.78   14.52   15.68   15.89   16.76   15.50   13.48

  Twa    ATwa    Tliqd    Tliqd2   Tvapr   Psat    Tsat    Tsump
 6.23   15.34    2.29     2.36     2.25   10.94    2.29   -10.0
    Vr          Ir         Cc
  1.74        .37      7.367E+02
 Thetab     Htube       Qdp       Athetab   Ahtube      AuQdp
 3.936   6.801E+02  2.577E+03   13.053   2.368E+02   3.744E+03
```

```
Data Set Number =  22  Bulk Oil % =  0.0
TIME:      13:42:13

TC No:     1       2       3       4       5       6       7       8
Temp :   4.38    4.40    4.39    4.37    4.33    4.31  -99.99  -99.99
TC No:     9      10      11      12      13      14      15      16
Temp : -99.99   15.98   14.70   15.33   16.07   16.36   15.38   13.55

  Twa    ATwa    Tliqd    Tliqd2   Tvapr   Psat    Tsat    Tsumo
  4.47   15.31    2.45     2.31     2.35   11.06    2.41   -10.1
     Vr          Ir         Cc
   1.33        .27      3.225E+02
 Thetab     Htube       Qdo       Athetab   Ahtube      AuQdo
  2.058   7.640E+02  1.572E+03   13.095   2.868E+02   3.755E+03


Data Set Number =  23  Bulk Oil % =  0.0
TIME:      13:43:07

TC No:     1       2       3       4       5       6       7       8
Temp :   3.58    3.53    3.52    3.47    3.43    3.30  -99.99  -99.99
TC No:     9      10      11      12      13      14      15      16
Temp : -99.99   15.98   14.54   15.38   15.98   16.39   15.54   13.42

  Twa    ATwa    Tliqd    Tliqd2   Tvapr   Psat    Tsat    Tsumo
  3.58   15.42    2.31     2.37     2.19   10.92    2.27   -10.0
     Vr          Ir         Cc
    .99        .20      1.825E+02
 Thetab     Htube       Qdo       Athetab   Ahtube      AuQdo
  1.317   6.529E+02  8.597E+02   13.153   2.808E+02   3.693E+03


Data Set Number =  24  Bulk Oil % =  0.0
TIME:      13:44:32

TC No:     1       2       3       4       5       6       7       8
Temp :   2.36    2.34    2.35    2.33    3.12    2.99  -99.99  -99.99
TC No:     9      10      11      12      13      14      15      16
Temp : -99.99   15.99   14.63   15.87   16.08   17.01   15.58   13.80

  Twa    ATwa    Tliqd    Tliqd2   Tvapr   Psat    Tsat    Tsumo
  2.38   15.52    2.46     2.48     2.34   11.05    2.40   -10.0
     Vr          Ir         Cc
    .70        .14      6.344E+01
 Thetab     Htube       Qdo       Athetab   Ahtube      AuQdo
   .574   7.393E+02  4.241E+02   13.120   2.847E+02   3.735E+03


NOTE: 24 data runs were stored in file D0907SC2
```

## APPENDIX D. SAMPLE CALCULATIONS[3]

Data file D0921ASC4 was used for sample calculations. The saturation temperature was 2.2 °C with a heat flux of 59,130 $W/m^2$ on the smooth upper test tube.

### A. SMOOTH TEST TUBE DIMENSIONS

Do = 0.015875 m

Di = 0.0127 m

D1 = 0.012446 m

L = 0.2032 m

Lu = 0.0762 m

### B. MEASURED PARAMETERS

V = Vr·25 = (7.76 V)(25) = 194.0 V

I = Ir·1.9182 = (1.66 A)(1.9182) = 3.18 A

T1 = 19.44 °C T2 = 20.03 °C

T3 = 19.75 °C T4 = 19.63 °C

T5 = 19.46 °C T6 = 19.38 °C

T7 and T8 not used, defective

[3]This analysis is essentially identical to the analysis done by Perry [Ref. 2] and therefore his procedure is largely reproduced.

Tsat = 2.20 °C

kc = 344 W/m·K

## C. OUTER WALL TEMPERATURE OF THE UPPER TEST TUBE

### 1. Surface Area of Smooth Tube

$P = \pi \cdot Do = \pi(0.015875\ m) = 0.04987\ m$

$Ac = \pi(Do^2-Di^2)/4 = \pi((0.015875\ m)^2-(0.0127)^2)/4$

$Ac = 7.13 \times 10^{-5}\ m^2$

### 2. Heater Power

$Qh = V \cdot I = (194.0\ V)(3.18\ A) = 616.92\ W$

### 3. Average Inside Tube Temperature

$Tavg = \Sigma_1^m\ Tn/m = \Sigma_1^6\ Tn/6 = (T1+T2+T3+T4+T5+T6)/6$

$Tavg = (19.44+20.03+19.75+19.63+19.46+19.38)/6$

$= 19.62\ °C$

### 4. Outside Wall Tube Temperature

Two is calculated using Fourier's Conduction Law, assuming uniform radial conduction and using a known Tavg:

$Two = Tavg - \{Qh(\ln(Do/Di))/(2\pi \cdot L \cdot kc)\}$

$Two = 19.62-\{616.92(\ln(0.015875/0.01245))/(2\pi \cdot 0.203 \cdot 344)\}$

$Two = 19.28\ °C$

### 5. Tube Wall Superheat

$\theta = Two - Tsat = 19.28 - 2.20 = 17.08\ °C$

## D. R-124 PROPERTIES AT FILM TEMPERATURE

The thermophysical properties of R-124 were computed at the film temperature using the REFPROP equations provided by Bertsch [Ref. 1]:

### 1. Film Temperature

$$T_f = (T_{wo} + T_{sat})/2 = (19.28 + 2.20)/2 = 10.74\ ^{\circ}C$$

### 2. Dynamic Viscosity

$$\mu = 3.4593-(0.0426)T_f+(3.9485\times10^{-4})T_f^2-(4.193\times10^{-6})T_f^3+(2.0709\times10^{-8})T_f^4$$

$$\mu = \{3.4593-(0.0426)10.74+(3.9485\times10^{-4})(10.74)^2-(4.193\times10^{-6})(10.74)^3+(2.0709\times10^{-8})(10.74)^4\}\times10^{-4}$$

$$\mu = 3.0424\times10^{-4}\ N\cdot s/m^2$$

### 3. Density

$$\rho = 1434.8-(2.8619)T_f-(6.7267\times10^{-3})T_f^2-(7.2852\times10^{-5})T_f^3$$

$$\rho = 1434.8-(2.8619)10.74-(6.7267\times10^{-3})(10.74)^2-(7.2852\times10^{-5})(10.74)^3$$

$$\rho = 1403.2\ kg/m^3$$

### 4. Kinematic Viscosity

$$\nu = \mu/\rho = 3.0422\times10^{-4}/1403.2 = 2.17\times10^{-7}\ m/s$$

### 5. Thermal Conductivity

$$k = 7.5191\times10^{-2}-(3.5436\times10^{-4})T_f-(1.9545\times10^{-7})T_f^2+(3.1835\times10^{-9})T_f^3$$

$$k = 7.5191\times10^{-2}-(3.5436\times10^{-4})(10.74)-(1.9545\times10^{-7})(10.74)^2+(3.1835\times10^{-9})(10.74)^3$$

$$k = 7.137\times10^{-2}\ W/m\cdot K$$

**6. Specific Heat**

$$Cp = 1.0542+(2.1405\times10^{-3})Tf+(1.0709\times10^{-5})Tf^{2}-(6.4721\times10^{-8})\cdot Tf^{3}-(1.4324\times10^{-9})Tf^{4}+(4.136\times10^{-11})Tf^{5}$$

$$Cp = \{1.0542+(2.1405\times10^{-3})(10.74)+(1.0709\times10^{-5})(10.74)^{2}-(6.4721\times10^{-8})(10.74)^{3}-(1.4324\times10^{-9})(10.74)^{4}+(4.136\times10^{-11})(10.74)^{5}\}\times10^{3}$$

$$Cp = 1078.35\ J/kg\cdot K$$

**7. Thermal Diffusivity**

$$\alpha = k/(\rho\cdot Cp) = 7.137\times10^{-2}/(1403.2\cdot1078.35)$$

$$\alpha = 4.717\times10^{-8}\ m^{2}/s$$

**8. Volumetric Thermal Expansion Coefficient**

$$\beta = -\Delta\rho/(\rho\cdot\Delta Tf) = -(1402.89-1403.50)/(1403.2\cdot0.2)$$

$$\beta = 2.174\times10^{-3}\ \ (1/K)$$

**9. Prandtl Number**

$$Pr = \nu/\alpha = 2.17\times10^{-7}/4.717\times10^{-8} = 4.60$$

## E. HEAT FLUX THROUGH NON-BOILING TUBE LENGTHS

Using the Churchill-Chu correlation [Ref. 9] for a smooth cylinder in natural convection, the average natural convection heat transfer coefficient of one non-boiling tube length is:

$$h = k/Do\{0.6+0.387[\Gamma/(1+(0.559/Pr)^{9/16})^{8/27}]\}^{2}$$

where $\Gamma = \{[g\cdot\beta\cdot Do^{3}\cdot\theta\cdot\tanh(m\cdot Lu)]/(\nu\cdot\alpha\cdot Lu\cdot m)\}^{1/6}$

$$m = \{(h\cdot P)/(kc\cdot Ac)\}^{1/2}$$

The program DRPJY computes the value of h by assuming a starting value of 190 $W/m^2 \cdot K$ and iterating to the final value. The resulting values of h and m are:

$h = 281.93\ W/m^2 \cdot K$

$m = 23.94\ (1/m)$

therefore,

$Qf = (h \cdot p \cdot kc \cdot Ac)^{1/2} \cdot \theta \cdot \tanh(m \cdot Lu) = 9.52\ W$

**F. HEAT FLUX THROUGH BOILING TUBE LENGTH**

$Q = Qh - 2 \cdot Qf = 616.92 - 2(9.52) = 597.88\ W$

$Ab = \pi \cdot Do \cdot L = \pi(0.015875)(.2032) = 1.013 \times 10^{-2}\ m^2$

$q'' = Q/Ab = 597.88/1.013 \times 10^{-2} = 59{,}021\ W/m^2$

$h = q''/\theta = 59021/17.08 = 3456\ W/m^2 \cdot K$

The following results were calculated by the data acquisition and reduction program DRPJY:

$q'' = 59{,}130\ W/m^2$

$h = 3463\ W/m^2 \cdot K$

$\theta = 17.08\ ^\circ C$

## APPENDIX E. UNCERTAINTY ANALYSIS[4]

The same data run used for the sample calculations (Appendix D) was used for the uncertainty analysis, thus all the measured and most of the calculated results still apply. A lower heat flux of 1561 $W/m^2$ was also analyzed from the same data run to show the difference between the two heat fluxes. All uncertainties are presented as a percentage of the calculated parameter, i.e. a relative uncertainty. The uncertainty analysis method suggested by Kline and McClintock [Ref. 29] was used. For example: If $R = R(x_1, x_2, x_3, \ldots\ldots x_n)$, then:

$$\delta R = \left[\left(\frac{\delta R}{\delta x_1}\delta X_1\right)^2 + \left(\frac{\delta R}{\delta x_2}\delta X_2\right)^2 + \ldots + \left(\frac{\delta R}{\delta x_3}\delta X_3\right)^2\right]^{\frac{1}{2}}$$

where:

$\delta R$ = uncertainty of the desired dependent variable

$x_n$ = measured variable

$\delta x_n$ = uncertainty in the measured variable

[4]This analysis is essentially identical to the analysis done by Perry [Ref. 2] and therefore his procedure is largely reproduced.

## A. HEAT TRANSFER RATE UNCERTAINTY

Ir = 1.66 amps  δIr = 0.025 amps

Vr = 7.76 volts  δVr = 0.05 volts

so we have:

$$\frac{\delta Qh}{Qh} = \left[\left(\frac{\delta Vr}{Vr}\right)^2 + \left(\frac{\delta Ir}{Ir}\right)^2\right]^{\frac{1}{2}}$$

$$\frac{\delta Qh}{Qh} = \left[\left(\frac{0.05}{7.76}\right)^2 + \left(\frac{0.025}{1.66}\right)^2\right]^{\frac{1}{2}} = 1.64\%$$

## B. SURFACE AREA UNCERTAINTY

The following dimensions were taken from the manufacturer's data sheet, and from actual measurements:

Do = 15.88 (mm)  δDo = 0.1 (mm)

L = 203.2 (mm)  δL = 0.1 (mm)

Ab = Do x L

$$\frac{\delta Ab}{Ab} = \left[\left(\frac{\delta Do}{Do}\right)^2 + \left(\frac{\delta L}{L}\right)^2\right]^{\frac{1}{2}}$$

$$\frac{\delta Ab}{Ab} = \left[\left(\frac{0.1}{15.88}\right)^2 + \left(\frac{0.1}{203.2}\right)^2\right]^{\frac{1}{2}} = 0.63\%$$

## C. WALL SUPERHEAT UNCERTAINTY

The following temperatures were measured:

T1 = 19.44 °C

T2 = 20.03 °C

T3 = 19.75 °C

T4 = 19.63 °C

T5 = 19.46 °C

T6 = 19.38 °C

Tavg = 19.62 °C

Standard Deviation = 0.245 °C

Tsat = 2.20 °C and $\delta$Tsat = 0.01 °C

$$Two = Tavg - Qh\left[\frac{\ln(\frac{Do}{D1})}{2\pi \cdot L \cdot kc}\right]$$

**Note**: The second term on the right hand side of the above equation is the Fourier heat transfer conduction term, and can be neglected for the uncertainty analysis since its value is less than the standard deviation, so:

Two = Tavg = 19.62 °C

$\Delta$T = Two - Tsat = 19.62 °C - 2.20 °C = 17.42 °C

therefore,

$$\frac{\delta \Delta T}{\Delta T} = \left[\left(\frac{\delta \Delta Two}{\Delta T}\right)^2 + \left(\frac{\delta Tsat}{\Delta T}\right)^2\right]^{\frac{1}{2}}$$

$$\frac{\delta \Delta T}{\Delta T} = \left[\left(\frac{0.245}{17.42}\right)^2 + \left(\frac{0.01}{17.42}\right)^2\right]^{\frac{1}{2}} = 1.41\%$$

**D. HEAT FLUX UNCERTAINTY**

$$q'' = \frac{(Qh - 2 \times Qf)}{Ab}$$

where: Qh = V x I = (194 V)(3.18 A) = 616.92 W

and $\delta Qh = (616.92)(0.0164) = 10.12$ W

$q'' = 59130$ W/m$^2$ (measured)

$Ab = 0.010137$ m$^2$

$Qh - 2.Qf = (q)(Ab) = (59130)(0.010137) = 599.40$ W

solving for Qf:

$$Qf = (616.92 - 599.40)/2 = 8.76 \text{ W}$$

assuming the same proportion uncertainty for Qf, we have:

$$\delta Qf = (8.76)(0.0164) = 0.144 \text{ W}$$

and for the uncertainty:

$$\frac{\delta q''}{q''} = \left[\left(\frac{\delta Qh}{Qh - 2Qf}\right)^2 + \left(\frac{2\delta Qf}{Qh - 2Qf}\right)^2 + \left(\frac{\delta Ab}{Ab}\right)^2\right]^{\frac{1}{2}}$$

$$\frac{\delta q''}{q''} = \left[\left(\frac{10.12}{599.4}\right)^2 + \left(\frac{2 \times 0.144}{599.4}\right)^2 + (0.0063)^2\right]^{\frac{1}{2}} = 1.80\%$$

## E. HEAT TRANSFER COEFFICIENT UNCERTAINTY

$$h = q''/\Delta T$$

therefore,

$$\frac{\delta h}{h} = \left[\left(\frac{\delta q''}{q''}\right)^2 + \left(\frac{\delta \Delta T}{\Delta T}\right)^2\right]^{\frac{1}{2}}$$

$$\frac{\delta h}{h} = [(0.018)^2 + (0.0141)^2]^{\frac{1}{2}} = 2.29\%$$

The above series of calculations was also conducted with a lower heat flux for the same data run and with a high and low heat flux from a TURBO-B data run (D1022FTBC4) with the results tabulated in Table 5.

**TABLE 5. RESULTS OF UNCERTAINTY ANALYSIS**

| PARAMETER | SMOOTH 1561 $W/m^2$ | SMOOTH 59130 $W/m^2$ | TURBO-B 1703 $W/m^2$ | TURBO-B 71270 $W/m^2$ |
|---|---|---|---|---|
| $\delta Qh/Qh$ (%) | 8.49 | 1.64 | 10.47 | 1.60 |
| $\delta Ab/Ab$ (%) | 0.63 | 0.63 | 0.63 | 0.63 |
| $\delta \Delta T/\Delta T$ (%) | 3.55 | 1.41 | 26.62 | 12.44 |
| $\delta q''/q''$ (%) | 13.05 | 1.80 | 9.26 | 1.55 |
| $\delta h/h$ (%) | 13.52 | 2.29 | 28.18 | 12.54 |

## LIST OF REFERENCES


1. Bertsch, G., *Nucleate Pool Boiling Characteristics of R-124,* M.S. Thesis, Naval Postgraduate School, Monterey, CA, March 1993.

2. Perry, G., *Effect of Oil on the Onset of Nucleate Pool Boiling of R-124 from a Single Horizontal Tube,* M.S. Thesis, Naval Postgraduate School, Monterey, CA, June 1993.

3. Lake, L., *The Influence of a Lower Heated Tube on Nucleate Pool Boiling from a Horizontal Tube,* Master's Thesis, Naval Postgraduate School, Monterey, CA, June 1992.

4. Bar-Cohen, A., *Hysteresis Phenomena at Onset of Nucleate Boiling,* Proceedings of the Engineering Foundation Conference on Pool and External Flow Boiling, Santa Barbara, CA, pp. 1-13, 1992.

5. You, S.M., Bar-Cohen, A., Simon, T.W., and Tong, W., *Experimental Investigation of Nucleate Boiling Incipience with a Highly-Wetting Dielectric Fluid (R-113),* International Journal Heat Mass Transfer, Vol. 33, No. 1, pp. 105-117, 1990.

6. Bar-Cohen, A., and Simon, T.W., *Wall Superheat Excursions in the Boiling Incipience of Dielectric Fluids,* Heat Transfer Engineering, Vol. 9, No. 3, pp. 19-31, 1988.

7. Tong, W., Bar-Cohen, A., Simon, T.W., and You, S.M., *Contact Angle Effects on Boiling Incipience of Highly-Wetting Liquids,* International Journal Heat Mass Transfer, Vol. 33, No. 1, pp. 91-103, 1990.

8. Thome, J.R., *Enhanced Boiling Heat Transfer,* Hemisphere Publishing Corp, pp. 5-7, 1990.

9. Churchill, S.W., and Chu, F.H.S., *Correlating Relations from a Laminar and Turbulent Free Convection from a Horizontal Cylinder,* International Journal Heat Mass Transfer, Vol. 18, pp.1049-1070, 1975.

10. Thome, J.R., *Enhanced Boiling Heat Transfer,* Hemisphere Publishing Corp, pp. 155-157, 1990.

11. Sparrow, E.M., and Niethammer, J.E., *Effect of Vertical Separation Distance and Cylinder-to-Cylinder Temperature Imbalance on Natural Convection for a Pair of Horizontal Cylinders,* Journal of Heat Transfer, Vol. 103, pp. 638-644, 1981.

12. Al-Alusi, T.R., and Bushnell, D.J., *An Experimental Study of Free Convection Heat Transfer From an Array of Horizontal Cylinders Parallel to a Vertical Wall,* Journal of Heat Transfer, Vol. 114, pp. 394-400, 1992.

13. Tokura, I., Saito, H., Kishinami, K., and Muramoto, K., *An Experimental Study of Free Convection Heat Transfer From a Horizontal Cylinder in a Vertical Array Set in Free Space Between Parallel Walls,* Journal of Heat Transfer, Vol. 105, pp. 102-107, 1983.

14. Sparrow, E.M., and Boessneck, D.S., *Effect of Transverse Misalignment on Natural Convection from a Pair of Parallel, Vertically Stacked, Horizontal Cylinders,* Journal of Heat Transfer, Vol. 105, pp. 241-247, 1983.

15. Inagaki, T., and Komori, K., *Natural Convection Heat Transfer from Two Horizontal Cylinders in Vertical Alignment,* Transactions of JSME, Vol. 56, pp. 3050-3055, 1990 (in Japanese): Translation in Heat Transfer - Japanese Research, Vol. 20, No. 6, pp. 549-559, 1991.

16. Cornwell, K., Duffin, N.W., and Schuller, R.B., *An Experimental Study of the Effects of Fluid Flow on Boiling Within a Kettle Reboiler Tube Bundle,* ASME Paper 80 HT-45, National Heat Transfer Conference, Orlando, 1980.

17. Cornwell, K., and Schuller, R.B., *A Study of Boiling Outside a Tube Bundle Using High Speed Photography,* International Journal Heat Mass Transfer, Vol. 25, pp. 683-690, 1982.

18. Cornwell, K., and Scoones, D.J., *Analysis of Low Quality Boiling on Plain and Low-Finned Tube Bundles,* 2nd UK National Heat Transfer Conference, Vol. 1, pp. 21-32, 1988.

19. Cornwell, K., *The Influence of Bubbly Flow on Boiling from a Tube in a Bundle,* Eurotherm Seminar No. 8, Advances in Pool Boiling Heat Transfer, FRG, pp. 177-183, 1989.

20. Fujita, Y., Ohta, H., Hidaka, S., and Nishikawa, K., *Nucleate Boiling Heat Transfer on Horizontal Tubes in*

*Bundles,* 8th International Heat Transfer Conference, Vol. 5, pp. 2131-2136, San Francisco, 1986.

21. Stephan, K., and Mitrovic, J., *Heat Transfer in Natural Convection/Boiling of Refrigerants and Refrigerant/Oil Mixtures in Bundles of T-Shaped Finned Tubes,* Advances in Enhanced Heat Transfer, ASME, pp. 131-146, 1981.

22. Hahne, E., and Muller, J., *Boiling on a Finned Tube and a Finned Tube Bundle,* International Journal Heat Mass Transfer, Vol. 26, No. 6, pp. 849-859, 1983.

23. Windisch, R., Hahne, E., and Kiss, V., *Heat Transfer for Boiling on Finned Tube Bundles,* International Committee Heat Mass Transfer, Vol. 12, pp. 355-368, 1985.

24. Hahne, E., Chen, Q., and Windisch, R., *Pool Boiling Heat Transfer on Finned Tubes - An Experimental and Theoretical Study,* International Journal Heat Mass Transfer, Vol. 34, No. 8, pp. 2071-2079, 1991.

25. Karasabun, M., *An Experimental Apparatus to Study Nucleate Pool Boiling of R-114 and Oil Mixtures,* M.S. Thesis, Naval Postgraduate School, Monterey, CA, 1984.

26. Reilley, J., *The Influence of Oil Contamination on the Nucleate Pool Boiling Behavior of R-114 from a Structured Surface,* M.S. Thesis, Naval Postgraduate School, Monterey, CA, 1985.

27. Sugiyama, D., *Nucleate Pool Boiling of R-114 and R-114/Oil Mixtures from Single Enhanced Tubes,* M.S. Thesis, Naval Postgraduate School, Monterey, CA, 1991.

28. Gallager, J., Mclinden, M., and Morrison, G., *NIST Thermodynamic Properties of Refrigerants and Refrigerant Mixtures Database,* RefProp Version 2.0, National Institute of Standards and Technology, Gaithersburg, MD, 1991.

29. Kline, S.J., and McClintock, F.A., *Describing Uncertainties in Single Sample Experiments,* Mechanical Engineering, p. 3, 1953.

## INITIAL DISTRIBUTION LIST

1. Defense Technical Information Center — 2
   Cameron Station
   Alexandria, Va 22304-6145

2. Library, Code 052 — 2
   Naval Postgraduate School
   Monterey, CA 93943-5002

3. Professor Matthew D. Kelleher, Code ME/Kk — 1
   Department of Mechanical Engineering
   Naval Postgraduate School
   Monterey, CA 93943-5002

4. Professor Paul J. Marto, Code ME/Mx — 2
   Department of Mechanical Engineering
   Naval Postgraduate School
   Monterey, CA 93943-5002

5. Professor Stephen B. Memory — 1
   Department of Mechanical Engineering
   McArthur Bldg.
   University of Miami
   Coral Gables, FL 33124-0624

6. Mr. R. Helmick, Code 2722 — 2
   Annapolis Detachment, C. D.
   Naval Surface Warfare Center
   Annapolis, MD 21402-5067

7. Mr. Bruce G. Unkel — 1
   NAVSEA (Code 56Y15)
   Department of the Navy
   Washington, D.C. 20362-5101

8. Naval Engineering Curricular Officer, Code 34 — 1
   Naval Postgraduate School
   Monterey, CA 93943-5002

9. LT Joseph E. Yusician, Jr. — 1
   9817 Dungan Road
   Philadelphia, PA 19115

DUDLEY KNOX LIBRARY
NAVAL POSTGRADUATE SCHOOL

3 2768 00307241 4